# EpCAM and CSPG4 scFv based fusion proteins for the treatment of triple negative breast cancer

Von der Fakultät für Mathematik, Informatik und Naturwissenschaften der RWTH Aachen University zur Erlangung des akademischen Grades einr Doktorin der Naturwissenschaften genehmigte Dissertation

vorgelegt von

Master of Science Medical science

**Manal Amoury**

aus Haifa (Palästina)

Berichter*:* Universitätsprofessor Dr. Rainer Fischer

Universitätsprofessor Dr. Fabian Kießling

Tag der mündlichen Prüfung*:* *27.1.2017*

Diese Dissertation ist auf den Internetseiten der Universitätsbibliothek verfügbar.

*In memory of my beloved father,* ***Nabeel Amoury***

*Thank you for passing the love of science and critical thinking to me.*

# ABSTRACT

Triple-negative breast cancer (TNBC) defines a heterogeneous group of breast tumors lacking the expression of estrogen receptor (ER), progesterone receptor (PR) and human epidermal growth factor receptor 2 (HER2). It has the poorest prognosis of all breast cancer subtypes and high prevalence among young premenopausal women. Unlike other breast cancer subtypes, no effective targeted immunotherapy is currently available. Due to the heterogeneity of TNBC, no single receptor can be expected to be effective in targeting all TNBCs. Therefore, in this study, we set out to develop a panel of receptors for targeted therapies which can, together, include the majority of TNBC tumors. Through a literature search two markers stood out as suitable targets, EpCAM- overexpressed in 60% of TNBC and CSPG4- overexpressed in 20-40% of TNBC. EpCAM and CSPG4 are differentially expressed and their expression on TNBC tumor does not overlap.

Therefore, novel single-chain variable fragment (scFv)-based human cytolytic fusion proteins (hCFPs) were constructed to target these receptors. Their activity and mechanism of action were compared to corresponding recombinant immunotoxins (ITs) utilizing the Pseudomonas Exotoxin A- deletion mutant (ETA') as the toxic moiety.

To target EpCAM expressing TNBC, a hCFP designated Gb-R201K-αEpCAM(scFv) was generated, in which an EpCAM-selective scFv was genetically fused to a human Granzyme B (Gb) mutant with reduced sensitivity to its natural inhibitor serpin B9. To target CSPG4 a CFP designated αCSPG4(scFv)-MAP was used, consisting of a CSPG4-selective scFv genetically fused to a functionally enhanced form of the human microtubule-associated protein (MAP) tau.

In vitro studies confirmed specific binding, internalization and subsequent potent cytotoxic activity of both hCFPs, with IC50 values of 200-300 nM for Gb-R201K-αEpCAM(scFv) towards TNBC cell lines MDA-MB-453 and MDA-MB-468 and 200-400nM for αCSPG4(scFv)-MAP toward MDA-MB-231 and Hs 578T. In vivo studies in subcutaneous tumor models revealed that treatment of mice bearing MDA-MB-468 tumors with Gb-R201K-αEpCAM(scFv) inhibited tumor growth of up to 50 %. Treatment of mice bearing MDA-MB-231 tumors with αCSPG4(scFv)-MAP resulted in prominent inhibition of tumor growth and to tumor regression of more than 50%.

Taken together, αCSPG4(scFv)-MAP and Gb-R201K-αEpCAM(scFv) appear to be clinically relevant and promising novel targeted agent for the treatment of TNBC.

## ZUSAMMENFASSUNG

Dreifach-negativer Brustkrebs (TNBC) bezieht sich auf eine heterogene Gruppe von Brusttumoren, die keine Östrogen-Rezeptoren (ER), keine Progesteronrezeptoren (PR) und keine humanen epidermalen Wachstumsfaktor 2 (HER2) Rezeptoren exprimieren. Er hat die schlechteste Prognose aller Brustkrebssubtypen und eine hohe Prävalenz bei jungen prämenopausalen Frauen. Im Gegensatz zu den anderen Brustkrebssubtypen ist derzeit keine wirksame gezielte Immuntherapie gegen TNBC verfügbar. Aufgrund der enormen Heterogenität von TNBC eignet sich dennoch kein einzelner Rezeptor als ultimatives Target für alle TNBC-Typen. Demzufolge wird in dieser Arbeit das Ziel gesetzt, geeignete und zielgerichtete Immuntherapien gegen die überwiegende Mehrheit der TNBC Tumoren zu entwickeln. Dabei wurden zwei Marker herausselektiert: EpCAM – überexprimiert in 60% der TNBC und CSPG4 – überexprimiert in 20-40% der TNBC. EpCAM und CSPG4 werden differenziell und nicht überlappend auf TNBC Tumoren exprimiert und eignen sich daher besonders gut für die direkte Immuntherapie.

Zu diesem Zweck wurden in dieser Arbeit neuartige zytolytischeh Fusionsproteine (hCFP) konstruiert. Diese bestehen aus einkettigen variablen Fragmenten (scFv) von Antikörpern gegen die ausgewählten TNBC Targets und einer zytotoxischen Domäne humanen Ursprungs. Die Aktivität und der Wirkungsmechanismus dieser hCFPs wurden mit den entsprechenden rekombinanten Immuntoxinen (ITs) mit der Pseudomonas Exotoxin A- Deletionsmutante (ETA‘) als toxische Einheit verglichen.

Für die EpCAM gerichtete Immuntherapie wurde ein auf Granzym B basiertes hCFP hergestellt, bezeichnet als GbR201K-αEpCAM(scFv). Dabei wurde ein EpCAM-selektives scFv genetisch an eine humanen Granzym B (GB) Mutante fusioniert, die minimale Empfindlichkeit gegenüber dem natürlichen Inhibitor von GB – Serpin B9 hat. Gegen CSPG4 wurde ein CFP generiert, das aus einem CSPG4-selektiven scFv besteht und als Fusionspartner eine funktionell verbesserte Form des humanen Mikrotubuli-assoziierten Protein tau (MAP) hat. Dieses Konstrukt wurde als αCSPG4(scFv)-MAP bezeichnet.

Die *in vitro* Studien in dieser Arbeit konnten erfolgreich die spezifische Bindung, Internalisierung und anschließend die starke zytotoxische Aktivität beider hCFPs bestätigen. Das Gb-R201K-αEpCAM(scFv) zeigte Zytotoxizität mit IC50-Werten im Bereich von 200-300 nM gegen die TNBC Zelllinien MDA-MB-453 und MDA-MB-468 gezeigt. Vergleichbare IC50-Werte (200-400 nM) gegen MDA-MB-231 und Hs 578T TNBC Zellen wurden mit dem αCSPG4(scFv)-MAP Konstrukt gemessen. Die präklinische Effizienz beider CFPs wurde in subkutanen Maustumormodellen gezeigt. Die Behandlung mit Gb-R201K-αEpCAM(scFv) von Mäusen mit MDA-MB-468-Tumoren hemmte das Tumorwachstum bis zu 50%. Eine stärkere Hemmung des Tumorwachstums und sogar zur Tumorrückbildung von mehr als 50% kam es bei der Behandlung von Mäusen mit MDA-MB-231-Tumoren.

Zum Schluss lässt sich zusammenfassen, dass die hier generierten αCSPG4(scFv)-MAP und GB-R201K-αEpCAM(scFv) CFPs sich gut als klinisch relevante und vielversprechende neue zielgerichtete Mittel für die Bekämpfung von TNBC eignen.

# Table of Contents

*ABSTRACT* ..... *I*

*ZUSAMMENFASSUNG* ..... *II*

*Table of Contents* ..... *III*

**I INTRODUCTION ..... 1**

I.1 BREAST CANCER ..... 1

*I.1.1 Intrinsic (molecular) breast cancer subtypes ..... 2*

*I.1.2 Triple negative breast cancer ..... 3*

I.2 TARGETED THERAPY OF BREAST CANCER ..... 5

I.3 POTENTIAL NEW TARGETS FOR TRIPLE NEGATIVE BREAST CANCER ..... 6

*I.3.1 The Epithelial cell adhesion molecule -EpCAM ..... 7*

*I.3.2 Melanoma chondroitin sulfate proteoglycan- CSPG4 ..... 8*

I.4 SELECTIVE TUMOR TARGETING USING IMMUNOTOXINS ..... 9

*I.4.1 ETA' immunotoxins ..... 10*

*I.4.2 Immunotoxins in the clinic ..... 11*

I.5 HUMAN CYTOLYTIC PROTEINS AS AN ALTERNATIVE TO BACTERIAL TOXINS ..... 12

*I.5.1 Granzyme B as a cytotoxic effector protein ..... 13*

*I.5.2 MAP tau as a new cytotoxic effector protein ..... 14*

I.6 SNAP TAG ..... 15

I.7 AIMS AND OBJECTIVES ..... 15

**II MATERIALS AND METHODS ..... 19**

II.1 MATERIALS ..... 19

*II.1.1 Chemicals and consumables ..... 19*

*II.1.2 Bacterial strains ..... 19*

*II.1.3 Mammalian cells – cell lines ..... 19*

*II.1.4 Buffers, media and solutions ..... 20*

*II.1.5 Chromatography resins and membranes ..... 22*

*II.1.6 Enzymes ..... 22*

*II.1.7 Kits ..... 22*

*II.1.8 Protein standards ..... 22*

*II.1.9 Nucleic acid standards ..... 23*

*II.1.10 Synthetic oligonucleotides ..... 23*

*II.1.11 Vectors ..... 23*

*II.1.12 Antibodies ..... 24*

*II.1.13 Equipment and software ..... 25*

II.2 METHODS ..... 27

*II.2.1 Molecular cloning ..... 27*

II.2.1.1 E. coli culturing and preservation ..... 27
II.2.1.2 Preparation of chemically competent E. coli ..... 27
II.2.1.3 Heat shock transformation of E. coli ..... 27
II.2.1.4 Periplasmic protein expression under osmotic stress ..... 27
II.2.1.5 Cell culture – mammary carcinoma cell lines ..... 28
II.2.1.6 Transfection of mammalian cells with recombinant DNA ..... 28
II.2.1.7 Expression of fusion proteins in HEK293T cells ..... 28
II.2.1.8 Isolation of plasmid DNA ..... 29
II.2.1.9 Agarose gel electrophoresis ..... 29
II.2.1.10 Determining DNA concentration ..... 29
II.2.1.11 Restriction enzymes digestion of DNA ..... 29
II.2.1.12 Ligations ..... 29
II.2.1.13 DNA sequencing and analysis ..... 30
*II.2.2 Protein preparation ..... 30*
II.2.2.1 Immobilized metal ion affinity chromatography (IMAC) ..... 30
II.2.2.2 Streptactin purification ..... 30
II.2.2.3 Size exclusion chromatography (SEC) ..... 30
II.2.2.4 Enterokinase digest ..... 31
*II.2.3 Proteins labeling ..... 31*
II.2.3.1 Labeling of SNAP tag fusion proteins ..... 31
II.2.3.2 Labeling of CFPs for live imaging ..... 31
*II.2.4 Protein analysis ..... 32*
II.2.4.1 Quantification of purified proteins ..... 32
II.2.4.2 Sodium dodecylsulfate polyacrylamide gel electrophoresis (SDS-PAGE) ..... 32
II.2.4.3 Protein Immuno-blotting ..... 32
II.2.4.4 Proteolytic activity of GB-R201K-αEpCAM(scFv) ..... 32
*II.2.5 Immunoassays ..... 33*
II.2.5.1 Flow cytometry ..... 33
II.2.5.2 Internalization analysis by confocal microscopy ..... 34
II.2.5.3 Internalization analysis by high-throughput confocal microscopy ..... 34
II.2.5.4 Immunofluorescence microscopy of mouse tissue sections ..... 34
II.2.5.5 Immunohistochemistry ..... 35
II.2.5.6 Detection of Serpin B9 (PI-9) expression in TNBC cell lines ..... 35
II.2.5.7 Co-Immunoprecipitation assay ..... 35
*II.2.6 Cytotoxic effect of CFPs on TNBC cell lines ..... 36*
II.2.6.1 Cell viability assay ..... 36
II.2.6.2 Apoptosis assay ..... 36
II.2.6.3 Caspase 3 and parp-1 cleavage assay ..... 36
II.2.6.4 Caspase-9 substrate assay ..... 37
II.2.6.5 Endonuclease G translocation assay ..... 37
II.2.6.6 Tubulin polymerization assay ..... 37
II.2.6.7 Cell cycle analysis ..... 38

*II.2.7 In vivo tumor xenograft models ..... 38*
II.2.7.1 Dose escalation studies and maximum tolerated dose determination ..... 38
II.2.7.2 Induction of subcutaneous tumors in BALB/c Nude mice ..... 38
II.2.7.3 In vivo efficacy of anti EpCAM CFPs ..... 39
II.2.7.4 In vivo efficacy of anti-CSPG4 CFPs ..... 39
II.2.7.5 Biodistribution assay ..... 39
II.2.7.6 Determination of tumor size by caliper measurements ..... 40
*II.2.8 Statistical analysis ..... 40*

**III RESULTS ..... 41**

III.1 scFv based Cytolytic fusion proteins targeting EpCAM ..... 41
*III.1.1 Generation and characterization of scFv based fusion proteins ..... 41*
III.1.1.1 Cloning and design of anti-EpCAM scFv fusion proteins ..... 41
III.1.1.2 Granzyme B activation and serpin B9 detection ..... 44
III.1.1.3 EpCAM expression on TNBC cell lines ..... 46
III.1.1.4 Binding analysis of αEpCAM fusion proteins on TNBC cell lines ..... 46
*III.1.2 Functional assays with αEpCAM fusion proteins ..... 49*
III.1.2.1 Internalization and cellular uptake kinetics of αEpCAM fusion proteins ..... 49
III.1.2.2 Cytotoxic effects of αEpCAM CFPs in TNBC cells in vitro ..... 51
III.1.2.3 Induction of apoptosis by αEpCAM fusion proteins in TNBC cell lines ..... 52
III.1.2.4 Activation of cellular apoptotic pathways by αEpCAM CFPs ..... 53
*III.1.3 in vivo evaluation of αEpCAM CFPs ..... 55*
III.1.3.1 Establishment of subcutaneous tumors in BALB/C Nude mice ..... 55
III.1.3.2 Tumor targeting and biodistribution studies in vivo ..... 56
III.1.3.3 In vivo toxicity and therapeutic activity of CFPs ..... 60
III.2 scFv based- CSPG4 targeting CFPs ..... 64
*III.2.1 Generation and characterization of scFv based fusion proteins ..... 64*
III.2.1.1 CSPG4 expression on TNBC cell lines ..... 64
III.2.1.2 Cloning and design of anti-CSPG4(scFv) CFPs ..... 65
III.2.1.3 Expression and purification of αCSPG4(scFv) CFPs ..... 67
III.2.1.4 Binding analysis of fusion proteins ..... 69
*III.2.2 Functional assays with αCSPG4 fusion proteins ..... 69*
III.2.2.1 αCSPG4(scFv) fusion proteins internalization and cellular uptake ..... 69
III.2.2.2 αCSPG4(scFv)-MAP Interaction with tubulin ..... 71
III.2.2.3 Cytotoxic effect of αCSPG4(scFv)-MAP on TNBC-derived cell lines ..... 73
III.2.2.4 Induction of apoptosis by αCSPG4(scFv) CFPs in MDA-MB-231 cell line ..... 74
III.2.2.5 Activation of mitochondrial stress apoptotic pathways by αCSPG4(scFv) fusion proteins ..... 76
III.2.2.6 Induction of cell cycle arrest by αCSPG4(scFv)-MAP ..... 77
*III.2.3 In vivo evaluation of αCSPG4 CFPs ..... 78*
III.2.3.1 Establishment of subcutaneous tumors in BALB/c Nude mice ..... 78
III.2.3.2 In vivo toxicity and therapeutic efficacy ..... 79
III.2.3.3 Tumor targeting and biodistribution studies in vivo ..... 81

**IV DISCUSSION ..... 84**

IV.1 TRIPLE NEGATIVE BREAST CANCER (TNBC) CURRENT THERAPY ..... 84

IV.2 TARGETING TNBC USING CSPG4 ..... 86

IV.3 TARGETING TNBC USING EPCAM ..... 87

IV.4 CANCER IMMUNOTHERAPYAS AN ALTERNATIVE TO TRADITIONAL CHEMOTHERAPY ..... 88

IV.5 SENSITIVITY OF TNBC CELL LINES TOWARDS ETA' IMMUNOTOXINS ..... 90

IV.6 HUMAN CYTOLYTIC FUSION PROTEINS AS AN ALTERNATIVE TO ITS ..... 92

IV.7 MECHANISM OF ACTION OF ACSPG4(SCFV)-MAP ..... 94

IV.8 MECHANISM OF ACTION OF GBR201K-AEPCAM(SCFV) ..... 96

IV.9 OUTLOOK AND POTENTIAL SCOPE OF ANTI-EPCAM AND ANTI-CSPG4 HCFPS ..... 98

**V REFERENCES ..... - 102 -**

**VI APPENDIX ..... - 118 -**

VI.1 INDEX OF FIGURES AND TABLES ..... - 118 -

*VI.1.1 Figures ..... - 118 -*

*VI.1.2 Tables ..... - 120 -*

VI.2 ABBREVIATIONS ..... - 120 -

VI.3 PLASMID SEQUENCES ..... - 122 -

*VI.3.1 PMT-anti-EpCAM(scFv)-ETA ..... - 122 -*

*VI.3.2 PMT-anti-CSPG4(scFv)-ETA ..... - 125 -*

*VI.3.3 PMS-L-EGB-anti-EPCAM(scFv)-IV_R201K ..... - 128 -*

*VI.3.4 pET-STREP-anti-CSPG4(ScFv)-ETA-KDEL ..... - 131 -*

*VI.3.5 PET-STREP-ANTI-CSPG4-MAP ..... - 134 -*

*VI.3.6 PMS-ANTI-EPCAM_SNAP_IV ..... - 137 -*

*VI.3.7 PMS-ANTI-CSPG4-SNAP_IV ..... - 140 -*

VI.4 PLASMID MAPS ..... - 144 -

*VI.4.1 pMT-anti-EpCAM-ETA ..... - 144 -*

*VI.4.2 pMT-anti-CSPG4-ETA ..... - 145 -*

*VI.4.3 pMS-L-EGB-anti-EpCAM-IV ..... - 145 -*

*VI.4.4 pET-strep-anti-CSPG4-ETA-KDEL ..... - 146 -*

*VI.4.5 pET-strep-anti-CSPG4-MAP ..... - 146 -*

*VI.4.6 pMS-anti-EpCAM-SNAP-IV ..... - 147 -*

*VI.4.7 pMS-anti-CSPG4-SNAP-IV ..... - 148 -*

**VII THESIS RELATED SCIENTIFIC PUBLICATIONS ..... - 149 -**

**VIII ACKNOWLEDGEMENTS ..... - 150 -**

# I Introduction

## *I.1 Breast cancer*

Breast cancer is a heterogeneous complex of tumors that originate from breast tissue, most commonly ductal carcinomas originating from the inner lining of milk ducts or lobular carcinomas originating from the lobules that supply the ducts with milk (1, 2). Prognosis and survival rates vary greatly depending on tumor type (3, 4). Many aspects are considered for the classification of breast cancer. Some rely on clinical aspects such as tumor staging or the TNM classification (5) which stands for: (T) the size of the tumor, (N) whether the tumor has spread to the lymph nodes (M) whether the tumor has metastasized. Other aspects include histopathological classification and tumor grade (6, 7). Newer approaches classify tumors using molecular and genetic profiling (6, 8-12). These methods utilize high-throughput methods to differentiate between tumors according to the expression levels or the lack of expression of different cellular molecules and pathways as well as gene abnormalities and mutations. These studies led to the identification of distinct molecular intrinsic subtypes (9, 11, 13). These subtypes greatly overlap -but not completely with the expression status of the following three receptors:

1. **Estrogen receptor (ER):** refers to the Estrogen receptor alpha, a 66kDa intracellular receptor, and is a member of the hormone receptors family(14).

ER has an important biological role in the development of the mammary gland and during pregnancy (15, 16). ER is expressed on 60-70% of all breast tumors (17, 18), and its role in breast cancer progression is complex and involves several mechanisms (17-20) - the major three being: 1) ER activation promotes cell proliferation and over-activation can lead to tumorigenesis. 2) Estrogen metabolism in mammary epithelial cells produces genotoxic byproducts 3) ER signaling in breast cancer promotes metastasis.

**2. Progesterone receptor (PR):** like ER, this is another intracellular hormone receptor. It remains inactive until the binding of progesterone, which leads to dimerization and activation of the DNA binding domain in the receptor. Activated PR binds to its target genes and promotes their transcription into mRNA (21).

In breast cancer, the role of PR is not well understood, and it is usually co-expressed with ER (22, 23), $PR^+$ $ER^-$ tumors are very rare, and account only for 3%-5%. Among $ER^+$

tumors, PR expression can indicate a favorable outcome (24, 25), less aggressive tumors and less tumor resistance to Tamoxifen therapy (26).

3. **Human epidermal growth factor receptor 2 (HER2):** HER2 is a transmembrane tyrosine kinase receptor (27). HER2 is over expressed in 20-30% of breast cancers (28-30), and its expression is associated with higher grade and disease recurrence. It is also overexpressed in other types of cancers, including ovarian, stomach, and aggressive forms of uterine cancer (31). In addition to overexpression, in some cancers, point mutations in HER2 genes lead to constant dimerization and activation of the receptor without the binding of its ligand (32).

### *I.1.1 Intrinsic (molecular) breast cancer subtypes*

As mentioned above I.1, the receptor status correlates to some degree, with the intrinsic subtypes that have been identified through gene expression and genetic profiling methods (9, 13). These subtypes have been classified according to intrinsic gene sets that are uniquely over expressed or downregulated in certain subsets (3, 11, 13, 33, 34). Gene amplifications, deletions and mutations were also considered as classification criteria of the different subtypes (35, 36). Several studies have identified and characterized breast cancer subtypes with slight differences but with many similarities between them, depending on the gene sets selected and the samples available(35-39). However, one study (4), has combined the data from many different studies, and came up with the following classification, which has been adopted in most of the subsequent published studies:

- Luminal like subtype: Mostly ER and/or PR positive (19, 24). These tumors express typical proteins and cytokeratin (CK) of luminal epithelial cells, in addition to the ER and PR hormones (4). The luminal subtype is further sub-classified into two subtypes: Luminal-A and Luminal-B.
- HER2 subtype: This subtype describes most tumors which are HER2 positive with no or very little expression of ER and PR. It is characterized by the downregulation of luminal markers and genes and with the overexpression of HER2 along with other genes associated with its proliferation pathway. This group of tumors is somewhat heterogeneous and some studies suggest they should be further sub-classified based on aggressiveness and their interaction with the immune system (40, 41).

- Basal-like subtype: This subtype contains the most aggressive, highly proliferative and metastasizing tumors (9). They are poorly differentiated with high histological grade and genomic instability. Most of these tumors (70%-80%) lack the expression of ER, PR and HER2 receptors (hence- triple negative) (9, 42). The expression of basal myoepithelial markers (CK5, 14 and 17) and Over-expression of proliferation genes are common features of these tumors (43, 44). TP53 (tumor protein 53) is also highly mutated in this subtype (45) and epidermal growth factor receptor (EGFR), vascular endothelial growth factor receptors (VEGFR) and P-cadherin are abundantly expressed (46). Genetically predisposed individuals with BRCA-1 mutations- tend to develop basal-like triple negative breast cancer (47).

These intrinsic subtypes are available in the research setting, where high throughput screening methods can be applied. However, in the clinical setting, this type of screening is unavailable, and the molecular phenotype- hence the receptor status, serves as a surrogate for the intrinsic subtype.

### *I.1.2 Triple negative breast cancer*

Triple negative breast cancer is the phenotype describing breast tumors which do not express the estrogen receptor ($ER^-$), the progesterone receptor ($PR^-$) and the human epidermal growth factor receptor-2 ($HER2^-$)(48, 49).

TNBCs account for approximately 15-30% of all breast tumors. Their frequency differs among different demographic groups according to different studies (2, 3, 8, 50). They are among the most aggressive and invasive breast tumors and are associated with advanced disease, high risk of recurrence within 3 years (2, 8), aggressive brain and lung metastases (29) and are more prevalent among young premenopausal women (3) as well as African American and Hispanic women in the USA (50).

There is about 80% overlap between TNBC and basal like tumors (9, 42). But they remain a heterogeneous group, with varying degrees of aggressiveness and sensitivities to chemotherapies. Further molecular and genetic profiling using high throughput methods categorized TNBC tumors into several subtypes.

Three such comprehensive studies identified 3 to 6 subtypes of TNBCs (11, 12, 34) with some differences between them but a lot of common characteristics. For the purposes of this work, the highlights of Lehman et al. (34) classification will be summarized. They have analyzed gene expression profiles from 21 breast cancer data sets and identified 587

TNBC cases. These tumors were then analyzed for their gene expression signature of unique gene ontologies and sub-classified into 6 subtypes:

- According to their classification the majority of tumors (51%) belonged to Basal like subtypes and were further classified into BL1 and BL2 and IM:

  Basal like 1 and 2 (BL1 & BL2) are characterized by overexpression of genes involved in cell cycle, DNA replication reactome, $G_2$ cell-cycle pathway, RNA polymerase, and $G_1$ to S cell cycle transition. BL1 tumors are enriched in DNA damage response (ATR/BRCA) pathways and increased Ki-67 expression. Some of the cell lines representing these subtypes are MDA-MB-468 and HCC2157. BL2 tumors are characterized in addition with enrichment of growth factor signaling such as EGF pathway, NGF pathway, MET pathway. Cell lines classified to this subtype are SUM149PT and cal-851.

  The IM (immune-modulatory) subtype displays enrichments in genes involved in the interaction, signaling and response to immune cells such as immune cell TH1/TH2 pathway, NK cell pathway, B cell receptor [BCR] signaling pathway, DC pathway, cytokine signaling pathway, IL-12 pathway and IL-7 pathway.

- Mesenchymal like tumors comprise 25% of TNBC tumors and were further classified into: M and MSL: The Mesenchymal like subtype M is heavily enriched in components and pathways involved in cell motility (regulation of actin by Rho), ECM receptor interaction, and cell differentiation pathways (Wnt pathway, anaplastic lymphoma kinase [ALK] pathway, and TGF signaling). The Mesenchymal stem like subtype (MSL) differs from the M subtype in the enrichment of genes and processes linked to growth factor signaling pathways that include Inositol phosphate metabolism, EGFR, PDGF, calcium signaling, G-protein coupled receptor, and ERK1/2 signaling as well as ABC transporter and adipocytokine signaling. Another unique feature of MSL type is the expression of genes associated with stem cells, numerous HOX genes, and mesenchymal stem cell–specific markers.

  Cell lines displaying similar characteristics to the MSL subtype are MDA-MB-231 and HS578T.

- Luminal like AR tumors (LAR): Approximately 12% of TNBC tumors were assigned to this subtype. LAR subtype is ER negative, but gene ontologies are heavily enriched in hormone regulated pathways including steroid synthesis,

porphyrin metabolism, and androgen receptor (AR) pathway. MDA-MB-453 and SUM185PE cell lines belong to this subtype.

The remaining tumors (13%) did not match any of the previous subtypes and could not be classified into any stable subtype.

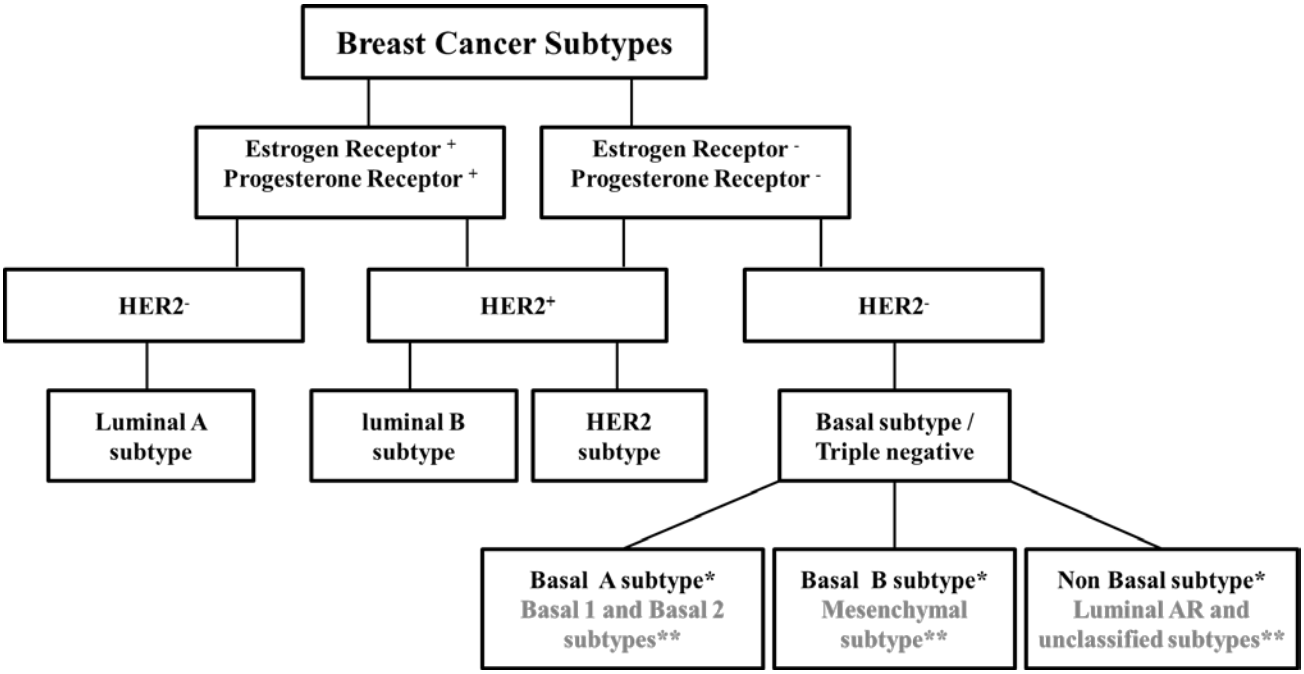



**Illustration 1. Breast cancer subtypes: receptor status and intrinsic subtypes**
* Classification according to Kao et al. (11)
** Classification according to Lehman et al. (34)

## *I.2 Targeted therapy of breast cancer*

Targeted therapy for breast cancer has proven to be a successful strategy (51). $HER2^+$ breast cancer patient receiving anti-HER2 antibodies in the adjuvant or neo-adjuvant setting have longer disease free survival and better prognosis (52). Trastuzumab is a monoclonal anti-HER2 antibody in widespread use. Treatment with Trastuzumab in the neo-adjuvant setting increased significantly the rate of pathologic complete response (pCR) in patients with HER2-positive breast cancer (53, 54). A 12-month course of Trastuzumab in addition to adjuvant chemotherapy significantly improves the disease-free survival (DFS) the overall survival (OS) (55). Lapatinib is a tyrosine kinase inhibitor which interrupts the signaling pathways of HER2/neu and epidermal growth factor receptor (EGFR) (53). Dual targeting approach with a combination of Trastuzumab and Lapatinib

improved progression-free survival (PFS) compared with Lapatinib alone in patients with metastatic breast cancer who did not respond to trastuzumab (53, 56).

Another successful approach is endocrine therapy. This type of therapy is given to $ER^+$ patients for both prevention and treatment of breast cancer. These classes of drugs target and block the estrogen pathway. The most well established and proven therapy in this aspect uses selective ER modulators such as Tamoxifen to disrupt the estrogen receptor activity (24, 57). Tamoxifen is regularly given to patients in the adjuvant setting for 5 years or more and it significantly decreases the risk of recurrence and increases overall survival (58, 59). Another approach targets aromatase enzyme using second generation aromatase inhibitors (AIs) such as formestane and exemestane. Aromatase is the enzyme involved in the last step of estrogen biosynthesis that converts testosterones to estrogens via aromatization process, which is the main pathway of estrogen synthesis in the breast of postmenopausal and non-pregnant women (57). AIs are commonly used as a first line treatment for postmenopausal women with metastatic hormone receptor-positive breast cancer. They are also beneficial in the adjuvant setting when given instead of Tamoxifen or in combination with Tamoxifen treatment (60). Although Tamoxifen has been in clinical use longer than second generation AIs, recent studies demonstrated superiority of AIs compared to Tamoxifen (59).

Patients with breast tumors lacking the expression of HER2 receptor and the Estrogen and Progesterone receptors do not benefit from these therapies (58).

### *I.3 Potential new targets for Triple negative breast cancer*

As TNBC tumors are very heterogeneous it is unlikely that a single therapeutic agent will be efficient to target them all. However, gene expression studies have identified several potential upregulated pathways which are differentially expressed in the different subtypes and therefore receptors in these pathways are being considered as potential targets.

Emerging targets currently being investigated for the treatment of TNBC are receptors and molecules involved in cell survival, proliferation and tumor angiogenesis (61). Several classes of drugs (62) specifically targeting cell surface receptors such as EGFR (46) and VEGFR are currently in clinical trials (61, 63, 64).

In addition to targeted immunotherapy, additional drugs targeting pathways that are over-expressed or damaged in TNBC are being studied in preclinical and clinical trials.

Some examples are PARP inhibitors (65), mTOR inhibitors (66) and Src tyrosine kinase inhibitors (67).

**Table 1. A list of targeted therapies in active clinical trials in the USA for the treatment of triple negative breast cancer in 2017 (61, 65-74):**

| Target | Drug | Phase | Patient population |
|---|---|---|---|
| VEGFR (69, 73) | Bevacizumab | Phase III | TNBC (adjuvant) |
| | Ramucirumab | Phase III | HER2-negative BC |
| | Sunitinib | Phase II | TNBC (neoadjuvant) |
| | Sorafenib | Phase II | TNBC (neoadjuvant) |
| | Apatinib | Phase II | mTNBC |
| | Cediranib | Phase II | Recurrent TNBC |
| EGFR (64, 70, 72, 74) | Cetuximab | Phase II | TNBC (neoadjuvant) |
| | Afatinib | Phase II | mTNBC |
| | Dasatinib | Phase II | mTNBC |
| | Erlotinib | Phase II | TNBC (neoadjuvant) |
| | Neratinib | Phase II | mTNBC |
| | Lapatinib | Phase II | Advanced/mTNBC |
| PARP (65) | Olaparib | Phase II | TNBC *BRCA*-mutated |
| | Talazoparib | Phase III | TNBC *BRCA*-mutated |
| Mutityrosine kinase | Dasatinib | Phase II | mTNBC |
| Immunotherapy – PD-1 PDL-1 blockade | Pembrolizumab | Phase II<br>Phase III | mTNBC (monotherapy)<br>mTNBC (single agent) |
| | Nivolumab | Phase II | TNBC (four-arms) |
| | Atezolizumab | Phase II<br>Phase III | TNBC (monotherapy)<br>TNBC (neoadjuvant) |
| mTOR (66) | Temsirolimus | Phase II | mTNBC |
| | Everolimus | Phase II<br>Phase III | mTNBC<br>mTNBC |

Abbreviations: Anth, anthracycline; CBp, carboplatin; Cp, cisplatin; EGFR, epidermal growth factor receptor; Gem, gemcitabine; mTNBC, metastatic triple-negative breast cancer; mTOR, mammalian target of rapamycin; P, paclitaxel; PARP, poly(adenosine diphosphate-ribose) polymerase; T, docetaxel; Tax, taxanes; TNBC, triple-negative breast cancer; VEGFR, vascular endothelial growth factor receptor.

### *I.3.1 The Epithelial cell adhesion molecule -EpCAM*

The epithelial cell adhesion molecule (EpCAM) is a 30-40 kDa $Ca^{2+}$-independent type 1 membrane glycoprotein which mediates cell-cell interactions such as cell aggregation and segregation (75). The intracellular domain of EpCAM plays a biological

role in cell proliferation and differentiation processes (76). It is expressed on human embryonic stem cells (hESC) and its expression is associated with the maintenance of the undifferentiated state of hESC (77).

EpCAM is expressed in low levels in healthy epithelia, but is overexpressed in many types of carcinomas. Its abundance on carcinomas established it as one of the most known and researched tumor-associated antigens (78). Moreover, EpCAM expression on many solid tumors is associated with poorer prognosis, more aggressive tumors and decreased overall survival of patients (79, 80). Extensive research in the past decade focusing on small subpopulations of tumor cells capable of initiating tumorigenesis and metastasis such as tumor initiating cells (TICs) and cancer stem cells (CSCs), identified EpCAM to be a marker of and actively involved in the tumorigenic activity of these cell subsets (76, 81, 82).

In the case of breast cancer, different studies detected EpCAM overexpression in 40-70% of breast tumors (83) and in general EpCAM overexpression strongly correlated with poor overall survival and higher risk of recurrence following conventional therapy. This was true for all breast cancer subtypes but it is particularly notable in the case of triple negative breast cancer (TNBC) (84).

Several monoclonal antibodies targeting EpCAM were and are being tested in clinical trials. Albeit its promising potential, so far, only one trifunctional antibody (Catumaxomab/Removab®, Fresenius Biotech) for the intraperitoneal treatment of malignant ascites in patients with EpCAM-positive carcinomas was approved (85).

### *I.3.2 Melanoma chondroitin sulfate proteoglycan- CSPG4*

Chondroitin sulfate proteoglycan 4 (CSPG4), also known as melanoma chondroitin sulfate proteoglycan (MCSP) is a membrane-bound proteoglycan consisting of an *N*-linked 280 kDa glycoprotein, a 450 kDa chondroitin sulfate proteoglycan and was initially characterized on the surface of melanoma cells (86, 87). Studies in the past years have identified CSPG4 as a potential marker of triple-negative breast cancer (88, 89). It has been is expressed on the surface of malignant cells and tumor-initiating cells in various types of tumors (90).

Wang *et al*. (88, 91) first reported that CSPG4 is differentially expressed in breast cancer tumors with significantly higher frequency in basal-like cancer. Medium to high levels of CSPG4 were expressed in 50% of basal-like TNBC tissue samples (91). They

also described four independent TNBC cell lines expressing CSPG4, namely MDA-MB-435, MDA-MB-231, Hs 578T and SUM149 (88, 91). According to molecular and genetic profiling studies of TNBC cell lines, these cell lines belong to a TNBC molecular subtype referred to as 'basal B subtype' (11) or 'mesenchymal subtype' (34). In both classifications, these subtypes are characterized by an increased gene expression in motility pathways and stem cell-like processes and are characterized as highly aggressive tumors.

## *I.4 Selective tumor targeting using immunotoxins*

The term immunotoxins (ITs) refers to a novel class of targeted therapy that gained popularity in the past three decades (92). They consist of an antibody based binding domain genetically fused to a cytotoxic domain (93). They combine the specificity of antibodies to selectively target cell subsets and the cell cytotoxicity of extremely toxic bacterial and plant toxins (94).

The binding domain is usually some form of antibody fragment. It can range from the full length antibody (95, 96) to a single chain antibody fragment (scFv) (97-99). Fab fragment (100), dia-bodies (101) and other forms of antibody fragments (102) have also been used. In some studies the binding domain used was not an antibody but a ligand of the target receptor such as EGF (92).

The toxic moiety can be any protein or peptide which can kill the target cells. First generation toxins were designed in the 1980s and 1990s and consist of bacterial and plant toxins such as Pseudomonas Exotoxin A (ETA') (103), Diphtheria toxin (DT) (104, 105) and ricin toxin (RT) (106). The native binding moiety of the toxins is usually deleted and the toxin is recombinantly fused to the antibody fragment (107-110). A short peptide linker is usually used to connect the two moieties (110, 111). The linker can be a random peptide or a specifically designed adapter. The adapter peptide is intended to increase the efficiency of the translocation of the internalized immunotoxin from the endosome into the cytosol. Such adapter can originate from naturally occurring peptides, such as the translocation domain sequence found in ETA', DT and RT (112-114). Other adapters are designed to contain a cleavable peptide (115, 116), pH sensitive peptide (111), or a membrane transfer peptide (117).

Bacterial and plant ITs are very toxic to cells, but they are also very immunogenic and cause severe side effects (118-120). In an attempt to reduce these side effects, and generate a more systemically "tolerable" and yet selectively toxic compounds, second and third

generation immunotoxins were designed (121-123). These "humanized" toxins include human pro apoptotic proteins such as proteases (e.g. Granzyme B) (124) and RNases (e.g. angiogenin) (125, 126) as the effector domain.

### *I.4.1 ETA' immunotoxins*

Pseudomonas Exotoxin A (ETA') is a toxin secreted by gram negative aerobic *Pseudomonas aeruginosa* pathogen. It consists of 3 domains: the binding domain (I), consisting of Ia and Ib, the translocation domain (II) and the catalytic domain (III) (127, 128).

The natural binding domain of Pseudomonas Exotoxin A binds to the low density lipoprotein receptor-related protein (LRP)1 or the closely related LRP1B leading to the internalization of the toxin (129).

The translocation domain II is thought to be involved in toxin translocation and intracellular trafficking (130); it contains a furin cleavage site (115) and a disulfide bond that enables conformational changes in the lower pH of the endosome (113).

The catalytic domain III is an adenosine diphosphate (ADP)-ribosyltransferase A, which catalyzes the inactivation of the elongation factor eEF2 (131). The mechanism of action involves the transfer an ADP-ribosyl group from $NAD^+$ to diphthamide residue (a highly conserved histidine residue in eEF2 with a post-translation modification), rendering the eEF2 irreversibly inactive and halting protein synthesis in the cell (132).

The ETA' sequence ends with a C-terminal endoplasmic reticulum (ER)-retention signal REDL which is required for its toxicity and is involved in the translocation of the toxin from the endosome into the cytosol (133, 134).

In order to prevent unspecific binding and allow selective targeting, deletion mutants of the Pseudomonas Exotoxin A were generated. In these mutants the native binding domain I is deleted. Several deletion mutants were developed for these purposes. The most commonly used mutants are ETA'- a 40 kDa sequence and PE38- a 38 kDa sequence (110). ETA' mutant encodes a truncated version coding for amino acids 252 to 613 of the wild-type toxin in which only the binding domain Ia was deleted (97). PE38 however, includes an additional partial deletion of binding domain Ib (Δ1–250 and Δ365–380) (135). To improve the endosomal escape, additional versions were generated in which the C-terminal REDL was exchanged with the native ER retention signal KDEL sequence (136).

In our group, my colleagues and myself have used the ETA' sequence (PE40) as a golden standard (97, 137). In special cases when the ETA' immunotoxins were not successful, other versions such as the ETA'-KDEL or the PE38KDEL were used. In this thesis, ETA' and ETA'-KDEL sequences were used.

To generate immunotoxin with selective targeting, these truncated versions were genetically fused to scFv as binding moiety.

### *I.4.2 Immunotoxins in the clinic*

Historically, immunotoxins emerged as potential therapeutics in the 80s and 90s, but these first generation immunotoxins showed severe side effects in the clinic, such as vascular leak syndrome (VLS) and had very limited therapeutic window due to their immunogenicity and the rapid development of neutralizing antibodies after one or two injections. Therefore, many initial trials failed to show therapeutic benefit and different strategies to administer these immunotoxins had to be developed, such as prior treatment with Pentostatin plus cyclophosphamide to reduce the development of neutralizing antibodies (93, 120, 138, 139).

Recent reviews by Dosio et al. 2014 (138) and Alewine et al. 2015 (139) named several immunotoxins that are currently undergoing active clinical trials in the US, and had already passed phase I successfully (Table 2). The most promising results are for those ITs targeting hematological malignancies. One of the first clinically approved immunotoxins is denileukin diftitox (140), which was approved in 2001 for treatment of cutaneous T-cell lymphoma (CTCL). This is a fusion protein of IL-2 and DT. Although it showed a good response rate, it is rarely used due to poor tolerability and severe side effects including flu-like symptom, infusion-related events, disruption of color vision, VLS with hypotension, and frequent grade 3–4 hypoalbuminemia (141).

SS1P is the one of the few immunotoxins currently in clinical trials for treatment of solid tumors. This is a PE38 based IT genetically fused to antibody targeting mesothelin (MSLN) (142). MSLN is expressed on many solid tumors and this IT is currently in a phase II trial with Mesothelioma patients in combination with chemotherapy (143).

Several anti-EpCAM immunotoxin are being tested in preclinical and clinical settings. MOC31PE and Vicinium are such immunotoxins. Vicinium, a scFv-PE38 IT is currently in phase III clinical trials for bladder cancer (144). Overall 44% of patients achieved a complete response with a median time to recurrence of 408 days. 16% of patients remained

disease free for the entire trial follows up period (18-25 months). At the time of writing this work, no protein based immunotoxins for the treatment triple negative breast cancer were being tested in clinical trials in the USA (144). Several such immunotoxins had been tested in Phase I in the past decades; however none of them succeeded in proceeding to phase II. Examples of such immunotoxins are scFv(FRP5)-PE38 (145) targeting HER2, and 260F9-rRTA (146) and multiple EGF and EGFR targeting immunotoxins (63, 70-72), recently, a new successful phase I trial was reported for EpCAM(scFv) immunotoxin MOC31PE (147).

**Table 2. Protein based immunotoxins that successfully passed phase I and are currently in active clinical trials in the USA:**

| Name | Target receptor | toxin | Population | Phase trial | Clinical trial reference |
|---|---|---|---|---|---|
| Denileukin diftitox | IL-2R | DT | Cutaneous T-cell lymphoma | Approved | (141) |
| Moxetumomab Pasudotox | CD22 | PE | Hairy cell leukemia | III | NCT01829711 |
| Resimmune A-dmDT390-bisFv(UCHT1) | CD3 | DT | Melanoma, in combination with Pembrolizumab | II | NCT02990416 |
| LMB-2 | CD25 | PE | Hairy cell leukemia<br>Adult T-cell leukemia | II<br>II | NCT00321555<br>NCT00924170 |
| SS1P | MSLN | PE | cyclophosphamide<br>Mesothelioma | II | NCT01362790 |
| Vicinium | EpCAM | PE | Carcinoma in situ of the bladder. | III | NCT00462488<br>NCT02449239 |
| LMB-100 | mesothelin | PE | Mesothelioma | II | NCT02810418 |
| Glembatumumab Vedotin | glycoprotein NMB | MMAE | Melanoma<br>ER negative breast cancer | I | NCT00038051 |

## *I.5 Human cytolytic proteins as an alternative to bacterial toxins*

Due to the severe side effects and immunogenicity of traditional ITs, novel approaches utilizing fully human cytolytic proteins (CFPs) were developed. These CFPS are comprised of a fully human targeting unit fused to a human pro-apoptotic protein and are

considered inherently safe. Several such proteins have been identified and they are gaining popularity as an alternative approach to ITs (111, 121, 122, 124). Some of these proteins that have been successfully applied in preclinical studies are Granzyme B (123), RNases (e.g. angiogenin) (125), tumor necrosis factor-related apoptosis-inducing ligand (TRAIL) (148) and MAP tau (149, 150). One of the aims of this thesis was to have a side by side comparison of the antitumor activity of immunotoxins vs. CFPs.

In the course of this study, many CFPs were generated and evaluated consisting of anti-EpCAM (scFv) or anti-CSPG4 (scFv)- genetically fused to Granzyme B, angiogenin, DAPK, MAP and SNAP tag which was later coupled to the photosensitizer agent IR-700. For this thesis, only the best preforming CFPs were discussed.

### *I.5.1 Granzyme B as a cytotoxic effector protein*

Granzyme B is a serine protease naturally found in the granules of natural killer (NK) cells and cytotoxic T cells (151). The secretion of these cytotoxic granules is the primary defense mechanism of the immune system against cancerous cells and viral pathogens (152). Granzyme B belongs to a family of proteases involved in immune defence. Granzyme B is secreted along with perforin and other materials that facilitate its endocytosis into the cell cytosol through pore forming or other vesicle disrupting mechanism (151). Once released into the cytoplasm Granzyme B is a potent inducer of apoptosis. It can directly and indirectly cleave caspase 3 and BID, thus activating multiple apoptotic pathways (152). Granzyme B mediates apoptosis in a similar manner to the Fas pathway by activating the caspase dependent apoptotic pathways as well as mitochondrial apoptosis pathway (152).

The utilization of Granzyme B in cytolytic fusion protein has been demonstrated by several groups, and preclinical studies of Granzyme B CFPs have shown promising results in the treatment of AML (124), Melanoma (98), Breast cancer (153) and ovarian and prostate carcinomas (154). CFPs containing Granzyme B have been successfully expressed in both bacterial and mammalian expression systems (124, 155). However, to protect the expressing cells form Granzyme B toxicity, these CFPs are expressed in an inactive form as a zymogen with a pre peptide in the N’ terminus followed by an Enterokinase cleavage site. In order for Granzyme B to be fully active, the N’ terminus has to be free. Therefore further processing with an Enterokinase digest is required to activate Granzyme B CFPs.

Granzyme B activity can be irreversibly inhibited by its natural inhibitor serpin B9 (PI-9). The mechanism of inhibition involves a stoichiometric interaction which leads to the inactivation of both Granzyme B and PI-9. Many tumors have been described to express PI-9, such as lung cancer (156) melanoma and breast cancer (157, 158) and leukemia (159).

PI-9 is a 42kDa protein belonging to the clade B serpin superfamily (160). It is expressed and accumulated in cytosol of immune system cells to regulate the protease activity of Granzyme, thus preventing self-inflicted injury to those cells (161). It is also found in many cells at immune-privileged sites that need to be protected from cell death caused by granule leakage (162). Cells that express the PI-9 are found in the ovaries, placenta, lens capsule, as well as dendritic cells, endothelial cells and peripheral blood mesenchymal cells (161-163).

Our group (Losasso et al.) recently developed a mutant version of Granzyme B with reduced sensitivity to PI-9 (164). Using molecular modeling of the PI-9 Granzyme B complex, the amino acids involved in this interaction were identified and rationally mutated (155, 164). The best performing mutant R201K was selected in which amino acid arginine in position 201 in the mature Granzyme B sequence was substituted with lysine. Using this mutated version, a Granzyme B-anti-CD30(scFv) fusion protein achieved promising *in vivo* anti-tumor activity in a Hodgkin's lymphoma xenograft mouse model (155).

### *I.5.2 MAP tau as a new cytotoxic effector protein*

Hristodorov et al. first generated and described the human microtubule-associated protein tau (Gene ID: 4137; from here on referred to as MAP). The smallest tau protein - Isoform 3 was selected as it still retains all four microtubule-binding repeats (165). MAP is microtubule stabilizing protein involved in the regulation of microtubule dynamics (165-167). While the dynamics of the microtubules in resting cells (interphase) are slow (minutes to hours), during mitosis spindle microtubule changes occur in a 100 fold faster rate (168). Fast changes in the microtubule during mitosis are crucial for successful cell division and are tightly controlled (169). The dynamics of microtubule assembly and disassembly are controlled by the phosphorylation of microtubule-associated proteins (165). Non-phosphorylated MAP binds to the tubulin and stabilizes the microtubule structure. Phosphorylation of MAP leads to its release from the tubulin (165). Following

this rationale, the main phosphorylation sites in MAP were rationally mutated in order to induce constant stabilization of microtubules thus reducing microtubule dynamics to a critical degree and inducing apoptosis (150, 170). MAP tau cytolytic fusion proteins targeting CD30, CD64 and EpCAM have been proven successful in killing various tumor cell in vivo and in xenograft mouse models (149, 150, 170).

## *I.6 SNAP tag*

SNAP-tag is a recombinant variant of the human repair enzyme O6-alkylguanine-DNA alkyl transferase that reacts in a site specific and stoichiometric manner with benzylguanine derivatives, leading to covalent binding (171, 172). Our group has successfully utilized the SNAP tag technology to generate scFv-SNAP tag fusion proteins for *in vitro* and *in vivo* studies (171, 173). In this thesis, scFv-SNAP tag fusion proteins were used as non cytolytic controls to the cytolytic fusion proteins (CFPs). They utilize the same binding domain (anti-EpCAM and anti-CSPG4 scFvs) with a similar binding affinity and similar protein size to the CFPs, but their effector domain- the SNAP tag is not toxic to the target cells (173).

## *I.7 Aims and objectives*

Targeted immunotherapy of breast cancer using tumor-specific antibodies has been shown to be effective in clinical settings (51). Breast cancer patients who were treated with HER2-specific immunotherapy in addition to chemotherapy showed a better overall survival and a better prognosis compared to patients who received only chemotherapy (52). Other therapeutic approaches are based on specific targeting of breast tumors expressing progesterone and/or estrogen receptors (57). However, for breast tumors lacking the expression of these receptors no targeted therapy is currently available. These ‘triple-negative breast cancer’ (TNBC) tumors are among the most aggressive and difficult to treat breast cancers (9, 174). The poor prognosis and prevalence of TNBC among young women highlight the urgent need of developing such therapies. Several disease-specific approaches are currently in preclinical and clinical trials including targeting receptors for vascular endothelial growth factor, epidermal growth factor and mesothelin (61, 142). However, the heterogeneity of TNBC tumors raises the need for identifying a panel of

surface markers to allow tailoring selective therapies to the specific needs of each patient(175-177).

Molecular and genetic profiling of TNBC tumors categorized them into several subtypes with specific genetic modifications and molecular markers distinguishing between the different subtypes (11, 12, 34). Two surface receptors were chosen to be the focus of this work and together they are overexpressed in approximately 80-90% of TNBC tumors:

1. Several studies identified CSPG4 as a potential target for TNBC tumors that is expressed on approximately 40-70% of TNBC tumors. More specifically, CSPG4 was found to be over-expressed mainly on 'basal B subtype' (11) or 'mesenchymal like subtype' (34). In both classifications, these subtypes are characterized by an increased gene expression in motility pathways and stem cell-like processes and are characterized as highly aggressive tumors (11, 34).
2. EpCAM overexpression has been reported in up to 70% of breast tumors (83). It strongly correlates with poor overall survival and higher risk of recurrence following conventional therapy. Furthermore, in breast cancer EpCAM strongly correlates with the tumorigenic capacity of tumor initiating cells and cancer stem cells subsets.

We obtained scFvs targeting these receptors from our collaboration partners (Prof. Helfrich, Groningen University and Prof. Fey, Erlangen University). The main objectives of this study were:

- ❖ To determine whether EpCAM and CSPG4 are suitableTNBC targets and to determine their expression patterns on a wide range of TNBC cell lines.
    - o To obtain as many TNBC cell lines as possible from collaboration partners.
    - o Flow cytometric analysis of the binding of EpCAM and CSPG4 antibodies on available TNBC cell lines.
- ❖ To generate scFv based fusion protein targeting EpCAM and CSPG4. To express and purify them and to study their binding and internalization kinetics in TNBC cell lines.
    - o Cloning of scFv into the available expression vectors in fusion with SNAP tag, ETA', Granzyme B, DAPK, Angiogenin and MAP.
    - o Small scale expression and purification using Ni-NTA agarose slurry.
    - o Analyzing the binding and internalization of the fusion proteins on TNBC cell lines using flow cytometry and confocal microscopy.

- To determine their cytotoxic effect *in vitro* and induction of apoptotic cellular pathways.
  - XTT assay with serial dilutions of the fusion proteins.
  - Annexin V assays with a few dilutions of the fusion proteins.
  - Activation of caspase dependent and caspase independent pathways.
- To select the most promising CFPs for *in vivo* studies in subcutaneous tumor models in mice.
  - Based on expression levels, purity achieved after purification, their binding affinity and specificity and their selective toxicity towards TNBC cell lines.
- To generate fluorescent TNBC cell lines by transfecting them with Katushka fluorescent protein and to determine the best protocol to establish fast growing subcutaneous tumors in BALB/c Nude mice
  - Transfection of TNBC cell lines with Katushka fluorescent protein.
  - FACS sorting of the most fluorescent cells.
  - Confirming EpCAM and CSPG4 expression levels are unchanged following transfection.
  - Inducing subcutaneous tumors in mice with or without Matrigel, with or without Katushka transfection and to determine the tumor take rate.
- Side by side evaluation of CFPs and immunotoxins biodistribution kinetics and tumor targeting.
  - Labeling of EpCAM and CSPG4 specific fusion proteins with a fluorescent DyLight747-NHS ester dye.
  - Studying *in vivo* biodistribution using live imaging CRi Maestro system.
  - Confirming the results using immunofluorescence and immunohistochemistry.
- *In vivo* efficacy and tumor growth inhibition of the fusion proteins in a subcutaneous tumor model in mice.

The final aim of this study is to come up with novel fully human cytolytic fusion proteins to target TNBC, to study their activity in the preclinical setting, and to demonstrate their potential as part of a larger panel of targeted therapeutics to tackle the heterogeneity of TNBC.

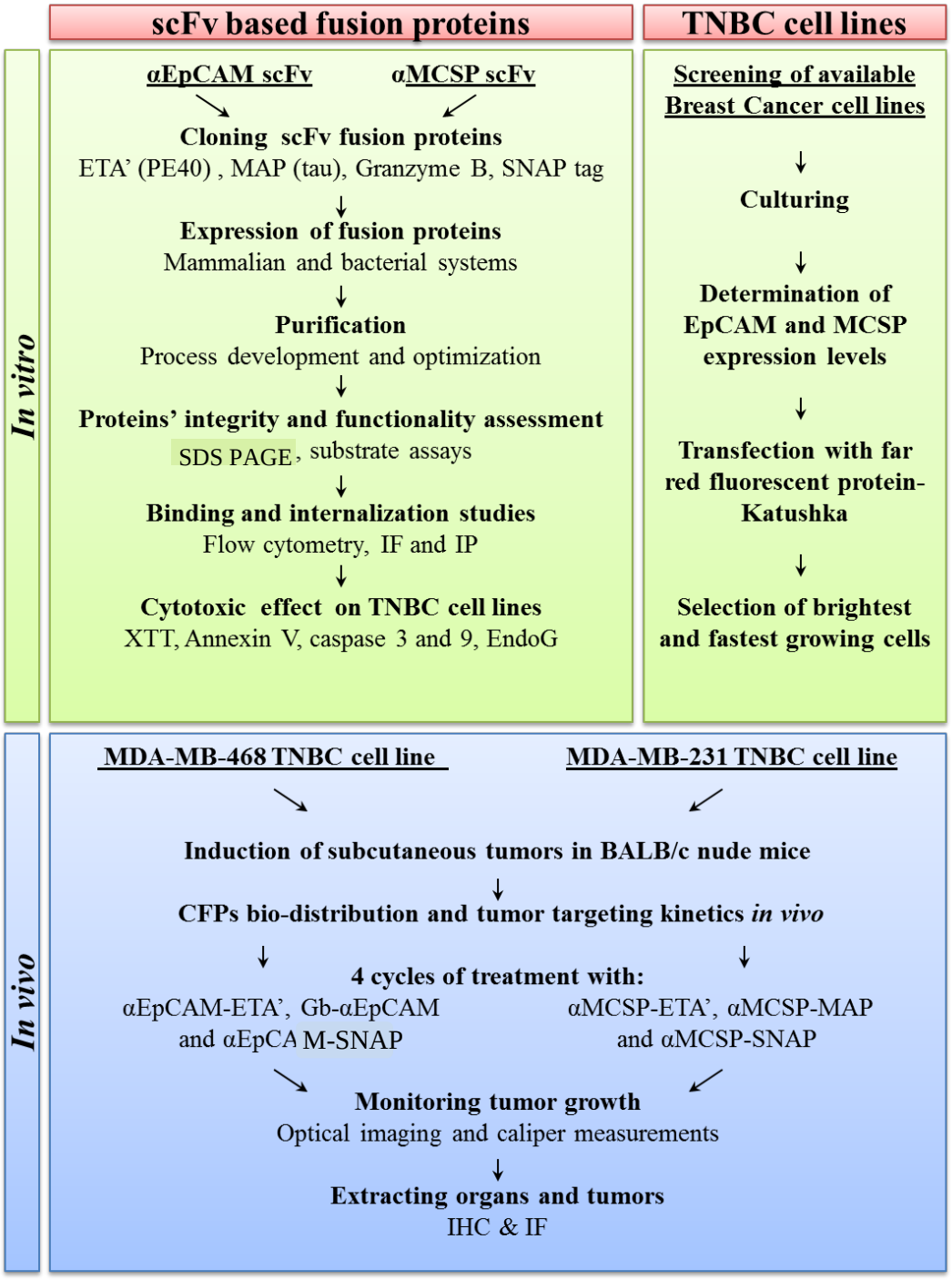



**Illustration 2. Schematic workflow**

Abbreviations:; EpCAM, Epithelial cell adhesion molecule; CSPG4, CSPG4 melanoma associated chondroitin sulfate proteoglycan; ETA' Pseudomonas Exotoxin A; MAP, microtubule-associated protein tau; XTT, cell viability assay; SDS-PAGE, sodium dodecyl sulfate polyacrylamide gel electrophoresis; IF, immunofluorescence; IP, immunoprecipitation; IHC, immunohistochemistry.

# II Materials and Methods

## *II.1 Materials*

### *II.1.1 Chemicals and consumables*

Unless otherwise noted, all chemicals and consumables were purchased from the following manufacturers: eBioscience; Invitrogen; New England BioLabs; Sigma; Pierce; Applied Biosystems; Thermo Fisher Scientific; MWG-Biotech; Roche; Qiagen; GE Healthcare; Stratagene; Fermentas; Promega; Roth; Merk; Dickinson Bioscience; BioRad; Biozym; Corning Inc.; Hewlett Packard; Eppendorf; Millipore; Novagen; Sarstedt; Schott-Glaswerke GmbH; Serva; Whatman; VWR; Labomedic; Falcon; Nalgene; Nunc™; Sartorius; Life Technologies; Jackson ImmunoResearch; Kisker Biotech; Menzel; Southern Biotech; Greiner, iba-lifescience.

### *II.1.2 Bacterial strains*

*E. coli* DH5α (F– Φ80*lac*ZΔM15 Δ(*lac*ZYA-*arg*F) U169 *rec*A1 *end*A1 *hsd*R17 (rK–, mK+) *pho*A *sup*E44 λ– *thi*-1 *gyr*A96 *rel*A1) was used for all intermediate cloning steps and for the amplification of plasmid DNA.

*E. coli* BL21(DE3) (F– *dcm ompT hsdS*(rB– mB–) *gal* λ(DE3)) was used for the expression of recombinant proteins.

### *II.1.3 Mammalian cells – cell lines*

HEK293T cells were used for recombinant protein expression.

mammary carcinoma cell lines: MCF7 (ATCC® HTB-22™), MDA-MB-231 (*ATCC*® HTB-26™), MDA-MB-453 (*ATCC*® HTB-131™) and MDA-MB-468 (*ATCC*® HTB-132™) were purchased from ATCC. Hs 578T (ATCC® HTB-126™) and BT-20 (ATCC® HTB-19™) were kindly provided by Prof. Dr. Edgar Dahl, University Hospital RWTH Aachen, Aachen, Germany).

### *II.1.4 Buffers, media and solutions*

Buffers and stock solutions were prepared according to standard procedures using deionized water ($dH_2O$). Ready-to-use RPMI1640 (Sigma) and MDEM medium (Lonza, Sigma and life biotechnologies) were supplemented with GlutaMAX™, 10% (v/v) fetal calf serum, 100 µg/ml penicillin and streptomycin. Antibiotics: Zeocin (Sigma) and Geneticin (Nalgene) were prepared as stock solutions, filter-sterilized (0.2 µm) and added to media (100 ng/ml and 500 ng/ml respectively). The composition of all common buffers is summarized below.

**Table 3. Buffers and media:**

| **Buffer** | **Composition** | **Concentration** | **Unit** |
|---|---|---|---|
| 10x PBS (pH 7.4) | NaCl | 1.37 | M |
| | KCl | 27 | mM |
| | $Na_2HPO_4$ x $12H_2O$ | 81 | mM |
| | $KH_2PO_4$ | 15 | mM |
| 1x PBST (pH 7.4) | 1x PBS | 99.95 | % (v/v) |
| | Tween 20 | 0.05 | |
| TGS (pH 8.3) | Tris-HCl (pH 8.3) | 25 | mM |
| | Glycine | 192 | mM |
| | SDS | 0.1 | % (w/v) |
| TAE (pH 8.2) | Tris | 40 | mM |
| | Glacial acetic acid | 5.7 | % (v/v) |
| | EDTA | 10 | mM |
| 5x OrangeG Loading buffer | Glycerol | 30 | % (w/v) |
| | OrangeG | 0.01 | % (v/v) |
| | 1x TAE | 70 | % (w/v) |
| Coomassie Staining Solution | Coomassie Brilliant Blue G-250 | 0.25 | %(w/v) |
| | Methanol | 50 | % (v/v) |
| | Glacial acetic acid | 9 | % (v/v) |
| Coomassie Destaining Solution | Methanol | 10 | % (v/v) |
| | Glacial acetic acid | 10 | % (v/v) |
| 5x Protein Loading Buffer (reducing) | Tris-HCl (pH 6.8) | 62.5 | mM |
| | Glycerol | 30 | % (v/v) |
| | SDS | 4 | % (w/v) |
| | Bromphenol blue | 0.05 | % (w/v) |
| | β-Mercaptoethanol | 10 | % (v/v) |
| SDS PAGE Gel (separating gel) | Acrylamide/Bisacrylamide (30/1) | 12 | % (w/v) |
| | Tris-HCl (pH 8.8) | 375 | mM |
| | SDS (10 %, w/v) | 0.1 | % (w/v) |

| | | | |
|---|---|---|---|
| | TEMED | 0.1 | % (v/v) |
| | APS | 0.1 | % (w/v) |
| SDS PAGE Gel | Acrylamide/Bisacrylamide (30/1) | 5 | % (w/v) |
| (stacking gel) | Tris-HCl (pH 6.8) | 150 | mM |
| | SDS | 0.1 | % (m/v) |
| | TEMED | 0.1 | % (v/v) |
| | APS | 0.1 | % (w/v) |
| Binding Buffer | $Na_2HPO_4$ | 200 | mM |
| (Ni-NTA purification, | NaCl | 1000 | mM |
| pH 7.5) | Imidazole | 5 | mM |
| Wash Buffer (Ni-NTA | $Na_2HPO_4$ | 50 | mM |
| purification, pH 7.5) | NaCl | 1000 | mM |
| | Imidazole | 25 | mM |
| Elution Buffer (Ni-NTA | $Na_2HPO_4$ | 50 | mM |
| purification, pH 7.5) | NaCl | 1000 | mM |
| | Imidazole | 500 | mM |
| Binding and wash buffer | Tris/HCl (pH 7.8) | 100 | mM |
| (Streptactin purification, | NaCl | 150 | mM |
| pH 7.8) | | | |
| Elution buffer | Tris/HCl (pH 7.8) | 100 | mM |
| (Streptactin purification, | NaCl | 150 | mM |
| pH 7.8) | D-Desthiobiotin | 5 | mM |
| Blotting Buffer | Tris-HCl, pH 8.3 | 25 | mM |
| | Glycine | 192 | mM |
| | Methanol | 20 | % (v/v) |
| AP Buffer | Tris-HCl, pH 9.6 | 100 | mM |
| | NaCl | 100 | mM |
| | $MgCl_2$ | 5 | mM |
| LB (pH 7.0) | NaCl | 1.0 | % (w/v) |
| | Peptone | 1.0 | % (w/v) |
| | Yeast extract | 0.5 | % (w/v) |
| SOC | Peptone | 2.0 | % (w/v) |
| | Yeast extract | 0.5 | % (w/v) |
| | NaCl | 10 | mM |
| | KCl | 25 | mM |
| | $MgCl_2$ | 10 | mM |
| | $MgSO_4$ | 10 | mM |
| | Glucose | 20 | mM |

### *II.1.5 Chromatography resins and membranes*

Immobilized metal ion affinity chromatography (IMAC) was performed with An XK16-20 column filled with Ni Sepharose 6 Fast Flow resin (GE Healthcare) for the enrichment of histidine (His)-tagged proteins. Streptactin® Superflow® 50% suspension (iba lifescience) was also packed in XK16-20 column for purification of protein with a strep tag. Preparative size exclusion chromatography (SEC) was carried out using an XK16-70 column packed with Superdex$^{TM}$ 75 resin. Zeba™ Spin Desalting Columns (Thermo Fisher Scientific, Germany) were used for buffer exchange.

### *II.1.6 Enzymes*

Restriction enzymes and T4 DNA ligase were purchased from New England BioLabs and used according to manufacturer's instructions. Novagen® Recombinant Enterokinase kit was used according to manufacturer's instructions.

### *II.1.7 Kits*

The following kits were used:

**Table 4. Names and suppliers of kits:**

| Name | Supplier |
|---|---|
| NucleoSpin Plasmid | Macherey-Nagel |
| NucleoSpin Extract II | Macherey-Nagel |
| Qproteome Cell Compartment Kit | Qiagen |
| Caspase-Glo® 9 Assay | Promega |
| GranzymeB substartae I assay colorimetric | Merck Millipore |
| Pierce™ BCA Protein Assay Kit | Thermo Fisher scientific |

### *II.1.8 Protein standards*

Pre-stained broad range marker: 175 / 80 / 58 / 46 / 30 / 25 / 17 / 7 kDa; #P7708, NEB (Frankfurt am Main).

### *II.1.9 Nucleic acid standards*

2-log ladder: 10.0 / 8.0 / 6.0 / 5.0 / 4.0 / **3.0** / 2.0 / 1.5 / 1.2 / **1.0** / 0.9 / 0.8 / 0.7 / 0.6 / **0.5** / 0.4 / 0.3/ 0.2 / 0.1 kb, #N3200, NEB (Frankfurt am Main).

### *II.1.10 Synthetic oligonucleotides*

Synthetic oligonucleotides were synthesized by MWG-Biotech (Ebersberg ,Germany) and used as primers for sequencing of plasmid DNA. The sequences of all oligonucleotides used for this thesis are listed below.

**Table 5. Sequences of oligonucleotides used for sequencing:**

| # | Name | Sequence |
|---|---|---|
| 1 | 5_E_NotI_tau3 | ATATATATATGAATTCGCGGCCGCAATGGCTGAACCCCGCCAGGAG |
| 2 | 3_H_BlpI_tau3 | ATATATATATAAGCTTGCTCAGCTCACAAACCCTGCTTGGCCAGGGAG |
| 3 | T7_promoter_f | AATACGACTCACTATAG |
| 4 | T7_terminator_r | GCTAGTTATTGCTCAGCGG |
| 5 | Hinterhis_r | CCAACAGCTGGCCCTCGCAGACAG |
| 6 | 5’ pMS | GGGCGGTAGGCGTGTACGGTGGG |

### *II.1.11 Vectors*

The following expression vectors were used:

1. pET27 vector was used for periplasmic stress expression of recombinant anti-CSPG4(scFv)-ETA’ and anti-CSPG4(scFv)-MAP in BL21 *E. coli.*
2. pMT was used for periplasmic stress expression of recombinant αEpCAM(scFv)-ETA’ in BL21 *E. coli*. This vector was derived from pET27b vector (Novagen).
3. pMS was used for expression of GB-R201K-αEpCAM(scFv), αEpCAM(scFv)-SNAP and αCSPG4(scFv)-SNAP in mammalian H293T cells.

### *II.1.12 Antibodies*

The antibodies used for this thesis are listed below.

**Table 6. List of antibodies used in this thesis:**

| Name | Supplier | Applications |
|---|---|---|
| Penta-His AlexaFluor488 | Qiagen | WB |
| Anti-Tau Monoclonal Antibody (HT7) | Thermo Fisher Scientific | WB |
| Goat-anti-Mouse-AP | Sigma | WB, IHC |
| goat anti-mouse IgG antibody 647-conjugated | Thermo Fisher Scientific | F, IF |
| anti-CSPG4 antibody | R&D Systems | F |
| anti-poly his antibody | Sigma | F, WB, IHC |
| Goat anti-mouse IgG FITC-conjugated | Dianova, | F, IF |
| Goat anti-mouse IgG PE-conjugated | Dianova, | F, IF |
| Rabbit anti-β-Tubulin antibody | Sigma | IP |
| Mouse anti-β-Tubulin antibody | Cell Signaling Technology | WB |
| Mouse-anti human EpCAM antibody (Abcam, United Kingdom | Abcam | F |
| Goat anti-mouse IgG antibody PO-conjugated (1:2000, Sigma Aldrich) | Sigma | WB |
| anti-cleaved caspase 3 antibody (1:500; Cell Signaling Technology), | Cell Signaling Technology | WB |
| anti-PARP-1 antibody (1:500; Cell Signaling Technology) | Cell Signaling Technology | WB |
| anti-actin antibody (1:2000, Sigma, Germany) | Cell Signaling Technology | WB |
| Goat anti-Rabbit IgG HRP-conjugated | Biomeda | WB, IHC |
| anti-endonuclease G antibody | AbDserotec, UK | WB |
| anti-Granzyme B | Santa Cruz Biotechnology | WB, F, IF |
| anti-ETA’ | TC1 clone (103), in-house preparation | F, IF, WB |

Abbreviations: WB, western blotting; F, flow cytometry; IHC, immunohistochemistry; IF, immunofluorescence microscopy; IP, immunoprecipitation.

### *II.1.13 Equipment and software*

**Table 7. List of equipment used in this thesis:**

| **Category** | **Name** | **manufacture** |
|---|---|---|
| Balances | Precision and analysis balances, Talent: TE6101, TE64, TE31025, TE12000 | Sartorius (Göttingen, Germany) |
| Centrifuges | Table centrifuge 5415D and 5415R<br>Multifuge 3 S-R / 1S<br>Avanti J-25I Centrifuge<br>Rotina 420 R | Eppendorf AG<br>Heraeus Instruments<br>Beckman Coulter<br>Hettich Zentrifuge |
| Rocker/Shaker | Eppendorf Thermomixer comfort,<br>Eppendorf Thermostat 5320 | Eppendorf AG<br>Eppendorf AG |
| vortex | Vortex-Genie 2 | Scientific Industries Inc. |
| Hoods | Hera Safe HS12 | Kendro |
| Incubators | Thermomixer compact<br>Function Line Type UT12<br>CD210 | Eppendorf AG<br>Heraeus Instruments<br>Binder |
| Sonication | Sonication Probe UW2070 | Bandelin Electronic |
| SDS-PAGE preparation | Mini Protean III Gel Chamber<br>Protein Gel-Apparatus<br>Supplies of Mini PROTEAN II™<br>Gel Air Dryer | BioRad |
| Electrophoresis and blotting | Mini Trans-Blot Cell | BioRad |
| Cryostat | Cryostat CM 3050 | Leica |
| Chromatography | Äkta Purifier | GE Healthcare |
| Spectrophotometer | Epoch Microplate Spectrophotometer Tecan<br>Genios Pro<br>Aminco Bowman Series 2 spectrometer | Biotek<br>Tecan<br>Polytec |
| Microscopes | TCS SP5 Confocal Laser Microscope<br>DMIL Inverted Microscope with Mercury Fluorescence Light Source<br>DM2000<br>Opera® QEHS 2.0 microscope | Leica<br>Leica<br><br>Leica<br>PerkinElmer |
| Flow Cytometer | FACSCalibur<br>FACSVantage Cell Sorter | Becton Dickinson |
| Cell Counter | Casy1 | Schärfe System (Reutlingen, Germany) |
| Cell Washer | Dade Serocent | Baxter |
| Sequencer | ABI Prism 3730 Capillary-Sequencer | Applied Biosystems |

| | | |
|---|---|---|
| Water Baths | TE31025, TE12000 | Sartorius |
| Trans illuminator | Molecular Imager Gel Doc XR System | BioRad |
| Chemiluminescence Imaging system | Stella 2000 Imaging System | raytest |
| In vivo optical imaging | Maestro CRi Imaging System | Maestro CRi Inc. |

**Table 8. Software used for data analysis:**

| **Category** | **Name** |
|---|---|
| Statistical analysis | Graphpad Prism v5.0 |
| Sequence analysis | CLC Main Workbench v6 |
| Gel Image analysis | AIDA Image Analyzer |
| Image analysis | Image J software |
| Optical imaging analysis | Maestro Cri software |
| FACS data analysis | Cyflogic, Flowjo |
| Graphs and data analysis | Microsoft Excel 2010 |
| Image editing | Microsoft PowerPoint 2010 |
| Documents | Microsoft Word 2010 |

## II.2 Methods

### II.2.1 Molecular cloning

#### II.2.1.1 E. coli culturing and preservation

To obtain single colonies DH5α or BL21 (DE3) *E.coli* cells were plated on LB agar plates with the appropriate antibiotics and plates were incubated over night at 37°C. Plates were stored at 4°C for short periods (1-2 weeks). Single colonies were picked and cultured in LB liquid medium containing the suitable antibiotic overnight at 37°C with vigorous shaking (225 rpm). Glycerol stocks were prepared by mixing 700 µl of an overnight culture with 300 µl of 75 % (v/v) sterile glycerol and were stored at –80°C.

#### II.2.1.2 Preparation of chemically competent E. coli

2-3 E.coli colonies were inoculated overnight in a shaking LB culture at 37°C. 1ml from over-night culture was sub-cultured in 100ml fresh LB at 28°C with shaking till $OD_{600}$ reached~ 0.25-0.35. The culture was then chilled on ice for 15min and spun down in a pre-cooled centrifuge at 3000 rpm for 10 min. The pellet was resuspended with 40 ml ice-cold 0.1 M $CaCl_2$ solution and kept on ice for 30 minutes. Centrifugation was done as before and the pellet was gently suspended with 5 mL ice-cold 0.1 M $CaCl_2$ solution containing 15% glycerol. Aliquots of 50 µL of cell suspension were prepared in 1.5 mL tubes and submerged in liquid nitrogen, then directly transferred to -80°C freezer.

#### II.2.1.3 Heat shock transformation of E. coli

Chemically competent *E. coli* cells (50 µl aliquots) (II.2.1.2) were thawed on ice and mixed gently with 50–100 ng of plasmid DNAII.2.1.8). The cells were incubated for 30 min on ice, next heat shocked at 42°C for 50 s and then cooled on ice for 2 min. 450 µl of LB medium was added and the cells were incubated at 37°C with shaking for 30–60 min. 100 µl of the cells were plated onto LB agar plates supplemented with appropriate antibiotics and incubated at 37°C overnight.

#### II.2.1.4 Periplasmic protein expression under osmotic stress

Recombinant proteins were expressed in *E. coli* BL21(DE3) cells using the protocol for periplasmic stress expression in the presence of compatible solutes as previously described (178). Briefly, *e. coli* BL21(DE3) cells were transformed II.2.1.3) with pMT or pET vectors carrying the recombinant DNA and single colonies were grown in pre cultures overnight.

Main culture was grown at 30°C to an OD of 1.6 followed by stress induction with 500 mM D-sorbitol, 10 mM betaine monohydrate and 4% (w/w) NaCl. After incubation at 26°C for 30 min with shaking (180 rpm), protein expression was induced with 2 mM IPTG. Bacteria were spun down 18 h after induction by centrifugation (4000 x *g*, 10 min, 4°C) and the pellet was frozen at –80°C overnight. The frozen pellet was resuspended in lysis buffer (50 mM Tris-HCl, 150 mM NaCl, 100 µg/ml lysozyme, 10% (v/v) glycerol, pH 8.0) containing a EDTA free protease inhibitor cocktail (Roche) at 4°C and sonicated five times for 60 s at 200 W. Cell debris was removed by centrifugation (24,000 x *g*, 20 min, 4°C) . The cleared bacterial lysate was then used for protein purification by IMAC.

#### *II.2.1.5 Cell culture – mammary carcinoma cell lines*

Mammalian cell lines were cultivated in complete R-10 medium in T-75 flasks: RPMI-1640 supplemented with 10% (v/v) fetal calf serum (FCS), 50 µg/ml penicillin and 100 µg/ml streptomycin (all Thermo Fisher Scientific, Germany). Cell cultures were incubated at 37°C, 100% humidity and 5% $CO_2$. Cells were passaged twice a week and split 1:4, adherent cells were detached by washing with PBS, followed by the addition of 1 ml Trypsin-EDTA solution (Sigma or Thermo Fisher) and incubation at 37° C for 3-5 minutes, once the cells started to detach, 5 ml of R-10 were added to deactivate the Trypsin, 1.5 ml of the cells were kept in the flask to achieve 1:4 split. Additional 9 ml of R-10 were added to the flask. Cell numbers were counted using the cell counter Casy1 (Schärfe System, Reutlingen, Germany).

#### *II.2.1.6 Transfection of mammalian cells with recombinant DNA*

Transfection of cells was performed using Roti-Fect (Roth, Germany) according to the manufacturer's instructions. 1 x $10^5$ cells were seeded in 12-well plates one day prior to transfection. Cells were transfected with a mixture of 1ug plasmid DNA and 7µl Roti-Fect for 4-6 hours. Cells were washed with cell media and successfully transfected cells were selected with appropriate antibiotics and sorted using the FACS Vantage Cell Sorter (Becton Dickinson, Germany).

#### *II.2.1.7 Expression of fusion proteins in HEK293T cells*

HEK293T cells were transfected as described in the previous section with pMS expression vector encoding the recombinant fusion proteins GB-R201K-αEpCAM(scFv), αEpCAM(scFv)-SNAP tag, and αCSPG4(scFv)-SNAP tag. Transfected cells were selected using Zeocin (100ug/ml) and were grown in triple flasks with selective cell media to induce

expression and secretion of the proteins; media was collected and replaced every 3-4 days. a total of 1-1.5 liters of supernatant was collected over the course of 3 weeks (155).

#### *II.2.1.8 Isolation of plasmid DNA*

Plasmid DNA was purified from 5 ml over-night DH5α bacteria cultures (II.2.1.3) using the NucleoSpin Plasmid Kit for minipreps (Macherey-Nagel) according to the manufacturer's instructions and stored at –20°C.

#### *II.2.1.9 Agarose gel electrophoresis*

DNA from PCR or DH5α minipreps (II.2.1.8) and restriction fragments were separated by electrophoresis using 0.8–1.2% (w/v) agarose gels prepared in TAE buffer containing 0.5 μg/ml ethidium bromide. OrangeG Loading Buffer (New England BioLabs) was mixed with DNA samples before loading. 2-Log DNA ladder (New England BioLabs) was used to evaluate sample size. The DNA was visualized at 302 nm and documented using a Molecular Imager Gel Doc XR System (BioRad). Preparative gel electrophoresis was used to isolate digested DNA fragments. Agarose bands containing the DNA fragment of interest were excised from the gel on an UV trans-illuminator with a sterile blade. DNA extraction was performed using a NuceloSpin Extract II kit (Macherey-Nagel) according to the manufacturer's guidelines and stored at –20°C.

#### *II.2.1.10 Determining DNA concentration*

DNA concentration was determined by measuring the $OD_{260nm}$ (1.0 corresponds to ~50 μg/ml of double stranded DNA). The purity of the nucleic acid was determined by measuring the $OD_{260/280nm}$ ratio.

#### *II.2.1.11 Restriction enzymes digestion of DNA*

Restriction endonucleases, 10x buffers 1, 2, 3 and 4, and bovine serum albumin (BSA) solution were obtained from New England BioLabs. DNA (II.2.1.8) was incubated with the corresponding enzyme and buffer in a heating block according to NEB recommendations for 2-16 hours. Reaction was stopped by running agarose gel electrophoresis.

#### *II.2.1.12 Ligations*

Ligation of DNA fragments and restricted vectors was carried out using T4 DNA Ligase (400,000 U/ml; New England BioLabs) and 10x ligase buffer as recommended in the manufacturer's protocol in a final volume of 20 μl. 1-4 fold molar excess of insert DNA to vector DNA (II.2.1.11) was used depending on their relative sizes. Ligation was carried out

for 30 min at room temperature or at 15°C overnight and *E. coli*. DH5α cells were used for the transformation.

#### *II.2.1.13 DNA sequencing and analysis*

DNA sequence analysis was carried out at the Fraunhofer IME sequencing facility using an ABI Prism 3700 Capillary-Sequencer (Applied Biosystems) with BigDye™ cycle sequencing terminator chemistry and the Applied Biosystems Sequencing Analysis Program. The sequences were analyzed with CLC workbench software.

### *II.2.2 Protein preparation*

#### *II.2.2.1 Immobilized metal ion affinity chromatography (IMAC)*

Äkta Purifier System (GE Healthcare) was used to enrich recombinant proteins by IMAC Sepharose 6 Fast Flow as resin (GE Healthcare). Bacterial lysates from periplasmic expression (II.2.1.4) or supernatant from HEK293 expression (II.2.1.7) were filtered by vacuum filtration using a 0.45µm Whatman filter before loading onto an XK16-20 column at a flow rate of 1–2 ml/min. After loading was complete, the column was washed with Wash Buffer (10 mM imidazole) followed by a second wash with 25mM imidazole until the baseline was reached. Elution was carried out at a flow rate of 1 ml/min using Elution Buffer (250 mM imidazole). The elution fraction was concentrated with a Vivaspin Ultrafiltration Device 30K (Sartorius). The elution buffer was exchanged with PBS using Zeba spin column (Pierce) or during subsequent size exclusion chromatography.

#### *II.2.2.2 Streptactin purification*

Anti-CSPG4 scFv fusion proteins (Figure 22) were further purified by ***Strep***-Tactin® Superflow® high capacity **(**iba lifesciences). The elution fraction from IMAC (II.2.2.1) was loaded onto the Streptactin column, washing steps were done using Streptactin loading buffer (Tris/NaCl), and the proteins were eluted using Streptactin elution buffer containing 5mM dis-biotin. The elution buffer was exchanged with PBS using Zeba spin column (Pierce) or during subsequent size exclusion chromatography

#### *II.2.2.3 Size exclusion chromatography (SEC)*

Preparative SEC was carried out following IMAC (II.2.2.1) or Streptactin purification (II.2.2.2) on an Äkta Purifier System (GE Healthcare) using an XK16-70 column packed with Superdex$^{TM}$ 75 (GE Healthcare). PBS (pH 7.4) was used as the mobile phase at a flow

rate of 1.0 ml/min. 2.5 ml fractions were collected and analyzed for their size and integrity by sodium dodecyl sulfate polyacrylamide gel electrophoresis II.2.4.2) (SDS-PAGE). Fractions of similar composition were combined and filter-sterilized (0.2 µm). The protein concentration was determined using BCA protein quantification kit (Pierce™, Thermo Fisher Scientific) and the proteins were aliquoted and stored at –20°C.

#### *II.2.2.4 Enterokinase digest*

Purified EGBR201K-αEpCAM(scFv) (II.2.2.1) was dialyzed against Enterokinase buffer (20mM TRIS, 150mM NaCl, 2nM $CaCl_2$) overnight at 14°C. 10 µg protein was cleaved with 0.4 units of Novagen® recombinant Enterokinase (Merck Millipore, Germany) at 21°C for 18 hours. Enterokinase buffer was subsequently exchanged to PBS using Zeba™ spin desalting columns (Thermo Fisher Scientific).

### *II.2.3 Proteins labeling*

#### *II.2.3.1 Labeling of SNAP tag fusion proteins*

Proteins containing the SNAP tag were labeled with benzyl guanine modified fluorescent dyes. The conjugation reaction with the BG-modified dyes BG Alexa-Fluor 647 (BG-647), BG Alexa-Fluor 747 (BG747) or BG Vista Green (Covalys Biosciences AG) was performed by incubation of the proteins in the dark at RT with 2-fold molar excess of the dye for 1 hour. Residual dye was removed using Zeba™ Spin Desalting Columns (Thermo Fisher Scientific). Labeled proteins were visualized after separation by SDS-PAGE using CRi Maestro imaging system using blue, red and near-infrared filter sets.

#### *II.2.3.2 Labeling of CFPs for live imaging*

Anti-CSPG4(scFv)-ETA’ and αCSPG4(scFv)-MAP were labeled with a DyLight 747-B3 NHS Ester dye (Thermo Fisher Scientific) according to manufacturer’s instructions. Briefly, CFPs and dye were added to a phosphate buffer (pH 7.0) in a 1:2 molar ratio for 1 hour. Excess dye was removed using Zeba™ Spin Desalting Columns (Thermo Fisher Scientific). Samples were analyzed by SDS-PAGE for detection of fluorescence and desalting efficiency.

### *II.2.4 Protein analysis*

#### *II.2.4.1 Quantification of purified proteins*

Purified protein (II.2.2) concentration was determined using the BCA protein assay kit (Thermo Fisher Scientific) according to manufactures instructions. Serially diluted BSA standards (provided with the kit) were used to generate the linear regression standard curve. The final concentration of the protein was calculated using excel software (Microsoft Office).

#### *II.2.4.2 Sodium dodecylsulfate polyacrylamide gel electrophoresis (SDS-PAGE)*

SDS-PAGE (12% acrylamide) was used for the separation of protein samples. Samples were mixed with 5x Protein Loading Buffer and heated at 95°C for 5 min before loading. Proteins were separated by electrophoresis at 140 V for 75 min.

Visualization of protein bands was performed by Coomassie Staining for 20 min at room temperature. Coomassie destaining solution was used for the removal of non-specific background staining.

#### *II.2.4.3 Protein Immuno-blotting*

Detection of purified proteins and determining their integrity was carried out using Immuno-blotting (Western blotting). Electro-tank blotting method was used to transfer proteins from SDS-PAGE (II.2.4.2) to a nitrocellulose membrane (250 mA; 60 min). The membrane was blocked with 2.5% (w/v) milk powder in PBST buffer or 3% BSA (w/v) in TBST buffer for 1 h at room temperature. The membrane was next incubated with the desired antibody to detect the different proteins. Detection of purified proteins was carried out using an anti-poly his mAb (1:2000, Sigma, Taufkirchen, Germany) and a goat anti-mouse IgG-Alkaline Phosphatase-conjugated antibody (1:5000; Sigma) and visualized using NBT/BCIP substrate (Life Technologies, Darmstadt, Germany). The reaction was stopped after the bands became visible by washing the membrane with water.

#### *II.2.4.4 Proteolytic activity of GB-R201K-αEpCAM(scFv)*

The enzymatic activity of Enterokinase cleaved GB-R201K-αEpCAM(scFv) II.2.2.4) and its undigested form EGB-R201K-αEpCAM(scFv) was determined by a colorimetric assay based on the synthetic Granzyme B substrate Ac-IETD-pNA Absorbance at 405 nm (Merck Millipore). 200 μM of the synthetic substrate was used per reaction with 1.5, 5 or 15 pmol of Enterokinase digested GB-R201K-αEpCAM(scFv) or the undigested CFP- EGB-R201K-

αEpCAM(scFv. 12 pmol Granzyme B standard was used as a positive control. reaction was monitored in a 2-min interval for 60 min at 37 °C.

### *II.2.5 Immunoassays*

#### *II.2.5.1 Flow cytometry*

##### *II.2.5.1.1 Binding analysis*

EpCAM and CSPG4 expression and the binding of CFPs to mammary carcinoma cells were evaluated by flow cytometry on a FACSCalibur (Becton Dickinson, Heidelberg, Germany). Data was analyzed using Cyflogic software (CyFlo Ltd, Turku, Finland). A total of $3 \times 10^5$ cells were washed with PBS and incubated with 1 µM of purified protein or 1 µg hEpCAM antibody (Abcam, Cambridge, United Kingdom) or 1 µg anti-CSPG4 antibody (R&D Systems, Wiesbaden, Germany) in 100 µl PBS for 30 min at 4 °C. After washing, cells incubated with CFPs were next incubated with anti-poly His mAb (1:1000, Sigma). Fluorescent staining with fluorescently labeled goat anti-mouse IgG- FITC-conjugated (1:100, Dianova, Hamburg, Germany) or PE-conjugated (1:200, Dianova) was performed for 30 min on ice in the dark.

##### *II.2.5.1.2 Saturation curve and dissociation constant determination assay*

The saturation analysis was performed as described previously (179). Briefly, different concentrations of Gb-αEp or αEpCAM(scFv)-ETA' (0, 0.1, 0.3, 1, 3, 10, 30, 100, 300 nM) were incubated for 1h at 4 °C with MDA-MB-468 cells followed by incubation with an anti-poly-his mAb (1:1000) and a goat anti-mouse IgG-647 (1:400, Thermo Fisher Scientific). Unspecific binding was measured by the addition of 3 µM unlabeled CFPs for 30 min, followed by FACS analysis. The mean fluorescence intensity (MFI) was evaluated and compared by non-linear-regression, the saturation curve interpolation and $K_d$ values were calculated using GraphPad (Prism 4.0, La Jolla, CA, USA).

##### *II.2.5.1.3 Cellular uptake rate of CFPs- internalization kinetics*

3 x $10^5$ cells per sample were incubated with 100 nM CFPs in PBS for 1 hour at 4 °C, subsequently washed and incubated at 37 °C for different time intervals (0, 1, 2 and 4 hours). 2 different samples per time point were prepared. Cells were next incubated with anti-poly-His mAb antibody (1:1000, sigma) for 30 min at 4 °C followed by staining with goat anti-mouse IgG-PE mAb (1:200) for the detection of the remaining surface-bound CFPs. MFIs

from the different time points were evaluated and compared to the 0 hour control which was defined as 100% surface signal. The percentage of internalized receptors was calculated by subtracting the relative percentage of surface signal.

#### *II.2.5.2 Internalization analysis by confocal microscopy*

TNBC cells were detached using Accutase (Thermo Fisher Scientific) and washed with PBS. 1 x $10^6$ cells were next stained with 0.5 nM αEpCAM(scFv)-SNAP or αCSPG4-SNAP previously coupled with BG-Alexa-647 fluorescent dye for 30 minutes. Cells were next washed and incubated with media for different time intervals (0, 1, 2, 4 hours). Cells were washed with PBS and analyzed by TCS SP5 Confocal Laser Microscope, 40x objective (Leica).

#### *II.2.5.3 Internalization analysis by high-throughput confocal microscopy*

$1 \times 10^4$ MDA-MB-231 or MDA-MB-468 cells per well were seeded overnight in 96-well plates. Cells were then incubated at 4 °C or 37 °C for different time intervals with 100 nM CFPs in 100 µl PBS or only in PBS as negative control. Cells were fixed 7 minutes with 3.7% (v/v) formaldehyde, blocked for 1 hour with 2% (w/v) BSA, stained with anti-Granzyme B (1:400, Santa Cruz Biotechnology, Heidelberg, Germany) or anti-ETA' (1:1000, TC1 clone, in-house preparation) antibodies for 2 hours, followed by goat anti-mouse IgG antibody FITC-conjugated (1:50) or 647 conjugated (1:400) for 1 hour. Cells were next counterstained with Hoechst dye for nuclear staining. Images were taken using an Opera® QEHS 2.0 microscope (PerkinElmer, MA, USA) at 40x magnification by Dr. Stefano DiFiore.

#### *II.2.5.4 Immunofluorescence microscopy of mouse tissue sections*

Sections from frozen tissues of mice bearing subcutaneous TNBC tumors II.2.7.5) (livers, kidneys, hearts, spleens and tumors) were cut into 12-µm sections on a Cryostat CM 3050 (Leica) and mounted on coated slides (Menzel). Sections were stained with anti poly-his tag antibody to detect tissue penetration of the CFPs. Sections were dried for minimum 48 hours and fixed with dry acetone (10 min), air-dried, blocked in 1% (v/v) normal goat serum (Sigma) in PBS (pH 7.4), and incubated overnight with the anti-his-Alexa 488 antibody (1:40, Sigma) at 4°C. Slides were washed three times for 5 min with 1x PBST and analyzed using a TCS SP5 Confocal Laser Microscope, 40x objective (Leica). Images were processed using Photoshop CS5 Extended software.

#### *II.2.5.5 Immunohistochemistry*

Sections from frozen livers, kidneys, hearts, spleens and tumors harvested from mice (II.2.7.5) were prepared as described above. Sections were stained with anti poly-His antibody (1:200, Rabbit Ab, Sigma) and washed three times for 5 min with 1x PBST, then incubated with AP-conjugated goat anti-rabbit antibody (1:1000, Sigma, Germany) in 1% (v/v) goat serum in PBS (pH 7.4; 45 min). After washing twice in PBST and once in Tris-HCl (0.1 M, pH 8.5), AP activity was detected using the substrate naphthol AS-BI phosphate (sodium salt, 500 mg/l; Sigma) and new fuchsine (100 mg/l; Merck) as the chromogen dissolved in 0.1 M Tris-HCl, pH 8.5, resulting in pink/red staining. Endogenous AP activity was inhibited by adding levamisole (350 mg/l, Sigma) to the reaction mixture. Slides were counterstained with hematoxylin. Images were taken on a Leica DM IL inverted microscope with 10x objective. Images were processed using Photoshop CS5 Extended software.

#### *II.2.5.6 Detection of Serpin B9 (PI-9) expression in TNBC cell lines*

1 x $10^6$ cells (MDA-MB468, MDA-MB-231, MDA-MB-453 and HS578T) were lysed by incubation with lysis buffer (150 mM sodium chloride, 1.0% (w/v) Triton X-100, 1 mM EDTA, 1 mM PMSF, 50 mM Tris, pH 7.5) for 30 minutes, centrifuged at 12,000 rpm for 20 minutes. Protein concentration was determined using the BCA protein assay kit (Thermo Fisher Scientific) and equal total protein amounts (40 µg) were separated on SDS-PAGE for subsequent western blot analysisII.2.4.2, II.2.4.3). Western blot analysis for the detection of PI-9 was performed using anti- Serpin B9 antibody (1:500, Santa Cruz Biotechnology, USA), followed by goat anti mouse IgG-AP conjugated antibody. NBT/BCIP substrate was used to visualize the signal. The reaction was stopped, once the bands became visible, by washing with water.

#### *II.2.5.7 Co-Immunoprecipitation assay*

Assay was carried according to *Abcam* protocol based on (180). MDA-MB-231 cells were treated with 200 nM αCSPG4-MAP or αCSPG4-ETA' or PBS as negative control for 24 hours. Samples were chilled on ice, and cell pellets were resuspended in non-denaturing lysis buffer. Cell lysates were precleared by incubation with Rabbit serum and protein G-Sepharose. The pre-cleared samples were incubated with β-tubulin antibody (Rabbit IgG, Cell Signaling Technology, USA) overnight at 4 °C. Protein G-Sepharose was added, and incubation was continued for another 4 h. The immune-complexes were washed 3 times with lysis buffer and eluted with glycine elution buffer pH 2.5. After centrifugation, the supernatants were analyzed by immunoblotting with MAP-tau antibody (mouse monoclonal,

Thermo Fisher Scientific, Germany) and β-Tubulin antibody (mouse monoclonal, Sigma, Germany) followed by goat anti mouse IgG antibody-PO conjugated (Sigma, Germany). ECL Western Blotting Substrate (*Pierce*™, Thermo Fisher Scientific) was used and the signal was measured using xStella camera (raytest, Germany).

### *II.2.6 Cytotoxic effect of CFPs on TNBC cell lines*

#### *II.2.6.1 Cell viability assay*

5-7 x $10^3$ cells per well were seeded 48 hours prior in 96 well plates. Serial dilutions of CFPs were added for 48 hours in triplicates. Subsequent dose-dependent evaluation of viability was carried out by measuring the conversion of XTT to a water soluble orange formazan dye as described previously (149). Briefly, at the end of the experiment, 50 µl of XTT/phenanzine methosulfate (100:1; Serva and Sigma-Aldrich) was added to each well and incubated for 2–3 h. The absorbance at 450 and 630 nm was measured using an Epoch Microplate Spectrophotometer (Biotek). $IC_{50}$ values were calculated relative to PBS treated control cell, statistical analysis of non-linear regression was done using GraphPad Prism v5 software. All experiments were carried out in triplicate.

#### *II.2.6.2 Apoptosis assay*

To confirm the cytotoxicity of CFPs, an AnnexinV/ propidium iodide (PI) apoptosis assay was performed. 3 x $10^5$ cells were seeded in 6-well plates. Cells were treated either with 250 nM of Gb-αEp or with 50 nM of αEpCAM(scFv)-ETA' or 200nM αCSPG4(scFv)-MAP or 40 nM αCSPG4(scFv)-ETA' for 48 hours. Next, cells were trypsinated, washed with Annexin buffer (10 mM HEPES, pH 7.4; 0.14 M NaCl; 2.5 mM CaCl) and incubated with supernatant containing secreted Annexin V-eGFP as described by Stöcker *et al.*(181). Cells were washed and 50 µg/ml propidium iodide (PI) was added to the cells. The frequency of early and late apoptotic cells was determined using a FACSCalibur (II.2.5.1).

#### *II.2.6.3 Caspase 3 and parp-1 cleavage assay*

1 x $10^6$ cells (MDA-MB468, MDA-MB-231, MDA-MB-453) were seeded and allowed to adhere over-night in T-25 flasks. Cells were next incubated with 50 nM αEpCAM(scFv)-ETA', 200 nM Gb-αEp, 40 nM αCSPG4(scFv)-ETA' or 200nM αCSPG4(scFv)-MAP for 48 hours. Cells were next lysed by incubation with lysis buffer (150 mM sodium chloride, 1.0% (v/v) Triton X-100, 1 mM EDTA, 1 mM PMSF, 50 mM Tris, pH 7.5) for 30 minutes,

centrifuged at 12,000 rpm for 20 minutes. Protein concentration was determined using the BCA protein assay kit (Pierce™, Thermo Fisher Scientific) and equal total protein amounts (25 µg) were separated on SDS PAGE for subsequent western blot analysis (II.2.4.2, II.2.4.3). Detection for apoptotic signaling was carried out using an anti-cleaved caspase 3 antibody (1:500; Cell Signaling Technology), an anti-PARP-1 antibody (1:500; Cell Signaling Technology) and an anti-actin antibody (1:2000, Sigma, Germany) followed by goat anti-rabbit IgG HRP-conjugated antibody (1:2000, Biomeda, Germany) or goat anti-mouse IgG-PO (1:5000, Sigma, Germany). The substrate reaction was carried out using ECL Western Blotting Substrate (Thermo Fisher Scientific) on a Stella 2000 Imaging System (raytest, Straubenhardt, Germany).

#### *II.2.6.4 Caspase-9 substrate assay*

In order to determine caspase-9 activity, a caspase-9 substrate (Caspase-Glo® 9 Assay, Promega GmbH, Mannheim, Germany) was added to 48 hours treated and non-treated MDA-MB-231 and MDA-MB-468 cells in a 96 well plate . Luminescence was measured using an Aminco Bowman Series 2 Spectrometer (Polytec, Waldbronn, Germany). The measured luminescence signal is directly proportional to the activity of caspase-9 and was normalized to the endogenous signal produced by non-treated cells.

#### *II.2.6.5 Endonuclease G translocation assay*

1 x $10^6$ MDA-MB-231 cells were treated with 200 nM of αCSPG4(scFv)-MAP for 48 hours; cells were lysed and sub-fractioned into cytosolic, nuclear and mitochondrial fractions using cell compartment kit (Qiagen) according to manufacturer's instructions. 14 µg protein from each sample were analyzed by Coomassie staining (II.2.4.2) and western blotting (II.2.4.3), Endonuclease G translocation from the mitochondria to nucleus was detected using Endonuclease G antibody (Rabbit polyclonal, AbDserotec, UK).

#### *II.2.6.6 Tubulin polymerization assay*

The stabilizing effect of H22(scFv)-MAP on tubulin polymerization was tested using a Tubulin Polymerization Assay Kit (Cytoskeleton) according to manufacturer's instructions. Paclitaxel and general tubulin buffer were used as controls. All measurements were carried out in duplicate. Vmax represents the slope of the linear phase in milli-extinction units (mE).

#### *II.2.6.7 Cell cycle analysis*

1 x $10^6$ MDA-MB-231cells were treated with αCSPG4-MAP or PBS buffer for 48 and 72 hours in T-25 small flasks, cells were fixed with cold Ethanol and stained with Propidium Iodide solution containing 0.01% (v/v) TritonX-100, RNAse 10 µg/ml, 50 µg/ml PI, in PBS. Cells were analyzed by Flow cytometry (II.2.5.1). PI signal was measured on FL2-A linear channel, gating on single cells; cell debris and duplicates were excluded.

### *II.2.7 In vivo tumor xenograft models*

All animal experiments were approved by the Landesamt für Natur, Umwelt und Verbraucherschutz NRW (LANUV) (AZ 87.-51.04.2010.A278). Six- to eight-week-old female BALB/c [nu/nu] mice (Charles River Laboratories, Sulzfeld, Germany) were kept in accordance with the requirements of the German Tierschutzgesetz, §8 Abs. 1 and with the guide for the care and use of laboratory animals published by the National Institutes of Health in 2011.

#### *II.2.7.1 Dose escalation studies and maximum tolerated dose determination*

To determine the maximum tolerated dose of GbR201K-αEpCAM(scFv), α CSPG4(scFv)-MAP and αCSPG4(scFv)-ETA', tumor-free B6 Mice (n=3 per group) received 4 *i.v.* doses of 0.5, 1.0, 2.0, or 4.0 mg/kg of CFPs on days (0,1,3 and 5). The overall health status and weight of the mice was monitored daily. Monitoring continued for another 10 days. Mice were then sacrificed and their internal organs (Kidney, Heart, spleen and Liver) were examined by eye, and extracted and frozen in liquid nitrogen.

#### *II.2.7.2 Induction of subcutaneous tumors in BALB/c Nude mice*

Frozen Aliquot of MDA-MB-468, MDA-MB-231 or Katushka transfected MDA-MB468/tdKat and MDA-MB-231/td Kat cells, were thawed in fresh R-10 culture media with an additional 10% (v/v) FCS added to the media, when the flasks reached confluency, the cells were detached using 0.3 ml Trypsin-EDTA(Sigma) and 0.3 ml Accutase (Sigma), the cells were then split into 4 flasks and passaged twice (with Geneticin antibiotic selection for the Katushka transfected cells). The cells were next detached, washed with PBS, counted, and spun down and resuspended in PBS to a concentration of 5 x $10^7$ cells / ml. the cells were chilled on ice until injection. 2.5 x $10^6$ cells were injected subcutaneously in the lower flanks of BALB/c Nude mice.

For induction of tumors with Matrigel, prior to injection, the cells were mixed with the same volume of Matrigel (1:1 v/v).

#### *II.2.7.3 In vivo efficacy of anti EpCAM CFPs*

7 x $10^6$ MDA-MB-468/tdKat cells transfected with the red fluorescent Katushka-2 protein (II.2.1.6) were suspended in a 1:1 mixture of PBS and Matrigel (pH 7.4) and subcutaneously injected (80 µL) into the right hind limb of 6–8-week-old female BALB/c Nude mice (N=40) (Charles River, Erkrath, Germany). For imaging experiments, mice were placed on a purified, chlorophyll-free diet (AIN93G, SSNIFF GmbH, Soest, Germany) 11 days before the starting the imaging experiments. Treatment started on day 15 after tumor induction, when the tumors reached an average size of 50 $mm^2$ The animals were injected intravenously with GB-R201K-αEpCAM(scFv) (2.5 mg/kg), αEpCAM(scFv)-ETA' (1.2 mg/kg), αEpCAM (scFv)-SNAP (2.5 mg/kg) or PBS (pH 7.4) on days 13, 14, 17 and 19. Tumor size was measured using a caliper and by optical imaging using the Maestro CRi Imaging System (Maestro CRi Inc., Woburn, MA, USA). Images were analyzed using the Maestro Spectral Imaging Software (Maestro CRi Inc.) as previously described (25,30).

#### *II.2.7.4 In vivo efficacy of anti-CSPG4 CFPs*

2 x $10^6$ MDA-MB-231/tdKat cells transfected with the red fluorescent Katushka-2 protein (II.2.1.6) were suspended in a 1:1 mixture of PBS and Matrigel (pH 7.4) and subcutaneously injected (80 µL) into the right hind limb of 6–8-week-old female BALB/c Nude mice (Charles River, Erkrath, Germany). For imaging experiments, mice were placed on a purified, chlorophyll-free diet (AIN93G, SSNIFF GmbH, Soest, Germany) 11 days before the starting the imaging experiments. Treatment started on day 22 after tumor induction, when the tumors reached an average size of 50 $mm^2$ The animals were injected intravenously with αCSPG4(scFv)-MAP (2.5 mg/kg), αCSPG4(scFv)-ETA' (1.2 mg/kg), αCSPG4(scFv)-SNAP (2.5 mg/kg) or PBS (pH 7.4) on days 22, 24, 27 and 29. Tumor size was measured using a caliper and by optical imaging using the Maestro CRi Imaging System (Maestro CRi Inc., Woburn, MA, USA). Images were analyzed using the Maestro Spectral Imaging Software (Maestro CRi Inc.) as previously described (25,30).

#### *II.2.7.5 Biodistribution assay*

Mice bearing MDA-MB-231/tdKat or MDA-MB-468/tdKat tumors (II.2.7.2) (n=3 per group) were injected *i.v.* with 1 mg/kg labeled CFP per mouse. Optical imaging was performed at 1, 8 and 24 hours after injection using the Maestro CRi Optical Imaging

System (Maestro CRi Inc.). Images were analyzed using the Maestro Spectral Imaging Software (Maestro Cri Inc.). The Katushka-2 signal was detected using the yellow filter set (630-850 nm, 10 nm increment), the Alexa-747 signal was detected using the deep red filter set (700-950 nm, 10 nm increment).

#### *II.2.7.6 Determination of tumor size by caliper measurements*

Tumor diameters were measured by caliper (Thermo Fisher Scientific). The subcutaneous tumors were measured at their longest part (length) and shortest part (width). At each time point, the tumors were measured blindly by two different individuals and the tumor area was calculated according to the ellipse area formula (½length x ½ width x π). The average from the two different measurements was considered as the tumor area for each time point.

### *II.2.8 Statistical analysis*

Statistical analysis was performed using GraphPad Prism 5 (GraphPad Software Inc., La Jolla, CA, USA). Data were expressed as mean ± standard deviation (SD), 95% confidence interval (CI) or standard error of mean (SEM) as indicated. Statistical comparisons were made using a two-tailed unpaired Student's *t* test or two-way ANOVA, where appropriate. Binding affinity, Kd value and IC-50 values were calculated based on nonlinear regression analysis. unless otherwise specified: * $p \leq 0.05$, ** $p \leq 0.01$, *** $p \leq 0.001$.

# III Results

This work aimed to study new potential immunotherapeutic approaches to target some of the most aggressive breast cancer tumors- triple negative breast cancers (TNBCs). As TNBCs are actually a heterogeneous group of tumors, multiple surface receptors would be required to target the different TNBC subtypes. In this study two candidate molecules EpCAM and CSPG4 were chosen as they are differentially expressed on TNBCs and the majority of TNBC cell lines are overexpressing one or the other. Therefore the results section is divided into two major chapters (one for each target), each containing three parts, as follows:

The first part summarizes the generation and characterization of the scFv based cytolytic fusion proteins and their binding on TNBC cell lines. The second part details the *in vitro* results of the functionality and cytotoxicity assays of the CFPs on TNBC cell lines, and finally the third parts demonstrates the *in vivo* efficacy of those CFPs in a mouse subcutaneous tumor model. The major findings of these results have been published in two scientific articles (182, 183).

## *III.1 scFv based Cytolytic fusion proteins targeting EpCAM*

### *III.1.1 Generation and characterization of scFv based fusion proteins*

#### *III.1.1.1 Cloning and design of anti-EpCAM scFv fusion proteins*

Anti-EpCAM scFv C54 (148) (here forth referred to as αEpCAM(scFv) was kindly provided by our collaboration partner Prof. W. Helfrich, Groningen University. It was digested with restriction enzymes SfiI and NotI and ligated into three plasmids (Figure 1) to generate the following fusion proteins:

1. Granzyme B R201K-anti-EpCAM (GB-R201K-αEpCAM(scFv), Gb-αEp): The pMS expression plasmid encoding EGb-Ki4(scFv)R201K (155) was used to clone pMS-EGB-R201K-αEpCAM by replacing the coding sequence for the single chain variable fragment Ki4(scFv) with αEpCAM(scFv) (148). The construct (Figure 1A) includes an Enterokinase cleavage site, which enables the removal of the N' terminal pre-peptide in order to activate

the Granzyme B and generate the final product GB-R201K-αEpCAM(scFv). The scFv is located 3' to the Granzyme B and the poly-His tag is at the C' terminus.

2. anti-EpCAM(scFv)-ETA' (αEpCAM(scFv)-ETA', αEp-ETA'): the H22 scFv was excised from the pMT-H22-ETA' plasmid (137) and replaced with αEpCAM scFv by SfiI – NotI digest and ligation. This construct (Figure 1B) contains an N' terminal periplasmic leader peptide (PelB), poly-His tag and Enterokinase cleavage site before the scFv sequence. The scFv is connected to ETA' by a short peptide composed of 10 amino acids. The ETA' sequence ends with the ER retention sequence REDL.

3. anti-EpCAM(scFv)-SNAP tag (αEpCAM(scFv)-SNAP, αEp-SNAP): pMS-L-2715-SNAP-IV vector was used (97, 171). The 2715 scFv was replaced with the αEpCAM scFv. This construct (Figure 1C) contains an N' terminal Igκ leader sequence and a C' terminal poly-His tag. αEpCAM(scFv)-SNAP was used throughout this work as a non-cytolytic αEpCAM fusion protein control.

Successful ligation products were confirmed by sequencing analysis. All plasmid schemes and sequences can be found in the appendix (Plasmid Plasmid sequences).

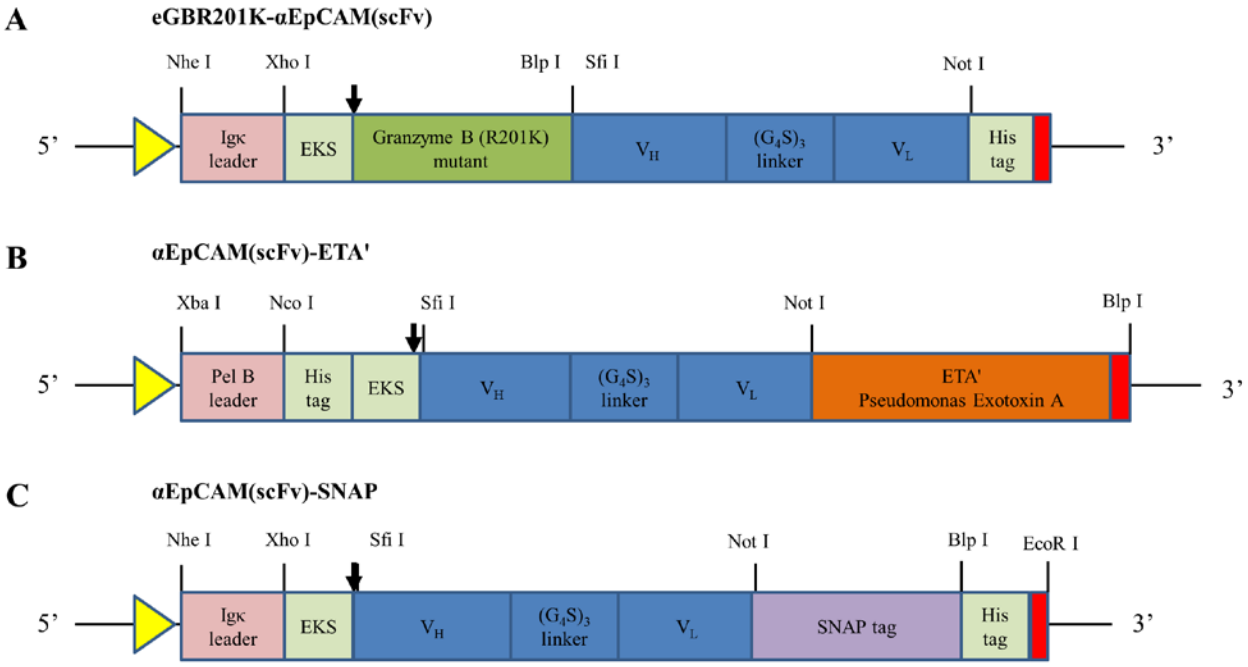



**Figure 1. Construction of EpCAM-specific fusion proteins.**

**A:** Schematic representation of GB-R201K-αEpCAM(scFv) open reading frame in the pMS vector VI.4.3 containing an Igκ leader sequence and an Enterokinase cleavage site (both at the N-terminus) and a polyhistidin tag (C-Terminus) **B:** Schematic representation of αEpCAM(scFv)-ETA' open

reading frame in the pMT vector VI.4.1 containing a pelB leader peptide, a poly-histidine tag and an Enterokinase cleavage site (all at the N-terminus) and a C' terminus 40 kDa truncated version of Pseudomonas aeruginosa Exotoxin A C: Schematic representation of αEpCAM(scFv)-SNAP open reading frame in the pMS vector VI.4.6 containing an Igκ leader sequence and an Enterokinase cleavage site (both at the N-terminus) and a polyhistidin tag (C-Terminus). Yellow triangle indicates start codon (ATG) and red rectangle indicates stop codon, black arrow indicates Enterokinase cleavage site, black lines indicate restriction enzyme positions. Abbreviations: EKS, Enterokinase site; $(G_4S)_3$; Glycine Serine linker containing three repeats of GGGGS peptide; $V_L$, light chain variable antibody fragment; $V_H$, heavy chain variable antibody fragment.

Unprocessed EGb-αEpCAM(scFv) and αEpCAM(scFv)-SNAP were expressed in HEK293T cells as described (II.2.1.7) and αEpCAM(scFv)-ETA' was expressed in BL21 bacteria (II.2.1.4). The poly Histidine tag was used for IMAC purification of EGb-αEpCAM(scFv) and αEpCAM(scFv)-SNAP, and was sufficient to achieve high purity (above 95%) of the protein. Yields were 8 mg per liter of culture medium for EGb-αEpCAM(scFv) (MW: 54 kDa, Figure 2 left panel) and 10 mg for αEpCAM(scFv)-SNAP (MW: 52kDa, Figure 2 Middle panel). In order to achieve high purity (>90%) αEpCAM(scFv)-ETA' was purified in a 2 step enrichment protocol using IMAC (II.2.2.1) followed by size exclusion chromotography (II.2.2.3), resulting in a yield of 4 mg per liter of bacterial culture (MW: 70 kDa, Figure 2 right panel). Proteins integrity, purity and identity were confirmed using SDS-PAGE and western blotting with anti-His tag antibody. Concentrating the proteins proved to be problematic, as both EGb-αEpCAM(scFv) and αEpCAM(scFv)-ETA' proteins appeared to aggregate, crystalize and precipitate during the dialysis or concentration processes (data not shown). Therefore the proteins were kept in concentrations between 0.2-0.4 mg/ml and stored at -20°C. Fusion proteins that were frozen for different periods of time up to 6 months, maintained high stability with low levels of degradation and retained their biological activities: selective binding and toxicity towards $EpCAM^+$ cells (data not shown).

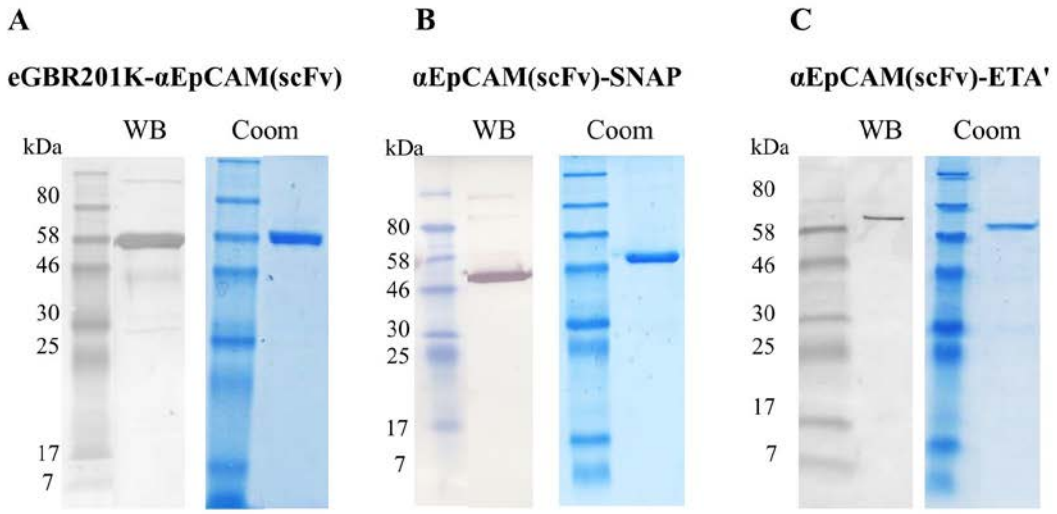



**Figure 2. Expression and purification of EpCAM specific fusion proteins.**

GB-R201K-αEpCAM(scFv) and αEpCAM(scFv)-SNAP proteins were expressed in HEK293T system (II.2.1.7) and the fusion proteins were purified from the supernatant via immobilized-metal affinity chromatography (IMAC) using a Ni-NTA super-flow column (II.2.2.1). αEpCAM(scFv)-ETA' was expressed periplasmically in *E. coli* BL21(DE3) under osmotic stress conditions in the presence of compatible solutes (II.2.1.4). Purification was carried out using IMAC followed by size exclusion chromatography (II.2.2.3). The purity and integrity of purified proteins was determined via SDS PAGE (II.2.4.2). 10 µl protein from each sample were separated by SDS PAGE and subsequent Western blot (II.2.4.3) and corresponding Coomassie-staining were performed for the following proteins: **A:** GB-R201K-αEpCAM(scFv), **B:** αEpCAM(scFv)-SNAP and **C:** αEpCAM(scFv)-ETA'. All proteins were detected using a mouse-anti-poly-His antibody (1:2000), followed by Alkaline Phosphatase conjugated-goat-anti-mouse IgG-antibody (1:5000) and visualized by NBT/BCIP substrate. Reaction was stopped by washing in water after the bands appeared clearly on the membrane (approximately 1-2 minutes exposure).

### *III.1.1.2 Granzyme B activation and serpin B9 detection*

In order to activate EGB-R201K-αEpCAM(scFv), Enterokinase digestion (II.2.2.4) was performed to release the pre peptide and free the amino terminus of Granzyme B, thus generating the enzymatically active GB-R201K-αEpCAM(scFv). The digest reaction was monitored using SDS-PAGE and stopped when a full cleavage of the EGB-R201K-αEpCAM(scFv) was observed (Figure 3 left). The proteolytic activity of GB-R201K-αEpCAM(scFv) before and after the cleavage was measured via colorimetric substrate assay (Figure 3 right). A comparable proteolytic activity was measured for GB-R201K-αEpCAM(scFv) and the Granzyme B commercial control.

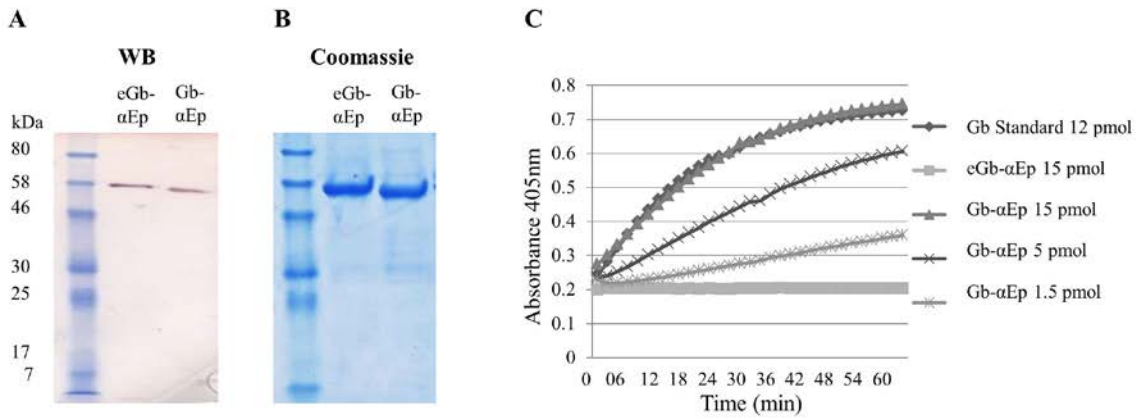



**Figure 3. Activation of GB-R201K-αEpCAM(scFv) proteolytic activity.**

Purified EGB-R201K-αEpCAM(scFv) (II.2.2.1) was digested using recombinant Enterokinase (0.4 units/ 10 µg protein (II.2.2.4) to remove the N-terminus pre-peptide. SDS PAGE (II.2.4.2) of EGB-R201K-αEpCAM(scFv) CFP before Enterokinase digest and GB-R201K-αEpCAM(scFv) after digest was carried out to confirm the digest **A:** 5 µg protein per sample were analyzed by Western blot analysis (II.2.4.3) and corresponding **B:** Coomassie staining (II.2.4.2) of 10 µg protein per sample before and after Enterokinase digest. Proteins were detected using anti His antibody as described in Figure 2. **C:** Proteolytic activity of GB-R201K-αEpCAM(scFv) (II.2.2.4). The enzymatic activity of GB-R201K-αEpCAM(scFv) and its undigested form EGB-R201K-αEpCAM(scFv) was determined by a colorimetric assay based on the synthetic Granzyme B substrate Ac-IETD-pNA Absorbance at 405 nm (II.2.4.4). The reaction was monitored in a 2-min interval for 60 min at 37 °C. Points on graph represent average of two reactions per sample. Abbreviations: eGb-αEp, undigested Granzyme B-αEpCAM (scFv); Gb-αEp, Enterokinase digested Granzyme B-αEpCAM (scFv); Gb standard, commercial Granzyme B.

Granzyme B inhibitor-Serpin B9 (PI-9) expression in TNBC cell lines was detected by western blotting (Figure 4). MDA-MB-231 cells tested positive for the full length PI-9 protein -MW 42 kDa. As for MDA-MB-468 cells, a positive band of approximately 20 kDa was detected. This size corresponds to one of PI-9 active splice variants (data from NCBI-AceView genes database (160). However, in the span of this work, no other available sources were found with information regarding serpin B9 expression in this cell line. In the case of MDA-MB-453 cell line, the cells appear to be PI-9 negative as no band was detected in the western blotting (Fig 4).

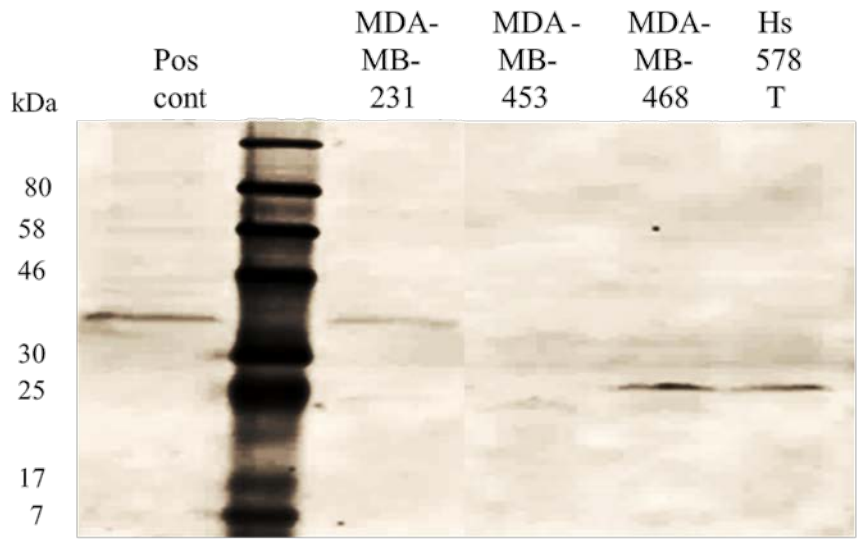



**Figure 4. Detection of Serpin B9 (PI-9) in TNBC cell lines.**

Triple-negative breast cancer cell lines MDA-MB-231, MDA-MB-453, MDA-MB-468 and Hs578T were lysed (II.2.5.6) and analyzed for PI-9 expression by western blotting (II.2.4.3). Serpin B9 was detected using a serpin B9-specific antibody (1:500, Santa Cruz, USA), followed by Goat anti-mouse IgG-AP conjugated antibody. The signal was visualized using NBT/BCIP substrate. Once the bands became visible, the membrane was washed with water to stop the reaction.

#### *III.1.1.3 EpCAM expression on TNBC cell lines*

EpCAM expression levels on TNBC cell lines were determined via flow cytometry using a commercial anti-EpCAM antibody (Figure 5). TNBC cell lines MDA-MB-453 and MDA-MB-486 and BT-20 had high expression levels of EpCAM, while MDA-MB-231 and Hs 578T had low or no expression of EpCAM.

#### *III.1.1.4 Binding analysis of αEpCAM fusion proteins on TNBC cell lines*

Specific binding of GB-R201K-αEpCAM(scFv) and αEpCAM(scFv)-ETA' on TNBC cell lines and their affinity constants $K_d$ were determined by flow cytometry in a binding and saturation assay as described before (179) (Figure 6 & Figure 7). Specific binding of αEpCAM fusion proteins was observed on MDA-MB-453 and MDA-MB-468, and no binding was detected on MDA-MB-231 cells which have very low expression levels of EpCAM (Figure 6).

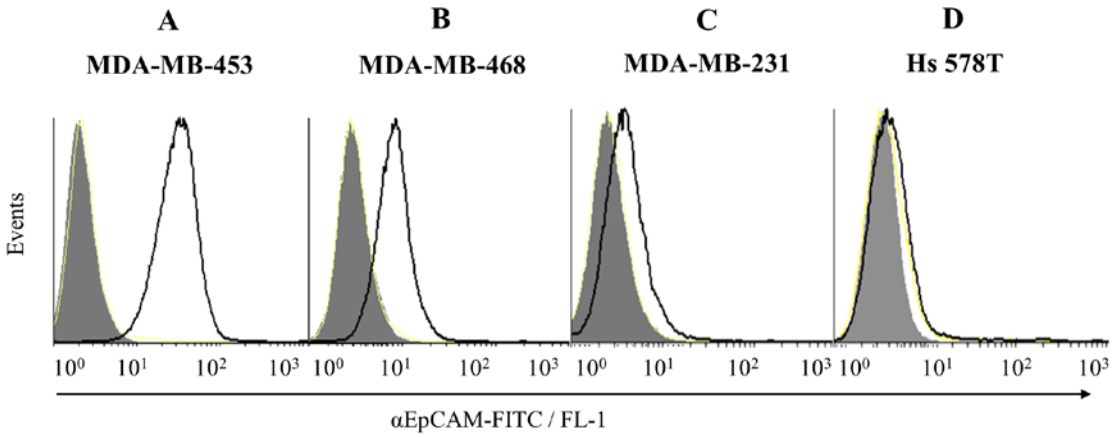



**Figure 5. Expression of EpCAM receptor in TNBC cell lines.**

EpCAM expression on the surface of indicated TNBC cell lines **A:** MDA-MB-453, **B:** MDA-MB-468, **C:** MDA-MB-231 and D: Hs578T was determined by flow cytometric analysis (II.2.5.1.1) using anti-EpCAM antibody. 1 x $10^5$ cultured cells per sample were stained with 0.5 µg anti-EpCAM antibody on ice for 20 minutes, followed by goat anti mouse IgG-FITC conjugated antibody. Cells were washed twice with PBS and the fluorescent signal was measured via FACSCalibur. Black lines indicate EpCAM-FITC signal, grey curve represents non stained control.

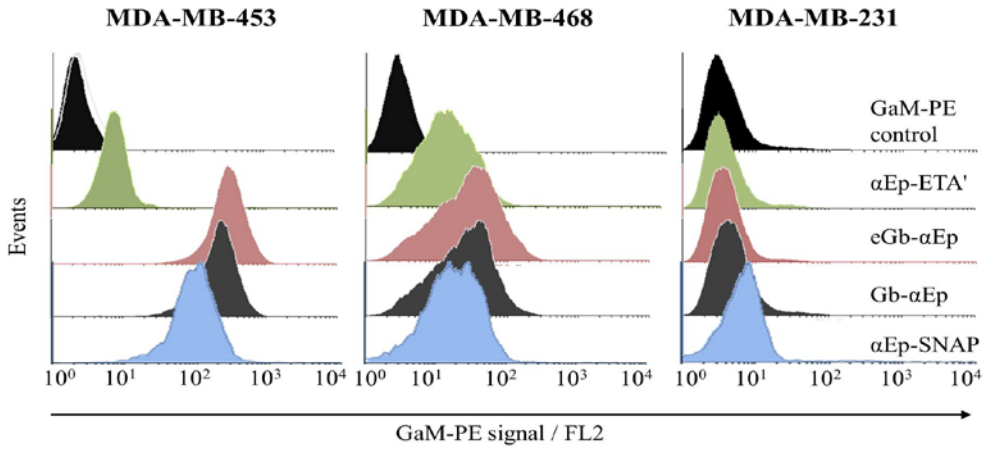
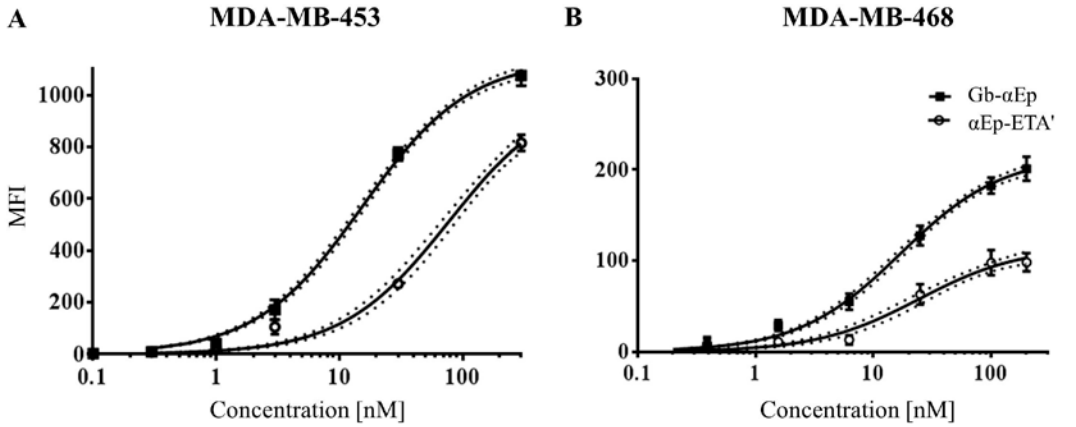



**Figure 6. Binding of purified EpCAM specific CFPs on TNBC cell lines.**

Binding analysis of EpCAM-specific CFPs to different TNBC cell lines using flow cytometry (II.2.5.1.1). 200 nM of the indicated CFPs (right side) were incubated with 1 x 105 of indicated cells on ice for 20 minutes, followed by incubation with mouse anti-His antibody and GaM-IgG-PE staining. Abbreviations: eGb-αEp, undigested Granzyme B-R201K-αEpCAM (scFv); Gb-αEp, Enterokinase digested Granzyme B-R201K-αEpCAM (scFv); αEp, αEpCAM (scFv); GaM-PE, PE-conjugated goat-anti-mouse IgG antibody.

A binding saturation assay was performed to determine the affinity by measuring the $K_d$ values. $K_d$ values were determined using One-site binding analysis in GraphPad PRISM software and a nonlinear fit regression was used to interpolate the standard curve. The $K_d$ values calculated indicated a slightly higher affinity for GB-R201K-αEpCAM(scFv) with slightly lower $K_d$ than that of αEpCAM(scFv)-ETA', 15.06 nM and 74.96 nM respectively for MDA-MB-453, and 17 nM and 24 nM for MDA-MB-468 cells (Figure 7).




| Best-Fit values | αEp-ETA' | Gb-αEp |
|---|---|---|
| Bmax (MFI) | 1025 | 1140 |
| Kd (nM) | 77.80 | 15.43 |

| Best-Fit values | αEp-ETA' | Gb-αEp |
|---|---|---|
| Bmax (MFI) | 115.6 | 215.8 |
| Kd (nM) | 24.39 | 17.04 |

**Figure 7. Saturation curve and binding affinity of EpCAM specific CFPs in TNBC cell lines.**

The binding saturation curves of CFPs on **A:** MDA-MB-453 and **B:** MDA-MB-468 cells were determined using a flow cytometric assay and nonlinear regression analysis (II.2.5.1.2). The $K_d$ and $B_{max}$ values were calculated using GraphPad Prism software (II.2.8). The curve represents the nonlinear regression interpolation, and the dotted lines represent the 95% confidence interval. Points on graph represent the mean of 3 measurements and error bars represent 95% confidence interval. Abbreviations: Gb-αEp, Granzyme B-R201K-αEpCAM (scFv); αEp-ETA', αEpCAM (scFv)-ETA'; Kd, equilibrium dissociation constant in nM; MFI, Mean Fluorescence intensity as calculated by cyflogic- FACS analysis software. Abbreviations: Gb-αEp, Granzyme B-R201K-αEpCAM(scFv); αEp-ETA', αEpCAM(scFv)-ETA'.

## *III.1.2 Functional assays with αEpCAM fusion proteins*

### *III.1.2.1 Internalization and cellular uptake kinetics of αEpCAM fusion proteins*

The cytolytic activity of the proteins depends not only on their specific binding but requires them to be efficiently internalized into the cells. Therefore, the specific binding and internalization of αEpCAM CFPs were confirmed by confocal microscopy. Surface binding of TNBC cell lines by both GB-R201K-αEpCAM(scFv) and αEpCAM(scFv)-ETA' proteins was observed at 4 °C (Figure 8). Gb and ETA' moieties were detected in vesicles inside the cells after 2 hours incubation at 37 °C with $EpCAM^{+}$ MDA-MB-468 (Figure 8, 1$^{st}$ and 3$^{rd}$ columns) but not in $EpCAM^{low}$ cell line MDA-MB-231 (Figure 8.2$^{nd}$ and 4$^{th}$ columns). 24 hours after, the signal was still visible and spread over the cell, indicating the delivery of Gb and ETA' into the cytosol of MDAMB-468 cells (Figure 8, bottom row).

Furthermore, to determine the kinetics of cellular uptake, an indirect internalization FACS assay was performed (II.2.5.1.3) in which the levels of surface receptor were quantified following different incubation periods with the CFPs at 37 °C. The results show that 50% internalization was achieved between 1 to 2 hours of incubation at 37 °C for GB-R201K-αEpCAM(scFv) and 2 hours for αEpCAM(scFv)-ETA' (Figure 9).

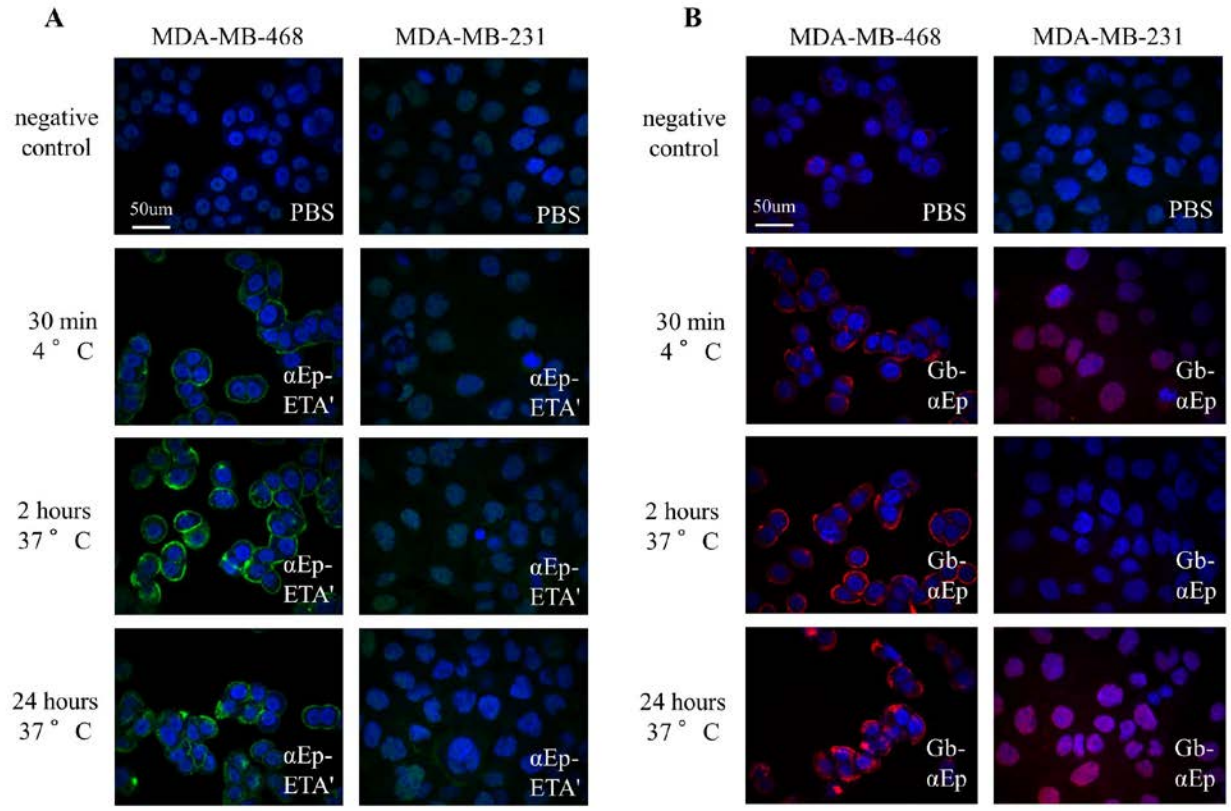



**Figure 8. Binding and internalization of CFPs in EpCAM positive MDA-MB-468 cell line.**

High throughput confocal microscopy imaging (0) of the binding and internalization of **A:** αEpCAM(scFv)-ETA' and **B:** GB-R201K-αEpCAM(scFv) on EpCAM$^{high}$ MDA-MB-468 cells (left) and EpCAM$^{low}$ MDA-MB-231 cells (right). αEpCAM(scFv)-ETA' was detected using anti-ETA' antibody followed by FITC-conjugated Goat-α-mouse IgG antibody and GB-R201K-αEpCAM(scFv) was detected using anti-Granzyme B antibody followed by Alexa-647-conjugated Goat-anti-mouse-IgG antibody (0). Images were taken on the Opera imaging system. Scale bar = 50 µm (upper left, equal for all). Abbreviations: Gb-αEp, Granzyme B-R201K-αEpCAM(scFv); αEp-ETA', αEpCAM(scFv)-ETA'.

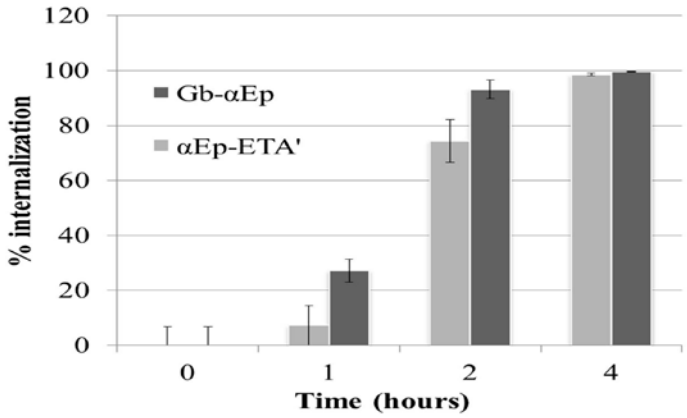
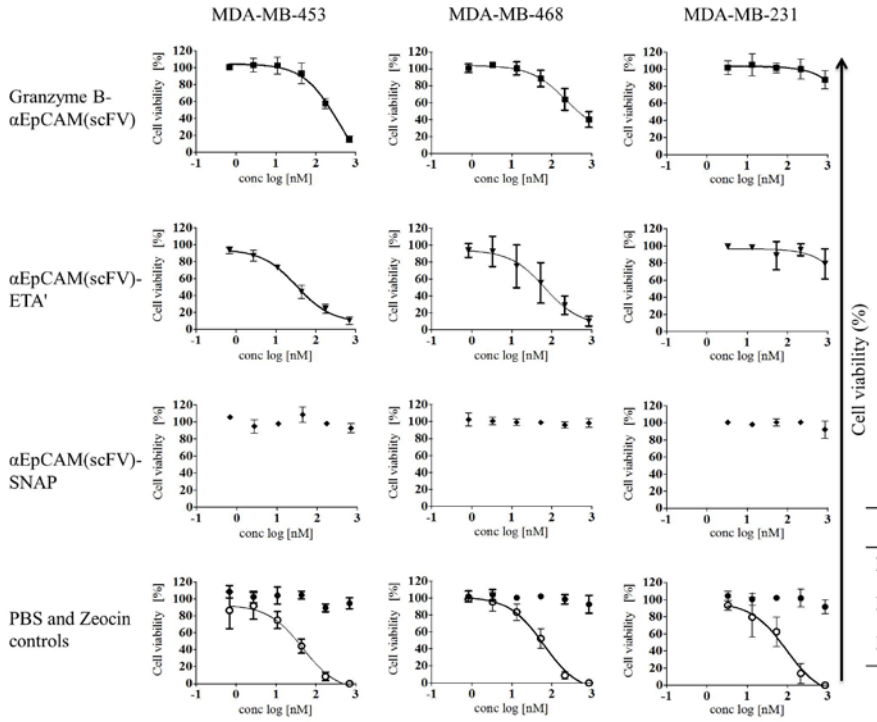



**Figure 9. Internalization kinetics of CFPs in MDA-MB-468 cell line.**

Graphical representation of the internalization rates at 37 C of GB-R201K-αEpCAM(scFv) and αEpCAM(scFv)-ETA' in MDA-MB-468 cells measured by flow cytometry in an indirect internalization assay (II.2.5.1.3). Cells were incubated for different intervals with the fusion proteins, the surface bound fusion protein was fluorescently labeled and the signal at each time point was expressed as percentage of the signal of control samples kept at 4°C. Values on graph represent the average of 2 independent experiments. Error bars represent standard deviation (SD). Statistical analysis was carried out using GraphPad PRISM (II.2.8). Abbreviations: Gb-αEp, Granzyme B-R201K-αEpCAM(scFv); αEp-ETA', αEpCAM(scFv)-ETA'.

### *III.1.2.2 Cytotoxic effects of αEpCAM CFPs in TNBC cells in vitro*

The cytotoxicity of GB-R201K-αEpCAM(scFv) and αEpCAM(scFv)-ETA' towards MDA-MB-468, MDA-MB-453 and MDA-MB-231 was determined by XTT cell viability assay. Cell growth inhibition was detected after 48 hours of treatment for both EpCAM-positive cell lines MDA-MB-453 and 468 in a dose dependent manner (Figure 10, 1st & 2nd columns). No significant effect was observed for EpCAM low MDA-MB-231 cells (Figure 10, 3rd column). αEpCAM(scFv)-ETA' had 4 to 5 folds higher toxicity than the GB-R201K-αEpCAM(scFv) CFP. The $IC_{50}$ values calculated were in the Nano molar range with approximately 50nM for αEpCAM(scFv)-ETA' and 250nM for GB-R201K-αEpCAM(scFv). The non cytolytic fusion protein αEpCAM(scFv)-SNAP which has comparable binding affinity and internalization kinetics to the αEpCAM(scFv) CFPs did not inhibit cell growth in any of the cell lines (Figure 10, 3rd row), suggesting that the mere binding and internalization of EpCAM using our scFv are not sufficient to induce a cytotoxic effect.




| IC50 (nM) | Gb-αEp | αEp-ETA' |
|---|---|---|
| MDA-MB-453 | 307 ± 21.36 | 32.9 ± 2.96 |
| MDA-MB-468 | 221.8 ± 10.27 | 66.4 ± 9.74 |
| MDA-MB-231 | No toxicity | No toxicity |

**Figure 10. Growth inhibition of TNBC cells *in vitro* by αEpCAM specific CFPs.**

XTT cell viability assay was carried out (II.2.6.1) with serial dilution of d EpCAM-specific CFPs: Gb-R201K-anti-EpCAM(scFv), anti-EpCAM(scFv)-ETA', anti-EpCAM(scFv)-SNAP and PBS and Zeocin controls (top to bottom), in MDA-MB-453, MDA-MB-468 and MDA-MB-231 cells respectively. The table represents non-linear regression analysis and $IC_{50}$ values that were calculated using GraphPad Prism 5 software (II.2.8). Values are represented as mean (n=4) ± SEM. Abbreviations: Gb-αEp, Granzyme B-R201K-αEpCAM(scFv); αEp-ETA', αEpCAM(scFv)-ETA'.

### *III.1.2.3 Induction of apoptosis by αEpCAM fusion proteins in TNBC cell lines*

To demonstrate that the cytotoxicity of αEpCAM CFPs in MDA-MB-468 cells is mediated by apoptosis an Annexin V apoptosis assay was performed Figure 11). Following 48 hours of treatment with the IC-50 concentration of each CFP (50 nM for ETA', 250nM for Gb), the percentage of cells detected in the early apoptotic phase (Annexin $V^+$, $PI^-$) increased from 3% in the PBS control to 30-40% in the treated cells. Many of the treated cells were already in the late apoptotic phase (Annexin $V^+$, $PI^+$, 20%-30%) or dead (Annexin $V^-$, $PI^+$) – cell debris were excluded from the analysis. No unspecific toxicity was observed in the Mock (scFv)-Granzyme B control, Gb-Ki4 (Figure 11).

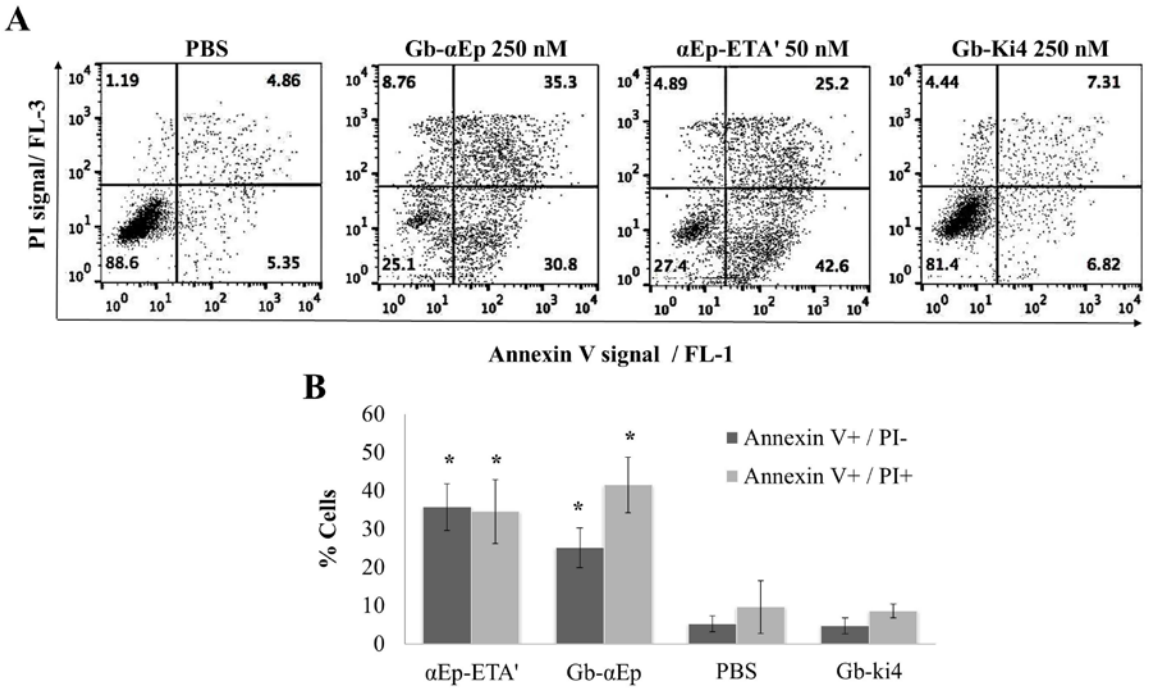



**Figure 11. Induction of apoptosis in MDA-MB-468 cells by EpCAM-specific CFPs.**

Annexin V apoptosis assay of different CFPs on MDA-MB-468 cells was carried out as described (II.2.6.2). **A:** Representative dot blots of cells stained with recombinant Annexin V-GFP and propidium iodide and analyzed by flow cytometry. The cells were incubated for 48 hours with 250 nM of GB-R201K-αEpCAM(scFv), 50 nM αEpCAM(scFv)-ETA' or the negative control GB-R201K-Ki4(scFv) (anti-CD30). **B:** Graph summarizing the results of 3 independent assays. The black bars represent % of cells in early apoptosis (Annexin $V^+$ / Propidium $Iodide^-$) and the grey bars represent late apoptotic cells (Annexin $V^+$ / Propidium $Iodide^+$). Error bars represent SEM. Statistical analysis was carried out using a two tailed unpaired t-test. *$p \leq 0.005$ compared to the PBS control. Abbreviations: Gb-αEp, Granzyme B-R201K-αEpCAM(scFv); αEp-ETA', αEpCAM(scFv)-ETA'.

### *III.1.2.4 Activation of cellular apoptotic pathways by αEpCAM CFPs*

The apoptotic features following treatment with CFPs were analyzed after 7 and 24 hours. Cleavage and activation of caspase 3 is one of the major processes that initiate cellular apoptosis through the caspase apoptotic pathway (184). Active caspase 3 was detected in the cell lysate by immunoblotting using a cleaved caspase 3-specific antibody (II.2.6.3). A strong signal of cleaved caspase 3 was observed after 7 h with GB-R201K-αEpCAM(scFv), and only moderate signal for αEpCAM(scFv)-ETA' (Figure 12, left panel). the cleavage of DNA repair polymerase Poly (ADP-Ribose) Polymerase 1 (PARP-1) which is a downstream process of several apoptotic pathways was also studied (185). Partial cleavage of PARP-1 was already detected after 7 hours, reaching almost full cleavage after 24 hours (Figure 12, middle panel). Additionally, the activation of another apoptotic pathway was analyzed,

namely caspase 9, known to be a substrate of cytochrome C and the mitochondrial apoptotic pathway (186). Both αEpCAM(scFv)-ETA' and GB-R201K-αEpCAM(scFV) treatment resulted in strong activation of caspase 9 in a colorimetric caspase 9 substrate assay, with approximately 7-fold activity for αEpCAM(scFv)-ETA' and 6-fold for GB-R201K-αEpCAM(scFv) compared to the basal level of caspase 9 activity (Figure 13).

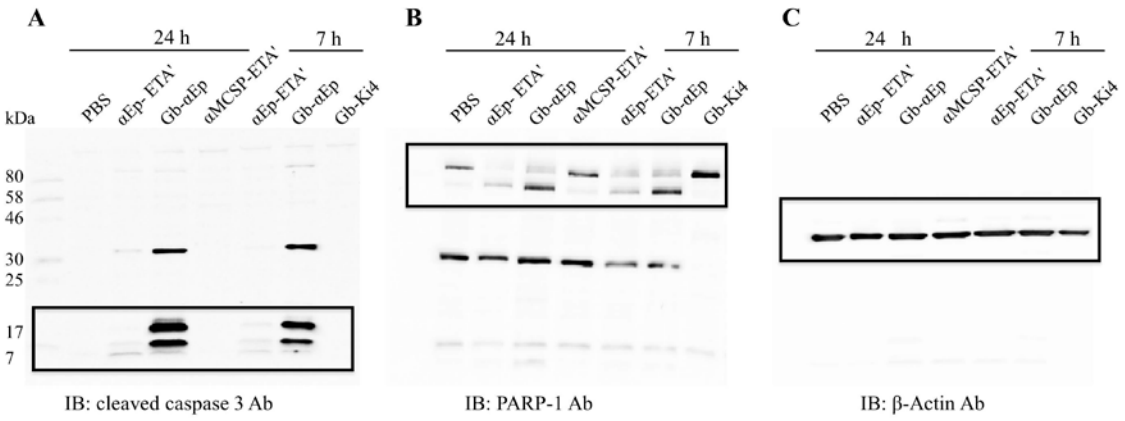



**Figure 12. Activation of caspase 3 apoptosis pathway by EpCAM specific CFPs.**

Western blot analysis (II.2.4.3) for the detection of **A:** caspase-3 and **B:** PARP-I cleavage in cell lysates (II.2.6.3) from MDA-MB-468 cells (II.2.1.5) treated for 24 hours or 7 hours with PBS (1st lane) or 50 nM αEpCAM(scFv)-ETA' (2nd & 5th lanes) or 200 nM GB-R201K-αEpCAM(scFv) (3rd & 6th lanes). αCSPG4(scFv)-ETA' (4th lane) and GB-R201K-Ki4(scFv) (7th lane) were used as negative controls. **C:** β-Actin immunoblotting was used as an equal loading control. Abbreviations: PARP-1, Poly (ADP-Ribose) Polymerase 1; IB, Immunoblotting; Ab, antibody. Abbreviations: Gb-αEp, Granzyme B-R201K-αEpCAM(scFv); αEp-ETA', αEpCAM(scFv)-ETA'.

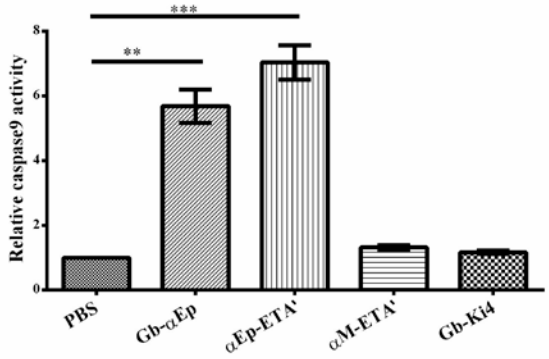



**Figure 13. Activation of caspase 9 apoptosis pathway by EpCAM specific CFPs.**

Induction of caspase-9 activity by αEpCAM CFPs in MDA-MB-468 cells was determined by a pre-luminescent caspase 9-DEVD-aminoluciferine substrate assay (II.2.6.4). Data are representatives of the mean (n=3) + SD. Results were normalized to the background signal of PBS control. GB-R201K-α CD30(scFv) (Gb-Ki4) and αCSPG4(scFv)-ETA' (M-ETA') were used as negative controls. Statistical analysis was carried out using a two-tailed unpaired Student's *t* test (II.2.8). ***p≤0.001, **p≤0.005

compared to the buffer control. Abbreviations: Gb-αEp, Granzyme B-R201K-αEpCAM(scFv); αEp-ETA', αEpCAM(scFv)-ETA'.

## *III.1.3 in vivo evaluation of αEpCAM CFPs*

### *III.1.3.1 Establishment of subcutaneous tumors in BALB/C Nude mice*

Initial in vivo studies sought to explore the best protocol for inducing the MDA-MB-468 tumor model. The following protocol was used (table 9) in an attempt to determine whether the cells transfected with Katushka fluorescent protein (II.2.1.6) would grow subcutaneously as well as non-transfected cells would, and whether the use of Matrigel would be beneficial to achieve a homogenous growth of the tumors compared to the injection of the cells alone.

**Table 9. Induction of subcutaneous MDA-MB-468 tumors in BALB/C nude mice (II.2.7.2):**

| | **Right lower flank** | **Left lower flank** |
|---|---|---|
| Group 1- (N=2) | Katushka transfected– with Matrigel (1:1) | Not transfected – with Matrigel (1:1) |
| Group 2- (N=3) | Katushka transfected- without Matrigel | Not transfected- without Matrigel |

Tumor growth was monitored by optical imaging with Cri Meastro system and by caliper measurements for 30 days. 100% take rate was observed. The results revealed similar growth pattern for the Katushka transfected cells compared to the non-transfected cell in the Matrigel set up (Figure 14 D). The group injected with the cells without Matrigel (Figure 14 C) had more variability in the tumor sizes and rate of growths independently from Katushka transfection status (Figure 14 A & B). Therefore, the protocol chosen for the following experiments was the induction of tumors using Katushka transfected cells with Matrigel-PBS mixture in a 1:1 ratio.

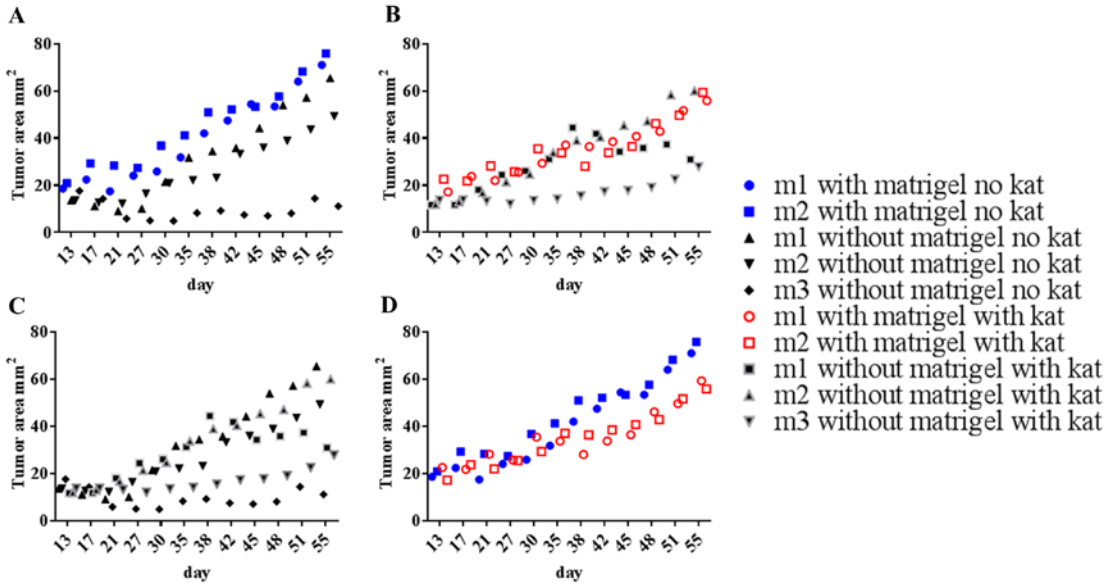



**Figure 14. Tumor take-rate of MDA-MB-468 cell line in a subcutaneous tumor model.**

**A:** MDA-MB-468 cells (II.2.1.5) or **B:** MDA-MB-468 transfected with Katushka fluorescent protein (II.2.1.6) were injected **C:** without or **D:** with Matrigel (1:1 ratio) in the hind flank of BALB/C Nude mice (II.2.7.2). Tumor width (W) and length (L) were measured using caliper and the tumor area (II.2.7.6) was calculated according to elliptical area formula (Pi x W/2 x L/2).

### *III.1.3.2 Tumor targeting and biodistribution studies in vivo*

αEpCAM(scFv)-ETA' and GB-R201K-αEpCAM(scFv) were labeled with a DyLight 747-NHS ester dye (Figure 15) as described (II.2.7.5). Fluorescence measurements were carried out using the CRi Meastro imaging system at elapsed time points of 1, 8 and 24 hours post-injection into BALB/c [nu/nu] mice bearing MDA-MB-468/tdKat subcutaneous tumors.

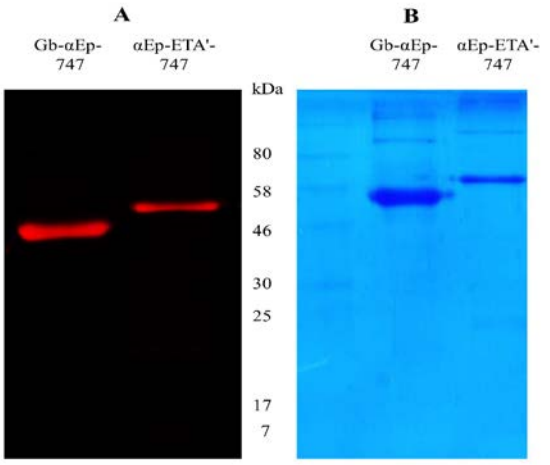



**Figure 15. Labeling of EpCAM specific CFPs with DyLight 747-NHS fluorescent dye**

GB-R201K-αEpCAM(scFv) (II.2.2.1) and αEpCAM(scFv)-ETA' (II.2.2.3) were labeled (II.2.3.2) with a 2 fold molar excess of DyLight-747-NHS ester dye for two hours. Excess dye was removed using zeba- desalting spin column. Samples were next separated on SDS PAGE (II.2.4.2). **A:** Visualization of fluorescent signal of labeled protein using CRi Maestro system, using the deep red filter set (II.1.13). **B:** subsequent Coomassie staining of the same SDS PAGE (II.2.4.2), to determine purity and degradation level. Abbreviations: Gb-αEp, Granzyme B-R201K-αEpCAM(scFv); αEp-ETA', αEpCAM(scFv)-ETA'.

Following *i.v.* administration of labeled CFPs, a fluorescent signal of DyLight 747 was observed in the injection site followed by rapid distribution to highly perfused organs (Figure 16). The results from αEpCAM(scFv)-ETA'-747 reveal rapid clearance of the fluorescent signal from most of the central compartment organs apart from the kidneys where the signal remained for up to 24h. Accumulation of αEpCAM(scFv)-ETA'-747 fluorescence in the tumor site was detected starting from 1 hour post injection and increased as the signal from the other compartments was fading. The signal in the tumor site remained detectable for at least 24 hours (Figure 16 A). Imaging of the primary fluorescent signal of the MDA-MB-468/tdKat cells clearly showed the co-localization of αEpCAM(scFv)-ETA'-747 in the tumor tissue.

As for GB-R201K-αEpCAM(scFv)-747, the fluorescent signal was retained in most of the central compartment organs, as well as in the stomach in 2 out of 3 mice (Figure 16 B). This signal was not observed in the αEpCAM(scFv)-ETA'-747 treated group. To avoid measurement errors and artifacts from the NHS ester labeling and limited tissue penetration of the fluorescent signal, unlabeled GB-R201K-αEpCAM(scFv)-747 and αEpCAM(scFv)-ETA' were injected *i.v.* to another group of mice bearing the MDA-MB-468/tdKat tumors.

In this case the mice were sacrificed at the different time points, and the tumors, kidneys, hearts, livers and spleens were extracted and frozen for sectioning. Representative tissue sections were prepared, CFP presence in the tumor tissue was detected by immunofluorescence 8 hours after injection (Figure 17) and immunohistochemistry was used to detect the CFPs in the kidney at different time points (Figure 18) using an anti-poly-His antibody as described in MM. The results confirmed the observations from the *in vivo* imaging experiment.

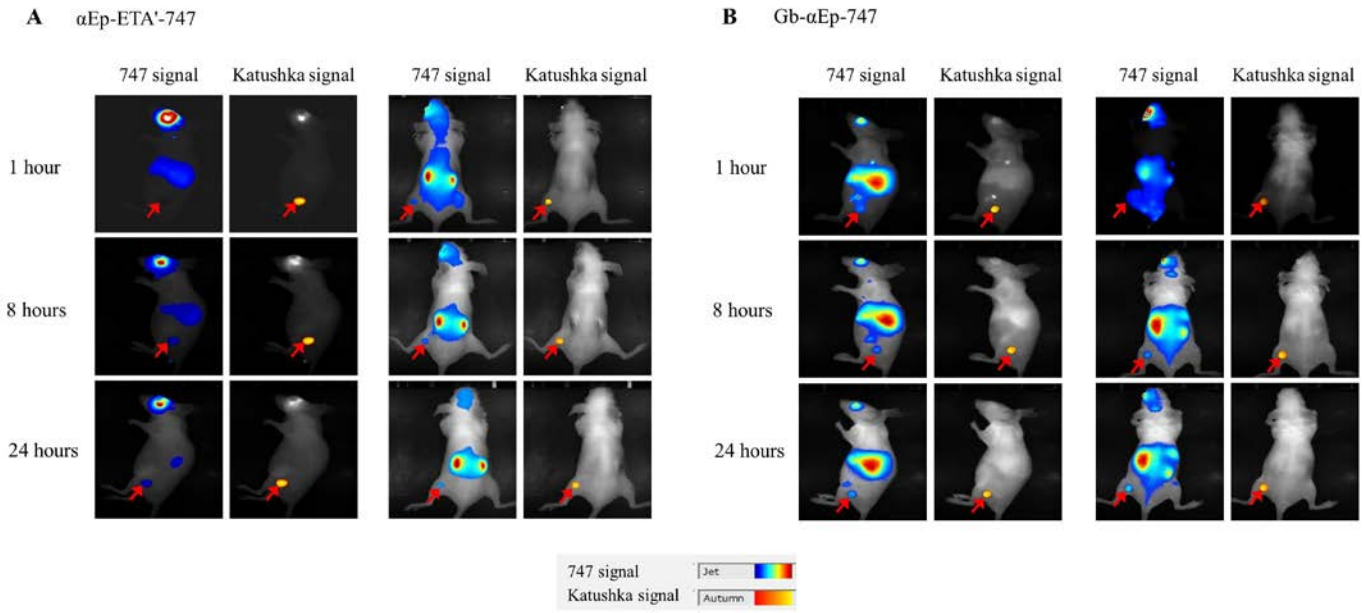



**Figure 16. Biodistribution of fluorescently-labeled αEpCAM CFPs in mice bearing MDA-MB-468 tumors.**

Whole body imaging of mice bearing Katushka-transfected MDA-MB-468/tdKAT (II.2.7.2) tumors injected *i.v.* with 1mg/kg of **A:** αEpCAM(scFv)-ETA' and **B:** GB-R201K-αEpCAM(scFv) labeled with NHS ester-DyLight 747 dye II.2.3.2). *In vivo* imaging was carried out 1 hour, 8 hours and 24 hours after injection (II.2.7.5). Fluorescent signal was converted into a heat-map using the Maestro software. Abbreviations: Gb-αEp, Granzyme B-R201K-αEpCAM(scFv); αEp-ETA', αEpCAM(scFv)-ETA'.

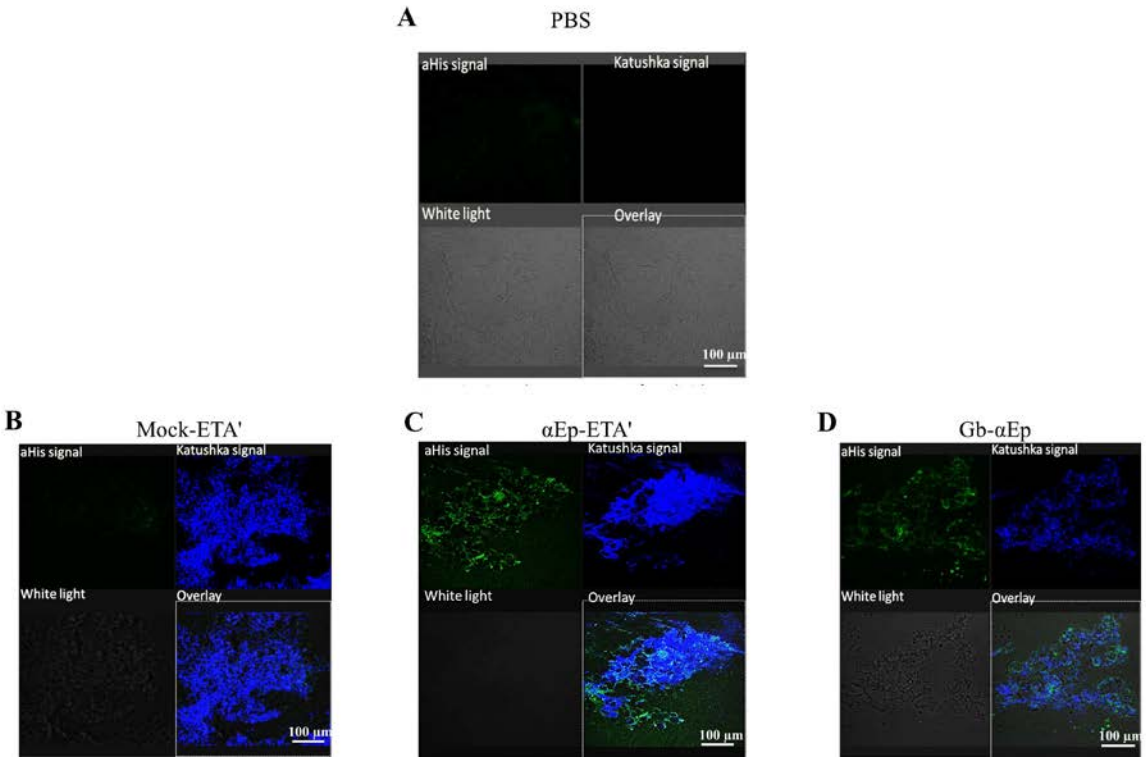



**Figure 17. Detection of EpCAM specific CFPs in tumor sections of MDA-MB-468 tumor-bearing mice 8 hours after treatment.**

Mice bearing (II.2.7.2) **A:** MDA-MB-468 and **B-D:** Katushka-transfected MDA-MB-468/tdKat (II.2.1.6) tumors were sacrificed 8 hours after *i.v.* administration of A: PBS, **B:** αCSPG4(scFv)-ETA', **C:** αEpCAM(scFv)-ETA' or **D:** GB-R201K-αEpCAM(scFv) and frozen tissue sections were prepared from extracted tumors for subsequent immunofluorescence staining (II.2.5.4). CFPs were detected using an anti-His-alexa488 antibody. Images were taken on a Leica TCS SP8 microscope with 40x objective. Scale bar = 100 µm (bottom right). Abbreviations: Gb-αEp, Granzyme B-R201K-αEpCAM(scFv); αEp-ETA', αEpCAM(scFv)-ETA'.

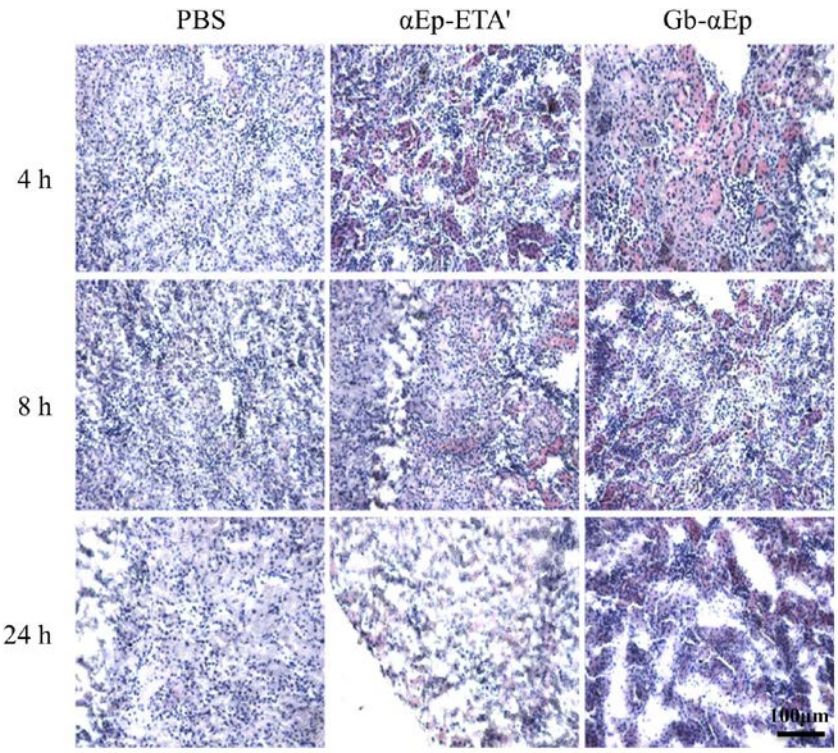



**Figure 18. Detection of EpCAM specific CFPs in kidney sections of treated mice 4 to 24 hours after treatment.**

Mice bearing MDA-MB-468/tdKat tumors (II.2.7.2) were sacrificed 4, 8 or 24 hours after *i.v.* injection of PBS, αEpCAM(scFv)-ETA' or GB-R201K-αEpCAM(scFv) and frozen tissue sections were prepared from harvested kidneys for immunohistochemistry (II.2.5.5). CFPs were detected using anti-His-tag rabbit antibody followed by alkaline phosphatase-labeled goat anti-rabbit antibody. Counterstaining was performed using hematoxylin. Images were taken on a Leica DM IL inverted microscope with 10x objective. Scale bar = 100 µm (bottom right, equal for all). Abbreviations: Gb-αEp, Granzyme B-R201K-αEpCAM(scFv); αEp-ETA', αEpCAM(scFv)-ETA'.

### *III.1.3.3 In vivo toxicity and therapeutic activity of CFPs*

#### *III.1.3.3.1 Maximum tolerated dose studies*

Prior to treatment experiments, the toxicity of GB-R201K-αEpCAM(scFv) was assessed in tumor-free mice. Three mice per treatment group received 4 doses *i.v.* of 0.5, 1.0, 2.0, or 4.0 mg/kg of GB-R201K-αEpCAM(scFv). The overall health status of the mice was monitored. No mortality or any significant body weight loss was observed following treatment (Table 10). 7 days after end of treatment the mice were sacrificed and their organs were harvested for further study. No visible tissue damage was observed for liver, spleen, and kidneys (data not shown). Maximum tolerated dose could not be reached, but these data

suggest that GB-R201K-αEpCAM(scFv) is well tolerated. Based on previously published studies, αEpCAM(scFv)-ETA' maximum tolerated dose was estimated between 1- 2mg/kg (187).

**Table 10. GB-R201K-αEpCAM(scFv) dose escalation study in mice:**

| **Dose** | **0.5 mg/kg** | **1 mg/kg** | **2 mg/kg** | **4 mg/kg** |
|---|---|---|---|---|
| Survival | 3/3 | 3/3 | 3/3 | 3/3 |
| Body weight loss | none | none | none | none |

Dose escalation and maximum tolerated dose of GB-R201K- αEpCAM(scFv) were determined (II.2.7.1). Four different doses (0.5, 1, 2 and 4 mg / Kg) were administered i.v. to mice (n=3) on days 0, 1, 3 and 5. The overall health, weight and survival of the mice were monitored every day.

### *III.1.3.3.2 Efficacy of EpCAM targeting CFPs in a Xenograft tumor model*

Next, the efficacy of GB-R201K-αEpCAM(scFv) was tested using a MDA-MB-468/tdKat xenograft mouse model. Due to the high viscosity and the tendency to precipitate in high concentrations of these fusion proteins and the limited volume that could be injected (100 ul per mouse a day), a 2.5 mg/kg GB-R201K-αEpCAM(scFv) concentration was used for the treatment studies. Tumor sizes were monitored using *in vivo* imaging of Katushka signal and caliper measurements, and comparable results were observed for both methods. Overall health condition and body weight were monitored throughout the experiment (Figure 19).

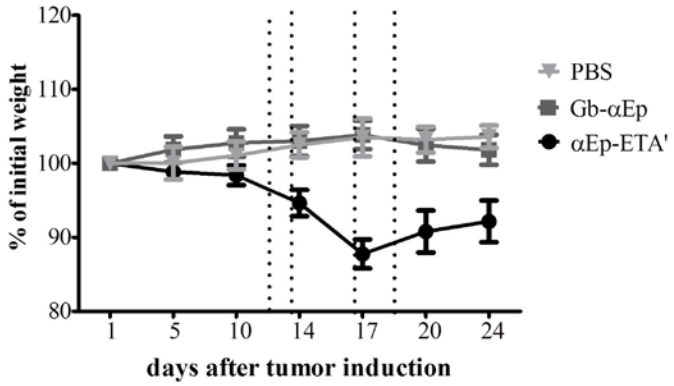



**Figure 19. General toxicity of EpCAM-specific CFPs in a MDA-MB-468 xenograft tumor model.**

Mice bearing Katushka-2-transfected (II.2.1.6) MDA-MB-468/tdKat tumors (n=7 per group) (II.2.7.3) were injected *i.v.* with PBS (▼), 2.5mg/kg GB-R201K-αEpCAM(scFv) (■), 1.25 mg/kg αEpCAM(scFv)-ETA' (●). Treatment was started when the tumors reached 50 $mm^2$, and was delivered 4 times over a period of 9 days (II.2.7.3). The weight of the mice was monitored. Graph

represents the weight loss of the animals during the treatment period. Values are represented as mean + SEM II.2.8). Dotted lines represent the days treatment was given.

Treatment started 13 days after tumor induction when tumor sizes reached approximately 50mm$^{2.}$ Treatment with either αEpCAM(scFv)-ETA' (4 x 1.2 mg/kg dose) or GB-R201K-αEpCAM(scFv) (4 x 2.5 mg/kg) resulted in approximately 50% growth inhibition when compared to the control group (Figure 20 A). αEpCAM(scFv)-ETA' treatment showed slightly better results than Gb-αEp, but the differences in growth inhibition were statistically insignificant. Moreover, treatment with a non-cytolytic control protein αEpCAM(scFv)-SNAP did not result in tumor growth inhibition (Figure 20 B) (171, 173), thus demonstrating that the anti-tumor activity of the CFPs is due to the effector proteins' domain and not simply the binding and internalization of EpCAM.

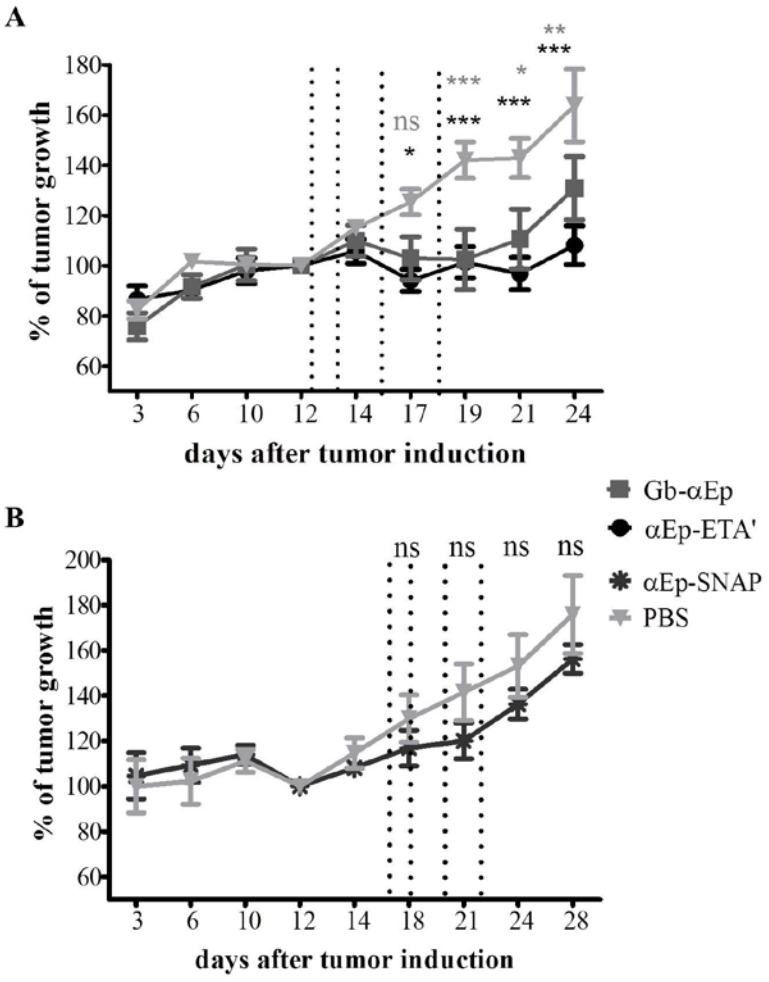



**Figure 20. Tumor growth inhibition by EpCAM-specific CFPs in a MDA-MB-468 xenograft tumor model.**

Mice bearing Katushka-2-transfected (II.2.1.6) MDA-MB-468/tdKat tumors (II.2.7.2) were injected *i.v.* with **A:** PBS (▼), 2.5 mg/kg GB-R201K-αEpCAM(scFv) (■), 1.25 mg/kg αEpCAM(scFv)-ETA' (●) or **B:** 2.5 mg/kg αEpCAM(scFv)-SNAP (✷).Treatment was started when the tumors reached 50

$mm^2$, and was delivered 4 times over a period of 9 days (II.2.7.3). Dotted lines represent the days treatment was given. Relative tumor growth following treatment was measured by *in vivo* imaging. Tumor size at each time point was normalized to the tumor size on day 12 (one day prior to initiating treatment), which was set to 100%. Values are represented as means ± SEM (n = 7). Dashed vertical lines represent dosing days. Statistical analysis was carried out using a two-way ANOVA test in GraphPad PRISM software (II.2.8). *$p \leq 0.05$, **$p \leq 0.01$, ***$p \leq 0.001$ compared to PBS control.

## *III.2 scFv based- CSPG4 targeting CFPs*

### *III.2.1 Generation and characterization of scFv based fusion proteins*

#### *III.2.1.1 CSPG4 expression on TNBC cell lines*

To verify published results (88, 91) and determine CSPG4 expression on other unpublished cell lines, Flow cytometric analysis was used to measure CSPG4 expression on all available breast cancer cell lines: MCF7, ZR-75, Hs 578T, BT-20, MDA-MB-231, MDA-MB-453, and MDA-MB-468. CSPG4 expression was confirmed only on TNBC cell lines MDA-MB-231 and Hs 578T by flow cytometry using a commercial CSPG4(scFv)-specific antibody (Figure 21 and Table 11), all other cell lines tested negative for CSPG4 expression. Both CSPG4$^{+}$ cell lines were previously identified as mesenchymal stem like TNBC subtype (34).

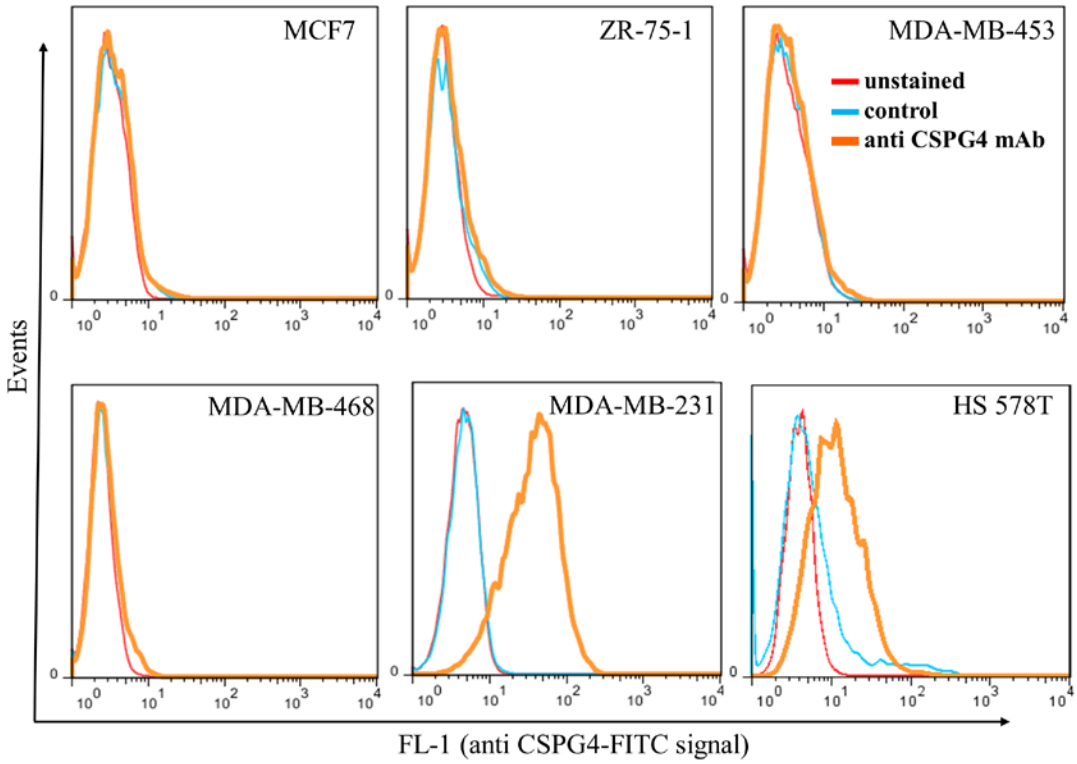



**Figure 21. CSPG4 expression on breast cancer cell lines.**

Breast cancer cell lines (II.2.1.5) (MCF7, ZR-75-1-MDA-MB-453, MDA-MB-468, MDA-MB-231 and HS 578T) were analyzed for their expression levels of CSPG4. Flow cytometric analysis (II.2.5.1.1) of CSPG4 expression was carried using anti-CSPG4 antibody followed by staining with

goat anti-mouse IgG-FITC on indicated breast cancer cell lines. Control staining was done using only the secondary antibody- goat anti-mouse IgG-FITC.

**Table 11. Expression of CSPG4 on breast cancer cell lines:**

| Cell line | Receptor status | *Molecular subtype (11) | **TNBC subtype (34) | ***CSPG4 expression (MFI) |
|---|---|---|---|---|
| MCF-7 | $ER^+$, $PR^+$ | Luminal | N/A | ^ |
| ZR-75-1 | $HER2^+$ | Luminal | N/A | ^ |
| MDA-MB-453 | TN | Luminal | Luminal AR | ^ |
| MDA-MB-468 | TN | Basal A | Basal-1 | ^ |
| BT-20 | TN | Basal A | Unclassified | ^ |
| MDA-MB-231 | TN | Basal B | Mesenchymal stem like | 69.5 $\pm$ 11.2 |
| HS 578T | TN | Basal B | Mesenchymal stem like | 25.7 $\pm$ 6.9 |

*Molecular subtype classification according to (11), **TNBC subtype classification according to (34), *** CSPG4 expression level were determined by FACS (II.2.5.1.1) and are described in MFI-( mean fluorescence intensity) calculated from at least 3 independent measurements. Values represent mean + SEM. ^ Non detectable- MFI value is equal to MFI of unstained cells (MFI values around 3-6). Abbreviations: ER, estrogen receptor; PR, progesterone receptor; HER2, human epidermal growth receptor-2; TN, Triple negative- $ER^-$, $PR^-$ and $HER2^-$, N/A; not available.

### *III.2.1.2 Cloning and design of anti-CSPG4(scFv) CFPs*

Initially αCSPG4(scFv) was kindly provided by Prof. Helfrich (Groningen University) (188) and cloned into pMT vector (as with the anti-EpCAM (scFv)) to generate αCSPG4(scFv)-ETA' immunotoxin (Figure 22 A and Plasmid sequences). However, expression levels were very low, and a pure product could not be purified (Figure 23A). Contaminant bacterial proteins were co eluting with the IT as was confirmed by mass spectrometry (MS) analysis which was kindly performed by Dr. Dr. Ivana Chudobová (Plant Biotechnology Departement, Fraunhofer IME, Aachen, Germany) (Figure 23b). Although positive and specific binding was confirmed, very low toxicity was measured for this compound on TNBC cell lines (data not shown).

Therefore, an alternative construct (anti-CSPG4(scFv)-ETA'-KDEL) was obtained from Prof. Fey (Erlangen University) (189). This anti-CSPG4(scFv) was received in a pET-27 vector already cloned in fusion with ETA' (Figure 22 B), N' terminal streptavidin-tag and a poly-his tag were included 5' to the scFv. A $(Gly4Ser)_4$ linker separates between the scFv and the ETA' toxin. Additionally, the REDLK sequence was modified with a KDEL ER retention signal at the C-terminus to increase endosomal escape and toxicity of the protein.

All following work with anti-CSPG4 (scFv) was done using the later scFv and expression plasmid.

The pET-αCSPG4(scFv)-ETA'-KDEL expression plasmid (VI.4.4) was used to generate αCSPG4(scFv)-MAP CFP. This was done by replacing the ETA' sequence with the MAP tau sequence using a NotI BlpI digest and ligation (Figure 22 C).

An additional αCSPG4(scFv) fusion protein was produced, carrying a SNAP-tag (173). αCSPG4(scFv)-SNAP: pMS-L-2715-SNAP-IV vector was used for cloning. The 2715 scFv was replaced with the αCSPG4 scFv. This construct (Figure 22D) contains a N' terminal Igκ leader sequence and a C' terminal poly-His tag (97, 173). The αCSPG4(scFv)-SNAP was used throughout this work as a non-cytolytic αCSPG4 fusion protein control (M-SNAP).

Successful ligation products were confirmed by sequencing analysis. All plasmid schemes and sequences can be found in the appendix.

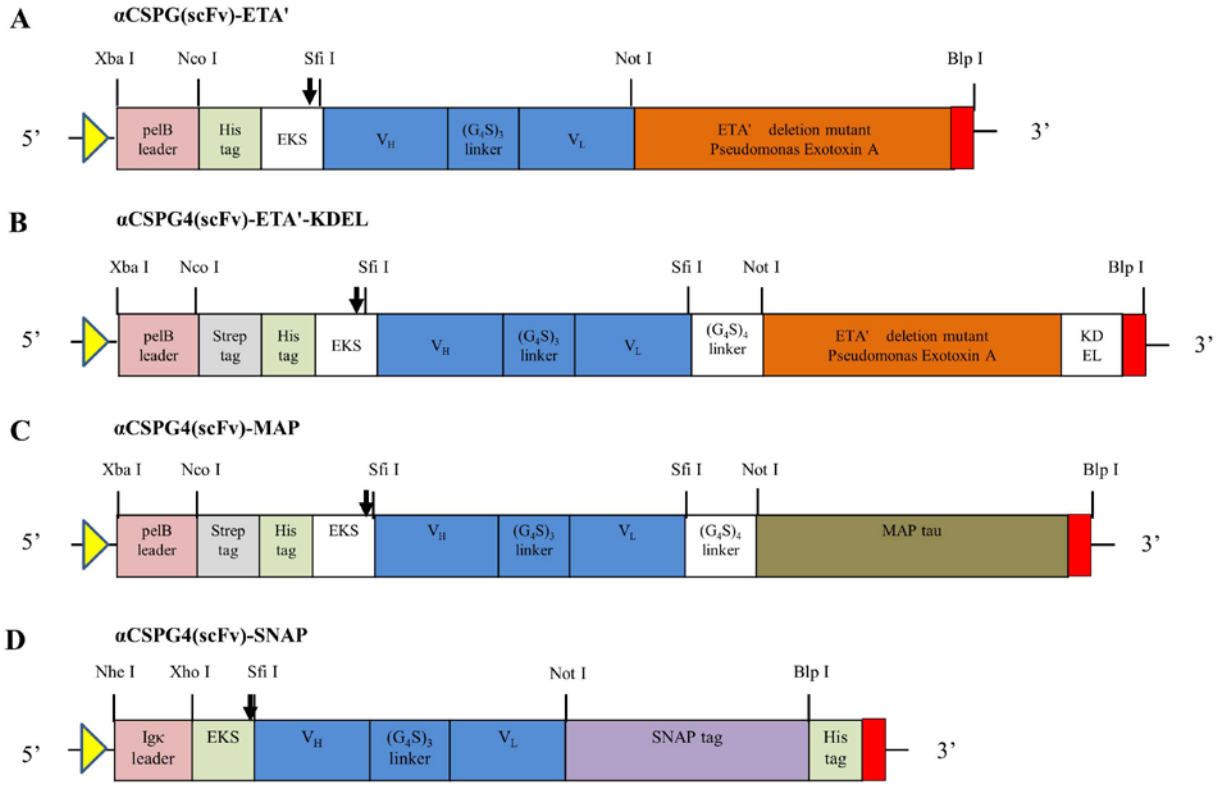
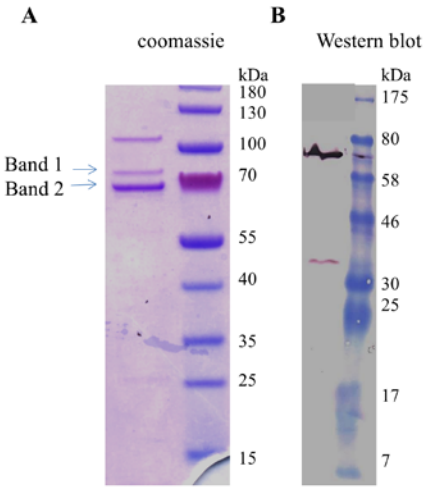



**Figure 22. CSPG4 specific CFP constructs' design.**

**A:** αCSPG4(scFv)-ETA' from pMT vectorVI.4.2, open reading frame containing a pelB leader peptide, a polyhistidin tag and an Enterokinase cleavage site (all at the N-terminus) and a C' terminus 40 kDa truncated version of Pseudomonas Exotoxin A **B:** αCSPG4(scFv)-ETA', from pET vector VI.4.4 containing a *pel*B leader peptide, a streptavidin-tag and a polyhistidin-tag for purification purposes (all at the N-terminus), the αCSPG4(scFv) and a 40- kDa deletion mutant of *Pseudomonas aeruginosa* Exotoxin A modified with a KDEL ER retention signal at the C-terminus. **C:** αCSPG4(scFv)-MAP from pET vector VI.4.5 containing the same elements, except for the

replacement of the ETA' sequence by the MAP tau cytolytic protein. **D:** Schematic representation of αEpCAM(scFv)-SNAP open reading frame from pMS vector VI.4.7 containing an Igκ leader sequence and an Enterokinase cleavage site (both at the N-terminus) and a polyhistidin tag (C-Terminus). Yellow triangle indicates start codon (ATG) and red rectangle indicates stop codon, black arrows indicate Enterokinase cleavage site, black lines indicate restriction enzyme positions. Abbreviations: EKS, Enterokinase site; $(G_4S)_3$; Glycine Serine linker containing three repeats of GGGGS peptide; $V_L$, light chain variable antibody fragment; $V_H$, heavy chain variable antibody fragment.




C

Mass spectrometry analysis of Band 1 and 2

Band 1:

| Accesion number | Protein name | Gene name | Mr | Score |
|---|---|---|---|---|
| gi\|170682848 | bifunctional UDP-glucuronic acid decarboxylase/UDP-4-amino-4-deoxy-L-arabinose formyltransferase [Escherichia coli SMS-3-5] | **arnA** | 74029 | 774 |
| gi\|76445989 | serum albumin [Bos indicus] | - | 53890 | 209 |
| gi\|290577 | glutamine amidotransferase [Escherichia coli] | **glmS** | 66833 | 148 |

Band 2:

| Accesion number | Protein name | Mr | Score |
|---|---|---|---|
| gi\|290577 | glutamine amidotransferase [Escherichia coli] | 66833 | 1075 |

**Figure 23. Contamination of αCSPG4(scFv)-ETA' elution fraction with co-eluting bacterial proteins.**

anti-CSPG4(scFv) was received from collaboration partner Prof. Helfrich (Groningen University) (188) and cloned via SfiI/NotI digest II.2.1.11) and ligation (II.2.1.12) in fusion with ETA' sequence in the pMT vector. Periplasmic expression (II.2.1.4) and purification via IMAC and size exclusion were carried out according to (II.2.2). **A:** Coomassie staining (II.2.4.2) of the purified anti-CSPG4(scFv) –ETA' rIT. **B:** western blotting II.2.4.3) using anti-poly-His mAb followed by goat anti mouse IgG-AP conjugated. **C:** mass spectrometry analysis of the separated band 1 and band 2 from A. the results from the analysis were run against known proteins database (Mass spectrometry analysis was kindly performed by **Dr. Ivana Chudobová).**

### *III.2.1.3 Expression and purification of αCSPG4(scFv) CFPs*

Both αCSPG4(scFv)-ETA' (74 kDa) and αCSPG4(scFv)-MAP (78 kDa) CFPs were expressed in *E.coli* BL21(DE3) under osmotic stress conditions in the presence of compatible solutes (178). Proteins were purified by immobilized metal ion affinity chromatography (IMAC) and Strep-Tactin affinity chromatography followed by size exclusion chromatography as described in MM (II.2.2.2). Purification yielded 4-5 mg protein per liter culture with a purity >90%.

αCSPG4(scFv)-SNAP was expressed in HEK293T cells as described (II.2.1.7). one step IMAC purification (II.2.2.1) was sufficient to achieve >95% purity. Purification yields were 8-10 mg protein per liter culture.

Proteins integrity, purity and identity were confirmed using SDS-PAGE and western blotting with anti-His tag antibody (Figure 24). The concentration of the proteins after all purification steps was determined using BCA protein quantification assay and the proteins were kept in concentrations between 0.5-0.8 mg/ml and stored at -20°C. Fusion proteins that were frozen for different periods of time up to 6 months, maintained high stability with low levels of degradation and retained their biological activity-binding and toxicity (data not shown).

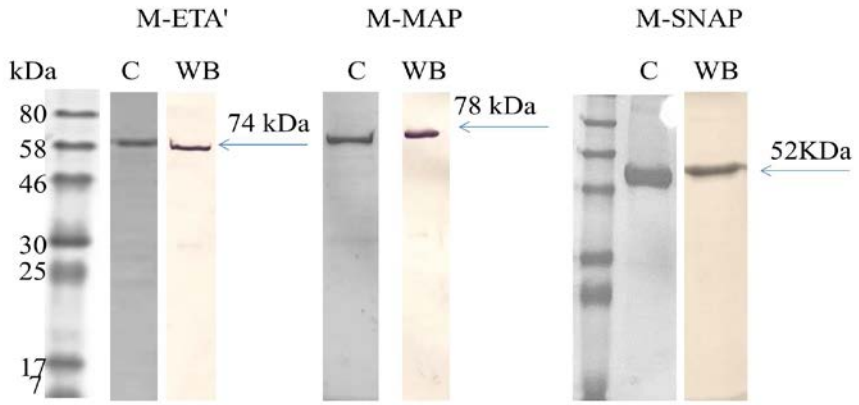



**Figure 24. Expression and purification of CSPG4 specific fusion proteins.**

Coomassie-stained (C) SDS gel (II.2.4.2) and corresponding western blot analysis (II.2.4.3) (WB) of purified (II.2.2.3) αCSPG4(scFv)-ETA', αCSPG4(scFv)-MAP and αCSPG4(scFv)-SNAP were carried out. αCSPG4(scFv)-ETA' and αCSPG4(scFv)-MAP were expressed periplasmically in *E. coli* BL21(DE3) under osmotic stress conditions in the presence of compatible solutes (II.2.1.4). Purification was carried out using two step purification with immobilized-metal affinity chromatography (IMAC) (II.2.2.1) using a Ni-NTA superflow column followed Streptactin affinity chromatography (II.2.2.2). An additional step of size exclusion chromatography was performed (II.2.2.3). αCSPG4(scFv)-SNAP proteins were expressed in HEK293T system II.2.1.7) and the fusion proteins were purified from the supernatant via IMAC column (II.2.2.1). All proteins were detected using a mouse-anti-poly-His antibody, followed by Alkaline Phosphatase conjugated-goat-anti-mouse IgG-antibody and visualized by NBT/BCIP substrate. Abbreviations: C, Coomassie staining; WB, western blot; M-SNAP, αCSPG4(scFv)-SNAP tag; M-MAP: αCSPG4(scFv)-MAP, M-ETA': αCSPG4(scFv)-ETA'.

#### *III.2.1.4 Binding analysis of fusion proteins*

Flow cytometric analysis of the binding of CFPs on TNBC cell lines confirmed specific and comparable binding affinity of αCSPG4(scFv)-MAP and αCSPG4(scFv)-ETA' on CSPG4$^{+}$ MDA-MB-231 and Hs 578T cells, but not on CSPG4(scFv)$^{neg}$ cell line MDA-MB-468 (Figure 25).

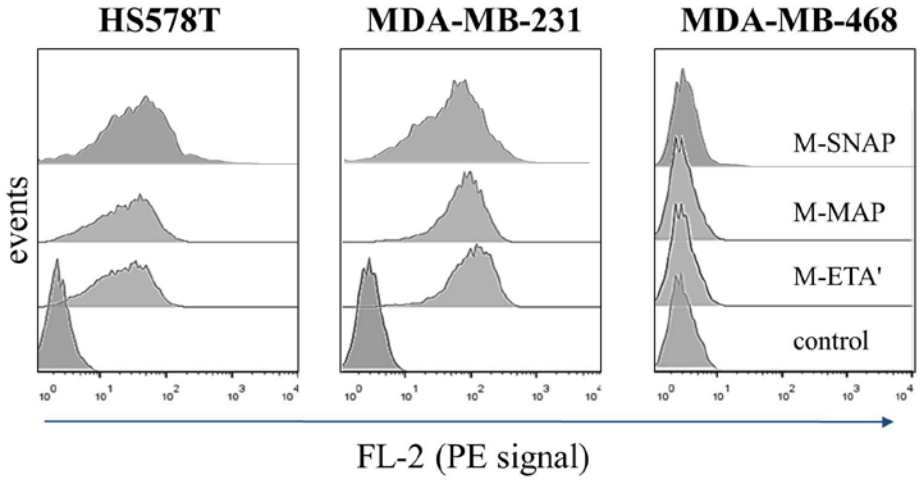



**Figure 25. Binding of CSPG4 specific fusion proteins on TNBC cell lines.**

Flow cytometric binding analysis (II.2.5.1.1) of purified II.2.2.3) αCSPG4(scFv)-SNAP, αCSPG4(scFv)-MAP, and αCSPG4(scFv)-ETA' on CSPG4-positive TNBC-derived cell lines (II.2.1.5) Hs 578T, MDA-MB-231 and CSPG4-negative MDA-MB-468 cell line. 200nM fusion proteins were incubated for 20 minutes on ice with 3 x $10^5$ Cells and binding was detected using mouse-anti-poly-His antibody and subsequent PE-conjugated goat-anti-mouse-IgG antibody. Abbreviations: M-SNAP, αCSPG4(scFv)-SNAP tag; M-MAP: αCSPG4(scFv)-MAP, M-ETA': αCSPG4(scFv)-ETA'.

### *III.2.2 Functional assays with αCSPG4 fusion proteins*

#### *III.2.2.1 αCSPG4(scFv) fusion proteins internalization and cellular uptake*

Specific internalization of αCSPG4(scFv)-MAP by MDA-MB-231 cells was detected using immunofluorescent staining with anti-MAP antibody. Confocal microscopy confirmed specific binding of αCSPG4(scFv)-MAP to CSPG4$^{+}$ MDA-MB-231, but not to CSPG4(scFv)- MDA-MB-468 cells. After 2 h of incubation at 37°C, αCSPG4(scFv)-MAP signal was mainly detected on the cell surface and in the cytosol of MDA-MB-231 cells, while after 24 h it was even distributed all over cytosol and nucleus (Figure 26 A). αCSPG4(scFv)-ETA' signal was similarly detected using anti ETA' antibody. 2 h incubation

resulted in a visible signal on the cell surface and in vesicles inside the cytosol. 24 h later the signal remained strong in the cytosol in a pattern typical to receptor mediated endocytosis (Figure 26 B).

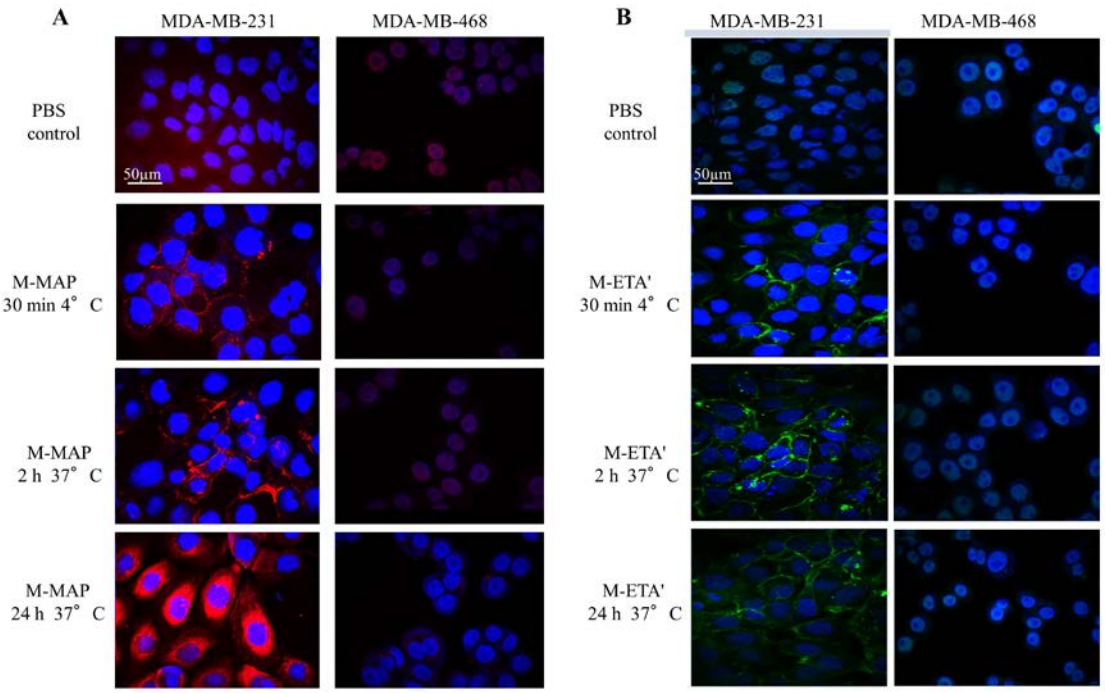



**Figure 26. Binding and internalization of CSPG4 specific CFPs on MDA-MB-231 cell line.**

High throughput confocal microscopy imaging (0) of the binding and internalization of **A:** Acspg4(scFv)-MAP and **B:** αCSPG4(scFv)-ETA' on CSPG4$^{high}$ MDA-MB-231 cells (left) and CSPG4$^{neg}$ MDA-MB-468 cells (right). αCSPG4(scFv)-ETA' was detected using anti-ETA' antibody followed by FITC-conjugated goat-anti-mouse IgG antibody and αCSPG4(scFv)-MAP was detected using anti-MAP tau antibody followed by Alexa-647-conjugated Goat-anti-mouse-IgG antibody as described (0). Images were taken by Dr. Stefano Di Fiore on the Opera imaging system. Abbreviations: h, hour; M-MAP: αCSPG4(scFv)-MAP, M-ETA': αCSPG4(scFv)-ETA'. Scale bar = 50 µm, same for all images.

An indirect internalization FACS assay (II.2.5.1.3) was performed to determine cellular uptake kinetics of the CFPs on MDA-MB-231 cells. The results show that 50% internalization was achieved between 2 hours to 4 hours of incubation at 37 °C for both CFPs (Figure 27).

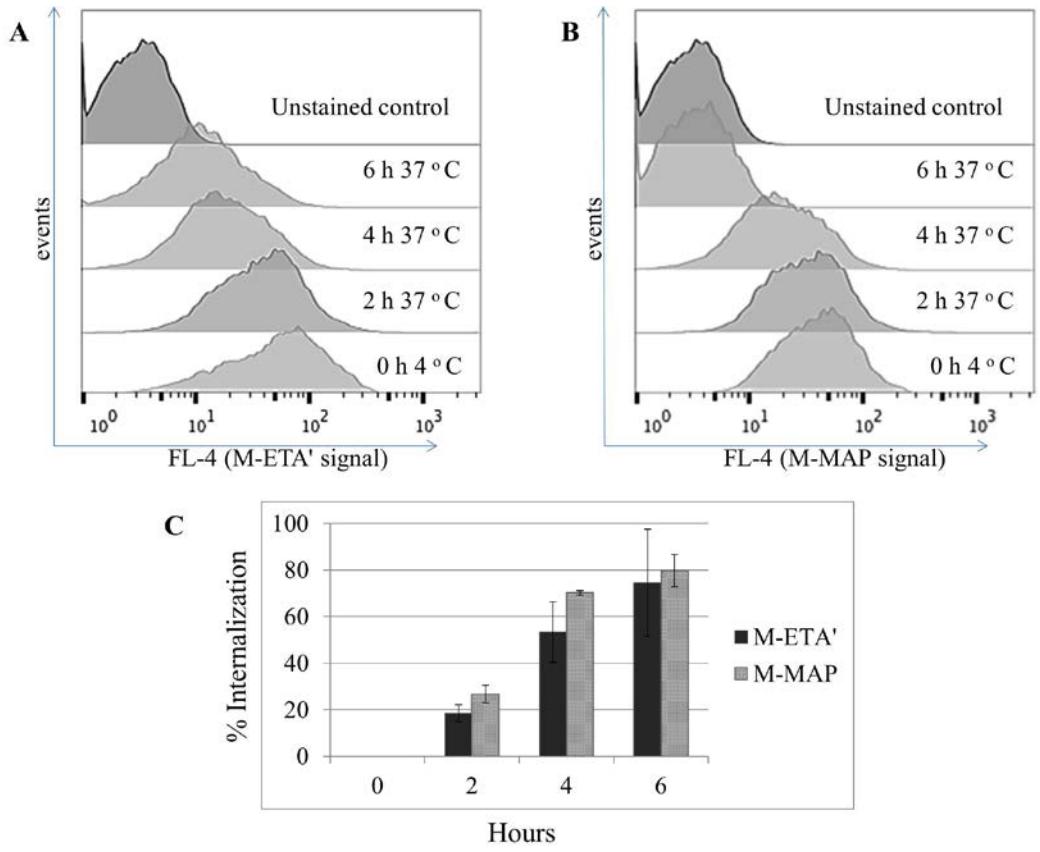



**Figure 27. Internalization kinetics of CSPG specific CFPs in MDA-MB-231 cells.**

Internalization rates at 37ºC of **A:** αCSPG4(scFv)-ETA' and **B:** αCSPG4-MAP in MDA-MB-231 cells were measured by flow cytometry in an indirect internalization assay (II.2.5.1.3). **C:** graphic representation of the percentage of internalized CFPS determined by calculating the ratio of the surface signal at each time point compared to the signal of control samples kept at 4°C. Values on graph are represented as mean + SD (n = 3), statistical analysis was carried out using a two-tailed unpaired Student's *t*-test (II.2.8). Abbreviations: M-MAP: αCSPG4(scFv)-MAP, M-ETA': αCSPG4(scFv)-ETA'.

### *III.2.2.2 αCSPG4(scFv)-MAP Interaction with tubulin*

The interaction of MAP-based CFP with tubulin was further examined by a tubulin polymerization assay (II.2.6.6) demonstrating that αCSPG4(scFv)-MAP can in fact stabilize microtubules and promote polymerization. 100 nM of αCSPG4(scFv)-MAP were able to stabilize microtubules effectively by promoting tubulin polymerization to an extent similar to 10 μM paclitaxel control (Figure 28).

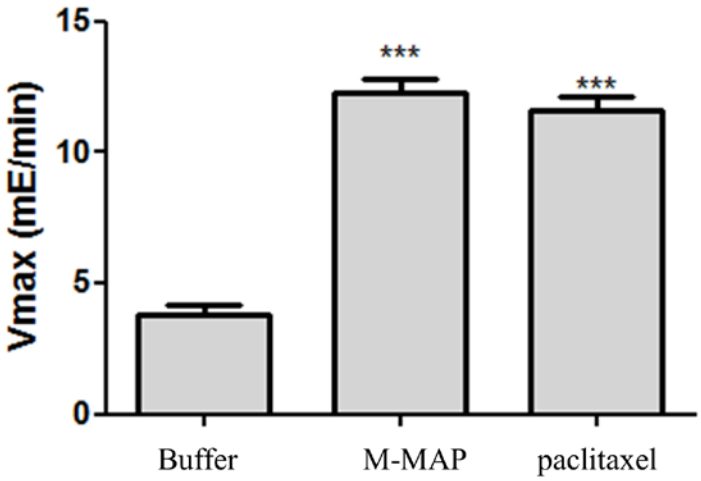



**Figure 28. Induction of Tubulin polymerization by αCSPG4(scFv)-MAP.**

Tubulin polymerization assay (II.2.6.6) comparing tubulin polymerization induced by 100 nM αCSPG4(scFv)-MAP and paclitaxel (10 μM), $v_{max}$ values were calculated using the slope of the linear phase (mE, milli-extinction). Statistical analysis (II.2.8) was carried out using a two-tailed unpaired Student's *t*-test. Values on graph represent the mean (n=3) + SEM ***p≤0.001 compared to the buffer control. Abbreviations: M-MAP: αCSPG4(scFv)-MAP.

Furthermore, in order to examine MAP-tubulin interaction inside the cells, to confirm endosomal escape and binding of αCSPG4(scFv)-MAP to tubulin once internalized into the cells, a co-immunoprecipitation assay was carried out as described (II.2.5.7). αCSPG4(scFv)-MAP was incubated with MDA-MB-231 cells for 24 hours. Cell lysates were analyzed by immunoprecipitation with tubulin-specific antibodies followed by detection with MAP tau specific antibody. The results confirm the co-localization of MAP and tubulin within the cells (Figure 29). The signal was specific to cells treated with αCSPG4(scFv)-MAP, but not in cells treated with αCSPG4(scFv)-ETA' or PBS, thus indicating that the signal is due to the internalization and binding of αCSPG4(scFv)-MAP to tubulin, and not to endogenous MAP tau protein.

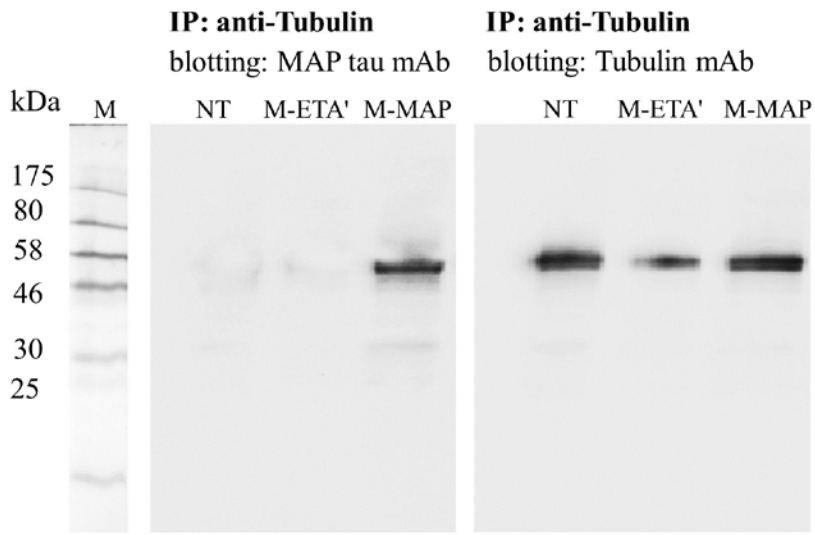
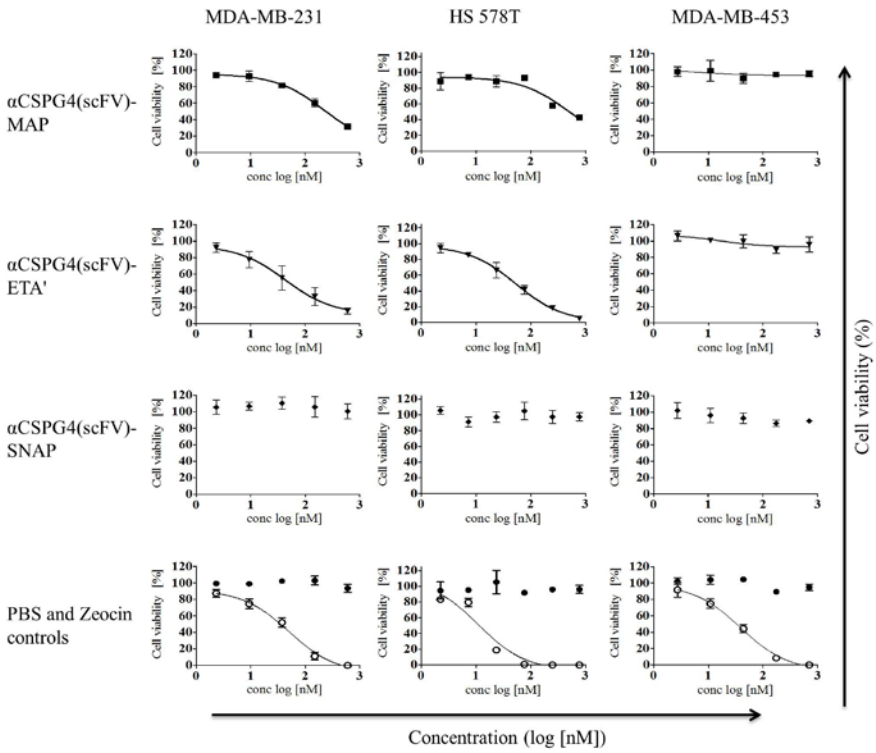



**Figure 29. Intracellular interaction of αCSPG4(scFv)-MAP with Tubulin following internalization in MDA-MB-231 cells.**

Co-immunoprecipitation (II.2.5.7) of αCSPG4(scFv)-MAP with tubulin. MDA-MB-231 Cells (II.2.1.5) were treated for 24 h with 100 nM of αCSPG4(scFv)-MAP or αCSPG4(scFv)-ETA' (II.2.2.3), lysed and tubulin was immune-precipitated using a tubulin-specific antibody. The immune complexes were eluted and analyzed by western blotting (II.2.4.3) using an anti-MAP tau antibody and a tubulin-specific antibody as a control. Abbreviations: NT: non-treated control, M-MAP: αCSPG4(scFv)-MAP, M-ETA': αCSPG4(scFv)-ETA'.

### *III.2.2.3 Cytotoxic effect of αCSPG4(scFv)-MAP on TNBC-derived cell lines*

Treatment of MDA-MB-231 and Hs-578T cells with αCSPG4(scFv)-MAP for 48 h resulted in inhibition of cell growth as determined by XTT cell viability assay (II.2.6.1). However, the cytotoxicity of the αCSPG4(scFv)-MAP measured in XTT cell viability assay was lower than that of αCSPG4(scFv)-ETA', with $IC_{50}$ values around 50 nM for αCSPG4(scFv)-ETA' and 200-400 nM for αCSPG4(scFv)-MAP (Figure 30). MDA-MB-231 were 2 folds more susceptible to αCSPG4(scFv)-MAP compared to Hs-578T. Cytotoxic effects induced by αCSPG4(scFv) alone were excluded using αCSPG4(scFv)-SNAP in TNBC cell lines. The cytotoxicity of αCSPG4(scFv) CFPs was specific to CSPG4 expressing cell lines. No off target toxicity was detected in CSPG4 negative cell line MDA-MB-468.




| IC50 (nM) | M-ETA' | M-MAP | CSPG4 expression level |
|---|---|---|---|
| MDA-MB-231 | 43.1 ± 5.6 | 219.5 ± 6.5 | High |
| HS 578T | 53.8 ± 4.6 | 480 ± 29.3 | Medium |
| MDA-MB-453 | No toxicity | No toxicity | No expression |

**Figure 30. Growth inhibition and cytotoxicity of CSPG4 specific CFPs in TNBC cell lines.**

XTT Cell viability assay (II.2.6.1) with CSPG4-positive MDA-MB-231 (left panel), HS 578T (middle) and CSPG4$^-$ MDA-MB-453 (right) cell lines treated for 48 h with serial dilutions of αCSPG4(scFv)-MAP, αCSPG4(scFv)-ETA' or the non-cytolytic control αCSPG4(scFv)-SNAP. PBS buffer and Zeocin were used as controls, XTT substrate was used to determine cell viability. $IC_{50}$ values in nM were extrapolated by non-linear regression analysis (II.2.8) from 3 independent experiments (each performed in triplicates) and are summed in the table in the lower pane. Abbreviations: M-MAP: αCSPG4(scFv)-MAP, M-ETA': αCSPG4(scFv)-ETA'.

### *III.2.2.4 Induction of apoptosis by αCSPG4(scFv) CFPs in MDA-MB-231 cell line*

Based on XTT toxicity assay results, MDA-MB-231 cells were used for further studies, and the determined IC-50 concentrations were used for subsequent apoptosis studies (40 nM αCSPG4(scFv)-ETA' and 200 nM αCSPG4(scFv)-MAP). Specific cytotoxicity was further demonstrated using an Annexin V/propidium iodide (PI) apoptosis assay (II.2.6.2). Treatment with αCSPG4(scFv)-MAP led to an increase in the fractions of apoptotic cells positive for Annexin V (4 folds) and PI positive (5 folds). αCSPG4(scFv)-ETA' treatment resulted in similar increase in the PI positive fraction,and a 6 fold increase in the Annexin V positive cells (Figure 31). No cytotoxic effects were induced by a negative control MAP CFP- Ki4-MAP.

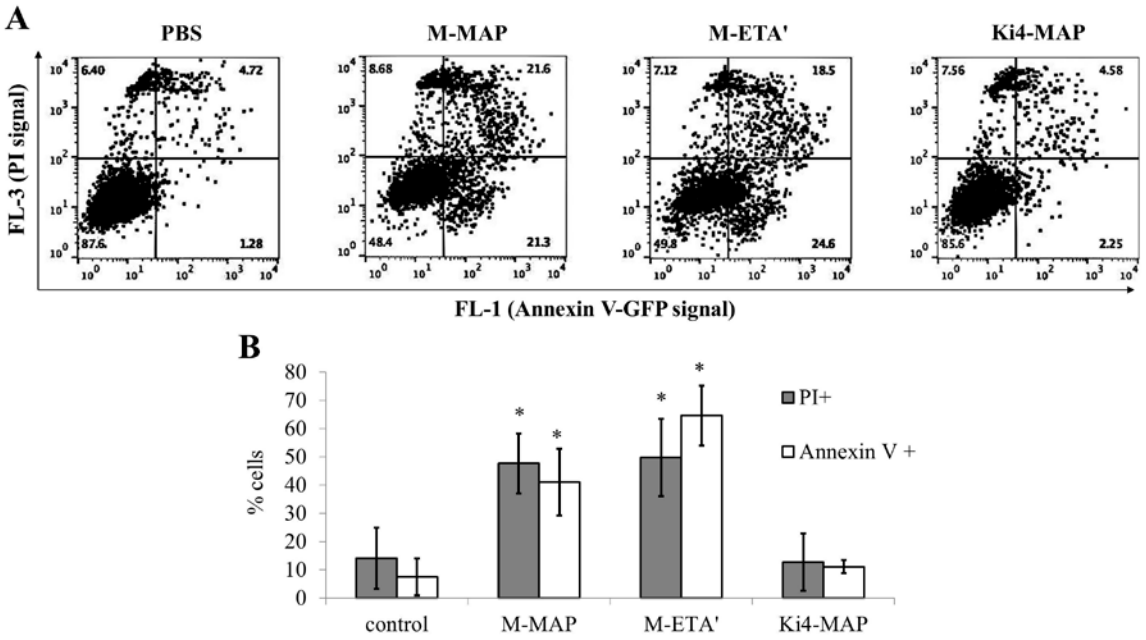



**Figure 31. Induction of apoptosis by CSPG4 specific CFPs in MDA-MB-231 cells.**

Annexin V Apoptosis assay (II.2.6.2) with MDA-MB-231 cells treated with (left to right): PBS, 250 nM αCSPG4(scFv)-MAP, 50 nM αCSPG4(scFv)-ETA' and 250 nM Ki4-MAP for 48 h. cells were washed and stained with supernatant containing AnnexinV-GFP and Propidium iodide. Cells were analyzed by flow cytometry (II.2.5.1). **A:** Dot plots were gated on single cells and represent annexinV-eGFP vs. PI staining. Ki4-MAP (α-CD30(scFv)-MAP) was used as negative control. **B:** Graph summarizing the results of 3 independent assays. The black bars represent % of cells in early apoptosis (Annexin $V^+$ / Propidium $Iodide^-$) and the grey bars represent late apoptotic cells (Annexin $V^+$ / Propidium $Iodide^{+)}$. Error bars represent SEM. Statistical analysis was carried out using a two tailed unpaired t-test. *$p \leq 0.005$ compared to the PBS control. Abbreviations: M-MAP: αCSPG4(scFv)-MAP, M-ETA': αCSPG4(scFv)-ETA'.

To explore the cellular apoptotic pathways activated by αCSPG4(scFv)-MAP, MDA-MB-231 cells were treated for 24 h with CFPs. Caspase-3 and PARP-1 cleavage was detected via western blot analysis of cell lysates (II.2.6.3). While strong activation of caspase-3 and cleavage of PARP-1 in cells treated with αCSPG4(scFv)-ETA' were observed (Figure 32), a much milder effect was seen in αCSPG4(scFv)-MAP treated cells, only very faint bands of cleaved caspase 3 were observed.

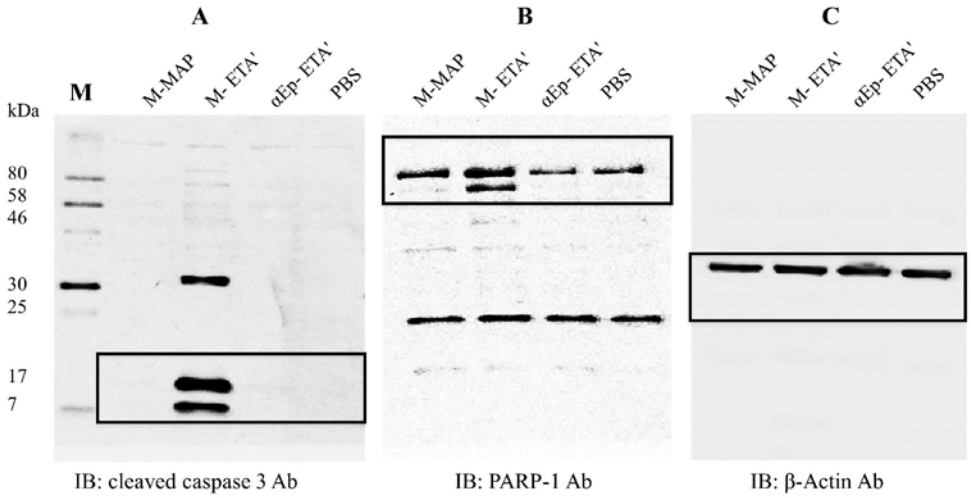



**Figure 32. Induction of caspase 3 dependent apoptosis by CSPG4 specific CFPs in MDA-MB-231 cells.**

Western blot analysis (II.2.6.3) of **A:** caspase-3 and **B:** PARP-1 cleavage in MDA-MB-231 cells (II.2.1.5) treated for 24 hours with 200 nM αCSPG4(scFv)-MAP (1st lane) or 50 nM αCSPG4(scFv)-ETA' (2nd lane) (II.2.2.3). αEpCAM(scFv)-ETA' (3rd lane) and PBS (4th lane) were used as negative controls. **C:** Immunoblotting with β-Actin was used as an equal loading control. Abbreviations: PARP-1, Poly (ADP-Ribose) Polymerase 1; IB, Immunoblotting; Ab, antibody; M, prestained protein marker; M-MAP: αCSPG4(scFv)-MAP, M-ETA': αCSPG4(scFv)-ETA' and αEp-ETA', αEpCAM(scFv)-ETA'.

### *III.2.2.5 Activation of mitochondrial stress apoptotic pathways by αCSPG4(scFv) fusion proteins*

Further investigation to reveal the cell death pathways induced by αCSPG4(scFv)-MAP was conducted. Activation of the mitochondrial stress apoptotic pathway was investigated: The subcellular location of endonuclease G (EndoG) was determined 48 h after treatment of MDA-MB-231 cells with αCSPG4(scFv)-MAP or αCSPG4(scFv)-ETA' as described in MM (II.2.6.5). 10µg total protein from each sample was used for Coomassie staining to verify proper separation of fractions and as a loading control (Figure 33B). Treatment resulted in the translocation of EndoG from the mitochondria to the nucleus for both fusion proteins (Figure 33A) compared to the PBS-treated control.

Furthermore, activation of the cytochrome C/caspase-9 pathway was analyzed in a caspase-9 substrate assay (II.2.6.4), 48 h after CFP treatment. Lower activation levels were measured for αCSPG4(scFv)-MAP compared to αCSPG4(scFv)-ETA' (Figure 33C).

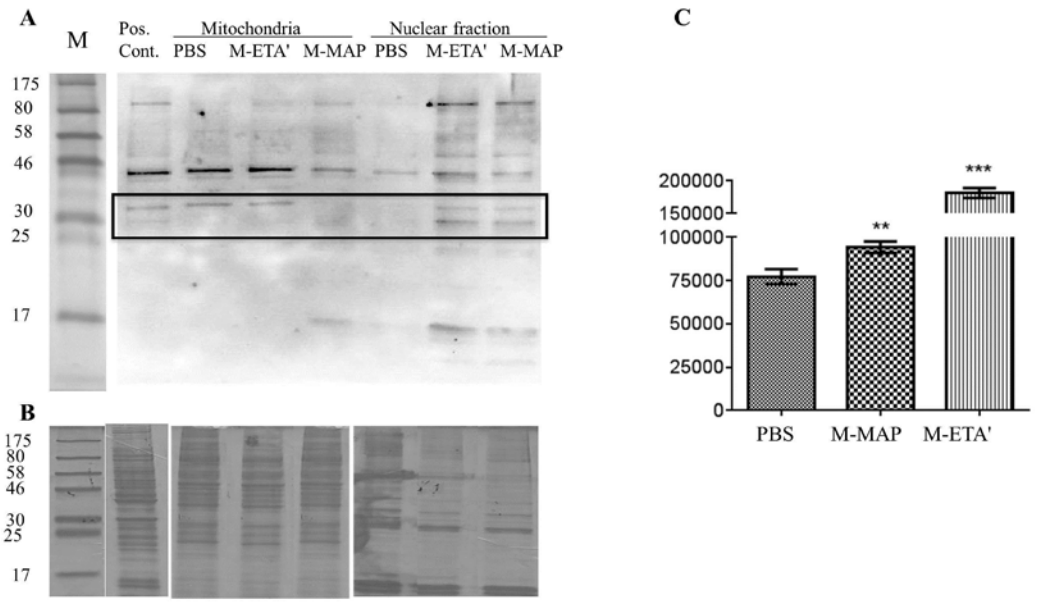



**Figure 33. Activation of the mitochondrial stress apoptotic pathway by CSPG4 specific CFPs.**

**A:** Detection of Endonuclease G translocation from the mitochondria to the nucleus (II.2.6.5) following treatment with αCSPG4(scFv)-MAP or αCSPG4(scFv)-ETA' II.2.2.3). Cells treated with CFPs for 48 h were sub-fractioned into mitochondrial and nuclear fractions and analyzed by SDS-PAGE (II.2.4.2) and western blotting II.2.4.3) using an anti-EndoG antibody. **B:** 10µ total protein from each sample was used for Coomassie staining II.2.4.2) to verify proper separation of fractions and as a loading control. **C:** Caspase-9 activity II.2.6.4) following 48 h treatment with 200 nM αCSPG4(scFv)-MAP or 40 nM αCSPG4(scFv)-ETA' on MDA-MB-231. Activation levels were determined using a caspase-9 pre-luminescent substrate II.2.6.4); the luminescence signal is directly proportional to the activity of caspase-9 and was normalized to the endogenous signal produced by non-treated cells, the results were analyzed using a two-tailed unpaired Student's *t*-test. Values on graph represent the mean (n=3) + SD (II.2.8). Abbreviations: M-MAP: αCSPG4(scFv)-MAP, M-ETA': αCSPG4(scFv)-ETA'.

### *III.2.2.6 Induction of cell cycle arrest by αCSPG4(scFv)-MAP*

We hypothesized that MAP stabilization of microtubules induces cell death by disturbing the cell cycle and reducing cell division, similar to other microtubule-stabilizing therapies (190). To verify this, a PI cell cycle analysis was performed for the quantification of DNA at different time points (II.2.6.7.). The results revealed an increase in the cells with doubled amount of DNA, thus confirming a partial cell cycle arrest (approximately 50% of

the cells) in the G2/M phase of the αCSPG4(scFv)-MAP-treated cells compared to the PBS-treated cells (less than 20%, Figure 34).

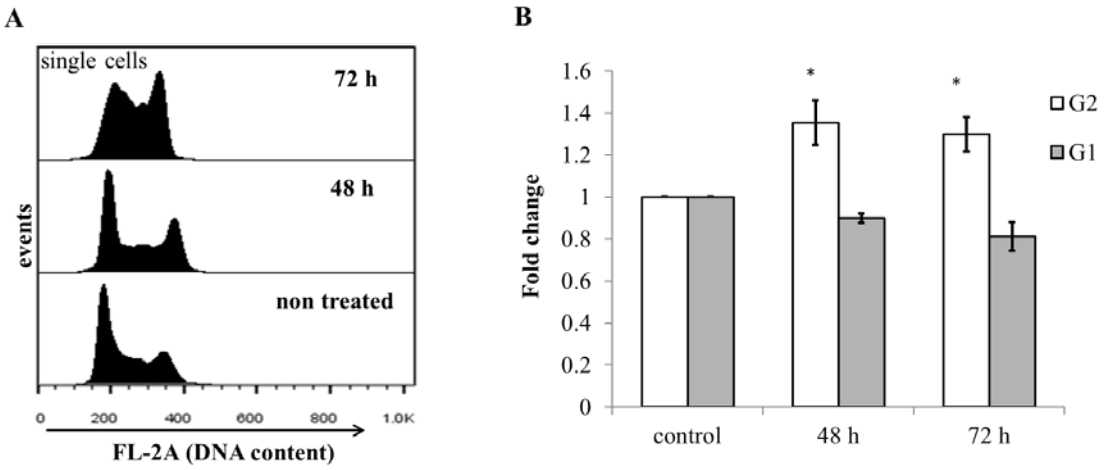



**Figure 34. Induction of cell cycle arrest by αCSPG4(scFv)-MAP in MDA-MB-231 cells.**

**A:** Cell cycle analysis of cells treated with αCSPG4(scFv)-MAP for 48 and 72 hours was determined by flow cytometry II.2.6.7). The DNA content was quantified by propidium iodide (PI) staining. PI signal was measured in the FL-2A channel gating on single cells; cell debris were excluded. **B:** graphical representation of the results from A. The average frequency (n=3) of cells in G1 phase (grey) and G2 phase (white) were calculated as fold change of the frequency in treated samples compared to the control. Statistical analysis (II.2.8) was carried using a two tailed *t*-test, data is representative of mean (n=3) + SD. *$p < 0.05$.

## *III.2.3 In vivo evaluation of αCSPG4 CFPs*

### *III.2.3.1 Establishment of subcutaneous tumors in BALB/c Nude mice*

As with the MDA-MB-468 cells (III.1.3.1), an initial experiment was performed to determine the best protocol to induce subcutaneous tumors in BALB/c Nude mice. (Table 12)

**Table 12. Tumor take rate study design- induction of MDA-MB-231 subcutaneous tumor in BALB/c Nude mice (II.2.7.2):**

| | **Right lower flank** | **Left lower flank** |
|---|---|---|
| **Group 1- (N=3)** | Katushka transfected– With Matrigel (1:1) | Katushka transfected- Without Matrigel |
| **Group 2- (N=3)** | Not transfected – With Matrigel (1:1) | Not transfected- Without Matrigel |

Tumor growth was monitored by optical imaging with Cri Maestro system and by caliper measurements for 30 days. There was 80% tumor take rate (5 out of 6 mice). The results

(data not shown) revealed similar growth pattern for the Katushka transfected cells compared to the non-transfected cell in the Matrigel set up. However 2 of the Katushka transfected tumors lost their fluorescence when injected without Matrigel. Furthermore, although the group injected with the cells without Matrigel had on average a higher tumor growth, there was more variability in the tumor sizes and rates of growth independently from Katushka transfection. Therefore the Katushka transfected cells with Matrigel protocol was chosen for the following studies.

#### *III.2.3.2 In vivo toxicity and therapeutic efficacy*

##### *III.2.3.2.1 Maximum tolerated dose studies*

Prior to treatment studies, the toxicity of the CFPs was assessed in tumor-free mice. Three mice per treatment group received 4 identical doses *i.v.* of either 0.5, 1.0, 2.0, or 4.0 mg/kg of αCSPG4(scFv)-MAP or αCSPG4(scFv)-ETA'. The overall health status of the mice was monitored daily. No adverse effects or body weight loss were observed even in the highest dosage of αCSPG4(scFv)-MAP (Table 13), however in the case of αCSPG4(scFv)-ETA' weight loss was observed at the 2 mg/kg dosage and all mice died at the highest dosage of 4 mg/kg (Fig 5B). The maximum tolerated dose was not reached for αCSPG4(scFv)-MAP and for αCSPG4(scFv)-ETA' the maximum tolerated dose was 2 mg/kg. Due to the high viscosity and the tendency to precipitate in high concentrations of αCSPG4(scFv)-MAP and the limited volume that could be injected (100ul per mouse a day) 2.5 mg/ kg concentration was chosen for the treatment studies.

**Table 13. Dose escalation studies *in vivo* of CSPG4 specific CFPs in mice (II.2.7.1):**

| Dose escalation studies | CFP | 0.5 mg/kg | 1 mg/kg | 2 mg/kg | 4 mg/kg |
|---|---|---|---|---|---|
| **survival** | M-MAP | 3/3 | 3/3 | 3/3 | 3/3 |
| | M-ETA' | 3/3 | 3/3 | 3/3 | 0/3 |
| **Average loss of body weight after 4 doses** | M-MAP | None | None | None | None |
| | M-ETA' | None | 5% ± 2.3% | 13% ± 4.6% | |

Values were calculated as mean + SEM (n=3). Abbreviations: M-MAP: αCSPG4(scFv)-MAP, M-ETA': αCSPG4(scFv)-ETA'

##### *III.2.3.2.2 Establishment of MDA-MB-231/ tdKat tumors for in vivo studies*

39 BALB/c Nude mice were injected in the lower right flank with Katushka transfected MDA-MB-231 cells (II.2.7.4). Tumor growth was monitored every other day using live imaging and caliper measurements. 80% tumor take rate was observed (32 / 39 mice). Treatment started 15 days after tumor induction at an average tumor size of 50 $mm^2$. 7 mice per group were used.

#### *III.2.3.2.3 Efficacy of EpCAM targeting CFPs in a Xenograft tumor model*

Biological efficacy of αCSPG4(scFv)-MAP *in vivo* was tested using a subcutaneous MDA-MB-231/tdKat xenograft model (II.2.7.4). Treatment with either αCSPG4(scFv)-ETA' (4 x 1.2 mg/kg dose) or αCSPG4(scFv)-MAP (4 x 2.5 mg/kg) resulted in significant tumor regression (Figure 35 A). Tumor sizes were monitored using both *in vivo* imaging of Katushka signal and caliper measurements. Treatment with αCSPG4(scFv)-MAP and αCSPG4(scFv)-ETA' resulted in comparable inhibition of tumor growth. Moreover, treatment with αCSPG4(scFv)-SNAP-tag (Figure 35 B) did not result in any tumor growth inhibition, thus demonstrating that the antitumor activity of both CFPs was mediated by their effector domains.

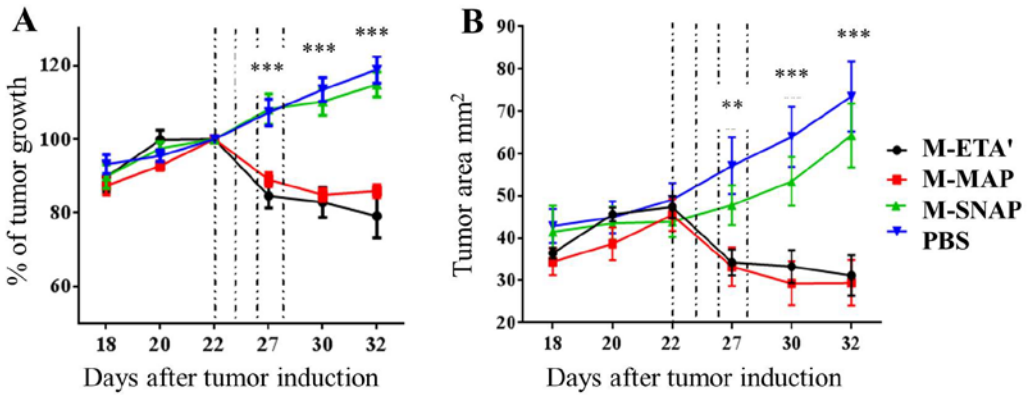



**Figure 35. Inhibition of tumor growth *in vivo* by CSPG4 specific CFPs in MDA-MB-231 subcutaneous tumor model.**

Mice bearing Katushka-2-transfected MDA-MB-231/tdKat tumors (II.2.7.2) were injected *i.v.* with PBS (▼), 2.5mg/kg αCSPG4-MAP(scFv) (■),1.25 mg/kg αCSPG4(scFv)-ETA' (●) and (▼)αCSPG4(scFv)-SNAP. Treatment was started when the tumors reached 50 $mm^2$, and was delivered 4 times over a period of 8 days (II.2.7.4). **A:** Relative tumor growth following treatment as measured by *in vivo* imaging. Tumor size at each time point was normalized to the tumor size on day 21 (one day prior to initiating treatment) which was set to 100%. **B:** actual tumor size as measured by caliper and calculated according to ellipse area formula. Values are presented as means ± SEM (n = 7).

Statistical analysis was carried out II.2.8) using a two-way ANOVA, ***p ≤ 0.001 comparing treatment groups to the PBS control. Dashed vertical lines represent dosing days. Abbreviations: M-SNAP: αCSPG4(scFv)-SNAP tag; M-MAP: αCSPG4(scFv)-MAP, M-ETA': αCSPG4(scFv)-ETA'.

### *III.2.3.3 Tumor targeting and biodistribution studies in vivo*

#### *III.2.3.3.1 In vivo accumulation of αCSPG4(scFv)-SNAP in tumor site*

Initial targeting studies were done in the same mice that were used for tumor establishment studies (Table 12) at the end point of the experiment (30 days after tumor induction). This was done using αCSPG4(scFv)-SNAP protein coupled to BG-Alexa 747 dye (II.2.3.1 ,Figure 36 A). 20 µg of proteins were injected *i.v.* and the signal was monitored after 8 hours and 24 hours. These studies revealed that αCSPG4(scFv)-SNAP-Alexa 747 was distributed to highly perfused organs and rapid clearance through the kidneys. αCSPG4(scFv)-SNAP-Alexa 747 could reach and accumulate in the tumor site within few hours (Figure 36B). The signal remained in the tumor site and in the kidneys for 24 hours. However a strong background signal was present in all time points and in all mice in the injection site and the neck and upper back of the mice.

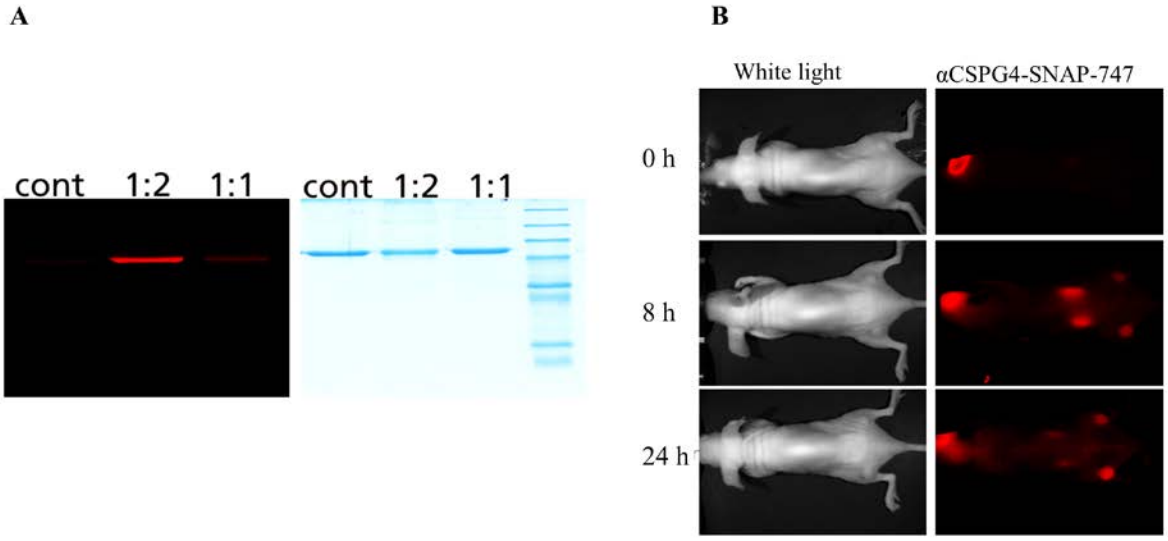



**Figure 36. *In vivo* imaging of the accumulation of αCSPG4(scFv)-SNAP in MDA-MB-231 subcutaneous tumors in mice.**

**A:** SNAP tag fusion protein was labeled with a 2 fold molar excess of Benzyl-Guanine modified Alexa-747 for two hours (II.2.3.1). Excess dye was removed using Zeba™ Spin Desalting Columns. Fluorescent visualization of SDSPAGE (II.2.4.2) (Left panel) and subsequent Coomassie staining (II.2.4.2) (right panel) of the labeled proteins after removal of the free dye were performed. **B:** Whole

body imaging of mice bearing (II.2.7.2) MDA-MB-231 and MDA-MB-231/tdKat (II.2.1.6) tumors injected *i.v.* with 20 µg of αCSPG4(scFv)-SNAP labeled with Alexa-747 (II.2.7.5). *In vivo* imaging was carried out 1 hour, 8 hours and 24 hours after injection. Fluorescent signal was converted into a color intensity map using the Maestro Cri software.

#### *III.2.3.3.2 In vivo tumor targeting and biodistribution of αCSPG4(scFv) CFPs*

αCSPG4(scFv)-MAP and αCSPG4(scFv)-ETA' were labeled with DyLight 747-B3 NHS ester dye, and injected *i.v.* into BALB/c Nude mice bearing MDA-MB-231/tdKat subcutaneous tumors as described in MM (II.2.7.5) (12 mice from the different treatment groups were randomly selected for this experiment). Fluorescence measurements were taken using the CRi Maestro Imaging System at elapsed time points of 0, 4, 8 and 24 h post-injection

Upon *i.v.* administration, a strong fluorescent signal of DyLight 747 at the injection site and rapid distribution to highly perfused organs (e.g. liver, lung, kidney, spleen, and gut) was observed (Figure 37). The results revealed clearance of the fluorescent signal from blood stream and most of the central compartment organs within few hours, apart from the kidneys where the signal remained for up to 24 h. Accumulation of αCSPG4(scFv)-MAP-747 fluorescence in the tumor site was detected starting 1 h post-injection and increased as the signal from the other compartments was fading (Figure 37 A). The signal in the tumor site remained detectable for at least 24 h. Imaging of the primary fluorescent signal of the MDA-MB-231/tdKat cells clearly showed the co-localization of αCSPG4(scFv)-MAP-747 in the tumor tissue. Similar results were observed for αCSPG4(scFv)-ETA'-747 (Figure 37 B).

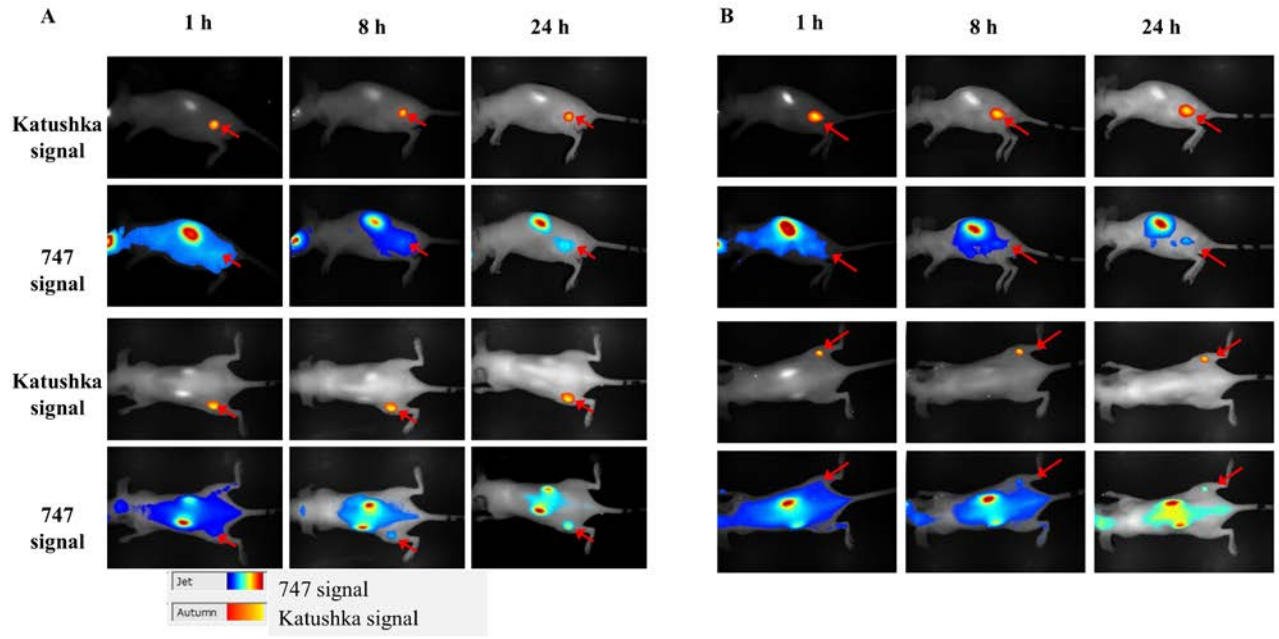



**Figure 37. Biodistribution kinetics of CSPG4 specific CFPs in xenograft mouse model.**

**A:** αCSPG4(scFv)-MAP and **B:** αCSPG4(scFv)-ETA' were labeled (II.2.3.2) with DyLight 747-B3 and 1.2 mg/kg were injected *i.v.* into mice bearing MDA-MB-231/tdKat tumors (II.2.7.2). Whole body live imaging of the fluorescent signal of the labeled CFP was performed 1, 8 and 24 h after injection (II.2.7.5). Imaging of the primary Katushka fluorescent signal of the MDA-MB-231/tdKat cells was done to confirm the colocalization of the CFPs signal with tumor site. Red arrows indicate the tumor site. Fluorescent signal was converted into a heat map using the Maestro Cri software.

# IV Discussion

## *IV.1 Triple negative breast cancer (TNBC) current therapy*

Breast cancer is the most common cancer in women worldwide. Triple negative breast cancer defined by the absence of expression of ER, PR and HER2 receptors comprises 12%-30% of breast tumors depending on population, age and ethnicity (42, 50). TNBC tumors are among the most aggressive breast tumors, and are associated with higher grade and brain metastasis (3, 8). The poor prognosis and prevalence of TNBC among young women highlight the urgent need of developing efficient therapies (48, 175). TNBC patients cannot benefit from the well-established available targeted therapies for other breast cancer subtypes, such as aromatase therapy (60), tamoxifen (59) and trastuzumab (51, 52) targeting the hormone receptors ER and PR and the HER2 receptor. The traditional course of treatment for TNBC is surgery and chemotherapy (176, 191-193). Despite several reports describing a good response of TNBCs to chemotherapy (192, 193), recurrence and aggressive metastasis are common among TNBC patients that receive traditional therapy (48, 175). Additional therapies such as taxanes and anthracyclines are being used in the adjuvant and neoadjuvant settings, but their benefit remains unclear (192). While some trials show positive role for their use in TNBC patients (62, 194) others have found no significant added benefits (192, 195). Several approaches for targeted therapies have been evaluated in clinical trials in the past years including targeting of the receptors for vascular endothelial growth factor (VEGF) (68, 69, 196, 197), epidermal growth factor (EGF) (70, 72, 198) and mesothelin (142, 143). The initial results illustrate only a modest if any benefit of these therapies (61, 73). So far the results from targeting EGFR have been disappointing, with little to no benefit observed for the use of these antibodies in combination with chemotherapy. Many anti-EGFR agents are already clinically available for many different types of cancer (74, 199-201). The monoclonal antibody cetuximab (74) has been tested in patients with TNBC when combined with single-agent carboplatin and with carboplatin/irinotecan with mixed results ranging from minor improvement to a moderate improvement in the response rate (objective response rate (ORR) = 18% and ORR = 49% in the TNBC population) (63, 64, 67).

The anti-vascular endothelial growth factor (VEGF) monoclonal antibody, bevacizumab, has been shown to increase response rate (RR) of patients with metastatic breast cancer when added to first-line chemotherapy, the results from three clinical trials were mixed, with some patients showing improvement in the response rate but others showing no advantage, and its approval for use in metastatic breast cancer has now been rescinded by the FDA (68, 196, 197, 202).

More recently (2015), the monoclonal antibody ramucirumab (IMC-1121B, ImClone) targeting VEGFR-2 in combination with docetaxel failed in a phase III clinical trial in patients with HER2- negative metastatic breast cancer (203). Addition of ramucirumab to docetaxel to this patients group did not meaningfully improve clinical outcomes (ClinicalTrials.gov NCT00703326).

mTOR and PARP-1 inhibitors therapies are also being investigated in the adjuvant setting. The results from these trials are more promising (65-67, 204-206). The DNA repair protein PARP-1 is involved in the repair of DNA breaks. Basal like tumors (80% of TNBC tumors), especially tumors with BRCA mutations tend to have defects in repair of DNA breaks by homologous recombination. Therefore, inhibition of PARP-1 might lead to accumulation of DNA breaks and apoptosis. PARP-1 inhibitor BSI-201 was combined with chemotherapy (gembcitabine and carboplatin) for treatment of TNBC patients who had two previous lines of chemotherapy and the overall response rate improved from 16% to 48% (207). Other approaches such as targeting chaperone protein HsP90 have also shown positive results (208).

However, one has to keep in mind that TNBC is a heterogeneous disease. Gene expression studies (32, 34) and molecular profiling (11) have classified TNBC tumors and cell lines into three (11) or six (34) molecular subtypes. The heterogeneity of TNBC tumors raises the need for developing a panel of targeted therapies which can, together, include the vast majority of TNBC tumors and enable the specific tailoring of therapies for the particular needs and disease of each patient. In this thesis, two markers EpCAM and CSPG4 were singled out, which are both differentially overexpressed on TNBC tumors. The results show little to no overlapping expression for these markers in TNBC cell lines (Figure 5, Figure 21), each being overexpressed in different TNBC cell lines representing different subtypes of TNBC. Furthermore, the expression of these markers on biopsy samples of TNBC patients by immunofluorescent staining with αEpCAM(scFv)-SNAP and αCSPG4(scFv)-SNAP confirmed this hypothesis. (*Data was acquired by Ahmad F. Hussain, and prepared for publication in Oncotarget: Amoury M et al. photoimmuno-*

*theranostics for triple negative breast cancer diagnosis and treatment that can be activated on demand*). In 90% of the samples one of the two receptors was expressed (36 / 60 $EpCAM^+$ and 18/ 60 $CSPG4^+$), and together, these receptors are expressed on the majority of TNBC tumors. The results from this study indicate that the assembly of a panel of markers and therapeutics, which includes EpCAM and CSPG4, represents a highly promising approach for targeting TNBC.

## *IV.2 Targeting TNBC using CSPG4*

CSPG4 expression is up-regulated in several cancer types (86). Its expression in high levels in normal tissue is mainly limited to fetal development stages, although protein expression at lower levels could be detected on internal tissues (209, 210). Studies suggest its involvement in stem cells niche maintenance and development and in vascular tissue development (86, 89, 211). Evidence for these roles comes from studies demonstrating CSPG4 expression on many stem and pluripotent cell populations where it plays an important role in regulating their motility and positioning within the niche (209, 212). Additionally, mice lacking NG2 (CSPG4 mouse orthologue) suffer from defects in vasculature (213). Most of the research focusing on CSPG4 in cancer was done on melanomas due to its abundance and high expression in these tumors (more than 70% of superficial spreading and nodular human melanomas) (86, 214). Many of these studies highlight CSPG4 role in cancer initiation, as it seems to be expressed on malignant cells in a very early stage of cancer (188, 214, 215). Additionally CSPG4 plays a role in metastasis and is associated with more aggressive tumors (215). Altogether, these data make CSPG4 an attractive target for antibody-based therapies (86). So far, immunotherapies targeting CSPG4 have not shown any significant or severe side effects, and patients who developed anti-CSPG4 antibodies had improved responses and better outcomes (216).

In breast cancer patients, high CSPG4 expression correlates with poor prognosis (89). Analysis of breast cancer cell lines revealed that CSPG4 expression is limited to subtypes characterized as basal B or ‘mesenchymal’ subtype’ (11, 34), which is in agreement with the findings of this study (expression in Mesenchymal cell lines MDA-MB-231 and Hs 578T, Figure 21). These subtypes are characterized by increased expression of genes associated with epithelial-mesenchymal transition and cell motility, signaling pathways prominent in stem cell-like $CD44^+/CD24^-$ normal mammary cells (217). CSPG4 expression correlates with a higher frequency of $CD44^+/CD24^{low}$ tumor cells with an

aggressive phenotype in TNBC tumors (88, 90, 91). Therefore, targeting CSPG4-expressing tumor cells in breast cancer patients is a valid and potentially beneficial approach.

### *IV.3 Targeting TNBC using EpCAM*

EpCAM is one of the first "cancer antigens" discovered. It is expressed on most carcinomas, and has been extensively studied for its role in supporting cancer stem cell proliferation and in cancer circulating cells and metastasis (75, 80, 218-222).

In this study, we tested EpCAM expression on cell lines representing the different TNBC subtypes (Figure 5). MDA-MB-468 was classified by Kao *et al.* (11) as belonging to the basal A subtype. MDA-MB-453 was classified as luminal subtype, and MDA-MB-231 and Hs 578T as basal B. EpCAM overexpression was detected on both MDA-MB-468 and MDA-MB-453 cells, but not on the basal B cell lines MDA-MB-231 and Hs 578T (Figure 5, Interestingly, this is an opposite picture to the expression of CSPG4, Figure 21).

Even though EpCAM is also expressed on the surface of healthy epithelial tissues it is mainly expressed on the basolateral surface where EpCAM is less accessible to antibodies than in tumors (223). Additionally, EpCAM expression and glycosylation levels are strongly elevated in cancer cells compared to EpCAM on normal cells (219). Several clinical trials using anti-EpCAM antibodies indicated that the affinities of the respective antibodies played a significant role in their therapeutic benefit (96, 224). It was shown that an antibody with moderate binding affinity rather than high affinity showed a better therapeutic activity and reduced side effects (224). High affinity was also shown to restrict tumor penetration of scFv (225). Following this rationale, a fully human, moderately binding single chain was chosen with $K_d$ values in the Nano-molar range rather than other scFvs with $K_d$ values in the Pico-molar range (187). Moreover, we (Hristodorv D and Amoury M) (149) have previously shown the efficacy of a novel CFP consisting of an anti-EpCAM(scFv) and a MAP tau protein to eliminate different carcinoma cell lines. The results in this study reveal that this scFv binds moderately to cells expressing high levels of EpCAM and is internalized effectively (Figure 8), but does not affect cells expressing low levels of EpCAM such as MDA-MB-231. This characteristic may help to reduce possible side effects such as acute pancreatitis observed for high affinity EpCAM-specific antibodies ING-1 and 3622W94 (224, 226-229). Indeed no such side effects were observed for the moderately binding anti-EpCAM antibody adecatumumab (224). This is especially

significant given the fact that EpCAM is expressed in low levels on many other normal cells and tissues.

### *IV.4 Cancer Immunotherapy as an alternative to traditional chemotherapy*

Immunotherapy using full length "naked" antibodies revolutionized cancer therapy. Specific targeting of cellular markers that are enriched on the malignant cells has proved to be beneficial in hematologic tumors and in some solid tumors such as $HER2^+$ breast cancer. Several antibodies are currently in clinical trials and some have already been approved. Trastuzumab for breast cancer (targeting HER2) (51), cetuximab for colon cancer (EGFR) (64), bevacizumab (VEGF) (230, 231), and rituximab for lymphomas (CD20) (232), are among the most successful antibodies that gained FDA approval. However, many other antibodies failed to show significant improvement in clinical trials. The failure of many mAbs may be associated to the way they exert their therapeutic effect (233). There are 3 main pathways in which antibodies lead to cell death: 1. the binding of the antibody to the receptor leads to the abrogation of cell signaling which leads to apoptosis. 2. The fragment crystallizable region (Fc) of the antibody is recognized by cells in the immune system that express the FC-receptor, which in turn stimulates these cells and initiates an immune response. This leads to the activation of cytotoxic cells which then attack and eliminate cancer cells through antibody-dependent cellular cytotoxicity (ADCC) and complement dependent cytotoxicity (CDC). 3. Some antibodies such bevacizumab target tumor environment and therefore inhibit tumor vasculature and stroma (234, 235). The dependence of antibody mediated toxicity on a functional host immune system is one problem, especially in people who received chemotherapy and or radiation therapy and have a compromised immune system. Additionally many tumor cells have developed escape mechanisms from the effects of antibodies, by changing the tumor microenvironment leading to the induction of immune tolerance towards the tumor cells, and preventing immune response. Moreover, the selective pressure exerted on tumor cells by repetitive administration of the antibody leads to resistance of the cells to the abrogated signaling or the downregulation of the targeted receptor (236). Therefore, many efforts have been focusing on the use of antibodies as "magic bullets" to deliver chemotherapeutic and toxic reagents selectively to the tumor cells, instead of relying on the limited toxicity exerted by these mAbs alone (99, 118, 237).

Traditional cancer therapy relies on the killing of rapidly dividing cells. The toxins used are not specific and are very toxic to normal dividing cells as well, which results in systemic toxicity (192). Methods that allow the selective delivery of these therapeutic molecules to cancer cells can reduce side effects and greatly improve patients' quality of life (200, 238).

Passive immunotherapy addresses these issues, by using bifunctional molecules with an antibody or antibody fragments binding domains suitable for selective targeting of tumor cells and cytotoxic effector domain to kill targeted cells.

Antibody drug conjugates (ADCs) are usually comprised of mAbs which are cross-linked to small cytotoxic agents or plant and bacterial proteins using chemical conjugation methods (118, 239). Many reagents have been used as a toxic moiety. Interestingly, some of the most promising ADCs utilize reagents disrupting tubulin dynamics such as taxanes. Trastuzumab-emtansine (T-DM1), is such an ADC targeting HER2. T-DM1 therapy resulted in improved response rate and overall survival in patients who had previouslydeveloped resistance to the HER2 monoclonal antibody therapy (240). Brentuximab vedotin, is another ADC inhibiting tubulin polymerization that has been approved by the FDA for the treatment of anaplastic large cell and Hodgkin lymphoma (237, 241).

Some of the shortcomings and challenges of ADCs are their heterogeneous integrity and undefined stoichiometry by chemical conjugation, their reduced serum stability and their immunogenicity (242).

In this study we utilize single chain variable antibody fragments (scFv) as the binding moiety to generate cytotoxic fusion proteins (e.g. recombinant immunotoxins ITs). The use of ITs as opposed to full length antibody-drug conjugates (ADCs) remains continuous subject to discussion (52, 99, 109, 122). The main potential advantages for using recombinant fusion proteins include their reduced size for better tumor penetration and their ease of purification as homogenous recombinant drug formulations (99, 122, 243). This class of protein therapeutics can be easily produced as a single recombinant molecule in high yields and subsequently purified resulting in a homogenous product. The results presented in this thesis with EpCAM targeting scFv-based fusion proteins demonstrate this, with high purity (>90%) achieved in a two-step purification process and high stability with very low degradation within 6 months (Figure 2). CSPG4 targeting scFv-based fusion proteins proved to be more difficult to purify, but this could be solved by the addition of a strep-tag (Figure 23Figure 24). Additionally, the internalization and the routing of scFv

fusion proteins compared to antibody drug conjugates seem to be different (244-246). Due to their bivalent binding, ADCs generally have a stronger binding affinity and rapid internalization compared to a monovalent scFv which recognize the same epitope. ADCs binding of two adjunct receptors can lead to their dimerization and rapid internalization which makes them prone to the lysosomal compartments and degradation (246, 247). Alternatively, due to slow $k_{off}$ rates of ADCs, they can be immediately recycled to the cell surface following internalization, without releasing their toxic moiety (248-250). In both cases, these properties seem to limit the tumor penetration and retention of ADCs (251). On the other hand scFv based immunotoxins and CFPs can only bind one receptor, do not induce receptor dimerization, and have weaker affinities as well as faster $K_{off}$ rates than full length antibodies, which allow for increased tumor penetration and retention (99, 225, 252-254). Indeed the results from the binding affinity assays show that EpCAM and CSPG4 scFv-based fusion proteins have moderate affinities in the Nano-molar range (Figure 7, Figure 26) and are internalized slowly with 50% internalization achieved around 2 hours (Figure 9, Figure 27).

Similarly to ADCs, a major disadvantage of first generation ITs is their immunogenicity. The use of bacterial or plant toxins can induce undesirable immune responses and dose limitations due to severe side effects (93, 108). Many clinical trials have shown that the incidence of immunogenicity after a single dose of IT ranges from 50–100% for solid tumors. However, in many instances, patients that have developed neutralizing antibodies to the ITs were still responsive to subsequent IT treatments, indicating that these ITs could be successfully used despite their immunogenicity (255), additionally, administration of Pentostatin plus cyclophosphamide prior to treatment with immunotoxins was shown to reduce the development of neutralizing antibodies (138, 139, 255).

### *IV.5 Sensitivity of TNBC cell lines towards ETA' immunotoxins*

The mechanism in which ETA' (Pseudomonas Exotoxin A deletion mutant) immunotoxins exert their toxicity depends greatly on their internalization through the endosome in a receptor mediated endocytosis (115, 128, 133, 256). ETA' is then processed through several steps that facilitate its translocation from the endosome to the cytosol: The immunotoxin (IT) undergoes retrograde transport through endosomes to the *trans*-site of the Golgi apparatus. This process is dependent on the protein Rab9, which functions in the

transport between late endosomes and the trans Golgi network (257). There, ETA' catalytic domain can be cleaved from the rest of the immunotoxin through its Furin cleavage site. Furin is a protease localized in the trans-Golgi (114-116) This step which allows the toxic domain to separate from the binding domain and translocate alone to the cytosol has been shown to increase the cytotoxicity of immunotoxins (114, 256, 258). Finally, ETA' is then transported to the ER using Rab6- and Arf1-dependent pathways with the mediation of KDEL- ER retention signal (or the ETA' homologue REDL) (93, 113, 132, 133).

The final step is the execution of cytotoxicity. Once ETA' is catalytically active in the cytosol, it catalyzes the ADP-ribosylation of EF2 (elongation factor 2), which leads to its inactivation thus halting protein synthesis in the cell (131, 259, 260).

In this study ETA' was used as a "gold standard". Both EpCAM and CSPG4 targeting scFvs- ETA' fusion immunotoxins (ITs) did bind specifically, were internalized (Figure 8, Figure 26) and were selectively cytotoxic towards TNBC cell lines that express their target antigen (Figure 10, Figure 30). However, it is noteworthy that the initial studies with the traditional immunotoxin αCSPG4(scFv)-ETA' which was cloned using the PPD group's "golden standard" ETA' vector-" pMT" (VI.3.2, Figure 22A), failed to generate positive results. This IT proved to be difficult to produce and purify. The amounts of purified and functional proteins that were generated were too low and contaminated with bacterial protein (Figure 23), and the results of subsequent functionality assays were disappointing. Consiquently, we replaced this IT with an "improved" version. The optimized version (VI.3.4) was generated and reported by Schwenkert et al. (189). This αCSPG4(scFv)-ETA' (Figure 22B) consists of an additional Streptavidin tag to allow for an additional purification step to achieve better purity when compared to the enrichment by the poly-Histidine tag alone. Additionally the ETA' ER retention signal homologue- REDL was replaced with the native ER retention sequence- KDEL, to enhance endosomal escape and translocation into the cytosol (136). And, finally a $(Gly_4Ser)_4$ linker was inserted between the scFv and ETA' sequence to increase the flexibility and stability of the construct (patent WO 2008131940 A2 (261)) . Indeed, with the new construct, better results were obtained in terms of purity (>90%) without visible bacterial protein contaminants. The improved construct also proved to be more toxic, with 10-20 folds improvement in IC-50 values approximately 300- 800 nM with the standard αCSPG4(scFv)-ETA' (data not shown, rough estimate due to low purity of protein, Figure 23), compared to 20-40 nM with the optimized αCSPG4(scFv)-ETA' Figure 30). Therefore, all experiments in this thesis were performed using the optimized version of αCSPG4(scFv)-ETA' (VI.3.4).

Both αEpCAM(scFv)-ETA' and the optimized αCSPG4(scFv)-ETA' performed well in the cytotoxicity assays, with IC-50 values in the Nano-molar range (20-80 nM, Figure 10 & Figure 30) and had higher toxicity *in vitro* compared to the hCFPs. Both rITs induced apoptosis in a dose and receptor selective manner. However, *in vivo* studies in mice revealed that ETA' ITs were not well tolerated, caused weight loss (Figure 19, Table 13) of 10% - 20% in the 2 mg/kg concentration, and were lethal at the 4 mg/ml concentration (Table 13). The MTD values measured for these ITs were 1-2mg/kg, Table 13, (96). Treatment of mice bearing TNBC tumors with ETA' rITs resulted in significant tumor growth inhibition of 50% with αEpCAM(scFv)-ETA' treatment (Figure 20) and 60% tumor regression with αCSPG4(scFv)-ETA', but did not abolish the tumors completely.

Our results are consistent with other published data using ETA' ITs and the maximum tolerated doses of ETA' are usually under 1 mg / kg (120, 138, 144, 262-264). Fusion of scFvs to plant and bacterial toxins such as ETA' can result in highly toxic anti-tumor compounds. However these compounds are associated with dose-limiting side effects and cause severe side effects such as vascular leak syndrome (VLS), liver toxicity and adverse immune reactions (109, 265-267). To this end, point mutations and deletions were introduced to the toxin domains to reduce their immunogenicity, including the removal of potential T- and B-cell epitopes on ETA' (110, 268, 269). Furthermore, localized administration of the ITs and the addition of immunosuppression therapy as well as premedication with dexamethasone, which has been shown to diminish severity of VLS are new approaches currently being tested in clinical trials (270-272). However, the search continues for better alternatives with reduced immunogenicity, and little off site toxicity.

### *IV.6 Human cytolytic fusion proteins as an alternative to ITs*

To overcome the limitations of ITs alternative approaches have been developed in which the bacterial toxins are replaced with cytotoxic human proteins creating so-called human cytolytic fusion proteins (CFP) (111, 123, 124, 149, 150, 155, 273).

The relative activity of CFPs is dependent on the characteristics of the corresponding tumor-associated cell surface antigen. Receptor concentrations, internalization and translocation rates are key factors in the efficacy of CFP. In comparison to ETA'-based IT, combinations of antibody fragments with human enzymes could strongly reduce immunogenicity but lack the intrinsic components driving translocation and endosomal escape. This may decrease the efficiency of these proteins to induce cell death and lead to

reduced anti-cancer activity (121). However, several studies published by our group have previously shown that combining the anti-CD64 antibody fragment H22 with human enzymes including Granzyme B, MAP and angiogenin result in CFPs with comparable activities to ETA'-based IT (125, 149, 153, 155). In this study, *in vitro* cell viability assays demonstrated that the CFPs resulted in a 5-10 fold lower toxicity than their ETA' counterparts in TNBC cell lines (Figure 10, Figure 30). The reduced toxicity could be attributed to the lack of translocation domains and endosomal escape mechanism. In order to facilitate and enhance endosomal escape, attempts to incorporate adapters into human CFPs design were done by our group as well as other groups (111, 274). These adapters facilitate endosomal escape, and have been shown to improve the translocation efficiency of the CFPs and increase their cytotoxicity. Such adapters can be inspired from the native translocation domains of bacterial and plant toxins, as well as the native signal peptides present in intracellular human proteins. Furthermore, Cao *et al.* (274) observed greater cytotoxicity when a pH-sensitive fusogenic peptide was incorporated into an anti HER2/ Granzyme B CFP. However, pH- sensitive adapter must be used with caution due to the possibility of reduced stability and the premature release of the toxins before reaching the target cells.

Although the mechanisms of endosomal escape of human CFPs remain unclear, the current results are supported by other studies in this field, such as the work of Liu *et al.* targeting $CSPG4^{+}$ melanoma cells using a Granzyme B-scFvMEL CFP that lacks an adapter or a translocation domain (98). In this study, we have also utilized a Granzyme B (152) CFP (Figure 1). Granzyme B is a serine protease, naturally found in the granulocytes of natural killer cells, and it is a strong inducer of apoptosis which has already been described as an effective cytotoxic domain to generate completely human cytolytic fusion proteins for targeted therapy (153, 154, 274). Our group, recently developed Granzyme B R201K mutant which is insensitive towards its natural inhibitor serpin B8 (PI9) (Losasso et al. (164)). By using the PI-9-insensitive R201K mutant, a broader range of cancer cells could be efficiently eliminated, including malignant cells overexpressing serpin B9 that would otherwise escape from Granzyme B-induced apoptotic cell death (155).

Another human cytolytic protein presented in this study is MAP tau (Figure 22). MAP tau is a modified version of human microtubule-associated protein tau, which has recently been exploited to generate human CFPs that can efficiently eliminate different types of cancer cells (149, 150, 170). Major serine phosphorylation sites (S156 and S204) in MAP tau were deleted to prevent negative regulation (275) as well as pathologically relevant

formation of paired helical filaments (275, 276). This recombinant MAP tau protein when fused with a binding moiety is able to specifically and efficiently induce apoptosis in proliferating cancer cells by binding to and stabilizing tubulin (149, 150, 170).

### *IV.7 Mechanism of action of αCSPG4(scFv)-MAP*

In the current study, we are presenting a MAP-based CFP with pro-apoptotic activity towards CSPG4-expressing TNBC cell lines (Figure 22). The αCSPG4(scFv)-MAP fusion protein combines a mode of action comparable to that of taxanes with the specific targeting of $CSPG4^+$ cells. Similar strategies- targeting tubulin polymerization have been used by others to generate ADCs linking taxanes to monoclonal antibodies. Some of these ADC's are currently in clinical trials such as ado-trastuzumab emtansine (240) which consists of a HER2-specific antibody linked to the microtubule inhibitor emtansine. This ADC has been approved by the FDA for treatment of metastatic breast cancer (277), showing improved patient's survival, but at the cost of severe side effects. CFPs such as αCSPG4(scFv)-MAP are considered inherently safer due to their uniformity and stability when produced as a single recombinant protein (242). The use of recombinant αCSPG4(scFv)-MAP provides an alternative to chemical conjugation of microtubule inhibitory agents to full length antibodies which often results in a heterogeneous product with a different drug-to-antibody ratio (DAR) and different drug load distribution (118, 278). Moreover, taxanes are small immunogenic molecules while MAP is a human protein. It cannot be internalized into cells without the addition of a binding domain, while free taxanes can be internalized in a nonspecific manner and cause off target toxicity (118, 243, 245).

Our results indicate that αCSPG4(scFv)-MAP worked in a similar manner to conventional microtubule-stabilizing therapeutics (168, 279), by binding to tubulin polymers inside the cells (Figure 28), inhibiting cell growth by causing a partial cell cycle arrest (Figure 34), and inducing cell death (Figure 31). This mode of action confines its cytotoxic activity mainly to rapidly proliferating cells, thus reducing toxicity to normal cells expressing the same target antigen.

Interestingly, αCSPG4(scFv)-MAP-mediated induction of cell death in MDA-MB-231 cells appears not to be exclusively caspase-dependent with little to no activation of caspase 3 (Figure 32). These results are in line with several reports discussing mechanism of action of taxanes, especially in MDA-MB-231 cells (279, 280). These studies have shown that while taxanes can induce apoptosis in some cell lines, they mostly cause cell death through

mitotic catastrophe or other caspase independent pathways in more resistant cell lines such as MDA-MB-231. In an attempt to further dissect αCSPG4(scFv)-MAP-mediated cytotoxicity, caspase-9 activation was explored. Caspase 9 activation can be achieved in a caspase-independent pathway through loss of mitochondrial membrane potential and release of cytochrome C. Our results indicate that some activation of caspase-9 did occur (Figure 33), but the levels of active caspase 9 were not potent enough to account for the total effect of MAP. Interestingly, αCSPG4(scFv)-MAP treatment resulted in translocation and activation of the mitochondrial endonuclease G (281) apoptotic pathway (Figure 33). This mechanism was previously demonstrated in cells subjected to ultraviolet irradiation or treated with TNF or taxanes, whereas the translocation of endonuclease G from mitochondria to nuclei was observed, which led to cleavage of nuclear DNA and to cell death (282). It was also shown that the translocation of endonuclease G and its nuclease activity can induce apoptosis in a caspase-independent manner, which occurs prior to the loss of mitochondrial membrane potential (281, 283). At this point several questions regarding the mechanism of action of αCSPG4(scFv)-MAP remain unanswered. Further studies are required to fully demonstrate how αCSPG4(scFv)-MAP induces cell death: To this end, experiments with different caspase inhibitors in combination with αCSPG4(scFv)-MAP can be utilized to determine whether cell death can be completely caspase-independent (284, 285). To explore the effects on cell cycle dynamics, studies of the phosphorylation and association of cyclins and CDKs at the different check points of the cell cycle should be performed (286). Also, one could explore whether cell death by αCSPG4(scFv)-MAP involves events that lead to mitotic catastrophe (280, 287) by fluorescent microscopy and transmission electronic microscopy (TEM).

Our *in vivo* studies demonstrate that αCSPG4(scFv)-MAP has no general or systemic toxicity and dose escalation studies revealed toleration even at concentrations up to 4 mg/kg (Table 13). In addition the results demonstrate that αCSPG4(scFv)-MAP efficiently inhibits tumor growth (Figure 35). Its activity *in vivo* proved to be comparably potent to ETA' rIT although $IC_{50}$ values of αCSPG4(scFv)-MAP compared to αCSPG4(scFv)-ETA' were 5- to 9-fold lower *in vitro* (Figure 30). The treatment regimen comprised of 4 doses of 2.5 mg/kg αCSPG4(scFv)-MAP lead to tumor regression but not tumor ablation. The treatment outcome could possibly be improved by increasing the treatment cycle to 6 or 8 doses, by increasing the dosage or by repeating the cycle several times. Longer treatment cycles and higher concentrations have been used successfully for other CFPs. For example, Liu et al. treated mice with 5 doses of 37.5 mg/kg of GrB/scFvMEL(98). In our group,

colleagues have used longer cycles with 6 or 7 doses per treatment to elucidate massive tumor remission (155, 288). The absence of off-target toxicity of αCSPG4(scFv)-MAP (Table 13) even at 4 mg/kg dosage combined with a good efficiency in tumor inhibition *in vivo* highlights the possibility of further increasing efficiency when using a higher dosage and increasing the treatment cycle. However, further in depth studies are necessary to confirm this.

In conclusion, αCSPG4(scFv)-MAP holds a great potential as a novel human cytolytic fusion protein for targeting some of the most aggressive breast tumors, which so far lack any targeted therapy.

### *IV.8 Mechanism of action of GbR201K-αEpCAM(scFv)*

In this study, we show that the fusion protein comprised of Granzyme B with an anti-EpCAM scFv retains the tumor-selective binding activity of the scFv and the cleavage activity of the Granzyme B (Figure 6). Moreover, Granzyme B mutant R201K (164) is toxic in cells expressing its natural inhibitor serpin B9 (164, 289). This was demonstrated here, with the serpin B9 positive cell line MDA-MB-468 (Figure 4). The cytotoxic activity of GB-R201K-αEpCAM(scFv) compared to αEpCAM(scFv)-ETA' was 5-10-fold lower *in vitro* (Figure 10), which could be attributed to the lack of a translocation domain and to different toxicity mechanism e.g. by activation of different apoptotic pathways by GB-R201K-αEpCAM(scFv) compared to αEpCAM(scFv)-ETA' (for example Gb is a potent caspase 3 activator while ETA' is a weak caspase 3 activator but a potent caspase 9 activator) (Figure 12, Figure 13).

Dose escalation studies *in vivo* revealed that the general toxicity in mice of GbR201K-αEpCAM(scFv) was at least 3-folds lower than that of αEpCAM(scFv)-ETA' (MTD between 1-2 mg/kg for ETA' and MTD > 4 mg/kg for GbR201K, Figure 19). In the tumor inhibition studies a comparable overall inhibition of tumor growth of 40-50% was observed for both fusion proteins (Figure 20). However, our short treatment regimen consisting of a single course of 4 doses could not achieve full tumor remission. As with the MAP CFP, We hypothesize that longer or repeated course of treatment would be required to achieve better outcome. The absent off-target toxicity of GbR201K-αEpCAM(scFv) combined with a good efficiency in tumor inhibition *in vivo* highlights the possibility of better tolerability and efficiency when using a higher dosage. Further studies in this direction are necessary to confirm this. Our initial biodistribution studies suggest different

kinetics of clearance and tumor accumulation for GbR201K-αEpCAM(scFv) and αEpCAM(scFv)-ETA'. These differences might be further analyzed using more accurate measurements, such as radiolabeling of the CFPs and quantification of the signal in each organ separately. One possible explanation for the prolonged signal in central compartments of GbR201K-αEpCAM(scFv) might be due to the difference in the electrical charges of ETA' and Granzyme B (290). Several studies suggest that Granzyme B binds to cell surface mostly via unspecific charge interactions (290, 291). Bird *et al.* identified two positively charged residues involved in this unspecific binding and showed that mutating these amino acids, interferes with the interaction between Granzyme B and the cell membrane (290). Further study of these differences could be crucial when determining the best treatment regimen and dosage.

Taken together, in this study we present a novel, fully human and structurally stable therapeutic fusion protein with a high translational potential for targeted elimination of TNBC including the associated tumor-initiating cells.

## *IV.9 Outlook and potential scope of anti-EpCAM and anti-CSPG4 hCFPs*

anti-HER2 immunotherapy has been a major success story, and women with $HER2^+$ tumors have benefited greatly, with improved life quality as well as prolonged disease free survival (51, 52). In fact, HER2 immunotherapy has opened a door to a new world of cancer therapy. The ability to have an effective therapy together with very few side effects for cancer patients is now an important consideration for the development of any therapeutic approach (95, 199, 292). In light of this success, many surface receptors have been considered for targeted therapy leading to the development of many new immunotherapeutic agents in the form of antibodies, antibody drug conjugates and recombinant immunotoxins (139, 292, 293). Evaluation of these agents in the preclinical setting showed a great potential and raised the hopes of many. However, in most clinical trials, the results have been disappointing (68, 93, 238, 242). Some forms such as immunotoxins and ADCs caused severe side effects (93, 118). Many other antibodies and ADCs failed to show significant results when given as a single agent (68, 94). Even more, no added benefit was observed for most in the adjuvant and even in the neoadjuvant settings (68).

The success story of HER2 therapy combined with the failure of other immunotherapeutic agents highlights the need to continue searching for newer and better strategies for immunotherapy.

In this work, it was demonstrated that our novel fully human cytolytic fusion proteins can induce a cytotoxic effect in triple negative breast cancer (TNBC) cell lines that express their target receptors EpCAM and CSPG4. These hCFPs were rationally designed, while keeping in mind the lessons learned from the failure of other approaches. Our main guidelines when choosing our target receptors and effector domains were tackling the heterogeneity of TNBC (34, 238), the escape mechanisms cancer cells develop towards therapeutics compounds (156, 159), the immunogenicity and dose limitations of ITs and ADCs.

Bearing all this in mind, the chosen receptors EpCAM and CSPG4 proved to be highly and differentially expressed on the majority of TNBC cells lines. In our opinion, these two targets are important markers to be considered towards the assembly of a panel of receptors which can together contain the heterogeneity of TNBC tumors, and allow the tailoring of personalized immunotherapies for TNBC specifically and for breast cancer in general.

While the use of “Naked” antibodies immunotherapy was beneficial in cases such as HER2, the monoclonal antibodies against EpCAM failed so far to show such effect for TNBC patients. EpCAM antibodies with very high affinity caused severe side effects and had limited success at improving patient prognosis (96, 224, 226). Many other studies have shown that antibodies and scFv with very high binding affinities have limited tumor penetration and are less effective *in vivo* (224, 225, 247, 254).

To this end, a scFv with moderate binding affinity was used, and the results demonstrated efficient binding and internalization in cells expressing high levels of EpCAM, but did not have an effect on MDAMB-231 cells which express low levels of EpCAM. We hypothesize that this might be helpful in reducing off target toxicity when targeting EpCAM, which is expressed in lower levels in healthy tissue. This however remains to be studied, and the binding of this scFv to normal human tissue expressing basal levels of EpCAM should be tested. Initial results in this regard, confirm our hypothesis. In collaboration with Ahmad F Hussain (University hospital, RWTH Aachen), the binding of αEpCAM(scFv)-SNAP on biopsy samples from healthy and TNBC patients was tested. No binding was detected on any of the 10 healthy samples, while approximately 60% of 60 TNBC samples tested positive for EpCAM using our scFv-SNAP protein. This study is still ongoing, and further samples are being collected and tested. Additional testing with a commercial EpCAM antibody is also planned (data not shown, and is being prepared for publication).

Our effector domains: MAP tau and Granzyme B R201K were also designed with the purpose of maximizing toxicity while reducing immunogenicity and off target side effects(121). The choice of fully human proteins reduces significantly the chances of the development of neutralizing antibodies against them or the development of a strong immune response.

Granzyme B is a potent apoptosis initiator and has been used and studied by our group and others as a cytotoxic domain (123, 124). However, it has been shown that many tumors develop an escape mechanism to Granzyme B by the expression of its inhibitor serpin B9. Our group has developed a novel Granzyme B mutant R201K, with reduced sensitivity to serpin B9 (164). In this study, the selective toxicity and *in vivo* anti-tumor activity of GB-R201K-αEpCAM hCFP towards a serpin B9 positive cell line (MDA-MB-468) was demonstrated. This hCFP was very well tolerated and did not cause side effects in the mouse model even with the high concentration of 4 mg/kg, unlike the corresponding

immunotoxin αEpCAM-ETA' which caused weight loss and some side effects at a much lower dosage of 1.2 mg/ kg.

Initial biodistribution studies confirmed that GB-αEpCAM can reach and accumulate in the tumor site, but revealeded some unspecific accumulation in central organs and sometimes in the stomach of mice. Further study of distribution and clearance kinetics will be crucial to determining the best treatment regimen and dosage.

Unlike Granzyme B, MAP toxicity does not rely on its enzymatic activity. Its mere presence in the cell is sufficient to change the dynamics of tubulin leading to cell cycle arrest and the inhibition of cell growth. αCSPG4(scFv)-MAP proved to be a potent inhibitor of tumor growth in vivo in a subcutaneous tumor model. In this thesis we conducted a series of assays in an attempt to elucidate αCSPG4(scFv)-MAP mechanism of action in tumor cells. We confirmed its ability to internalize and bind to tubulin inside the cell and to induce cell cycle arrest and apoptosis, mainly through the mitochondrial stress apoptotic pathway. Future studies can focus on demonstrating the endosomal escape mechanism of MAP CFPs. Furthermore, special adapters, signal peptides and Furin cleavage sites can be incorporated to enhance the translocation to the cytosol and perhaps increase the cytotoxic activity of αCSPG4(scFv)-MAP (111).

Future studies with αCSPG4(scFv)-MAP and GB-R201K-αEpCAM(scFv) should focus on optimizing their expression and purification, mainly addressing their tendency to aggregate and precipitate in high concentrations. Their high tolerability cannot be utilized if higher concentration of active proteins cannot be reached.

The IC-50 values of MAP and Granzyme B hCFPs are in the high Nano molar range. The relatively "low" toxicity compared to other ADCs and ITs can pose a hurdle on the way to clinical studies. Although these CFPs are inherently safe and well tolerated, treatment with extremely high concentrations is usually disfavored. Therefore, further optimization of the constructs' design should focus on increasing their toxicity. This could be done as discussed above by designing linkers and adapters to facilitate their endosomal escape, and the release of the effector domain in the cytosol.

In terms of elucidating the mechanism of action, studies should focus on determining internalization routes and translocation into the cytosol of the human CFPs. In the case of MAP, its effect on cell cycle should be further confirmed by studying the changes in the tightly regulated signaling of cell cycle proteins such as cyclins.

Surprisingly, the results from *in vivo* studies revealed that GB-R201K-αEpCAM and αCSPG4(scFv)-MAP hCFPs resulted in efficient tumor growth inhibition at a 2.5 mg/kg despite the low IC-50 values measured *in vitro.* These results are especially encouraging in light of the short treatment course. Perhaps longer or repeated treatment courses will demonstrate complete and long term tumor remission. Indeed, longer and more elaborate *in vivo* studies are required to discover the full potential of these hCFPs.

# V REFERENCES

1. Al-Hajj M, Wicha MS, Benito-Hernandez A, Morrison SJ, Clarke MF. Prospective identification of tumorigenic breast cancer cells. Proceedings of the National Academy of Sciences of the United States of America. 2003;100(7):3983-8.
2. Carey LA, Perou CM, Livasy CA, Dressler LG, Cowan D, Conway K, et al. Race, breast cancer subtypes, and survival in the Carolina Breast Cancer Study. Jama. 2006;295(21):2492-502.
3. Azim HA, Jr., Michiels S, Bedard PL, Singhal SK, Criscitiello C, Ignatiadis M, et al. Elucidating prognosis and biology of breast cancer arising in young women using gene expression profiling. Clinical cancer research : an official journal of the American Association for Cancer Research. 2012;18(5):1341-51.
4. Wirapati P, Sotiriou C, Kunkel S, Farmer P, Pradervand S, Haibe-Kains B, et al. Meta-analysis of gene expression profiles in breast cancer: toward a unified understanding of breast cancer subtyping and prognosis signatures. Breast cancer research : BCR. 2008;10(4):R65.
5. Singletary SE, Greene FL. Revision of breast cancer staging: the 6th edition of the TNM Classification. Seminars in surgical oncology. 2003;21(1):53-9.
6. Penault-Llorca F, Viale G. Pathological and molecular diagnosis of triple-negative breast cancer: a clinical perspective. Annals of oncology : official journal of the European Society for Medical Oncology / ESMO. 2012;23 Suppl 6:vi19-22.
7. Wilkinson NW, Shahryarinejad A, Winston JS, Watroba N, Edge SB. Concordance with breast cancer pathology reporting practice guidelines. Journal of the American College of Surgeons. 2003;196(1):38-43.
8. Kuroi K, Toi M, Ohno S, Nakamura S, Iwata H, Masuda N, et al. Prognostic significance of subtype and pathologic response in operable breast cancer; a pooled analysis of prospective neoadjuvant studies of JBCRG. Breast cancer (Tokyo, Japan). 2015;22(5):486-95.
9. Bertucci F, Finetti P, Birnbaum D. Basal breast cancer: a complex and deadly molecular subtype. Current molecular medicine. 2012;12(1):96-110.
10. Farmer P, Bonnefoi H, Becette V, Tubiana-Hulin M, Fumoleau P, Larsimont D, et al. Identification of molecular apocrine breast tumours by microarray analysis. Oncogene. 2005;24(29):4660-71.
11. Kao J, Salari K, Bocanegra M, Choi YL, Girard L, Gandhi J, et al. Molecular profiling of breast cancer cell lines defines relevant tumor models and provides a resource for cancer gene discovery. PloS one. 2009;4(7):e6146.
12. Keller PJ, Lin AF, Arendt LM, Klebba I, Jones AD, Rudnick JA, et al. Mapping the cellular and molecular heterogeneity of normal and malignant breast tissues and cultured cell lines. Breast cancer research : BCR. 2010;12(5):R87.
13. Eroles P, Bosch A, Perez-Fidalgo JA, Lluch A. Molecular biology in breast cancer: intrinsic subtypes and signaling pathways. Cancer treatment reviews. 2012;38(6):698-707.
14. Marino M, Galluzzo P, Ascenzi P. Estrogen signaling multiple pathways to impact gene transcription. Current genomics. 2006;7(8):497-508.
15. Nilsson S, Makela S, Treuter E, Tujague M, Thomsen J, Andersson G, et al. Mechanisms of estrogen action. Physiological reviews. 2001;81(4):1535-65.
16. Hall JM, Couse JF, Korach KS. The multifaceted mechanisms of estradiol and estrogen receptor signaling. The Journal of biological chemistry. 2001;276(40):36869-72.
17. Renoir JM, Marsaud V, Lazennec G. Estrogen receptor signaling as a target for novel breast cancer therapeutics. Biochemical pharmacology. 2013;85(4):449-65.
18. Pearce ST, Jordan VC. The biological role of estrogen receptors alpha and beta in cancer. Critical reviews in oncology/hematology. 2004;50(1):3-22.
19. Duffy MJ. Estrogen receptors: role in breast cancer. Critical reviews in clinical laboratory sciences. 2006;43(4):325-47.

20. Yager JD. Mechanisms of estrogen carcinogenesis: The role of E2/E1-quinone metabolites suggests new approaches to preventive intervention--A review. Steroids. 2015;99(Pt A):56-60.
21. Kastner P, Krust A, Turcotte B, Stropp U, Tora L, Gronemeyer H, et al. Two distinct estrogen-regulated promoters generate transcripts encoding the two functionally different human progesterone receptor forms A and B. The EMBO journal. 1990;9(5):1603-14.
22. Diep CH, Daniel AR, Mauro LJ, Knutson TP, Lange CA. Progesterone action in breast, uterine, and ovarian cancers. Journal of molecular endocrinology. 2015;54(2):R31-53.
23. Yip CH, Rhodes A. Estrogen and progesterone receptors in breast cancer. Future oncology (London, England). 2014;10(14):2293-301.
24. Bardou VJ, Arpino G, Elledge RM, Osborne CK, Clark GM. Progesterone receptor status significantly improves outcome prediction over estrogen receptor status alone for adjuvant endocrine therapy in two large breast cancer databases. Journal of clinical oncology : official journal of the American Society of Clinical Oncology. 2003;21(10):1973-9.
25. Horwitz KB, Koseki Y, McGuire WL. Estrogen control of progesterone receptor in human breast cancer: role of estradiol and antiestrogen. Endocrinology. 1978;103(5):1742-51.
26. Lakhani SR, Van De Vijver MJ, Jacquemier J, Anderson TJ, Osin PP, McGuffog L, et al. The pathology of familial breast cancer: predictive value of immunohistochemical markers estrogen receptor, progesterone receptor, HER-2, and p53 in patients with mutations in BRCA1 and BRCA2. Journal of clinical oncology : official journal of the American Society of Clinical Oncology. 2002;20(9):2310-8.
27. Roskoski R, Jr. The ErbB/HER family of protein-tyrosine kinases and cancer. Pharmacological research. 2014;79:34-74.
28. Engel RH, Kaklamani VG. HER2-positive breast cancer: current and future treatment strategies. Drugs. 2007;67(9):1329-41.
29. Heitz F, Harter P, Lueck HJ, Fissler-Eckhoff A, Lorenz-Salehi F, Scheil-Bertram S, et al. Triple-negative and HER2-overexpressing breast cancers exhibit an elevated risk and an earlier occurrence of cerebral metastases. European journal of cancer (Oxford, England : 1990). 2009;45(16):2792-8.
30. Mitri Z, Constantine T, O'Regan R. The HER2 Receptor in Breast Cancer: Pathophysiology, Clinical Use, and New Advances in Therapy. Chemotherapy research and practice. 2012;2012:743193.
31. English DP, Roque DM, Santin AD. HER2 expression beyond breast cancer: therapeutic implications for gynecologic malignancies. Molecular diagnosis & therapy. 2013;17(2):85-99.
32. Bose R, Kavuri SM, Searleman AC, Shen W, Shen D, Koboldt DC, et al. Activating HER2 mutations in HER2 gene amplification negative breast cancer. Cancer discovery. 2013;3(2):224-37.
33. Neve RM, Chin K, Fridlyand J, Yeh J, Baehner FL, Fevr T, et al. A collection of breast cancer cell lines for the study of functionally distinct cancer subtypes. Cancer Cell. 2006;10(6):515-27.
34. Lehmann BD, Bauer JA, Chen X, Sanders ME, Chakravarthy AB, Shyr Y, et al. Identification of human triple-negative breast cancer subtypes and preclinical models for selection of targeted therapies. The Journal of clinical investigation. 2011;121(7):2750-67.
35. Sorlie T, Perou CM, Tibshirani R, Aas T, Geisler S, Johnsen H, et al. Gene expression patterns of breast carcinomas distinguish tumor subclasses with clinical implications. Proceedings of the National Academy of Sciences of the United States of America. 2001;98(19):10869-74.
36. Perou CM, Sorlie T, Eisen MB, van de Rijn M, Jeffrey SS, Rees CA, et al. Molecular portraits of human breast tumours. Nature. 2000;406(6797):747-52.
37. Naderi A, Teschendorff AE, Barbosa-Morais NL, Pinder SE, Green AR, Powe DG, et al. A gene-expression signature to predict survival in breast cancer across independent data sets. Oncogene. 2007;26(10):1507-16.
38. Sotiriou C, Neo SY, McShane LM, Korn EL, Long PM, Jazaeri A, et al. Breast cancer classification and prognosis based on gene expression profiles from a population-based study. Proceedings of the National Academy of Sciences of the United States of America. 2003;100(18):10393-8.
39. Curtis C, Shah SP, Chin SF, Turashvili G, Rueda OM, Dunning MJ, et al. The genomic and transcriptomic architecture of 2,000 breast tumours reveals novel subgroups. Nature. 2012;486(7403):346-52.

40. Staaf J, Jonsson G, Ringner M, Vallon-Christersson J, Grabau D, Arason A, et al. High-resolution genomic and expression analyses of copy number alterations in HER2-amplified breast cancer. Breast cancer research : BCR. 2010;12(3):R25.
41. Prat A, Carey LA, Adamo B, Vidal M, Tabernero J, Cortes J, et al. Molecular features and survival outcomes of the intrinsic subtypes within HER2-positive breast cancer. Journal of the National Cancer Institute. 2014;106(8).
42. Badve S, Dabbs DJ, Schnitt SJ, Baehner FL, Decker T, Eusebi V, et al. Basal-like and triple-negative breast cancers: a critical review with an emphasis on the implications for pathologists and oncologists. Modern pathology : an official journal of the United States and Canadian Academy of Pathology, Inc. 2011;24(2):157-67.
43. Nielsen TO, Hsu FD, Jensen K, Cheang M, Karaca G, Hu Z, et al. Immunohistochemical and clinical characterization of the basal-like subtype of invasive breast carcinoma. Clinical cancer research : an official journal of the American Association for Cancer Research. 2004;10(16):5367-74.
44. Livasy CA, Karaca G, Nanda R, Tretiakova MS, Olopade OI, Moore DT, et al. Phenotypic evaluation of the basal-like subtype of invasive breast carcinoma. Modern pathology : an official journal of the United States and Canadian Academy of Pathology, Inc. 2006;19(2):264-71.
45. Bertheau P, Lehmann-Che J, Varna M, Dumay A, Poirot B, Porcher R, et al. p53 in breast cancer subtypes and new insights into response to chemotherapy. Breast (Edinburgh, Scotland). 2013;22 Suppl 2:S27-9.
46. Gilbert JA, Goetz MP, Reynolds CA, Ingle JN, Giordano KF, Suman VJ, et al. Molecular analysis of metaplastic breast carcinoma: high EGFR copy number via aneusomy. Molecular cancer therapeutics. 2008;7(4):944-51.
47. Valentin MD, da Silva SD, Privat M, Alaoui-Jamali M, Bignon YJ. Molecular insights on basal-like breast cancer. Breast cancer research and treatment. 2012;134(1):21-30.
48. Bauer KR, Brown M, Cress RD, Parise CA, Caggiano V. Descriptive analysis of estrogen receptor (ER)-negative, progesterone receptor (PR)-negative, and HER2-negative invasive breast cancer, the so-called triple-negative phenotype: a population-based study from the California cancer Registry. Cancer. 2007;109(9):1721-8.
49. Onitilo AA, Engel JM, Greenlee RT, Mukesh BN. Breast cancer subtypes based on ER/PR and Her2 expression: comparison of clinicopathologic features and survival. Clinical medicine & research. 2009;7(1-2):4-13.
50. Amirikia KC, Mills P, Bush J, Newman LA. Higher population-based incidence rates of triple-negative breast cancer among young African-American women : Implications for breast cancer screening recommendations. Cancer. 2011;117(12):2747-53.
51. Gianni L, Dafni U, Gelber RD, Azambuja E, Muehlbauer S, Goldhirsch A, et al. Treatment with trastuzumab for 1 year after adjuvant chemotherapy in patients with HER2-positive early breast cancer: a 4-year follow-up of a randomised controlled trial. The Lancet Oncology. 2011;12(3):236-44.
52. Zardavas D, Cameron D, Krop I, Piccart M. Beyond trastuzumab and lapatinib: new options for HER2-positive breast cancer. American Society of Clinical Oncology educational book / ASCO American Society of Clinical Oncology Meeting. 2013.
53. Vrbic S, Pejcic I, Filipovic S, Kocic B, Vrbic M. Current and future anti-HER2 therapy in breast cancer. Journal of BUON : official journal of the Balkan Union of Oncology. 2013;18(1):4-16.
54. Pernas Simon S. Neoadjuvant therapy of early stage human epidermal growth factor receptor 2 positive breast cancer: latest evidence and clinical implications. Therapeutic advances in medical oncology. 2014;6(5):210-21.
55. Mavroudis D, Saloustros E, Malamos N, Kakolyris S, Boukovinas I, Papakotoulas P, et al. Six versus 12 months of adjuvant trastuzumab in combination with dose-dense chemotherapy for women with HER2-positive breast cancer: a multicenter randomized study by the Hellenic Oncology Research Group (HORG). Annals of oncology : official journal of the European Society for Medical Oncology / ESMO. 2015;26(7):1333-40.
56. Blackwell KL, Burstein HJ, Storniolo AM, Rugo HS, Sledge G, Aktan G, et al. Overall survival benefit with lapatinib in combination with trastuzumab for patients with human epidermal growth factor receptor 2-positive metastatic breast cancer: final results from the EGF104900 Study.

Journal of clinical oncology : official journal of the American Society of Clinical Oncology. 2012;30(21):2585-92.
57. Lumachi F, Luisetto G, Basso SM, Basso U, Brunello A, Camozzi V. Endocrine therapy of breast cancer. Current medicinal chemistry. 2011;18(4):513-22.
58. Abdulkareem IH, Zurmi IB. Review of hormonal treatment of breast cancer. Nigerian journal of clinical practice. 2012;15(1):9-14.
59. Cuzick J, Sestak I, Baum M, Buzdar A, Howell A, Dowsett M, et al. Effect of anastrozole and tamoxifen as adjuvant treatment for early-stage breast cancer: 10-year analysis of the ATAC trial. The Lancet Oncology. 2010;11(12):1135-41.
60. Chumsri S. Clinical utilities of aromatase inhibitors in breast cancer. International journal of women's health. 2015;7:493-9.
61. Crown J, O'Shaughnessy J, Gullo G. Emerging targeted therapies in triple-negative breast cancer. Annals of oncology : official journal of the European Society for Medical Oncology / ESMO. 2012;23 Suppl 6:vi56-65.
62. Hugh J, Hanson J, Cheang MC, Nielsen TO, Perou CM, Dumontet C, et al. Breast cancer subtypes and response to docetaxel in node-positive breast cancer: use of an immunohistochemical definition in the BCIRG 001 trial. Journal of clinical oncology : official journal of the American Society of Clinical Oncology. 2009;27(8):1168-76.
63. Carey LA, Rugo HS, Marcom PK, Mayer EL, Esteva FJ, Ma CX, et al. TBCRC 001: randomized phase II study of cetuximab in combination with carboplatin in stage IV triple-negative breast cancer. Journal of clinical oncology : official journal of the American Society of Clinical Oncology. 2012;30(21):2615-23.
64. Baselga J, Gomez P, Greil R, Braga S, Climent MA, Wardley AM, et al. Randomized phase II study of the anti-epidermal growth factor receptor monoclonal antibody cetuximab with cisplatin versus cisplatin alone in patients with metastatic triple-negative breast cancer. Journal of clinical oncology : official journal of the American Society of Clinical Oncology. 2013;31(20):2586-92.
65. U.S. National Institutes of Health. search term: triple negative breast cancer and PARP inhibitors. Internet [cited 29/09/2015]. Available from: https://clinicaltrials.gov/ct2/results?term=triple+negative+breast+cancer+and+parp+inhibitor&recr=&rslt=&type=Intr&cond=&intr=&titles=&outc=&spons=&lead=&id=&state1=&cntry1=&state2=&cntry2=&state3=&cntry3=&locn=&gndr=&rcv_s=&rcv_e=&lup_s=&lup_e=
66. U.S. National Institutes of Health. search term: triple negative breast cancer and mTOR. Internet [cited 29/09/2015]. Available from: https://clinicaltrials.gov/ct2/results?term=triple+negative+breast+cancer+and+mtor&recr=&rslt=&type=Intr&cond=&intr=&titles=&outc=&spons=&lead=&id=&state1=&cntry1=&state2=&cntry2=&state3=&cntry3=&locn=&gndr=&rcv_s=&rcv_e=&lup_s=&lup_e=
67. O'Shaughnessy J, Osborne C, Pippen JE, Yoffe M, Patt D, Rocha C, et al. Iniparib plus chemotherapy in metastatic triple-negative breast cancer. The New England journal of medicine. 2011;364(3):205-14.
68. Miller K, Wang M, Gralow J, Dickler M, Cobleigh M, Perez EA, et al. Paclitaxel plus bevacizumab versus paclitaxel alone for metastatic breast cancer. The New England journal of medicine. 2007;357(26):2666-76.
69. U.S. National Institutes of Health. search term: triple negative breast cancer and VEGF. Internet [cited 29/09/2015]. Available from: https://clinicaltrials.gov/ct2/results?term=triple+negative+breast+cancer+and+vegf&recr=&rslt=&type=Intr&cond=&intr=&titles=&outc=&spons=&lead=&id=&state1=&cntry1=&state2=&cntry2=&state3=&cntry3=&locn=&gndr=&rcv_s=&rcv_e=&lup_s=&lup_e=
70. U.S. National Institutes of Health. search term: triple negative breast cancer and EGFR. Internet [cited 29/09/2015]. Available from: https://clinicaltrials.gov/ct2/results?term=triple+negative+breast+cancer+and+egfr&recr=&rslt=&type=Intr&cond=&intr=&titles=&outc=&spons=&lead=&id=&state1=&cntry1=&state2=&cntry2=&state3=&cntry3=&locn=&gndr=&rcv_s=&rcv_e=&lup_s=&lup_e=
71. U.S. National Institutes of Health. TP-38 Toxin in Treating Young Patients With Recurrent or Progressive Supratentorial High-Grade Glioma. Internet [cited 10/04/2016]. Available from: https://clinicaltrials.gov/ct2/show/NCT00074334?term=egfr+immunotoxin&rank=1

72. U.S. National Institutes of Health. Phase II Study of Erlotinib, an EGFR Inhibitor in Metastatic EGFR-positive 'Triple Receptor-negative' Breast Cancer. Internet [cited 01/02/2016]. Available from: https://clinicaltrials.gov/ct2/show/NCT00739063?term=egfr+and+breast+cancer&rank=2.
73. Brufsky A, Valero V, Tiangco B, Dakhil S, Brize A, Rugo HS, et al. Second-line bevacizumab-containing therapy in patients with triple-negative breast cancer: subgroup analysis of the RIBBON-2 trial. Breast cancer research and treatment. 2012;133(3):1067-75.
74. Luedke E, Jaime-Ramirez AC, Bhave N, Carson WE, 3rd. Monoclonal antibody therapy of pancreatic cancer with cetuximab: potential for immune modulation. Journal of immunotherapy (Hagerstown, Md : 1997). 2012;35(5):367-73.
75. Litvinov SV, Balzar M, Winter MJ, Bakker HA, Briaire-de Bruijn IH, Prins F, et al. Epithelial cell adhesion molecule (Ep-CAM) modulates cell-cell interactions mediated by classic cadherins. The Journal of cell biology. 1997;139(5):1337-48.
76. Lin CW, Liao MY, Lin WW, Wang YP, Lu TY, Wu HC. Epithelial cell adhesion molecule regulates tumor initiation and tumorigenesis via activating reprogramming factors and epithelial-mesenchymal transition gene expression in colon cancer. The Journal of biological chemistry. 2012;287(47):39449-59.
77. Lu TY, Lu RM, Liao MY, Yu J, Chung CH, Kao CF, et al. Epithelial cell adhesion molecule regulation is associated with the maintenance of the undifferentiated phenotype of human embryonic stem cells. The Journal of biological chemistry. 2010;285(12):8719-32.
78. Went PT, Lugli A, Meier S, Bundi M, Mirlacher M, Sauter G, et al. Frequent EpCam protein expression in human carcinomas. Human pathology. 2004;35(1):122-8.
79. Spizzo G, Went P, Dirnhofer S, Obrist P, Moch H, Baeuerle PA, et al. Overexpression of epithelial cell adhesion molecule (Ep-CAM) is an independent prognostic marker for reduced survival of patients with epithelial ovarian cancer. Gynecologic oncology. 2006;103(2):483-8.
80. Spizzo G, Went P, Dirnhofer S, Obrist P, Simon R, Spichtin H, et al. High Ep-CAM expression is associated with poor prognosis in node-positive breast cancer. Breast cancer research and treatment. 2004;86(3):207-13.
81. Baccelli I, Schneeweiss A, Riethdorf S, Stenzinger A, Schillert A, Vogel V, et al. Identification of a population of blood circulating tumor cells from breast cancer patients that initiates metastasis in a xenograft assay. Nature biotechnology. 2013;31(6):539-44.
82. Munz M, Baeuerle PA, Gires O. The emerging role of EpCAM in cancer and stem cell signaling. Cancer research. 2009;69(14):5627-9.
83. Abd El-Maqsoud NM, Abd El-Rehim DM. Clinicopathologic implications of EpCAM and Sox2 expression in breast cancer. Clinical breast cancer. 2014;14(1):e1-9.
84. Schmidt M, Hasenclever D, Schaeffer M, Boehm D, Cotarelo C, Steiner E, et al. Prognostic effect of epithelial cell adhesion molecule overexpression in untreated node-negative breast cancer. Clinical cancer research : an official journal of the American Association for Cancer Research. 2008;14(18):5849-55.
85. Seimetz D. Novel monoclonal antibodies for cancer treatment: the trifunctional antibody catumaxomab (removab). Journal of Cancer. 2011;2:309-16.
86. Campoli MR, Chang CC, Kageshita T, Wang X, McCarthy JB, Ferrone S. Human high molecular weight-melanoma-associated antigen (HMW-MAA): a melanoma cell surface chondroitin sulfate proteoglycan (MSCP) with biological and clinical significance. Critical reviews in immunology. 2004;24(4):267-96.
87. Wilson BS, Imai K, Natali PG, Ferrone S. Distribution and molecular characterization of a cell-surface and a cytoplasmic antigen detectable in human melanoma cells with monoclonal antibodies. International journal of cancer. 1981;28(3):293-300.
88. Wang X, Osada T, Wang Y, Yu L, Sakakura K, Katayama A, et al. CSPG4 protein as a new target for the antibody-based immunotherapy of triple-negative breast cancer. Journal of the National Cancer Institute. 2010;102(19):1496-512.
89. Hsu NC, Nien PY, Yokoyama KK, Chu PY, Hou MF. High chondroitin sulfate proteoglycan 4 expression correlates with poor outcome in patients with breast cancer. Biochemical and biophysical research communications. 2013;441(2):514-8.
90. Wang X, Wang Y, Yu L, Sakakura K, Visus C, Schwab JH, et al. CSPG4 in cancer: multiple roles. Current molecular medicine. 2010;10(4):419-29.

91. Wang X, Osada T, Wang Y, Miyazato P, Thorne S, DeLeo A, et al. Antibody-based immunotherapy: targeting CSPG4 on human basal breast cancer stem cells. Cancer research. 2009;69(2 Supplement):5046.
92. Blythman HE, Casellas P, Gros O, Gros P, Jansen FK, Paolucci F, et al. Immunotoxins: hybrid molecules of monoclonal antibodies and a toxin subunit specifically kill tumour cells. Nature. 1981;290(5802):145-6.
93. Kreitman RJ. Immunotoxins for targeted cancer therapy. The AAPS journal. 2006;8(3):E532-51.
94. Carter PJ, Senter PD. Antibody-drug conjugates for cancer therapy. Cancer journal (Sudbury, Mass). 2008;14(3):154-69.
95. Carter PJ. Potent antibody therapeutics by design. Nature reviews Immunology. 2006;6(5):343-57.
96. Schmidt M, Scheulen ME, Dittrich C, Obrist P, Marschner N, Dirix L, et al. An open-label, randomized phase II study of adecatumumab, a fully human anti-EpCAM antibody, as monotherapy in patients with metastatic breast cancer. Annals of oncology : official journal of the European Society for Medical Oncology / ESMO. 2010;21(2):275-82.
97. Bruell D, Bruns CJ, Yezhelyev M, Huhn M, Muller J, Ischenko I, et al. Recombinant anti-EGFR immunotoxin 425(scFv)-ETA' demonstrates anti-tumor activity against disseminated human pancreatic cancer in nude mice. International journal of molecular medicine. 2005;15(2):305-13.
98. Liu Y, Zhang W, Niu T, Cheung LH, Munshi A, Meyn RE, Jr., et al. Targeted apoptosis activation with GrB/scFvMEL modulates melanoma growth, metastatic spread, chemosensitivity, and radiosensitivity. Neoplasia (New York, NY). 2006;8(2):125-35.
99. Ahmad ZA, Yeap SK, Ali AM, Ho WY, Alitheen NB, Hamid M. scFv antibody: principles and clinical application. Clinical & developmental immunology. 2012;2012:980250.
100. Bera TK, Onda M, Kreitman RJ, Pastan I. An improved recombinant Fab-immunotoxin targeting CD22 expressing malignancies. Leukemia research. 2014;38(10):1224-9.
101. Kim GB, Wang Z, Liu YY, Stavrou S, Mathias A, Goodwin KJ, et al. A fold-back single-chain diabody format enhances the bioactivity of an anti-monkey CD3 recombinant diphtheria toxin-based immunotoxin. Protein engineering, design & selection : PEDS. 2007;20(9):425-32.
102. Ranft K, Thepen T, Fischer R, Barth S, Stocker M. Recombinant bispecific single chain antibody fragments induce Fc gamma-receptor-mediated elimination of CD30+ lymphoma cells. Cancer letters. 2009;282(2):187-94.
103. Galloway DR, Hedstrom RC, Pavlovskis OR. Production and characterization of monoclonal antibodies to exotoxin A from Pseudomonas aeruginosa. Infection and immunity. 1984;44(2):262-7.
104. Murphy JR, Bishai W, Borowski M, Miyanohara A, Boyd J, Nagle S. Genetic construction, expression, and melanoma-selective cytotoxicity of a diphtheria toxin-related alpha-melanocyte-stimulating hormone fusion protein. Proceedings of the National Academy of Sciences of the United States of America. 1986;83(21):8258-62.
105. Williams DP, Parker K, Bacha P, Bishai W, Borowski M, Genbauffe F, et al. Diphtheria toxin receptor binding domain substitution with interleukin-2: genetic construction and properties of a diphtheria toxin-related interleukin-2 fusion protein. Protein engineering. 1987;1(6):493-8.
106. Cawley DB, Herschman HR, Gilliland DG, Collier RJ. Epidermal growth factor-toxin A chain conjugates: EGF-ricin A is a potent toxin while EGF-diphtheria fragment A is nontoxic. Cell. 1980;22(2 Pt 2):563-70.
107. Ferreras JM, Citores L, Iglesias R, Jimenez P, Girbes T. Use of ribosome-inactivating proteins from Sambucus for the construction of immunotoxins and conjugates for cancer therapy. Toxins. 2011;3(5):420-41.
108. Li Z, Yu T, Zhao P, Ma J. Immunotoxins and cancer therapy. Cellular & molecular immunology. 2005;2(2):106-12.
109. Weidle UH, Tiefenthaler G, Schiller C, Weiss EH, Georges G, Brinkmann U. Prospects of bacterial and plant protein-based immunotoxins for treatment of cancer. Cancer genomics & proteomics. 2014;11(1):25-38.
110. Weldon JE, Pastan I. A guide to taming a toxin--recombinant immunotoxins constructed from Pseudomonas exotoxin A for the treatment of cancer. The FEBS journal. 2011;278(23):4683-700.

111. Hetzel C, Bachran C, Fischer R, Fuchs H, Barth S, Stocker M. Small cleavable adapters enhance the specific cytotoxicity of a humanized immunotoxin directed against CD64-positive cells. Journal of immunotherapy (Hagerstown, Md : 1997). 2008;31(4):370-6.
112. Lemichez E, Bomsel M, Devilliers G, vanderSpek J, Murphy JR, Lukianov EV, et al. Membrane translocation of diphtheria toxin fragment A exploits early to late endosome trafficking machinery. Molecular microbiology. 1997;23(3):445-57.
113. Ogata M, Chaudhary VK, Pastan I, FitzGerald DJ. Processing of Pseudomonas exotoxin by a cellular protease results in the generation of a 37,000-Da toxin fragment that is translocated to the cytosol. The Journal of biological chemistry. 1990;265(33):20678-85.
114. Wesche J, Rapak A, Olsnes S. Dependence of ricin toxicity on translocation of the toxin A-chain from the endoplasmic reticulum to the cytosol. The Journal of biological chemistry. 1999;274(48):34443-9.
115. Chiron MF, Fryling CM, FitzGerald DJ. Cleavage of pseudomonas exotoxin and diphtheria toxin by a furin-like enzyme prepared from beef liver. The Journal of biological chemistry. 1994;269(27):18167-76.
116. Mallet WG, Maxfield FR. Chimeric forms of furin and TGN38 are transported with the plasma membrane in the trans-Golgi network via distinct endosomal pathways. The Journal of cell biology. 1999;146(2):345-59.
117. Kaul P, Silverman J, Shen WH, Blanke SR, Huynh PD, Finkelstein A, et al. Roles of Glu 349 and Asp 352 in membrane insertion and translocation by diphtheria toxin. Protein science : a publication of the Protein Society. 1996;5(4):687-92.
118. Janthur WD, Cantoni N, Mamot C. Drug conjugates such as Antibody Drug Conjugates (ADCs), immunotoxins and immunoliposomes challenge daily clinical practice. International journal of molecular sciences. 2012;13(12):16020-45.
119. Liu W, Onda M, Lee B, Kreitman RJ, Hassan R, Xiang L, et al. Recombinant immunotoxin engineered for low immunogenicity and antigenicity by identifying and silencing human B-cell epitopes. Proceedings of the National Academy of Sciences of the United States of America. 2012;109(29):11782-7.
120. Madhumathi J, Verma RS. Therapeutic targets and recent advances in protein immunotoxins. Current opinion in microbiology. 2012;15(3):300-9.
121. Mathew M, Verma RS. Humanized immunotoxins: a new generation of immunotoxins for targeted cancer therapy. Cancer science. 2009;100(8):1359-65.
122. Lorberboum-Galski H. Human toxin-based recombinant immunotoxins/chimeric proteins as a drug delivery system for targeted treatment of human diseases. Expert opinion on drug delivery. 2011;8(5):605-21.
123. Hehmann-Titt G, Schiffer S, Berges N, Melmer G, Barth S. Improving the therapeutic potential of hhuman granzyme B for targeted cancer therapy. Antibodies. 2013;2(1):19.
124. Stahnke B, Thepen T, Stocker M, Rosinke R, Jost E, Fischer R, et al. Granzyme B-H22(scFv), a human immunotoxin targeting CD64 in acute myeloid leukemia of monocytic subtypes. Molecular cancer therapeutics. 2008;7(9):2924-32.
125. Huhn M, Sasse S, Tur MK, Matthey B, Schinkothe T, Rybak SM, et al. Human angiogenin fused to human CD30 ligand (Ang-CD30L) exhibits specific cytotoxicity against CD30-positive lymphoma. Cancer research. 2001;61(24):8737-42.
126. Schiffer S, Hristodorov D, Mladenov R, Aslanian E, Huhn M, Fischer R, et al. Species-dependent functionality of the human cytolytic fusion proteins Granzyme B-H22(scFv) and H22(scFv)-Angiogenin in Macrophages. Antibodies. 2013;2(1):9.
127. Allured VS, Collier RJ, Carroll SF, McKay DB. Structure of exotoxin A of Pseudomonas aeruginosa at 3.0-Angstrom resolution. Proceedings of the National Academy of Sciences of the United States of America. 1986;83(5):1320-4.
128. Hwang J, Fitzgerald DJ, Adhya S, Pastan I. Functional domains of Pseudomonas exotoxin identified by deletion analysis of the gene expressed in E. coli. Cell. 1987;48(1):129-36.
129. Pastrana DV, Hanson AJ, Knisely J, Bu G, Fitzgerald DJ. LRP 1 B functions as a receptor for Pseudomonas exotoxin. Biochimica et biophysica acta. 2005;1741(3):234-9.
130. Siegall CB, Chaudhary VK, FitzGerald DJ, Pastan I. Functional analysis of domains II, Ib, and III of Pseudomonas exotoxin. The Journal of biological chemistry. 1989;264(24):14256-61.

131. Iglewski BH, Liu PV, Kabat D. Mechanism of action of Pseudomonas aeruginosa exotoxin Aiadenosine diphosphate-ribosylation of mammalian elongation factor 2 in vitro and in vivo. Infection and immunity. 1977;15(1):138-44.
132. Liu PV. The roles of various fractions of Pseudomonas aeruginosa in its pathogenesis. 3. Identity of the lethal toxins produced in vitro and in vivo. The Journal of infectious diseases. 1966;116(4):481-9.
133. Chaudhary VK, Jinno Y, FitzGerald D, Pastan I. Pseudomonas exotoxin contains a specific sequence at the carboxyl terminus that is required for cytotoxicity. Proceedings of the National Academy of Sciences of the United States of America. 1990;87(1):308-12.
134. Capitani M, Sallese M. The KDEL receptor: new functions for an old protein. FEBS letters. 2009;583(23):3863-71.
135. Tsutsumi Y, Onda M, Nagata S, Lee B, Kreitman RJ, Pastan I. Site-specific chemical modification with polyethylene glycol of recombinant immunotoxin anti-Tac(Fv)-PE38 (LMB-2) improves antitumor activity and reduces animal toxicity and immunogenicity. Proceedings of the National Academy of Sciences of the United States of America. 2000;97(15):8548-53.
136. Kreitman RJ, Pastan I. Importance of the glutamate residue of KDEL in increasing the cytotoxicity of Pseudomonas exotoxin derivatives and for increased binding to the KDEL receptor. The Biochemical journal. 1995;307 ( Pt 1):29-37.
137. Tur MK, Huhn M, Jost E, Thepen T, Brummendorf TH, Barth S. In vivo efficacy of the recombinant anti-CD64 immunotoxin H22(scFv)-ETA' in a human acute myeloid leukemia xenograft tumor model. International journal of cancer. 2011;129(5):1277-82.
138. Dosio F, Stella B, Cerioni S, Gastaldi D, Arpicco S. Advances in anticancer antibody-drug conjugates and immunotoxins. Recent patents on anti-cancer drug discovery. 2014;9(1):35-65.
139. Alewine C, Hassan R, Pastan I. Advances in anticancer immunotoxin therapy. The oncologist. 2015;20(2):176-85.
140. Duvic M, Talpur R. Optimizing denileukin diftitox (Ontak) therapy. Future oncology (London, England). 2008;4(4):457-69.
141. Manoukian G, Hagemeister F. Denileukin diftitox: a novel immunotoxin. Expert opinion on biological therapy. 2009;9(11):1445-51.
142. Alewine C, Xiang L, Yamori T, Niederfellner G, Bosslet K, Pastan I. Efficacy of RG7787, a next-generation mesothelin-targeted immunotoxin, against triple-negative breast and gastric cancers. Molecular cancer therapeutics. 2014;13(11):2653-61.
143. Hassan R, Miller AC, Sharon E, Thomas A, Reynolds JC, Ling A, et al. Major cancer regressions in mesothelioma after treatment with an anti-mesothelin immunotoxin and immune suppression. Science translational medicine. 2013;5(208):208ra147.
144. Kowalski M, Entwistle J, Cizeau J, Niforos D, Loewen S, Chapman W, et al. A Phase I study of an intravesically administered immunotoxin targeting EpCAM for the treatment of nonmuscle-invasive bladder cancer in BCGrefractory and BCG-intolerant patients. Drug design, development and therapy. 2010;4:313-20.
145. von Minckwitz G, Harder S, Hovelmann S, Jager E, Al-Batran SE, Loibl S, et al. Phase I clinical study of the recombinant antibody toxin scFv(FRP5)-ETA specific for the ErbB2/HER2 receptor in patients with advanced solid malignomas. Breast cancer research : BCR. 2005;7(5):R617-26.
146. Weiner LM, O'Dwyer J, Kitson J, Comis RL, Frankel AE, Bauer RJ, et al. Phase I evaluation of an anti-breast carcinoma monoclonal antibody 260F9-recombinant ricin A chain immunoconjugate. Cancer research. 1989;49(14):4062-7.
147. Andersson Y, Engebraaten O, Juell S, Aamdal S, Brunsvig P, Fodstad O, et al. Phase I trial of EpCAM-targeting immunotoxin MOC31PE, alone and in combination with cyclosporin. British journal of cancer. 2015;113(11):1548-55.
148. Bremer E, Kuijlen J, Samplonius D, Walczak H, de Leij L, Helfrich W. Target cell-restricted and -enhanced apoptosis induction by a scFv:sTRAIL fusion protein with specificity for the pancarcinoma-associated antigen EGP2. International journal of cancer. 2004;109(2):281-90.
149. Hristodorov D, Amoury M, Mladenov R, Niesen J, Arens K, Berges N, et al. EpCAM-selective elimination of carcinoma cells by a novel MAP-based cytolytic fusion protein. Molecular cancer therapeutics. 2014;13(9):2194-202.

150. Hristodorov D, Mladenov R, Pardo A, Pham AT, Huhn M, Fischer R, et al. Microtubule-associated protein tau facilitates the targeted killing of proliferating cancer cells in vitro and in a xenograft mouse tumour model in vivo. British journal of cancer. 2013;109(6):1570-8.
151. Pinkoski MJ, Waterhouse NJ, Heibein JA, Wolf BB, Kuwana T, Goldstein JC, et al. Granzyme B-mediated apoptosis proceeds predominantly through a Bcl-2-inhibitable mitochondrial pathway. The Journal of biological chemistry. 2001;276(15):12060-7.
152. Lord SJ, Rajotte RV, Korbutt GS, Bleackley RC. Granzyme B: a natural born killer. Immunological reviews. 2003;193:31-8.
153. Dalken B, Giesubel U, Knauer SK, Wels WS. Targeted induction of apoptosis by chimeric granzyme B fusion proteins carrying antibody and growth factor domains for cell recognition. Cell death and differentiation. 2006;13(4):576-85.
154. Kanatani I, Lin X, Yuan X, Manorek G, Shang X, Cheung LH, et al. Targeting granzyme B to tumor cells using a yoked human chorionic gonadotropin. Cancer chemotherapy and pharmacology. 2011;68(4):979-90.
155. Schiffer S, Hansen HP, Hehmann-Titt G, Huhn M, Fischer R, Barth S, et al. Efficacy of an adapted granzyme B-based anti-CD30 cytolytic fusion protein against PI-9-positive classical Hodgkin lymphoma cells in a murine model. Blood cancer journal. 2013;3:e106.
156. Soriano C, Mukaro V, Hodge G, Ahern J, Holmes M, Jersmann H, et al. Increased proteinase inhibitor-9 (PI-9) and reduced granzyme B in lung cancer: mechanism for immune evasion? Lung cancer (Amsterdam, Netherlands). 2012;77(1):38-45.
157. Jiang X, Ellison SJ, Alarid ET, Shapiro DJ. Interplay between the levels of estrogen and estrogen receptor controls the level of the granzyme inhibitor, proteinase inhibitor 9 and susceptibility to immune surveillance by natural killer cells. Oncogene. 2007;26(28):4106-14.
158. Fritsch K, Finke J, Grullich C. Suppression of granzyme B activity and caspase-3 activation in leukaemia cells constitutively expressing the protease inhibitor 9. Annals of hematology. 2013;92(12):1603-9.
159. Classen CF, Ushmorov A, Bird P, Debatin KM. The granzyme B inhibitor PI-9 is differentially expressed in all main subtypes of pediatric acute lymphoblastic leukemias. Haematologica. 2004;89(11):1314-21.
160. Danielle Thierry-Mieg and Jean Thierry-Mieg. Homo sapiens complex locus SERPINB9, encoding serpin peptidase inhibitor, clade B (ovalbumin), member 9. Internet [cited 10/05/2016]. Available from: http://www.ncbi.nlm.nih.gov/IEB/Research/Acembly/av.cgi?db=human&c=Gene&l=SERPINB9.
161. Hirst CE, Buzza MS, Bird CH, Warren HS, Cameron PU, Zhang M, et al. The intracellular granzyme B inhibitor, proteinase inhibitor 9, is up-regulated during accessory cell maturation and effector cell degranulation, and its overexpression enhances CTL potency. Journal of immunology (Baltimore, Md : 1950). 2003;170(2):805-15.
162. Buzza MS, Hirst CE, Bird CH, Hosking P, McKendrick J, Bird PI. The granzyme B inhibitor, PI-9, is present in endothelial and mesothelial cells, suggesting that it protects bystander cells during immune responses. Cellular immunology. 2001;210(1):21-9.
163. Kanamori H, Krieg S, Mao C, Di Pippo VA, Wang S, Zajchowski DA, et al. Proteinase inhibitor 9, an inhibitor of granzyme B-mediated apoptosis, is a primary estrogen-inducible gene in human liver cells. The Journal of biological chemistry. 2000;275(8):5867-73.
164. Losasso V, Schiffer S, Barth S, Carloni P. Design of human granzyme B variants resistant to serpin B9. Proteins. 2012;80(11):2514-22.
165. Billingsley ML, Kincaid RL. Regulated phosphorylation and dephosphorylation of tau protein: effects on microtubule interaction, intracellular trafficking and neurodegeneration. The Biochemical journal. 1997;323 ( Pt 3):577-91.
166. Maney T, Wagenbach M, Wordeman L. Molecular dissection of the microtubule depolymerizing activity of mitotic centromere-associated kinesin. The Journal of biological chemistry. 2001;276(37):34753-8.
167. Giodini A, Kallio MJ, Wall NR, Gorbsky GJ, Tognin S, Marchisio PC, et al. Regulation of microtubule stability and mitotic progression by survivin. Cancer research. 2002;62(9):2462-7.
168. Saxton WM, Stemple DL, Leslie RJ, Salmon ED, Zavortink M, McIntosh JR. Tubulin dynamics in cultured mammalian cells. The Journal of cell biology. 1984;99(6):2175-86.

169. Zhai Y, Kronebusch PJ, Simon PM, Borisy GG. Microtubule dynamics at the G2/M transition: abrupt breakdown of cytoplasmic microtubules at nuclear envelope breakdown and implications for spindle morphogenesis. The Journal of cell biology. 1996;135(1):201-14.
170. Hristodorov D, Nordlohne J, Mladenov R, Huhn M, Fischer R, Thepen T, et al. Human microtubule-associated protein tau mediates targeted killing of CD30(+) lymphoma cells in vitro and inhibits tumour growth in vivo. British journal of haematology. 2014;164(2):251-7.
171. Amoury M, Blume T, Brehm H, Niesen J, Tenhaef N, Barth S, et al. SNAP-tag based agents for preclinical in vitro imaging in malignant diseases. Current pharmaceutical design. 2013;19(30):5429-36.
172. Hussain AF, Amoury M, Barth S. SNAP-tag technology: a powerful tool for site specific conjugation of therapeutic and imaging agents. Current pharmaceutical design. 2013;19(30):5437-42.
173. Kampmeier F, Niesen J, Koers A, Ribbert M, Brecht A, Fischer R, et al. Rapid optical imaging of EGF receptor expression with a single-chain antibody SNAP-tag fusion protein. European journal of nuclear medicine and molecular imaging. 2010;37(10):1926-34.
174. Criscitiello C, Azim HA, Jr., Schouten PC, Linn SC, Sotiriou C. Understanding the biology of triple-negative breast cancer. Annals of oncology : official journal of the European Society for Medical Oncology / ESMO. 2012;23 Suppl 6:vi13-8.
175. Dent R, Trudeau M, Pritchard KI, Hanna WM, Kahn HK, Sawka CA, et al. Triple-negative breast cancer: clinical features and patterns of recurrence. Clinical cancer research : an official journal of the American Association for Cancer Research. 2007;13(15 Pt 1):4429-34.
176. De Laurentiis M, Cianniello D, Caputo R, Stanzione B, Arpino G, Cinieri S, et al. Treatment of triple negative breast cancer (TNBC): current options and future perspectives. Cancer treatment reviews. 2010;36 Suppl 3:S80-6.
177. Liedtke C, Mazouni C, Hess KR, Andre F, Tordai A, Mejia JA, et al. Response to neoadjuvant therapy and long-term survival in patients with triple-negative breast cancer. Journal of clinical oncology : official journal of the American Society of Clinical Oncology. 2008;26(8):1275-81.
178. Barth S, Huhn M, Matthey B, Klimka A, Galinski EA, Engert A. Compatible-solute-supported periplasmic expression of functional recombinant proteins under stress conditions. Applied and environmental microbiology. 2000;66(4):1572-9.
179. Krauss J, Arndt MA, Martin AC, Liu H, Rybak SM. Specificity grafting of human antibody frameworks selected from a phage display library: generation of a highly stable humanized anti-CD22 single-chain Fv fragment. Protein engineering. 2003;16(10):753-9.
180. Bonifacino JS, Dell'Angelica EC. Immunoprecipitation. Current Protocols in Cell Biology: John Wiley & Sons, Inc.; 2001.
181. Stocker M, Pardo A, Hetzel C, Reutelingsperger C, Fischer R, Barth S. Eukaryotic expression and secretion of EGFP-labeled annexin A5. Protein expression and purification. 2008;58(2):325-31.
182. Amoury M, Kolberg K, Pham AT, Hristodorov D, Mladenov R, Di Fiore S, et al. Granzyme B-based cytolytic fusion protein targeting EpCAM specifically kills triple negative breast cancer cells in vitro and inhibits tumor growth in a subcutaneous mouse tumor model. Cancer letters. 2016;372(2):201-9.
183. Amoury M, Mladenov R, Nachreiner T, Pham AT, Hristodorov D, Di Fiore S, et al. A novel approach for targeted elimination of CSPG4-positive triple-negative breast cancer cells using a MAP tau-based fusion protein. International journal of cancer. 2016.
184. Trejo-Solis C, Palencia G, Zuniga S, Rodriguez-Ropon A, Osorio-Rico L, Luvia ST, et al. Cas IIgly induces apoptosis in glioma C6 cells in vitro and in vivo through caspase-dependent and caspase-independent mechanisms. Neoplasia (New York, NY). 2005;7(6):563-74.
185. Chaitanya GV, Steven AJ, Babu PP. PARP-1 cleavage fragments: signatures of cell-death proteases in neurodegeneration. Cell communication and signaling : CCS. 2010;8:31.
186. Zou H, Li Y, Liu X, Wang X. An APAF-1.cytochrome c multimeric complex is a functional apoptosome that activates procaspase-9. The Journal of biological chemistry. 1999;274(17):11549-56.
187. Di Paolo C, Willuda J, Kubetzko S, Lauffer I, Tschudi D, Waibel R, et al. A recombinant immunotoxin derived from a humanized epithelial cell adhesion molecule-specific single-chain

antibody fragment has potent and selective antitumor activity. Clinical cancer research : an official journal of the American Association for Cancer Research. 2003;9(7):2837-48.
188. de Bruyn M, Rybczynska AA, Wei Y, Schwenkert M, Fey GH, Dierckx RA, et al. Melanoma-associated Chondroitin Sulfate Proteoglycan (MCSP)-targeted delivery of soluble TRAIL potently inhibits melanoma outgrowth in vitro and in vivo. Molecular cancer. 2010;9:301.
189. Schwenkert M, Birkholz K, Schwemmlein M, Kellner C, Kugler M, Peipp M, et al. A single chain immunotoxin, targeting the melanoma-associated chondroitin sulfate proteoglycan, is a potent inducer of apoptosis in cultured human melanoma cells. Melanoma research. 2008;18(2):73-84.
190. Pasquier E, Kavallaris M. Microtubules: a dynamic target in cancer therapy. IUBMB life. 2008;60(3):165-70.
191. Joensuu H, Gligorov J. Adjuvant treatments for triple-negative breast cancers. Annals of oncology : official journal of the European Society for Medical Oncology / ESMO. 2012;23 Suppl 6:vi40-5.
192. Verma S, Provencher L, Dent R. Emerging trends in the treatment of triple-negative breast cancer in Canada: a survey. Current oncology (Toronto, Ont). 2011;18(4):180-90.
193. Yadav BS, Sharma SC, Chanana P, Jhamb S. Systemic treatment strategies for triple-negative breast cancer. World journal of clinical oncology. 2014;5(2):125-33.
194. Gluz O, Nitz UA, Harbeck N, Ting E, Kates R, Herr A, et al. Triple-negative high-risk breast cancer derives particular benefit from dose intensification of adjuvant chemotherapy: results of WSG AM-01 trial. Annals of oncology : official journal of the European Society for Medical Oncology / ESMO. 2008;19(5):861-70.
195. Cheang MC, Voduc KD, Tu D, Jiang S, Leung S, Chia SK, et al. Responsiveness of intrinsic subtypes to adjuvant anthracycline substitution in the NCIC.CTG MA.5 randomized trial. Clinical cancer research : an official journal of the American Association for Cancer Research. 2012;18(8):2402-12.
196. Robert NJ, Dieras V, Glaspy J, Brufsky AM, Bondarenko I, Lipatov ON, et al. RIBBON-1: randomized, double-blind, placebo-controlled, phase III trial of chemotherapy with or without bevacizumab for first-line treatment of human epidermal growth factor receptor 2-negative, locally recurrent or metastatic breast cancer. Journal of clinical oncology : official journal of the American Society of Clinical Oncology. 2011;29(10):1252-60.
197. Thomssen C, Pierga JY, Pritchard KI, Biganzoli L, Cortes-Funes H, Petrakova K, et al. First-line bevacizumab-containing therapy for triple-negative breast cancer: analysis of 585 patients treated in the ATHENA study. Oncology. 2012;82(4):218-27.
198. Reis-Filho JS, Pinheiro C, Lambros MB, Milanezi F, Carvalho S, Savage K, et al. EGFR amplification and lack of activating mutations in metaplastic breast carcinomas. The Journal of pathology. 2006;209(4):445-53.
199. Weiner LM, Dhodapkar MV, Ferrone S. Monoclonal antibodies for cancer immunotherapy. Lancet (London, England). 2009;373(9668):1033-40.
200. Arnedos M, Soria JC, Andre F, Tursz T. Personalized treatments of cancer patients: a reality in daily practice, a costly dream or a shared vision of the future from the oncology community? Cancer treatment reviews. 2014;40(10):1192-8.
201. Berge EM, Doebele RC. Re-examination of maintenance therapy in non-small cell lung cancer with the advent of new anti-cancer agents. Drugs. 2013;73(6):517-32.
202. The American Food and Drug Administration. Revoking Avastin approval for metastaitc breast cancer. Internet [cited 3/10/2015]. Available from: http://www.fda.gov/NewsEvents/Newsroom/ucm280533.htm.
203. Sledge GW. Anti-vascular endothelial growth factor therapy in breast cancer: game over? Journal of clinical oncology : official journal of the American Society of Clinical Oncology. 2015;33(2):133-5.
204. Isakoff S, Overmoyer B, Tung N, Gelman R, Giranda V, Bernhard K, et al., editors. A phase II trial of the PARP inhibitor veliparib (ABT888) and temozolomide for metastatic breast cancer. ASCO Annual Meeting Proceedings; 2010.
205. Pajk B, Cufer T, Canney P, Ellis P, Cameron D, Blot E, et al. Anti-tumor activity of capecitabine and vinorelbine in patients with anthracycline- and taxane-pretreated metastatic breast

cancer: findings from the EORTC 10001 randomized phase II trial. Breast (Edinburgh, Scotland). 2008;17(2):180-5.
206. Ellard SL, Clemons M, Gelmon KA, Norris B, Kennecke H, Chia S, et al. Randomized phase II study comparing two schedules of everolimus in patients with recurrent/metastatic breast cancer: NCIC Clinical Trials Group IND.163. Journal of clinical oncology : official journal of the American Society of Clinical Oncology. 2009;27(27):4536-41.
207. Ossovskaya V, Li L, Broude E, Lim C-U, Roninson I, Bradley C, et al., editors. Abstract# 5552: BSI-201 enhances the activity of multiple classes of cytotoxic agents and irradiation in triple negative breast cancer. Cancer research; 2009.
208. Caldas-Lopes E, Cerchietti L, Ahn JH, Clement CC, Robles AI, Rodina A, et al. Hsp90 inhibitor PU-H71, a multimodal inhibitor of malignancy, induces complete responses in triple-negative breast cancer models. Proceedings of the National Academy of Sciences of the United States of America. 2009;106(20):8368-73.
209. Biname F. Transduction of extracellular cues into cell polarity: the role of the transmembrane proteoglycan NG2. Molecular neurobiology. 2014;50(2):482-93.
210. Pantazaka E, Papadimitriou E. Chondroitin sulfate-cell membrane effectors as regulators of growth factor-mediated vascular and cancer cell migration. Biochimica et biophysica acta. 2014;1840(8):2643-50.
211. Fukushi J, Makagiansar IT, Stallcup WB. NG2 proteoglycan promotes endothelial cell motility and angiogenesis via engagement of galectin-3 and alpha3beta1 integrin. Molecular biology of the cell. 2004;15(8):3580-90.
212. Eisenmann KM, McCarthy JB, Simpson MA, Keely PJ, Guan JL, Tachibana K, et al. Melanoma chondroitin sulphate proteoglycan regulates cell spreading through Cdc42, Ack-1 and p130cas. Nature cell biology. 1999;1(8):507-13.
213. Petrini S, Tessa A, Stallcup WB, Sabatelli P, Pescatori M, Giusti B, et al. Altered expression of the MCSP/NG2 chondroitin sulfate proteoglycan in collagen VI deficiency. Molecular and cellular neurosciences. 2005;30(3):408-17.
214. Iida J, Pei D, Kang T, Simpson MA, Herlyn M, Furcht LT, et al. Melanoma chondroitin sulfate proteoglycan regulates matrix metalloproteinase-dependent human melanoma invasion into type I collagen. The Journal of biological chemistry. 2001;276(22):18786-94.
215. Yang J, Price MA, Li GY, Bar-Eli M, Salgia R, Jagedeeswaran R, et al. Melanoma proteoglycan modifies gene expression to stimulate tumor cell motility, growth, and epithelial-to-mesenchymal transition. Cancer research. 2009;69(19):7538-47.
216. Mittelman A, Chen ZJ, Yang H, Wong GY, Ferrone S. Human high molecular weight melanoma-associated antigen (HMW-MAA) mimicry by mouse anti-idiotypic monoclonal antibody MK2-23: induction of humoral anti-HMW-MAA immunity and prolongation of survival in patients with stage IV melanoma. Proceedings of the National Academy of Sciences of the United States of America. 1992;89(2):466-70.
217. Mani SA, Guo W, Liao MJ, Eaton EN, Ayyanan A, Zhou AY, et al. The epithelial-mesenchymal transition generates cells with properties of stem cells. Cell. 2008;133(4):704-15.
218. Agboola AJ, Paish EC, Rakha EA, Powe DG, Macmillan RD, Ellis IO, et al. EpCAM expression is an indicator of recurrence in basal-like breast cancer. Breast cancer research and treatment. 2012;133(2):575-82.
219. Baeuerle PA, Gires O. EpCAM (CD326) finding its role in cancer. British journal of cancer. 2007;96(3):417-23.
220. Imrich S, Hachmeister M, Gires O. EpCAM and its potential role in tumor-initiating cells. Cell adhesion & migration. 2012;6(1):30-8.
221. van der Gun BTF, Melchers LJ, Ruiters MHJ, de Leij LFMH, McLaughlin PMJ, Rots MG. EpCAM in carcinogenesis: the good, the bad or the ugly. Carcinogenesis. 2010;31(11):1913-21.
222. Yamashita T, Ji J, Budhu A, Forgues M, Yang W, Wang HY, et al. EpCAM-positive hepatocellular carcinoma cells are tumor-initiating cells with stem/progenitor cell features. Gastroenterology. 2009;136(3):1012-24.
223. Xie X, Wang CY, Cao YX, Wang W, Zhuang R, Chen LH, et al. Expression pattern of epithelial cell adhesion molecule on normal and malignant colon tissues. World journal of gastroenterology. 2005;11(3):344-7.

224. Munz M, Murr A, Kvesic M, Rau D, Mangold S, Pflanz S, et al. Side-by-side analysis of five clinically tested anti-EpCAM monoclonal antibodies. Cancer cell international. 2010;10:44.
225. Adams GP, Schier R, McCall AM, Simmons HH, Horak EM, Alpaugh RK, et al. High affinity restricts the localization and tumor penetration of single-chain fv antibody molecules. Cancer research. 2001;61(12):4750-5.
226. Goel S, Bauer RJ, Desai K, Bulgaru A, Iqbal T, Strachan BK, et al. Pharmacokinetic and safety study of subcutaneously administered weekly ING-1, a human engineere monoclonal antibody targeting human EpCAM, in patients with advanced solid tumors. Annals of oncology : official journal of the European Society for Medical Oncology / ESMO. 2007;18(10):1704-7.
227. Lewis LD. Technology evaluation: ING-1, XOMA. Current opinion in molecular therapeutics. 2003;5(4):433-6.
228. Saleh M, Posey J, Khazaeli M, Thurmond L, Khor S, Lampkin T, et al., editors. Phase I trial testing multiple doses of humanized monoclonal antibody 3622W94. PROCEEDINGS OF THE ANNUAL MEETING-AMERICAN SOCIETY OF CLINICAL ONCOLOGY; 1998: AMERICAN SOCIETY OF CLINICAL ONCOLOGY.
229. LoBuglio A, Saleh M, Braddock J, Lampkin T, Khor S, Wissel P, et al., editors. A phase I trial of the humanized anti-EGP40 monoclonal antibody 3622W94. Proc Am Soc Clin Oncol; 1997.
230. Eskander RN, Randall LM. Bevacizumab in the treatment of ovarian cancer. Biologics : targets & therapy. 2011;5:1-5.
231. Strickler JH, Hurwitz HI. Bevacizumab-based therapies in the first-line treatment of metastatic colorectal cancer. The oncologist. 2012;17(4):513-24.
232. Gisselbrecht C, Glass B, Mounier N, Singh Gill D, Linch DC, Trneny M, et al. Salvage regimens with autologous transplantation for relapsed large B-cell lymphoma in the rituximab era. Journal of clinical oncology : official journal of the American Society of Clinical Oncology. 2010;28(27):4184-90.
233. Scott AM, Wolchok JD, Old LJ. Antibody therapy of cancer. Nature reviews Cancer. 2012;12(4):278-87.
234. Green MC, Murray JL, Hortobagyi GN. Monoclonal antibody therapy for solid tumors. Cancer treatment reviews. 2000;26(4):269-86.
235. Schrama D, Reisfeld RA, Becker JC. Antibody targeted drugs as cancer therapeutics. Nature reviews Drug discovery. 2006;5(2):147-59.
236. Reichert JM. Monoclonal antibodies in the clinic. Nature biotechnology. 2001;19(9):819-22.
237. Lambert JM. Drug-conjugated antibodies for the treatment of cancer. British journal of clinical pharmacology. 2013;76(2):248-62.
238. Clark O, Botrel TE, Paladini L, Ferreira MB. Targeted therapy in triple-negative metastatic breast cancer: a systematic review and meta-analysis. Core evidence. 2014;9:1-11.
239. Lambert JM. Drug-conjugated monoclonal antibodies for the treatment of cancer. Current opinion in pharmacology. 2005;5(5):543-9.
240. Boyraz B, Sendur MA, Aksoy S, Babacan T, Roach EC, Kizilarslanoglu MC, et al. Trastuzumab emtansine (T-DM1) for HER2-positive breast cancer. Current medical research and opinion. 2013;29(4):405-14.
241. Sievers EL, Senter PD. Antibody-drug conjugates in cancer therapy. Annual review of medicine. 2013;64:15-29.
242. Firer MA, Gellerman G. Targeted drug delivery for cancer therapy: the other side of antibodies. Journal of hematology & oncology. 2012;5:70.
243. Boswell CA, Mundo EE, Zhang C, Bumbaca D, Valle NR, Kozak KR, et al. Impact of drug conjugation on pharmacokinetics and tissue distribution of anti-STEAP1 antibody-drug conjugates in rats. Bioconjugate chemistry. 2011;22(10):1994-2004.
244. Bornstein GG. Antibody Drug Conjugates: Preclinical Considerations. The AAPS journal. 2015;17(3):525-34.
245. Ducry L, Stump B. Antibody-drug conjugates: linking cytotoxic payloads to monoclonal antibodies. Bioconjugate chemistry. 2010;21(1):5-13.

246. Ritchie M, Tchistiakova L, Scott N. Implications of receptor-mediated endocytosis and intracellular trafficking dynamics in the development of antibody drug conjugates. mAbs. 2013;5(1):13-21.
247. Rudnick SI, Lou J, Shaller CC, Tang Y, Klein-Szanto AJ, Weiner LM, et al. Influence of affinity and antigen internalization on the uptake and penetration of Anti-HER2 antibodies in solid tumors. Cancer research. 2011;71(6):2250-9.
248. Pellinen T, Ivaska J. Integrin traffic. Journal of cell science. 2006;119(Pt 18):3723-31.
249. Dautry-Varsat A, Ciechanover A, Lodish HF. pH and the recycling of transferrin during receptor-mediated endocytosis. Proceedings of the National Academy of Sciences of the United States of America. 1983;80(8):2258-62.
250. Trivedi RR, Bhattacharyya S. Constitutive internalization and recycling of metabotropic glutamate receptor 5 (mGluR5). Biochemical and biophysical research communications. 2012;427(1):185-90.
251. Ackerman ME, Pawlowski D, Wittrup KD. Effect of antigen turnover rate and expression level on antibody penetration into tumor spheroids. Molecular cancer therapeutics. 2008;7(7):2233-40.
252. Schmidt MM, Thurber GM, Wittrup KD. Kinetics of anti-carcinoembryonic antigen antibody internalization: effects of affinity, bivalency, and stability. Cancer immunology, immunotherapy : CII. 2008;57(12):1879-90.
253. Viti F, Tarli L, Giovannoni L, Zardi L, Neri D. Increased binding affinity and valence of recombinant antibody fragments lead to improved targeting of tumoral angiogenesis. Cancer research. 1999;59(2):347-52.
254. Zhou Y, Goenaga AL, Harms BD, Zou H, Lou J, Conrad F, et al. Impact of intrinsic affinity on functional binding and biological activity of EGFR antibodies. Molecular cancer therapeutics. 2012;11(7):1467-76.
255. Olsen E, Duvic M, Frankel A, Kim Y, Martin A, Vonderheid E, et al. Pivotal phase III trial of two dose levels of denileukin diftitox for the treatment of cutaneous T-cell lymphoma. Journal of clinical oncology : official journal of the American Society of Clinical Oncology. 2001;19(2):376-88.
256. Tagge E, Harris B, Burbage C, Hall P, Vesely J, Willingham M, et al. Synthesis of green fluorescent protein-ricin and monitoring of its intracellular trafficking. Bioconjugate chemistry. 1997;8(5):743-50.
257. Smith DC, Spooner RA, Watson PD, Murray JL, Hodge TW, Amessou M, et al. Internalized Pseudomonas exotoxin A can exploit multiple pathways to reach the endoplasmic reticulum. Traffic (Copenhagen, Denmark). 2006;7(4):379-93.
258. Mohanraj D, Ramakrishnan S. Cytotoxic effects of ricin without an interchain disulfide bond: genetic modification and chemical crosslinking studies. Biochimica et biophysica acta. 1995;1243(3):399-406.
259. Van Ness BG, Howard JB, Bodley JW. ADP-ribosylation of elongation factor 2 by diphtheria toxin. NMR spectra and proposed structures of ribosyl-diphthamide and its hydrolysis products. The Journal of biological chemistry. 1980;255(22):10710-6.
260. Endo Y, Mitsui K, Motizuki M, Tsurugi K. The mechanism of action of ricin and related toxic lectins on eukaryotic ribosomes. The site and the characteristics of the modification in 28 S ribosomal RNA caused by the toxins. The Journal of biological chemistry. 1987;262(12):5908-12.
261. Fey GHM, Stieglmaier J, Schwenkert M, Schwemmlein M. Combination of immunological agent and sensitizing agent for the treatment of cancer. Google Patents; 2008.
262. Stish BJ, Chen H, Shu Y, Panoskaltsis-Mortari A, Vallera DA. Increasing anticarcinoma activity of an anti-erbB2 recombinant immunotoxin by the addition of an anti-EpCAM sFv. Clinical cancer research : an official journal of the American Association for Cancer Research. 2007;13(10):3058-67.
263. Francisco JA, Schreiber GJ, Comereski CR, Mezza LE, Warner GL, Davidson TJ, et al. In vivo efficacy and toxicity of a single-chain immunotoxin targeted to CD40. Blood. 1997;89(12):4493-500.
264. Kioi M, Seetharam S, Puri RK. Targeting IL-13Ralpha2-positive cancer with a novel recombinant immunotoxin composed of a single-chain antibody and mutated Pseudomonas exotoxin. Molecular cancer therapeutics. 2008;7(6):1579-87.

265. Frankel AE. Reducing the immune response to immunotoxin. Clinical cancer research : an official journal of the American Association for Cancer Research. 2004;10(1 Pt 1):13-5.
266. Hertler AA, Spitler LE, Frankel AE. Humoral immune response to a ricin A chain immunotoxin in patients with metastatic melanoma. Cancer drug delivery. 1987;4(4):245-53.
267. Hall PD, Virella G, Willoughby T, Atchley DH, Kreitman RJ, Frankel AE. Antibody response to DT-GM, a novel fusion toxin consisting of a truncated diphtheria toxin (DT) linked to human granulocyte-macrophage colony stimulating factor (GM), during a phase I trial of patients with relapsed or refractory acute myeloid leukemia. Clinical immunology (Orlando, Fla). 2001;100(2):191-7.
268. Roscoe DM, Jung SH, Benhar I, Pai L, Lee BK, Pastan I. Primate antibody response to immunotoxin: serological and computer-aided analysis of epitopes on a truncated form of Pseudomonas exotoxin. Infection and immunity. 1994;62(11):5055-65.
269. Roscoe DM, Pai LH, Pastan I. Identification of epitopes on a mutant form of Pseudomonas exotoxin using serum from humans treated with Pseudomonas exotoxin containing immunotoxins. European journal of immunology. 1997;27(6):1459-68.
270. Kelly KR, Chanan-Khan A, Somlo G, Heffner LT, Demand M, Haeder T, et al., editors. Indatuximab Ravtansine (BT062) in Combination with Lenalidomide and Low-Dose Dexamethasone in Patients with Relapsed and/or Refractory Multiple Myeloma: Clinical Activity in Len/Dex-Refractory Patients. Blood; 2014.
271. Berdeja JG. Lorvotuzumab mertansine: antibody-drug-conjugate for CD56+ multiple myeloma. Frontiers in bioscience (Landmark edition). 2014;19:163-70.
272. Verma RS, Bonavida B. Resistance to Immunotoxins in Cancer Therapy: Springer; 2015.
273. Tur MK, Neef I, Jost E, Galm O, Jager G, Stocker M, et al. Targeted restoration of down-regulated DAPK2 tumor suppressor activity induces apoptosis in Hodgkin lymphoma cells. Journal of immunotherapy (Hagerstown, Md : 1997). 2009;32(5):431-41.
274. Cao Y, Mohamedali KA, Marks JW, Cheung LH, Hittelman WN, Rosenblum MG. Construction and characterization of novel, completely human serine protease therapeutics targeting Her2/neu. Molecular cancer therapeutics. 2013;12(6):979-91.
275. Alonso AC, Zaidi T, Grundke-Iqbal I, Iqbal K. Role of abnormally phosphorylated tau in the breakdown of microtubules in Alzheimer disease. Proceedings of the National Academy of Sciences of the United States of America. 1994;91(12):5562-6.
276. Feinstein SC, Wilson L. Inability of tau to properly regulate neuronal microtubule dynamics: a loss-of-function mechanism by which tau might mediate neuronal cell death. Biochimica et biophysica acta. 2005;1739(2-3):268-79.
277. Guerin M, Sabatier R, Goncalves A. [Trastuzumab emtansine (Kadcyla((R))) approval in HER2-positive metastatic breast cancers]. Bulletin du cancer. 2015;102(4):390-7.
278. Behrens CR, Liu B. Methods for site-specific drug conjugation to antibodies. mAbs. 2014;6(1):46-53.
279. Blagosklonny MV, Robey R, Sheikh MS, Fojo T. Paclitaxel-induced FasL-independent apoptosis and slow (non-apoptotic) cell death. Cancer biology & therapy. 2002;1(2):113-7.
280. Morse DL, Gray H, Payne CM, Gillies RJ. Docetaxel induces cell death through mitotic catastrophe in human breast cancer cells. Molecular cancer therapeutics. 2005;4(10):1495-504.
281. Bajt ML, Cover C, Lemasters JJ, Jaeschke H. Nuclear translocation of endonuclease G and apoptosis-inducing factor during acetaminophen-induced liver cell injury. Toxicological sciences : an official journal of the Society of Toxicology. 2006;94(1):217-25.
282. Li LY, Luo X, Wang X. Endonuclease G is an apoptotic DNase when released from mitochondria. Nature. 2001;412(6842):95-9.
283. Hahn HP, Pang M, He J, Hernandez JD, Yang RY, Li LY, et al. Galectin-1 induces nuclear translocation of endonuclease G in caspase- and cytochrome c-independent T cell death. Cell death and differentiation. 2004;11(12):1277-86.
284. Lee TJ, Kim EJ, Kim S, Jung EM, Park JW, Jeong SH, et al. Caspase-dependent and caspase-independent apoptosis induced by evodiamine in human leukemic U937 cells. Molecular cancer therapeutics. 2006;5(9):2398-407.
285. van Loo G, Schotte P, van Gurp M, Demol H, Hoorelbeke B, Gevaert K, et al. Endonuclease G: a mitochondrial protein released in apoptosis and involved in caspase-independent DNA degradation. Cell death and differentiation. 2001;8(12):1136-42.

286. Zhu R, Zou ST, Wan JM, Li W, Li XL, Zhu W. BTG1 inhibits breast cancer cell growth through induction of cell cycle arrest and apoptosis. Oncology reports. 2013;30(5):2137-44.
287. Vitale I, Galluzzi L, Castedo M, Kroemer G. Mitotic catastrophe: a mechanism for avoiding genomic instability. Nature reviews Molecular cell biology. 2011;12(6):385-92.
288. Pardo A, Stocker M, Kampmeier F, Melmer G, Fischer R, Thepen T, et al. In vivo imaging of immunotoxin treatment using Katushka-transfected A-431 cells in a murine xenograft tumour model. Cancer immunology, immunotherapy : CII. 2012;61(10):1617-26.
289. Bladergroen BA, Strik MC, Bovenschen N, van Berkum O, Scheffer GL, Meijer CJ, et al. The granzyme B inhibitor, protease inhibitor 9, is mainly expressed by dendritic cells and at immune-privileged sites. Journal of immunology (Baltimore, Md : 1950). 2001;166(5):3218-25.
290. Bird CH, Sun J, Ung K, Karambalis D, Whisstock JC, Trapani JA, et al. Cationic sites on granzyme B contribute to cytotoxicity by promoting its uptake into target cells. Molecular and cellular biology. 2005;25(17):7854-67.
291. Shi L, Keefe D, Durand E, Feng H, Zhang D, Lieberman J. Granzyme B binds to target cells mostly by charge and must be added at the same time as perforin to trigger apoptosis. Journal of immunology (Baltimore, Md : 1950). 2005;174(9):5456-61.
292. Weiner LM, Surana R, Wang S. Monoclonal antibodies: versatile platforms for cancer immunotherapy. Nature reviews Immunology. 2010;10(5):317-27.
293. Brinkmann U, Reiter Y, Jung SH, Lee B, Pastan I. A recombinant immunotoxin containing a disulfide-stabilized Fv fragment. Proceedings of the National Academy of Sciences of the United States of America. 1993;90(16):7538-42.

# VI Appendix

## *VI.1 Index of Figures and Tables*

### *VI.1.1 Figures*

Figure 1. Construction of EpCAM-specific fusion proteins. ..... 42
Figure 2. Expression and purification of EpCAM specific fusion proteins. ..... 44
Figure 3. Activation of GB-R201K-αEpCAM(scFv) proteolytic activity. ..... 45
Figure 4. Detection of Serpin B9 (PI-9) in TNBC cell lines. ..... 46
Figure 5. Expression of EpCAM receptor in TNBC cell lines. ..... 47
Figure 6. Binding of purified EpCAM specific CFPs on TNBC cell lines. ..... 47
Figure 7. Saturation curve and binding affinity of EpCAM specific CFPs in TNBC cell lines. ..... 48
Figure 8. Binding and internalization of CFPs in EpCAM positive MDA-MB-468 cell line. ..... 50
Figure 9. Internalization kinetics of CFPs in MDA-MB-468 cell line. ..... 51
Figure 10. Growth inhibition of TNBC cells *in vitro* by αEpCAM specific CFPs ..... 52
Figure 11. Induction of apoptosis in MDA-MB-468 cells by EpCAM-specific CFPs. ..... 53
Figure 12. Activation of caspase 3 apoptosis pathway by EpCAM specific CFPs. ..... 54
Figure 13. Activation of caspase 9 apoptosis pathway by EpCAM specific CFPs. ..... 54
Figure 14. Tumor take-rate of MDA-MB-468 cell line in a subcutaneous tumor model. ..... 56
Figure 15. Labeling of EpCAM specific CFPs with DyLight 747-NHS fluorescent dye ..... 57
Figure 16. Biodistribution of fluorescently-labeled αEpCAM CFPs in mice bearing MDA-MB-468 tumors. ..... 58
Figure 17. Detection of EpCAM specific CFPs in tumor sections of MDA-MB-468 tumor-bearing mice 8 hours after treatment. ..... 59
Figure 18. Detection of EpCAM specific CFPs in kidney sections of treated mice 4 to 24 hours after treatment. ..... 60

Figure 19. General toxicity of EpCAM-specific CFPs in a MDA-MB-468 xenograft tumor model. ..... 61
Figure 20. Tumor growth inhibition by EpCAM-specific CFPs in a MDA-MB-468 xenograft tumor model. ..... 62
Figure 21. CSPG4 expression on breast cancer cell lines. ..... 64
Figure 22. CSPG4 specific CFP constructs' design. ..... 66
Figure 23. Contamination of αCSPG4(scFv)-ETA' elution fraction with co-eluting bacterial proteins. ..... 67
Figure 24. Expression and purification of CSPG4 specific fusion proteins. ..... 68
Figure 25. Binding of CSPG4 specific fusion proteins on TNBC cell lines. ..... 69
Figure 26. Binding and internalization of CSPG4 specific CFPs on MDA-MB-231 cell line. ..... 70
Figure 27. Internalization kinetics of CSPG specific CFPs in MDA-MB-231 cells. 71
Figure 28. Induction of Tubulin polymerization by αCSPG4(scFv)-MAP. ..... 72
Figure 29. Intracellular interaction of αCSPG4(scFv)-MAP with Tubulin following internalization in MDA-MB-231 cells. ..... 73
Figure 30. Growth inhibition and cytotoxicity of CSPG4 specific CFPs in TNBC cell lines. ..... 74
Figure 31. Induction of apoptosis by CSPG4 specific CFPs in MDA-MB-231 cells... ..... 75
Figure 32. Induction of caspase 3 dependent apoptosis by CSPG4 specific CFPs in MDA-MB-231 cells. ..... 76
Figure 33. Activation of the mitochondrial stress apoptotic pathway by CSPG4 specific CFPs. ..... 77
Figure 34. Induction of cell cycle arrest by αCSPG4(scFv)-MAP in MDA-MB-231 cells. ..... 78
Figure 35. Inhibition of tumor growth *in vivo* by CSPG4 specific CFPs in MDA-MB-231 subcutaneous tumor model. ..... 80
Figure 36. *In vivo* imaging of the accumulation of αCSPG4(scFv)-SNAP in MDA-MB-231 subcutaneous tumors in mice ..... 81
Figure 37. Biodistribution kinetics of CSPG4 specific CFPs in xenograft mouse model. ..... 83

### *VI.1.2 Tables*

Table 1. A list of targeted therapies in active clinical trials in the USA for the treatment of triple negative breast cancer in 2015: ..... 7
Table 2. Protein based immunotoxins that successfully passed phase I and are currently in active clinical trials in the USA:..... 12
Table 3. Buffers and media:..... 20
Table 4. Names and suppliers of kits:..... 22
Table 5. Sequences of oligonucleotides used for sequencing: ..... 23
Table 6. List of antibodies used in this thesis:..... 24
Table 7. List of equipment used in this thesis: ..... 25
Table 8. Software used for data analysis: ..... 26
Table 9. Induction of subcutaneous MDA-MB-468 tumors in BALB/C Nude mice:... ..... 55
Table 10. GB-R201K-αEpCAM(scFv) dose escalation study in mice:..... 61
Table 11. Expression of CSPG4 on breast cancer cell lines:..... 65
Table 12. Tumor take rate study design- induction of MDA-MB-231subcutaneous tumor in BALB/c Nude mice:..... 78
Table 13. Dose escalation studies *in vivo* of CSPG4 specific CFPs in mice:..... 79

### *VI.2 Abbreviations*

| | |
|---|---|
| Ab | antibody |
| Ag | antigen |
| Ang | angiogenin |
| AP | alkaline phosphatase |
| APS | ammonium persulfate |
| ATCC | American Type Culture Collection |
| bp | base pair |
| BSA | bovine serum albumin |
| $dH_2O$ | deionized water |
| DMF | dimethylformamide |
| DNA | deoxyribonucleic acid |
| dNTP | deoxy nucleotide triphosphate |
| DSMZ | Deutsche Stammsammlung von Mikroorganismen und Zellkulturen |
| DT | diphtheria toxin |
| DTT | dithiothreitol |
| ECP | endosomal cleavable peptide |
| EDTA | ethylenediaminetetraacetic acid |

| | |
|---|---|
| EF | eukaryotic elongation factor |
| EGF | epidermal growth factor |
| ELISA | enzyme linked immunosorbent assay |
| ER | endoplasmic reticulum |
| ETA | Pseudomonas Exotoxin A, deletion mutant |
| Fab | fragment antigen binding |
| FACS | fluorescence-activated cell sorting |
| FC | antibody fragment crystallizable region |
| FCS | fetal calf serum |
| FITC | fluorescein isothiocyanate |
| g | relative centrifuge force |
| Gb | Granzyme B |
| hCD64 | human CD64 |
| CFP | cytolytic fusion protein |
| His-tag | polyhistidine motif |
| HRP | horseradish peroxidase |
| $IC_{50}$ | inhibitory concentration at 50% survival |
| IF | immunofluorescence |
| IFN-γ | interferon-γ |
| IgG | immunoglobulin G |
| IHC | immunohistochemistry |
| IL | interleukin |
| IMAC | immobilized metal ion affinity chromatography |
| iNOS | inducible nitric oxide synthase |
| IPTG | isopropyl-beta-D-thiogalactopyranoside |
| IT | immunotoxin |
| Kan | kanamycin |
| kb | kilobase |
| kDa | kilo Dalton |
| Kd | Dissociation constant |
| LB | Luria broth |
| mAb | monoclonal antibody |
| MAP | microtubule-associated protein |
| MFI | mean fluorescence intensity |
| MTP | membrane transfer peptide |
| NBT-BCIP | nitro blue tetrazolium chloride/5-bromo-4-chloro-3-indolyl phosphate |
| neg | negative |
| NK | natural killer cell(s) |
| NLS | nuclear localization sequence |
| NTA | nitrilotriacetic acid |
| OD | optical density |
| ORF | open reading frame |
| ori | origin of replication |
| PAGE | polyacrylamide gel electrophoresis |
| PBMCs | peripheral blood mononuclear cells |
| PBS | phosphate buffered saline |
| PBST | phosphate buffered saline + 0.05% (v/v) Tween 20 |
| PCR | polymerase chain reaction |
| pH | negative logarithm of the concentration of hydrogen ions in solution |

| | |
|---|---|
| PI | propidium iodide |
| RNA | ribonucleic acid |
| RNI | reactive nitrogen intermediates |
| ROI | reactive oxygen intermediates |
| PE | (R-)phycoerythrin |
| rpm | rotations per minute |
| scFv | single chain fragment variable |
| SD | standard deviation |
| SDS | sodium dodecyl sulfate |
| SEC | size exclusion chromatography |
| SEM | standard error of mean |
| SLS | sodium lauryl sulfate (=SDS) |
| TAE | trisacetate EDTA buffer |
| TEMED | tetramethylethylenediamine |
| TGF-β | tumor growth factor-β |
| TNF | tumor necrosis factor |
| Tris | tris(hydroxymethyl)aminomethane |
| Tween 20 | polyoxyethylene (20) sorbitan monolaurate |
| U | unit(s) |
| UV | ultraviolet |
| v/v | volume per volume |
| VEGF | vascular endothelial growth factor |
| w/v | weight per volume |
| WB | western blotting |
| XTT | sodium 3'-[1-(phenylaminocarbonyl)-3,4-tetrazolium]-bis(4-methoxy-6-nitro)benzenesulfonic acid hydrate |

## *VI.3 Plasmid sequences*

### *VI.3.1 PMT-anti-EpCAM(scFv)-ETA*

TGGCGAATGGGACGCGCCCTGTAGCGGCGCATTAAGCGCGGCGGGTGTGGTGGTTACGCGCAG
CGTGACCGCTACACTTGCCAGCGCCCTAGCGCCCGCTCCTTTCGCTTTCTTCCCTTCCTTTCTCGC
CACGTTCGCCGGCTTTCCCCGTCAAGCTCTAAATCGGGGGCTCCCTTTAGGGTTCCGATTTAGTG
CTTTACGGCACCTCGACCCCAAAAAACTTGATTAGGGTGATGGTTCACGTAGTGGGCCATCGCC
CTGATAGACGGTTTTTCGCCCTTTGACGTTGGAGTCCACGTTCTTTAATAGTGGACTCTTGTTCC
AAACTGGAACAACACTCAACCCTATCTCGGTCTATTCTTTTGATTTATAAGGGATTTTGCCGATT
TCGGCCTATTGGTTAAAAAATGAGCTGATTTAACAAAAATTTAACGCGAATTTTAACAAAATAT
TAACGTTTACAATTTCAGGTGGCACTTTTCGGGGAAATGTGCGCGGAACCCCTATTTGTTTATTT
TTCTAAATACATTCAAATATGTATCCGCTCATGAATTAATTCTTAGAAAAACTCATCGAGCATCA
AATGAAACTGCAATTTATTCATATCAGGATTATCAATACCATATTTTTGAAAAAGCCGTTTCTGT
AATGAAGGAGAAAACTCACCGAGGCAGTTCCATAGGATGGCAAGATCCTGGTATCGGTCTGCG
ATTCCGACTCGTCCAACATCAATACAACCTATTAATTTCCCCTCGTCAAAAATAAGGTTATCAA
GTGAGAAATCACCATGAGTGACGACTGAATCCGGTGAGAATGGCAAAAGTTTATGCATTTCTTT

CCAGACTTGTTCAACAGGCCAGCCATTACGCTCGTCATCAAAATCACTCGCATCAACCAAACCG
TTATTCATTCGTGATTGCGCCTGAGCGAGACGAAATACGCGATCGCTGTTAAAAGGACAATTAC
AAACAGGAATCGAATGCAACCGGCGCAGGAACACTGCCAGCGCATCAACAATATTTTCACCTG
AATCAGGATATTCTTCTAATACCTGGAATGCTGTTTTCCCGGGGATCGCAGTGGTGAGTAACCA
TGCATCATCAGGAGTACGGATAAAATGCTTGATGGTCGGAAGAGGCATAAATTCCGTCAGCCA
GTTTAGTCTGACCATCTCATCTGTAACATCATTGGCAACGCTACCTTTGCCATGTTTCAGAAACA
ACTCTGGCGCATCGGGCTTCCCATACAATCGATAGATTGTCGCACCTGATTGCCCGACATTATC
GCGAGCCCATTTATACCCATATAAATCAGCATCCATGTTGGAATTTAATCGCGGCCTAGAGCAA
GACGTTTCCCGTTGAATATGGCTCATAACACCCCTTGTATTACTGTTTATGTAAGCAGACAGTTT
TATTGTTCATGACCAAAATCCCTTAACGTGAGTTTTCGTTCCACTGAGCGTCAGACCCCGTAGAA
AAGATCAAAGGATCTTCTTGAGATCCTTTTTTTCTGCGCGTAATCTGCTGCTTGCAAACAAAAAA
ACCACCGCTACCAGCGGTGGTTTGTTTGCCGGATCAAGAGCTACCAACTCTTTTTCCGAAGGTA
ACTGGCTTCAGCAGAGCGCAGATACCAAATACTGTCCTTCTAGTGTAGCCGTAGTTAGGCCACC
ACTTCAAGAACTCTGTAGCACCGCCTACATACCTCGCTCTGCTAATCCTGTTACCAGTGGCTGCT
GCCAGTGGCGATAAGTCGTGTCTTACCGGGTTGGACTCAAGACGATAGTTACCGGATAAGGCGC
AGCGGTCGGGCTGAACGGGGGGTTCGTGCACACAGCCCAGCTTGGAGCGAACGACCTACACCG
AACTGAGATACCTACAGCGTGAGCTATGAGAAAGCGCCACGCTTCCCGAAGGGAGAAAGGCGG
ACAGGTATCCGGTAAGCGGCAGGGTCGGAACAGGAGAGCGCACGAGGGAGCTTCCAGGGGGA
AACGCCTGGTATCTTTATAGTCCTGTCGGGTTTCGCCACCTCTGACTTGAGCGTCGATTTTTGTG
ATGCTCGTCAGGGGGGCGGAGCCTATGGAAAAACGCCAGCAACGCGGCCTTTTTACGGTTCCTG
GCCTTTTGCTGGCCTTTTGCTCACATGTTCTTTCCTGCGTTATCCCCTGATTCTGTGGATAACCGT
ATTACCGCCTTTGAGTGAGCTGATACCGCTCGCCGCAGCCGAACGACCGAGCGCAGCGAGTCA
GTGAGCGAGGAAGCGGAAGAGCGCCTGATGCGGTATTTTCTCCTTACGCATCTGTGCGGTATTT
CACACCGCATATATGGTGCACTCTCAGTACAATCTGCTCTGATGCCGCATAGTTAAGCCAGTAT
ACACTCCGCTATCGCTACGTGACTGGGTCATGGCTGCGCCCCGACACCCGCCAACACCCGCTGA
CGCGCCCTGACGGGCTTGTCTGCTCCCGGCATCCGCTTACAGACAAGCTGTGACCGTCTCCGGG
AGCTGCATGTGTCAGAGGTTTTCACCGTCATCACCGAAACGCGCGAGGCAGCTGCGGTAAAGCT
CATCAGCGTGGTCGTGAAGCGATTCACAGATGTCTGCCTGTTCATCCGCGTCCAGCTCGTTGAG
TTTCTCCAGAAGCGTTAATGTCTGGCTTCTGATAAAGCGGGCCATGTTAAGGGCGGTTTTTTCCT
GTTTGGTCACTGATGCCTCCGTGTAAGGGGGATTTCTGTTCATGGGGGTAATGATACCGATGAA
ACGAGAGAGGATGCTCACGATACGGGTTACTGATGATGAACATGCCCGGTTACTGGAACGTTGT
GAGGGTAAACAACTGGCGGTATGGATGCGGCGGGACCAGAGAAAAATCACTCAGGGTCAATGC
CAGCGCTTCGTTAATACAGATGTAGGTGTTCCACAGGGTAGCCAGCAGCATCCTGCGATGCAGA
TCCGGAACATAATGGTGCAGGGCGCTGACTTCCGCGTTTCCAGACTTTACGAAACACGGAAACC
GAAGACCATTCATGTTGTTGCTCAGGTCGCAGACGTTTTGCAGCAGCAGTCGCTTCACGTTCGCT
CGCGTATCGGTGATTCATTCTGCTAACCAGTAAGGCAACCCCGCCAGCCTAGCCGGGTCCTCAA
CGACAGGAGCACGATCATGCGCACCCGTGGGGCCGCCATGCCGGCGATAATGGCCTGCTTCTCG
CCGAAACGTTTGGTGGCGGGACCAGTGACGAAGGCTTGAGCGAGGGCGTGCAAGATTCCGAAT
ACCGCAAGCGACAGGCCGATCATCGTCGCGCTCCAGCGAAAGCGGTCCTCGCCGAAAATGACC
CAGAGCGCTGCCGGCACCTGTCCTACGAGTTGCATGATAAAGAAGACAGTCATAAGTGCGGCG
ACGATAGTCATGCCCCGCGCCCACCGGAAGGAGCTGACTGGGTTGAAGGCTCTCAAGGGCATC

GGTCGAGATCCCGGTGCCTAATGAGTGAGCTAACTTACATTAATTGCGTTGCGCTCACTGCCCG
CTTTCCAGTCGGGAAACCTGTCGTGCCAGCTGCATTAATGAATCGGCCAACGCGCGGGGAGAG
GCGGTTTGCGTATTGGGCGCCAGGGTGGTTTTTCTTTTCACCAGTGAGACGGGCAACAGCTGAT
TGCCCTTCACCGCCTGGCCCTGAGAGAGTTGCAGCAAGCGGTCCACGCTGGTTTGCCCCAGCAG
GCGAAAATCCTGTTTGATGGTGGTTAACGGCGGGATATAACATGAGCTGTCTTCGGTATCGTCG
TATCCCACTACCGAGATATCCGCACCAACGCGCAGCCCGGACTCGGTAATGGCGCGCATTGCGC
CCAGCGCCATCTGATCGTTGGCAACCAGCATCGCAGTGGGAACGATGCCCTCATTCAGCATTTG
CATGGTTTGTTGAAAACCGGACATGGCACTCCAGTCGCCTTCCCGTTCCGCTATCGGCTGAATTT
GATTGCGAGTGAGATATTTATGCCAGCCAGCCAGACGCAGACGCGCCGAGACAGAACTTAATG
GGCCCGCTAACAGCGCGATTTGCTGGTGACCCAATGCGACCAGATGCTCCACGCCCAGTCGCGT
ACCGTCTTCATGGGAGAAAATAATACTGTTGATGGGTGTCTGGTCAGAGACATCAAGAAATAAC
GCCGGAACATTAGTGCAGGCAGCTTCCACAGCAATGGCATCCTGGTCATCCAGCGGATAGTTAA
TGATCAGCCCACTGACGCGTTGCGCGAGAAGATTGTGCACCGCCGCTTTACAGGCTTCGACGCC
GCTTCGTTCTACCATCGACACCACCACGCTGGCACCCAGTTGATCGGCGCGAGATTTAATCGCC
GCGACAATTTGCGACGGCGCGTGCAGGGCCAGACTGGAGGTGGCAACGCCAATCAGCAACGAC
TGTTTGCCCGCCAGTTGTTGTGCCACGCGGTTGGGAATGTAATTCAGCTCCGCCATCGCCGCTTC
CACTTTTTCCCGCGTTTTCGCAGAAACGTGGCTGGCCTGGTTCACCACGCGGGAAACGGTCTGA
TAAGAGACACCGGCATACTCTGCGACATCGTATAACGTTACTGGTTTCACATTCACCACCCTGA
ATTGACTCTCTTCCGGGCGCTATCATGCCATACCGCGAAAGGTTTTGCGCCATTCGATGGTGTCC
GGGATCTCGACGCTCTCCCTTATGCGACTCCTGCATTAGGAAGCAGCCCAGTAGTAGGTTGAGG
CCGTTGAGCACCGCCGCCGCAAGGAATGGTGCATGCAAGGAGATGGCGCCCAACAGTCCCCCG
GCCACGGGGCCTGCCACCATACCCACGCCGAAACAAGCGCTCATGAGCCCGAAGTGGCGAGCC
CGATCTTCCCCATCGGTGATGTCGGCGATATAGGCGCCAGCAACCGCACCTGTGGCGCCGGTGA
TGCCGGCCACGATGCGTCCGGCGTAGAGGATCGAGATCTCGATCCCGCGAAATTAATACGACTC
ACTATAGGGGAATTGTGAGCGGATAACAATTCCCCTCTAGAAATAATTTTGTTTAACTTTAAGA
AGGAGATATACATATGAAATACCTGCTGCCGACCGCTGCTGCTGGTCTGCTGCTCCTCGCTGCC
CAGCCGGCGATGGCCATGGGCCATCATCATCATCATCATCATCATCACAGCAGCGGCCATA
TCGACGACGACGACAAGCATATGAAGCTTATGGCCCAGCCGGCCATGGCCCAGGTGCAGCTGG
TGCAGTCTGGGGCTGAGGTGAAGAAGCCTGG\GTCCTCGGTGAGGGTCTCCTGCAAGGCTTCTG
GAGGCACCTTCAGCAGCTATGCTATCAGCTGGGTGCGACAGGCCCCTGGACAAGGGCTTGAGT
GGATGGGAGGGATCATCCCTATCTTTGGTACAGCAAACTACGCACAGAAGTTCCAGGGCAGAG
TCACGATTACCGCGGACGAATCCACGAGCACAGCCTACATGGAGCTGAGCAGCCTGAGATCTG
AGGACACGGCTGTGTATTACTGTGCAAGAGACCCGTTTCTTCACTATTGGGGCCAAGGTACCCT
GGTCACCGTCTCGAGTGGTGGAGGCGGTTCAGGCGGAGGTGGCTCTGGCGGTGGCGGATCGGA
AATTGAGCTCACTCAGTCTCCACTCTCCCTGCCCGTCACCCCTGGAGAGCCGGCCTCCATCTCCT
GCAGGTCTAGTCAGAGCCTCCTGCATAGTAATGGATACAACTATTTGGATTGGTACCTGCAGAA
GCCAGGGCAGTCTCCACAGCTCCTGATCTATTTGGGTTCTAATCGGGCCTCCGGGGTCCCTGAC
AGGTTCAGTGGCAGTGGATCAGGCACAGATTTTACACTGAAAATCAGCAGAGTGGAGGCTGAG
GATGTTGGGGTTTATTACTGCATGCAAGCTCTACAAACTTTCACTTTCGGCCCTGGGACCAAGGT
GGAGATCAAACGTGCGGCCGCAGAGCTCGCTTCCGGAGGTCCCGAGGGCGGCAGCCTGGCCGC
GCTGACCGCGCACCAGGCCTGCCACCTGCCGCTGGAGACTTTCACCCGTCATCGCCAGCCGCGC

GGCTGGGAACAACTGGAGCAGTGCGGCTATCCGGTGCAGCGGCTGGTCGCCCTCTACCTGGCG
GCGCGACTGTCATGGAACCAGGTCGACCAGGTGATCCGCAACGCCCTGGCCAGCCCCGGCAGC
GGCGGCGACCTGGGCGAAGCGATCCGCGAGCAGCCGGAGCAGGCCCGTCTCGCGCTGACCCTG
GCCGCCGCCGAGAGCGAGCGCTTCGTCCGGCAGGGCACCGGCAACGACGAGGCGGGAGCGGCC
AACGCCGACGTGGTGAGCCTGACCTGCCCGGTCGCCGCCGGTGAATGCGCGGGCCCGGCGGAC
AGCGGCGACGCCCTGCTGGAGCGCAACTATCCCACTGGCGCGGAGTTCCTCGGCGACGGCGGC
GACGTCAGCTTCAGCACCCGCGGCACGCAGAACTGGACGGTGGAGCGGCTGCTCCAGGCGCAC
CGCCAACTGGAGGAGCGCGGCTATGTGTTCGTCGGCTACCACGGCACCTTCCTCGAAGCGGCGC
AAAGCATCGTCTTCGGCGGGGTGCGCGCGCGCAGCCAGGACCTCGACGCGATCTGGCGCGGTTT
CTATATCGCCGGCGATCCGGCGCTGGCCTACGCCTACGCCCAGGACCAGGAACCCGACGCACG
CGGCCGGATCCGCAACGGTGCCCTGCTGCGGGTCTATGTGCCGCGCTCTAGCCTGCCGGGCTTC
TACCGCACCAGCCTGACCCTGGCCGCGCCGGAGGCGGCGGGCGAGGTCGAACGGCTGATCGGC
CATCCGCTGCCGCTGCGCCTGGACGCCATCACCGGCCCCGAGGAGGAAGGCGGGCGCCTGGAG
ACCATTCTCGGCTGGCCGCTGGCCGAGCGCACCGTGGTGATTCCCTCGGCGATCCCCACCGACC
CGCGCAACGTCGGCGGCGACCTCGACCCGTCCAGCATCCCCGACAAGGAACAGGCGATCAGCG
CCCTGCCGGACTACGCCAGCCAGCCCGGCAAACCGCCGCGCGAGGACCTGAAGTAACTGCCGC
GACCGGCCGGCTCCCTTCGCAGGAGCCGGCCTTCTCGGGGCCTGGCCATACATCAGGTTTTCCT
GATGCCAGCCCAATCGAATATGAATTTCGACGCTGAGCAATAACTAGCATAACCCCTTGGGGCC
TCTAAACGGGTCTTGAGGGGTTTTTTGCTGAAAGGAGGAACTATATCCGGAT

### *VI.3.2 PMT-anti-CSPG4(scFv)-ETA*

TGGCGAATGGGACGCGCCCTGTAGCGGCGCATTAAGCGCGGCGGGTGTGGTGGTTACGCGCAG
CGTGACCGCTACACTTGCCAGCGCCCTAGCGCCCGCTCCTTTCGCTTTCTTCCCTTCCTTTCTCGC
CACGTTCGCCGGCTTTCCCCGTCAAGCTCTAAATCGGGGGCTCCCTTTAGGGTTCCGATTTAGTG
CTTTACGGCACCTCGACCCCAAAAAACTTGATTAGGGTGATGGTTCACGTAGTGGGCCATCGCC
CTGATAGACGGTTTTTCGCCCTTTGACGTTGGAGTCCACGTTCTTTAATAGTGGACTCTTGTTCC
AAACTGGAACAACACTCAACCCTATCTCGGTCTATTCTTTTGATTTATAAGGGATTTTGCCGATT
TCGGCCTATTGGTTAAAAAATGAGCTGATTTAACAAAAATTTAACGCGAATTTTAACAAAATAT
TAACGTTTACAATTTCAGGTGGCACTTTTCGGGGAAATGTGCGCGGAACCCCTATTTGTTTATTT
TTCTAAATACATTCAAATATGTATCCGCTCATGAATTAATTCTTAGAAAAACTCATCGAGCATCA
AATGAAACTGCAATTTATTCATATCAGGATTATCAATACCATATTTTTGAAAAAGCCGTTTCTGT
AATGAAGGAGAAAACTCACCGAGGCAGTTCCATAGGATGGCAAGATCCTGGTATCGGTCTGCG
ATTCCGACTCGTCCAACATCAATACAACCTATTAATTTCCCCTCGTCAAAAATAAGGTTATCAA
GTGAGAAATCACCATGAGTGACGACTGAATCCGGTGAGAATGGCAAAAGTTTATGCATTTCTTT
CCAGACTTGTTCAACAGGCCAGCCATTACGCTCGTCATCAAAATCACTCGCATCAACCAAACCG
TTATTCATTCGTGATTGCGCCTGAGCGAGACGAAATACGCGATCGCTGTTAAAAGGACAATTAC
AAACAGGAATCGAATGCAACCGGCGCAGGAACACTGCCAGCGCATCAACAATATTTTCACCTG
AATCAGGATATTCTTCTAATACCTGGAATGCTGTTTTCCCGGGGATCGCAGTGGTGAGTAACCA
TGCATCATCAGGAGTACGGATAAAATGCTTGATGGTCGGAAGAGGCATAAATTCCGTCAGCCA
GTTTAGTCTGACCATCTCATCTGTAACATCATTGGCAACGCTACCTTTGCCATGTTTCAGAAACA

ACTCTGGCGCATCGGGCTTCCCATACAATCGATAGATTGTCGCACCTGATTGCCCGACATTATC
GCGAGCCCATTTATACCCATATAAATCAGCATCCATGTTGGAATTTAATCGCGGCCTAGAGCAA
GACGTTTCCCGTTGAATATGGCTCATAACACCCCTTGTATTACTGTTTATGTAAGCAGACAGTTT
TATTGTTCATGACCAAAATCCCTTAACGTGAGTTTTCGTTCCACTGAGCGTCAGACCCCGTAGAA
AAGATCAAAGGATCTTCTTGAGATCCTTTTTTTCTGCGCGTAATCTGCTGCTTGCAAACAAAAAA
ACCACCGCTACCAGCGGTGGTTTGTTTGCCGGATCAAGAGCTACCAACTCTTTTTCCGAAGGTA
ACTGGCTTCAGCAGAGCGCAGATACCAAATACTGTCCTTCTAGTGTAGCCGTAGTTAGGCCACC
ACTTCAAGAACTCTGTAGCACCGCCTACATACCTCGCTCTGCTAATCCTGTTACCAGTGGCTGCT
GCCAGTGGCGATAAGTCGTGTCTTACCGGGTTGGACTCAAGACGATAGTTACCGGATAAGGCGC
AGCGGTCGGGCTGAACGGGGGGTTCGTGCACACAGCCCAGCTTGGAGCGAACGACCTACACCG
AACTGAGATACCTACAGCGTGAGCTATGAGAAAGCGCCACGCTTCCCGAAGGGAGAAAGGCGG
ACAGGTATCCGGTAAGCGGCAGGGTCGGAACAGGAGAGCGCACGAGGGAGCTTCCAGGGGGA
AACGCCTGGTATCTTTATAGTCCTGTCGGGTTTCGCCACCTCTGACTTGAGCGTCGATTTTTGTG
ATGCTCGTCAGGGGGGCGGAGCCTATGGAAAAACGCCAGCAACGCGGCCTTTTTACGGTTCCTG
GCCTTTTGCTGGCCTTTTGCTCACATGTTCTTTCCTGCGTTATCCCCTGATTCTGTGGATAACCGT
ATTACCGCCTTTGAGTGAGCTGATACCGCTCGCCGCAGCCGAACGACCGAGCGCAGCGAGTCA
GTGAGCGAGGAAGCGGAAGAGCGCCTGATGCGGTATTTTCTCCTTACGCATCTGTGCGGTATTT
CACACCGCATATATGGTGCACTCTCAGTACAATCTGCTCTGATGCCGCATAGTTAAGCCAGTAT
ACACTCCGCTATCGCTACGTGACTGGGTCATGGCTGCGCCCCGACACCCGCCAACACCCGCTGA
CGCGCCCTGACGGGCTTGTCTGCTCCCGGCATCCGCTTACAGACAAGCTGTGACCGTCTCCGGG
AGCTGCATGTGTCAGAGGTTTTCACCGTCATCACCGAAACGCGCGAGGCAGCTGCGGTAAAGCT
CATCAGCGTGGTCGTGAAGCGATTCACAGATGTCTGCCTGTTCATCCGCGTCCAGCTCGTTGAG
TTTCTCCAGAAGCGTTAATGTCTGGCTTCTGATAAAGCGGGCCATGTTAAGGGCGGTTTTTTCCT
GTTTGGTCACTGATGCCTCCGTGTAAGGGGGATTTCTGTTCATGGGGGTAATGATACCGATGAA
ACGAGAGAGGATGCTCACGATACGGGTTACTGATGATGAACATGCCCGGTTACTGGAACGTTGT
GAGGGTAAACAACTGGCGGTATGGATGCGGCGGGACCAGAGAAAAATCACTCAGGGTCAATGC
CAGCGCTTCGTTAATACAGATGTAGGTGTTCCACAGGGTAGCCAGCAGCATCCTGCGATGCAGA
TCCGGAACATAATGGTGCAGGGCGCTGACTTCCGCGTTTCCAGACTTTACGAAACACGGAAACC
GAAGACCATTCATGTTGTTGCTCAGGTCGCAGACGTTTTGCAGCAGCAGTCGCTTCACGTTCGCT
CGCGTATCGGTGATTCATTCTGCTAACCAGTAAGGCAACCCCGCCAGCCTAGCCGGGTCCTCAA
CGACAGGAGCACGATCATGCGCACCCGTGGGGCCGCCATGCCGGCGATAATGGCCTGCTTCTCG
CCGAAACGTTTGGTGGCGGGACCAGTGACGAAGGCTTGAGCGAGGGCGTGCAAGATTCCGAAT
ACCGCAAGCGACAGGCCGATCATCGTCGCGCTCCAGCGAAAGCGGTCCTCGCCGAAAATGACC
CAGAGCGCTGCCGGCACCTGTCCTACGAGTTGCATGATAAAGAAGACAGTCATAAGTGCGGCG
ACGATAGTCATGCCCCGCGCCCACCGGAAGGAGCTGACTGGGTTGAAGGCTCTCAAGGGCATC
GGTCGAGATCCCGGTGCCTAATGAGTGAGCTAACTTACATTAATTGCGTTGCGCTCACTGCCCG
CTTTCCAGTCGGGAAACCTGTCGTGCCAGCTGCATTAATGAATCGGCCAACGCGCGGGGAGAG
GCGGTTTGCGTATTGGGCGCCAGGGTGGTTTTTCTTTTCACCAGTGAGACGGGCAACAGCTGAT
TGCCCTTCACCGCCTGGCCCTGAGAGAGTTGCAGCAAGCGGTCCACGCTGGTTTGCCCCAGCAG
GCGAAAATCCTGTTTGATGGTGGTTAACGGCGGGATATAACATGAGCTGTCTTCGGTATCGTCG
TATCCCACTACCGAGATATCCGCACCAACGCGCAGCCCGGACTCGGTAATGGCGCGCATTGCGC

CCAGCGCCATCTGATCGTTGGCAACCAGCATCGCAGTGGGAACGATGCCCTCATTCAGCATTTG
CATGGTTTGTTGAAAACCGGACATGGCACTCCAGTCGCCTTCCCGTTCCGCTATCGGCTGAATTT
GATTGCGAGTGAGATATTTATGCCAGCCAGCCAGACGCAGACGCGCCGAGACAGAACTTAATG
GGCCCGCTAACAGCGCGATTTGCTGGTGACCCAATGCGACCAGATGCTCCACGCCCAGTCGCGT
ACCGTCTTCATGGGAGAAAATAATACTGTTGATGGGTGTCTGGTCAGAGACATCAAGAAATAAC
GCCGGAACATTAGTGCAGGCAGCTTCCACAGCAATGGCATCCTGGTCATCCAGCGGATAGTTAA
TGATCAGCCCACTGACGCGTTGCGCGAGAAGATTGTGCACCGCCGCTTTACAGGCTTCGACGCC
GCTTCGTTCTACCATCGACACCACCACGCTGGCACCCAGTTGATCGGCGCGAGATTTAATCGCC
GCGACAATTTGCGACGGCGCGTGCAGGGCCAGACTGGAGGTGGCAACGCCAATCAGCAACGAC
TGTTTGCCCGCCAGTTGTTGTGCCACGCGGTTGGGAATGTAATTCAGCTCCGCCATCGCCGCTTC
CACTTTTTCCCGCGTTTTCGCAGAAACGTGGCTGGCCTGGTTCACCACGCGGGAAACGGTCTGA
TAAGAGACACCGGCATACTCTGCGACATCGTATAACGTTACTGGTTTCACATTCACCACCCTGA
ATTGACTCTCTTCCGGGCGCTATCATGCCATACCGCGAAAGGTTTTGCGCCATTCGATGGTGTCC
GGGATCTCGACGCTCTCCCTTATGCGACTCCTGCATTAGGAAGCAGCCCAGTAGTAGGTTGAGG
CCGTTGAGCACCGCCGCCGCAAGGAATGGTGCATGCAAGGAGATGGCGCCCAACAGTCCCCCG
GCCACGGGGCCTGCCACCATACCCACGCCGAAACAAGCGCTCATGAGCCCGAAGTGGCGAGCC
CGATCTTCCCCATCGGTGATGTCGGCGATATAGGCGCCAGCAACCGCACCTGTGGCGCCGGTGA
TGCCGGCCACGATGCGTCCGGCGTAGAGGATCGAGATCTCGATCCCGCGAAATTAATACGACTC
ACTATAGGGGAATTGTGAGCGGATAACAATTCCCCTCTAGAAATAATTTTGTTTAACTTTAAGA
AGGAGATATACATATGAAATACCTGCTGCCGACCGCTGCTGCTGGTCTGCTGCTCCTCGCTGCC
CAGCCGGCGATGGCCATGGGCCATCATCATCATCATCATCATCATCATCACAGCAGCGGCCATA
TCGACGACGACGACAAGCATATGAAGCTTATGGCCCAGCCGGCCATGGCCCAGGTGAAACTGC
AGCAGTCTGGACCTGAGCTGGTGAAGCCTGGGGCCTCAGTGAAGATTTCCTGCAAAGCTTCTGG
CTACGCATTCAGTAGGTCTTGGATGAACTGGGTGAAGCAGAGGCCTGGACAGGGTCTTGAGTG
GATTGGACGGATTTATCCTGGAGATGGAGATACTAACTACAATGGGAAGTTCAAGGGCAAGGC
CACACTGACTGCAGACAAATCCTCCAGCACAGCCTACATGCAGGTCAGCAGCCTGACCTCTGTG
GACTCTGCGGTCTATTTCTGTGCAAGAGGGAATACGGTAGTAGTTCCCTATACTATGGACTACT
GGGGTCAAGGAACCACCGTGACCGTGAGTTCGGGTGGCGGTGGATCCGGTGGTGGCGGCAGCG
GTGGTGGCGGCAGCGATATTGAACTGACGCAATCTCCAGCTTCTTTGGCTGTGTCTCTAGGGCA
GAGGGCCACCATATCCTGCAGAGCCAGTGAAAGTGTTGATAGTTATGGCAATAGTTTTATGCAC
TGGTACCAGCAGAAACCAGGACAGCCACCCAAACTCCTCATCTATCTTGCATCCAACCTAGAAT
CTGGGGTCCCTGCCAGGTTCAGTGGCAGTGGATCTAGGACAGACTTCACCCTCACCATTGATCC
TGTGGAGGCTGATGATGCTGCAACCTATTACTGTCAACAAAATAATGAAGACCCTCTGACGTTT
GGCGGCGGGACCAAGCTGGAACTGAAACGGGCGGCCGCAGAGCTCGCTTCCGGAGGTCCCGAG
GGCGGCAGCCTGGCCGCGCTGACCGCGCACCAGGCCTGCCACCTGCCGCTGGAGACTTTCACCC
GTCATCGCCAGCCGCGCGGCTGGGAACAACTGGAGCAGTGCGGCTATCCGGTGCAGCGGCTGG
TCGCCCTCTACCTGGCGGCGCGACTGTCATGGAACCAGGTCGACCAGGTGATCCGCAACGCCCT
GGCCAGCCCCGGCAGCGGCGGCGACCTGGGCGAAGCGATCCGCGAGCAGCCGGAGCAGGCCC
GTCTCGCGCTGACCCTGGCCGCCGCCGAGAGCGAGCGCTTCGTCCGGCAGGGCACCGGCAACG
ACGAGGCGGGAGCGGCCAACGCCGACGTGGTGAGCCTGACCTGCCCGGTCGCCGCCGGTGAAT
GCGCGGGCCCGGCGGACAGCGGCGACGCCCTGCTGGAGCGCAACTATCCCACTGGCGCGGAGT

TCCTCGGCGACGGCGGCGACGTCAGCTTCAGCACCCGCGGCACGCAGAACTGGACGGTGGAGC
GGCTGCTCCAGGCGCACCGCCAACTGGAGGAGCGCGGCTATGTGTTCGTCGGCTACCACGGCAC
CTTCCTCGAAGCGGCGCAAAGCATCGTCTTCGGCGGGGTGCGCGCGCGCAGCCAGGACCTCGA
CGCGATCTGGCGCGGTTTCTATATCGCCGGCGATCCGGCGCTGGCCTACGCCTACGCCCAGGAC
CAGGAACCCGACGCACGCGGCCGGATCCGCAACGGTGCCCTGCTGCGGGTCTATGTGCCGCGCT
CTAGCCTGCCGGGCTTCTACCGCACCAGCCTGACCCTGGCCGCGCCGGAGGCGGCGGGCGAGG
TCGAACGGCTGATCGGCCATCCGCTGCCGCTGCGCCTGGACGCCATCACCGGCCCCGAGGAGG
AAGGCGGGCGCCTGGAGACCATTCTCGGCTGGCCGCTGGCCGAGCGCACCGTGGTGATTCCCTC
GGCGATCCCCACCGACCCGCGCAACGTCGGCGGCGACCTCGACCCGTCCAGCATCCCCGACAA
GGAACAGGCGATCAGCGCCCTGCCGGACTACGCCAGCCAGCCCGGCAAACCGCCGCGCGAGGA
CCTGAAGTAACTGCCGCGACCGGCCGGCTCCCTTCGCAGGAGCCGGCCTTCTCGGGGCCTGGCC
ATACATCAGGTTTTCCTGATGCCAGCCCAATCGAATATGAATTTCGACGCTGAGCAATAACTAG
CATAACCCCTTGGGGCCTCTAAACGGGTCTTGAGGGGTTTTTTGCTGAAAGGAGGAACTATATC
CGGAT

### *VI.3.3 PMS-L-EGB-anti-EPCAM(scFv)-IV_R201K*

GACGGATCGGGAGATCTCCCGATCCCCTATGGTCGACTCTCAGTACAATCTGCTCTGATGCCGC
ATAGTTAAGCCAGTATCTGCTCCCTGCTTGTGTGTTGGAGGTCGCTGAGTAGTGCGCGAGCAAA
ATTTAAGCTACAACAAGGCAAGGCTTGACCGACAATTGCATGAAGAATCTGCTTAGGGTTAGGC
GTTTTGCGCTGCTTCGCGATGTACGGGCCAGATATACGCGTTGACATTGATTATTGACTAGTTAT
TAATAGTAATCAATTACGGGGTCATTAGTTCATAGCCCATATATGGAGTTCCGCGTTACATAAC
TTACGGTAAATGGCCCGCCTGGCTGACCGCCCAACGACCCCCGCCCATTGACGTCAATAATGAC
GTATGTTCCCATAGTAACGCCAATAGGGACTTTCCATTGACGTCAATGGGTGGACTATTTACGG
TAAACTGCCCACTTGGCAGTACATCAAGTGTATCATATGCCAAGTACGCCCCCTATTGACGTCA
ATGACGGTAAATGGCCCGCCTGGCATTATGCCCAGTACATGACCTTATGGGACTTTCCTACTTG
GCAGTACATCTACGTATTAGTCATCGCTATTACCATGGTGATGCGGTTTTGGCAGTACATCAATG
GGCGTGGATAGCGGTTTGACTCACGGGGATTTCCAAGTCTCCACCCCATTGACGTCAATGGGAG
TTTGTTTTGGCACCAAAATCAACGGGACTTTCCAAAATGTCGTAACAACTCCGCCCCATTGACG
CAAATGGGCGGTAGGCGTGTACGGTGGGAGGTCTATATAAGCAGAGCTCTCTGGCTAACTAGA
GAACCCACTGCTTACTGGCTTATCGAAATTAATACGACTCACTATAGGGAGACCCAAGCTGGCT
AGCCACCATGGAGACAGACACACTCCTGCTATGGGTACTGCTGCTCTGGGTTCCAGGTTCCACT
GGTGACTCTAGACATATCGACGACGACGACAAGATCATCGGGGGACATGAGGCCAAGCCCCAC
TCCCGCCCCTACATGGCTTTTCTTATGATCTGGGATCAGAAGTCTCTGAAGAGGTGCGGTGGCTT
CCTGATACGAGACGACTTCGTGCTGACAGCTGCTCACTGTTGGGGAAGCTCCATAAATGTCACC
TTGGGGGCCCACAATATCAAGGAACAGGAGCCGACCCAGCAGTTTATCCCTGTGAAAAGAGCC
ATCCCCCATCCAGCCTATAATCCTAAGAACTTCTCCAATGACATCATGCTACTGCAGCTGGAGA
GAAAGGCCAAGCGGACCAGAGCTGTGCAGCCCCTCAGGCTACCTAGCAACAAGGCCCAGGTGA
AGCCAGGGCAGACATGCAGTGTGGCCGGCTGGGGGCAGACGGCCCCCCTGGGAAAACACTCAC
ACACACTACAAGAGGTGAAGATGACAGTGCAGGAAGATCGAAAGTGCGAATCTGACTTACGCC
ATTATTACGACAGTACCATTGAGTTGTGCGTGGGGGACCCAGAGATTAAAAAGACTTCCTTTAA

GGGGGACTCTGGAGGCCCTCTTGTGTGTAACAAGGTGGCCCAGGGCATTGTCTCCTATGGAAAA
AACAATGGCATGCCTCCACGAGCCTGCACCAAAGTCTCAAGCTTTGTACACTGGATAAAGAAA
ACCATGAAACGCTACGGATCCAAACTAGCTGAGCACGAAGGTGACGCGGCCCAGCCGGCCATG
GCCCAGGTGCAGCTGGTGCAGTCTGGGGCTGAGGTGAAGAAGCCTGGGTCCTCGGTGAGGGTC
TCCTGCAAGGCTTCTGGAGGCACCTTCAGCAGCTATGCTATCAGCTGGGTGCGACAGGCCCCTG
GACAAGGGCTTGAGTGGATGGGAGGGATCATCCCTATCTTTGGTACAGCAAACTACGCACAGA
AGTTCCAGGGCAGAGTCACGATTACCGCGGACGAATCCACGAGCACAGCCTACATGGAGCTGA
GCAGCCTGAGATCTGAGGACACGGCTGTGTATTACTGTGCAAGAGACCCGTTTCTTCACTATTG
GGGCCAAGGTACCCTGGTCACCGTCTCGAGTGGTGGAGGCGGTTCAGGCGGAGGTGGCTCTGG
CGGTGGCGGATCGGAAATTGAGCTCACTCAGTCTCCACTCTCCCTGCCCGTCACCCCTGGAGAG
CCGGCCTCCATCTCCTGCAGGTCTAGTCAGAGCCTCCTGCATAGTAATGGATACAACTATTTGG
ATTGGTACCTGCAGAAGCCAGGGCAGTCTCCACAGCTCCTGATCTATTTGGGTTCTAATCGGGC
CTCCGGGGTCCCTGACAGGTTCAGTGGCAGTGGATCAGGCACAGATTTTACACTGAAAATCAGC
AGAGTGGAGGCTGAGGATGTTGGGGTTTATTACTGCATGCAAGCTCTACAAACTTTCACTTTCG
GCCCTGGGACCAAGGTGGAGATCAAACGTGCGGCCGCAGGGCCCCATCATCATCATCATCATTG
AGTTTAATTCTGGAATTAATTCGCTGTCTGCGAGGGCCAGCTGTTGGGGTGAGTACTCCCTCTCA
AAAGCGGGCATGACTTCTGCGCTAAGATTGTCAGTTTCCAAAAACGAGGAGGATTTGATATTCA
CCTGGCCCGCGGTGATGCCTTTGAGGGTGGCCGCGTCCATCTGGTCAGAAAAGACAATCTTTTT
GTTGTCAAGCTTGAGGTGTGGCAGGCTTGAGATCTGGCCATACACTTGAGTGACAATGACATCC
ACTTTGCCTTTCTCTCCACAGGTGTCCACTCCCAGGTCCAACTGCAGGTCGAGCATGCATCTAGG
GCGGCCAATTCCGCCCCTCTCCCTCCCCCCCCCCTAACGTTACTGGCCGAAGCCGCTTGGAATA
AGGCCGGTGTGCGTTTGTCTATATGTGATTTTCCACCATATTGCCGTCTTTTGGCAATGTGAGGG
CCCGGAAACCTGGCCCTGTCTTCTTGACGAGCATTCCTAGGGGTCTTTCCCCTCTCGCCAAAGGA
ATGCAAGGTCTGTTGAATGTCGTGAAGGAAGCAGTTCCTCTGGAAGCTTCTTGAAGACAAACAA
CGTCTGTAGCGACCCTTTGCAGGCAGCGGAACCCCCCACCTGGCGACAGGTGCCTCTGCGGCCA
AAAGCCACGTGTATAAGATACACCTGCAAAGGCGGCACAACCCCAGTGCCACGTTGTGAGTTG
GATAGTTGTGGAAAGAGTCAAATGGCTCTCCTCAAGCGTATTCAACAAGGGGCTGAAGGATGC
CCAGAAGGTACCCCATTGTATGGGATCTGATCTGGGGCCTCGGTGCACATGCTTTACATGTGTTT
AGTCGAGGTTAAAAAAACGTCTAGGCCCCCCGAACCACGGGGACGTGGTTTTCCTTTGAAAAAC
ACGATGATAAGCTTGCCACAACCCGGGATCCACCGGTCGCCACCATGGTGAGCAAGGGCGAGG
AGCTGTTCACCGGGGTGGTGCCCATCCTGGTCGAGCTGGACGGCGACGTAAACGGCCACAAGTT
CAGCGTGTCCGGCGAGGGCGAGGGCGATGCCACCTACGGCAAGCTGACCCTGAAGTTCATCTG
CACCACCGGCAAGCTGCCCGTGCCCTGGCCCACCCTCGTGACCACCCTGACCTACGGCGTGCAG
TGCTTCAGCCGCTACCCCGACCACATGAAGCAGCACGACTTCTTCAAGTCCGCCATGCCCGAAG
GCTACGTCCAGGAGCGCACCATCTTCTTCAAGGACGACGGCAACTACAAGACCCGCGCCGAGG
TGAAGTTCGAGGGCGACACCCTGGTGAACCGCATCGAGCTGAAGGGCATCGACTTCAAGGAGG
ACGGCAACATCCTGGGGCACAAGCTGGAGTACAACTACAACAGCCACAACGTCTATATCATGG
CCGACAAGCAGAAGAACGGCATCAAGGTGAACTTCAAGATCCGCCACAACATCGAGGACGGCA
GCGTGCAGCTCGCCGACCACTACCAGCAGAACACCCCCATCGGCGACGGCCCCGTGCTGCTGCC
CGACAACCACTACCTGAGCACCCAGTCCGCCCTGAGCAAAGACCCCAACGAGAAGCGCGATCA
CATGGTCCTGCTGGAGTTCGTGACCGCCGCCGGGATCACTCTCGGCATGGACGAGCTGTACAAG

TAAGTTTAAACCCGCTGATCAGCCTCGACTGTGCCTTCTAGTTGCCAGCCATCTGTTGTTTGCCC
CTCCCCCGTGCCTTCCTTGACCCTGGAAGGTGCCACTCCCACTGTCCTTTCCTAATAAAATGAGG
AAATTGCATCGCATTGTCTGAGTAGGTGTCATTCTATTCTGGGGGGTGGGGTGGGGCAGGACAG
CAAGGGGGAGGATTGGGAAGACAATAGCAGGCATGCTGGGGATGCGGTGGGCTCTATGGCTTC
TGAGGCGGAAAGAACCAGCTGGGGCTCTAGGGGGTATCCCCACGCGCCCTGTAGCGGCGCATT
AAGCGCGGCGGGTGTGGTGGTTACGCGCAGCGTGACCGCTACACTTGCCAGCGCCCTAGCGCCC
GCTCCTTTCGCTTTCTTCCCTTCCTTTCTCGCCACGTTCGCCGGCTTTCCCCGTCAAGCTCTAAAT
CGGGGCATCCCTTTAGGGTTCCGATTTAGTGCTTTACGGCACCTCGACCCCAAAAAACTTGATT
AGGGTGATGGTTCACGTAGTGGGCCATCGCCCTGATAGACGGTTTTTCGCCCTTTGACGTTGGA
GTCCACGTTCTTTAATAGTGGACTCTTGTTCCAAACTGGAACAACACTCAACCCTATCTCGGTCT
ATTCTTTTGATTTATAAGGGATTTTGGGGATTTCGGCCTATTGGTTAAAAAATGAGCTGATTTAA
CAAAAATTTAACGCGAATTAATTCTGTGGAATGTGTGTCAGTTAGGGTGTGGAAAGTCCCCAGG
CTCCCCAGCAGGCAGAAGTATGCAAAGCATGCATCTCAATTAGTCAGCAACCAGGTGTGGAAA
GTCCCCAGGCTCCCCAGCAGGCAGAAGTATGCAAAGCATGCATCTCAATTAGTCAGCAACCATA
GTCCCGCCCCTAACTCCGCCCATCCCGCCCCTAACTCCGCCCAGTTCCGCCCATTCTCCGCCCCA
TGGCTGACTAATTTTTTTTATTTATGCAGAGGCCGAGGCCGCCTCTGCCTCTGAGCTATTCCAGA
AGTAGTGAGGAGGCTTTTTTGGAGGCCTAGGCTTTTGCAAAAAGCTCCCGGGAGCTTGTATATC
CATTTTCGGATCTGATCAGCACGTGTTGACAATTAATCATCGGCATAGTATATCGGCATAGTAT
AATACGACAAGGTGAGGAACTAAACCATGGCCAAGTTGACCAGTGCCGTTCCGGTGCTCACCG
CGCGCGACGTCGCCGGAGCGGTCGAGTTCTGGACCGACCGGCTCGGGTTCTCCCGGGACTTCGT
GGAGGACGACTTCGCCGGTGTGGTCCGGGACGACGTGACCCTGTTCATCAGCGCGGTCCAGGA
CCAGGTGGTGCCGGACAACACCCTGGCCTGGGTGTGGGTGCGCGGCCTGGACGAGCTGTACGC
CGAGTGGTCGGAGGTCGTGTCCACGAACTTCCGGGACGCCTCCGGGCCGGCCATGACCGAGAT
CGGCGAGCAGCCGTGGGGGCGGGAGTTCGCCCTGCGCGACCCGGCCGGCAACTGCGTGCACTT
CGTGGCCGAGGAGCAGGACTGACACGTGCTACGAGATTTCGATTCCACCGCCGCCTTCTATGAA
AGGTTGGGCTTCGGAATCGTTTTCCGGGACGCCGGCTGGATGATCCTCCAGCGCGGGGATCTCA
TGCTGGAGTTCTTCGCCCACCCCAACTTGTTTATTGCAGCTTATAATGGTTACAAATAAAGCAAT
AGCATCACAAATTTCACAAATAAAGCATTTTTTTCACTGCATTCTAGTTGTGGTTTGTCCAAACT
CATCAATGTATCTTATCATGTCTGTATACCGTCGACCTCTAGCTAGAGCTTGGCGTAATCATGGT
CATAGCTGTTTCCTGTGTGAAATTGTTATCCGCTCACAATTCCACACAACATACGAGCCGGAAG
CATAAAGTGTAAAGCCTGGGGTGCCTAATGAGTGAGCTAACTCACATTAATTGCGTTGCGCTCA
CTGCCCGCTTTCCAGTCGGGAAACCTGTCGTGCCAGCTGCATTAATGAATCGGCCAACGCGCGG
GGAGAGGCGGTTTGCGTATTGGGCGCTCTTCCGCTTCCTCGCTCACTGACTCGCTGCGCTCGGTC
GTTCGGCTGCGGCGAGCGGTATCAGCTCACTCAAAGGCGGTAATACGGTTATCCACAGAATCAG
GGGATAACGCAGGAAAGAACATGTGAGCAAAAGGCCAGCAAAAGGCCAGGAACCGTAAAAAG
GCCGCGTTGCTGGCGTTTTTCCATAGGCTCCGCCCCCCTGACGAGCATCACAAAAATCGACGCT
CAAGTCAGAGGTGGCGAAACCCGACAGGACTATAAAGATACCAGGCGTTTCCCCCTGGAAGCT
CCCTCGTGCGCTCTCCTGTTCCGACCCTGCCGCTTACCGGATACCTGTCCGCCTTTCTCCCTTCGG
GAAGCGTGGCGCTTTCTCAATGCTCACGCTGTAGGTATCTCAGTTCGGTGTAGGTCGTTCGCTCC
AAGCTGGGCTGTGTGCACGAACCCCCCGTTCAGCCCGACCGCTGCGCCTTATCCGGTAACTATC
GTCTTGAGTCCAACCCGGTAAGACACGACTTATCGCCACTGGCAGCAGCCACTGGTAACAGGAT

TAGCAGAGCGAGGTATGTAGGCGGTGCTACAGAGTTCTTGAAGTGGTGGCCTAACTACGGCTAC
ACTAGAAGGACAGTATTTGGTATCTGCGCTCTGCTGAAGCCAGTTACCTTCGGAAAAAGAGTTG
GTAGCTCTTGATCCGGCAAACAAACCACCGCTGGTAGCGGTGGTTTTTTTGTTTGCAAGCAGCA
GATTACGCGCAGAAAAAAAGGATCTCAAGAAGATCCTTTGATCTTTTCTACGGGGTCTGACGCT
CAGTGGAACGAAAACTCACGTTAAGGGATTTTGGTCATGAGATTATCAAAAAGGATCTTCACCT
AGATCCTTTTAAATTAAAAATGAAGTTTTAAATCAATCTAAAGTATATATGAGTAAACTTGGTC
TGACAGTTACCAATGCTTAATCAGTGAGGCACCTATCTCAGCGATCTGTCTATTTCGTTCATCCA
TAGTTGCCTGACTCCCCGTCGTGTAGATAACTACGATACGGGAGGGCTTACCATCTGGCCCCAG
TGCTGCAATGATACCGCGAGACCCACGCTCACCGGCTCCAGATTTATCAGCAATAAACCAGCCA
GCCGGAAGGGCCGAGCGCAGAAGTGGTCCTGCAACTTTATCCGCCTCCATCCAGTCTATTAATT
GTTGCCGGGAAGCTAGAGTAAGTAGTTCGCCAGTTAATAGTTTGCGCAACGTTGTTGCCATTGC
TACAGGCATCGTGGTGTCACGCTCGTCGTTTGGTATGGCTTCATTCAGCTCCGGTTCCCAACGAT
CAAGGCGAGTTACATGATCCCCCATGTTGTGCAAAAAAGCGGTTAGCTCCTTCGGTCCTCCGAT
CGTTGTCAGAAGTAAGTTGGCCGCAGTGTTATCACTCATGGTTATGGCAGCACTGCATAATTCT
CTTACTGTCATGCCATCCGTAAGATGCTTTTCTGTGACTGGTGAGTACTCAACCAAGTCATTCTG
AGAATAGTGTATGCGGCGACCGAGTTGCTCTTGCCCGGCGTCAATACGGGATAATACCGCGCCA
CATAGCAGAACTTTAAAAGTGCTCATCATTGGAAAACGTTCTTCGGGGCGAAAACTCTCAAGGA
TCTTACCGCTGTTGAGATCCAGTTCGATGTAACCCACTCGTGCACCCAACTGATCTTCAGCATCT
TTTACTTTCACCAGCGTTTCTGGGTGAGCAAAAACAGGAAGGCAAAATGCCGCAAAAAAGGGA
ATAAGGGCGACACGGAAATGTTGAATACTCATACTCTTCCTTTTTCAATATTATTGAAGCATTTA
TCAGGGTTATTGTCTCATGAGCGGATACATATTTGAATGTATTTAGAAAAATAAACAAATAGGG
GTTCCGCGCACATTTCCCCGAAAAGTGCCACCTGACGTC

### *VI.3.4 pET-STREP-anti-CSPG4(ScFv)-ETA-KDEL*

TGGCGAATGGGACGCGCCCTGTAGCGGCGCATTAAGCGCGGCGGGTGTGGTGGTTACGCGCAG
CGTGACCGCTACACTTGCCAGCGCCCTAGCGCCCGCTCCTTTCGCTTTCTTCCCTTCCTTTCTCGC
CACGTTCGCCGGCTTTCCCCGTCAAGCTCTAAATCGGGGGCTCCCTTTAGGGTTCCGATTTAGTG
CTTTACGGCACCTCGACCCCAAAAAACTTGATTAGGGTGATGGTTCACGTAGTGGGCCATCGCC
CTGATAGACGGTTTTTCGCCCTTTGACGTTGGAGTCCACGTTCTTTAATAGTGGACTCTTGTTCC
AAACTGGAACAACACTCAACCCTATCTCGGTCTATTCTTTTGATTTATAAGGGATTTTGCCGATT
TCGGCCTATTGGTTAAAAAATGAGCTGATTTAACAAAAATTTAACGCGAATTTTAACAAAATAT
TAACGTTTACAATTTCAGGTGGCACTTTTCGGGGAAATGTGCGCGGAACCCCTATTTGTTTATTT
TTCTAAATACATTCAAATATGTATCCGCTCATGAATTAATTCTTAGAAAAACTCATCGAGCATCA
AATGAAACTGCAATTTATTCATATCAGGATTATCAATACCATATTTTTGAAAAAGCCGTTTCTGT
AATGAAGGAGAAAACTCACCGAGGCAGTTCCATAGGATGGCAAGATCCTGGTATCGGTCTGCG
ATTCCGACTCGTCCAACATCAATACAACCTATTAATTTCCCCTCGTCAAAAATAAGGTTATCAA
GTGAGAAATCACCATGAGTGACGACTGAATCCGGTGAGAATGGCAAAAGTTTATGCATTTCTTT
CCAGACTTGTTCAACAGGCCAGCCATTACGCTCGTCATCAAAATCACTCGCATCAACCAAACCG
TTATTCATTCGTGATTGCGCCTGAGCGAGACGAAATACGCGATCGCTGTTAAAAGGACAATTAC
AAACAGGAATCGAATGCAACCGGCGCAGGAACACTGCCAGCGCATCAACAATATTTTCACCTG

AATCAGGATATTCTTCTAATACCTGGAATGCTGTTTTCCCGGGGATCGCAGTGGTGAGTAACCA
TGCATCATCAGGAGTACGGATAAAATGCTTGATGGTCGGAAGAGGCATAAATTCCGTCAGCCA
GTTTAGTCTGACCATCTCATCTGTAACATCATTGGCAACGCTACCTTTGCCATGTTTCAGAAACA
ACTCTGGCGCATCGGGCTTCCCATACAATCGATAGATTGTCGCACCTGATTGCCCGACATTATC
GCGAGCCCATTTATACCCATATAAATCAGCATCCATGTTGGAATTTAATCGCGGCCTAGAGCAA
GACGTTTCCCGTTGAATATGGCTCATAACACCCCTTGTATTACTGTTTATGTAAGCAGACAGTTT
TATTGTTCATGACCAAAATCCCTTAACGTGAGTTTTCGTTCCACTGAGCGTCAGACCCCGTAGAA
AAGATCAAAGGATCTTCTTGAGATCCTTTTTTTCTGCGCGTAATCTGCTGCTTGCAAACAAAAAA
ACCACCGCTACCAGCGGTGGTTTGTTTGCCGGATCAAGAGCTACCAACTCTTTTTCCGAAGGTA
ACTGGCTTCAGCAGAGCGCAGATACCAAATACTGTCCTTCTAGTGTAGCCGTAGTTAGGCCACC
ACTTCAAGAACTCTGTAGCACCGCCTACATACCTCGCTCTGCTAATCCTGTTACCAGTGGCTGCT
GCCAGTGGCGATAAGTCGTGTCTTACCGGGTTGGACTCAAGACGATAGTTACCGGATAAGGCGC
AGCGGTCGGGCTGAACGGGGGGTTCGTGCACACAGCCCAGCTTGGAGCGAACGACCTACACCG
AACTGAGATACCTACAGCGTGAGCTATGAGAAAGCGCCACGCTTCCCGAAGGGAGAAAGGCGG
ACAGGTATCCGGTAAGCGGCAGGGTCGGAACAGGAGAGCGCACGAGGGAGCTTCCAGGGGGA
AACGCCTGGTATCTTTATAGTCCTGTCGGGTTTCGCCACCTCTGACTTGAGCGTCGATTTTTGTG
ATGCTCGTCAGGGGGGCGGAGCCTATGGAAAAACGCCAGCAACGCGGCCTTTTTACGGTTCCTG
GCCTTTTGCTGGCCTTTTGCTCACATGTTCTTTCCTGCGTTATCCCCTGATTCTGTGGATAACCGT
ATTACCGCCTTTGAGTGAGCTGATACCGCTCGCCGCAGCCGAACGACCGAGCGCAGCGAGTCA
GTGAGCGAGGAAGCGGAAGAGCGCCTGATGCGGTATTTTCTCCTTACGCATCTGTGCGGTATTT
CACACCGCATATATGGTGCACTCTCAGTACAATCTGCTCTGATGCCGCATAGTTAAGCCAGTAT
ACACTCCGCTATCGCTACGTGACTGGGTCATGGCTGCGCCCCGACACCCGCCAACACCCGCTGA
CGCGCCCTGACGGGCTTGTCTGCTCCCGGCATCCGCTTACAGACAAGCTGTGACCGTCTCCGGG
AGCTGCATGTGTCAGAGGTTTTCACCGTCATCACCGAAACGCGCGAGGCAGCTGCGGTAAAGCT
CATCAGCGTGGTCGTGAAGCGATTCACAGATGTCTGCCTGTTCATCCGCGTCCAGCTCGTTGAG
TTTCTCCAGAAGCGTTAATGTCTGGCTTCTGATAAAGCGGGCCATGTTAAGGGCGGTTTTTTCCT
GTTTGGTCACTGATGCCTCCGTGTAAGGGGGATTTCTGTTCATGGGGGTAATGATACCGATGAA
ACGAGAGAGGATGCTCACGATACGGGTTACTGATGATGAACATGCCCGGTTACTGGAACGTTGT
GAGGGTAAACAACTGGCGGTATGGATGCGGCGGGACCAGAGAAAAATCACTCAGGGTCAATGC
CAGCGCTTCGTTAATACAGATGTAGGTGTTCCACAGGGTAGCCAGCAGCATCCTGCGATGCAGA
TCCGGAACATAATGGTGCAGGGCGCTGACTTCCGCGTTTCCAGACTTTACGAAACACGGAAACC
GAAGACCATTCATGTTGTTGCTCAGGTCGCAGACGTTTTGCAGCAGCAGTCGCTTCACGTTCGCT
CGCGTATCGGTGATTCATTCTGCTAACCAGTAAGGCAACCCCGCCAGCCTAGCCGGGTCCTCAA
CGACAGGAGCACGATCATGCGCACCCGTGGGGCCGCCATGCCGGCGATAATGGCCTGCTTCTCG
CCGAAACGTTTGGTGGCGGGACCAGTGACGAAGGCTTGAGCGAGGGCGTGCAAGATTCCGAAT
ACCGCAAGCGACAGGCCGATCATCGTCGCGCTCCAGCGAAAGCGGTCCTCGCCGAAAATGACC
CAGAGCGCTGCCGGCACCTGTCCTACGAGTTGCATGATAAAGAAGACAGTCATAAGTGCGGCG
ACGATAGTCATGCCCCGCGCCCACCGGAAGGAGCTGACTGGGTTGAAGGCTCTCAAGGGCATC
GGTCGAGATCCCGGTGCCTAATGAGTGAGCTAACTTACATTAATTGCGTTGCGCTCACTGCCCG
CTTTCCAGTCGGGAAACCTGTCGTGCCAGCTGCATTAATGAATCGGCCAACGCGCGGGGAGAG
GCGGTTTGCGTATTGGGCGCCAGGGTGGTTTTTCTTTTCACCAGTGAGACGGGCAACAGCTGAT

TGCCCTTCACCGCCTGGCCCTGAGAGAGTTGCAGCAAGCGGTCCACGCTGGTTTGCCCCAGCAG
GCGAAAATCCTGTTTGATGGTGGTTAACGGCGGGATATAACATGAGCTGTCTTCGGTATCGTCG
TATCCCACTACCGAGATATCCGCACCAACGCGCAGCCCGGACTCGGTAATGGCGCGCATTGCGC
CCAGCGCCATCTGATCGTTGGCAACCAGCATCGCAGTGGGAACGATGCCCTCATTCAGCATTTG
CATGGTTTGTTGAAAACCGGACATGGCACTCCAGTCGCCTTCCCGTTCCGCTATCGGCTGAATTT
GATTGCGAGTGAGATATTTATGCCAGCCAGCCAGACGCAGACGCGCCGAGACAGAACTTAATG
GGCCCGCTAACAGCGCGATTTGCTGGTGACCCAATGCGACCAGATGCTCCACGCCCAGTCGCGT
ACCGTCTTCATGGGAGAAAATAATACTGTTGATGGGTGTCTGGTCAGAGACATCAAGAAATAAC
GCCGGAACATTAGTGCAGGCAGCTTCCACAGCAATGGCATCCTGGTCATCCAGCGGATAGTTAA
TGATCAGCCCACTGACGCGTTGCGCGAGAAGATTGTGCACCGCCGCTTTACAGGCTTCGACGCC
GCTTCGTTCTACCATCGACACCACCACGCTGGCACCCAGTTGATCGGCGCGAGATTTAATCGCC
GCGACAATTTGCGACGGCGCGTGCAGGGCCAGACTGGAGGTGGCAACGCCAATCAGCAACGAC
TGTTTGCCCGCCAGTTGTTGTGCCACGCGGTTGGGAATGTAATTCAGCTCCGCCATCGCCGCTTC
CACTTTTTCCCGCGTTTTCGCAGAAACGTGGCTGGCCTGGTTCACCACGCGGGAAACGGTCTGA
TAAGAGACACCGGCATACTCTGCGACATCGTATAACGTTACTGGTTTCACATTCACCACCCTGA
ATTGACTCTCTTCCGGGCGCTATCATGCCATACCGCGAAAGGTTTTGCGCCATTCGATGGTGTCC
GGGATCTCGACGCTCTCCCTTATGCGACTCCTGCATTAGGAAGCAGCCCAGTAGTAGGTTGAGG
CCGTTGAGCACCGCCGCCGCAAGGAATGGTGCATGCAAGGAGATGGCGCCCAACAGTCCCCCG
GCCACGGGGCCTGCCACCATACCCACGCCGAAACAAGCGCTCATGAGCCCGAAGTGGCGAGCC
CGATCTTCCCCATCGGTGATGTCGGCGATATAGGCGCCAGCAACCGCACCTGTGGCGCCGGTGA
TGCCGGCCACGATGCGTCCGGCGTAGAGGATCGAGATCTCGATCCCGCGAAATTAATACGACTC
ACTATAGGGGAATTGTGAGCGGATAACAATTCCCCTCTAGATAACGAGGGCAAAAAATGAAAA
AGACAGCTATCGCGATTGCAGTGGCACTGGCTGGTTTCGCTACCGTAGCGCAGGCCGCTAGCTG
GAGCCACCCGCAGTTCGAAAAAATCGAAGGGCGCCATCACCATCACCATCACGGGGCCCAGCC
GGCCATGGCCGATTATAAACAGGTGAAACTGCAGCAGTCTGGACCTGAGCTGGTGAAGCCTGG
GGCCTCAGTGAAGATTTCCTGCAAAGCTTCTGGCTACGCATTCAGTAGGTCTTGGATGAACTGG
GNGAAGCAGAGGCCTGGACAGGGTCTTGAGTGGATTGGACGGATTTATCCTGGAGATGGAGAT
ACTAACTACAATGGGAAGTTCAAGGGCAAGGCCACACTGACTGCAGACAAATCCTCCAGCACA
GCCTACATGCAGGTCAGCAGCCTGACCTCTGTGGACTCTGCGGTCTATTTCTGTGCAAGAGGGA
ANACGGNAGTAGTTCCCTATACTATGGACTACTGGGGTCAAGGAACCACCGTGACCGTGAGTTC
GGGTGGCGGTGGATCCGGTGGTGGCGGCAGCGGTGGTGGCGGCAGCGATATTGAACTGACGCA
ATCTCCAGCTTCTTTGGCTGTGTCTCTAGGGCAGAGGGCCACCATATCCTGCAGAGCCAGTGAA
AGTGTTGATAGTTATGGCAATAGTTTTATGCACTGGTACCAGCAGAAACCAGGACAGCCACCCA
AACTCCTCATCTATCTTGCATCCAACCTAGAATCTGGGGTCCCTGCCAGGTTCAGTGGCAGTGG
ATCTAGGACAGACTTCACCCTCACCATTGATCCTGTGGAGGCTGATGATGCTGCAACCTATTAC
TGTCAACAAAATAATGAAGACCCTCTGACGTTTGGCGGCGGGACCAAGCTGGAACTGAAACGG
TCGGCCTCGGGGGCCGGTGGTGGCGGCAGTGGTGGTGGCGGCAGTGGTGGTGGCGGCAGTGGT
GGTGGCGGCAGTGCGGCCGCACTCGAGGGCGGCAGCCTGGCCGCGCTGACCGCGCACCAGGCC
TGCCACCTGCCGCTGGAGACTTTCACCCGTCATCGCCAGCCGCGCGGCTGGGAACAACTGGAGC
AGTGCGGCTATCCGGTGCAGCGGCTGGTCGCCCTCTACCTGGCGGCGCGACTGTCATGGAACCA
GGTCGACCAGGTGATCCGCAACGCCCTGGCCAGCCCCGGCAGCGGCGGCGACCTGGGCGAAGC

GATCCGCGAGCAGCCGGAGCAGGCCCGTCTGGCCCTGACCCTGGCCGCCGCCGAGAGCGAGCG
CTTCGTCCGGCAGGGCACCGGCAACGACGAGGCCGGCGCGGCCAGCGCCGACGTGGTGAGCCT
GACCTGCCCGGTCGCCGCCGGTGAATGCGCGGGCCCGGCGGACAGCGGCGACGCCCTGCTGGA
GCGCAACTATCCCACTGGCGCGGAGTTCCTCGGCGACGGTGGCGACGTCAGCTTCAGCACCCGC
GGCACGCAGAACTGGACGGTGGAGCGGCTGCTCCAGGCGCACCGCCAACTGGAGGAGCGCGGC
TATGTGTTCGTCGGCTACCACGGCACCTTCCTCGAAGCGGCGCAAAGCATCGTCTTCGGCGGGG
TGCGCGCGCGCAGCCAGGATCTCGACGCGATCTGGCGCGGTTTCTATATCGCCGGCGATCCGGC
GCTGGCCTACGGCTACGCCCAGGACCAGGAACCCGACGCGCGCGGCCGGATCCGCAACGGTGC
CCTGCTGCGGGTCTATGTGCCGCGCTCGAGCCTGCCGGGCTTCTACCGCACCGGCCTGACCCTG
GCCGCGCCGGAGGCGGCGGGCGAGGTCGAACGGCTGATCGGCCATCCGCTGCCGCTGCGCCTG
GACGCCATCACCGGCCCCGAGGAGGAAGGCGGGCGCCTGGAGACCATTCTCGGCTGGCCGCTG
GCCGAGCGCACCGTGGTGATTCCCTCGGCGATCCCCACCGACCCGCGCAACGTCGGCGGCGACC
TCGACCCGTCCAGCATCCCCGACAAGGAACAGGCGATCAGCGCCCTGCCGGACTACGCCAGCC
AGCCCGGCAAACCGCCGAAGGACGAGCTGTAATGAAAGCTTGCTGAGCAATAACTAGCATAAC
CCCTTGGGGCCTCTAAACGGGTCTTGAGGGGTTTTTTGCTGAAAGGAGGAACTATATCCGGATT
G

### *VI.3.5 PET-STREP-ANTI-CSPG4-MAP*

TGGCGAATGGGACGCGCCCTGTAGCGGCGCATTAAGCGCGGCGGGTGTGGTGGTTACGCGCAG
CGTGACCGCTACACTTGCCAGCGCCCTAGCGCCCGCTCCTTTCGCTTTCTTCCCTTCCTTTCTCGC
CACGTTCGCCGGCTTTCCCCGTCAAGCTCTAAATCGGGGGCTCCCTTTAGGGTTCCGATTTAGTG
CTTTACGGCACCTCGACCCCAAAAAACTTGATTAGGGTGATGGTTCACGTAGTGGGCCATCGCC
CTGATAGACGGTTTTTCGCCCTTTGACGTTGGAGTCCACGTTCTTTAATAGTGGACTCTTGTTCC
AAACTGGAACAACACTCAACCCTATCTCGGTCTATTCTTTTGATTTATAAGGGATTTTGCCGATT
TCGGCCTATTGGTTAAAAAATGAGCTGATTTAACAAAAATTTAACGCGAATTTTAACAAAATAT
TAACGTTTACAATTTCAGGTGGCACTTTTCGGGGAAATGTGCGCGGAACCCCTATTTGTTTATTT
TTCTAAATACATTCAAATATGTATCCGCTCATGAATTAATTCTTAGAAAAACTCATCGAGCATCA
AATGAAACTGCAATTTATTCATATCAGGATTATCAATACCATATTTTTGAAAAAGCCGTTTCTGT
AATGAAGGAGAAAACTCACCGAGGCAGTTCCATAGGATGGCAAGATCCTGGTATCGGTCTGCG
ATTCCGACTCGTCCAACATCAATACAACCTATTAATTTCCCCTCGTCAAAAATAAGGTTATCAA
GTGAGAAATCACCATGAGTGACGACTGAATCCGGTGAGAATGGCAAAAGTTTATGCATTTCTTT
CCAGACTTGTTCAACAGGCCAGCCATTACGCTCGTCATCAAAATCACTCGCATCAACCAAACCG
TTATTCATTCGTGATTGCGCCTGAGCGAGACGAAATACGCGATCGCTGTTAAAAGGACAATTAC
AAACAGGAATCGAATGCAACCGGCGCAGGAACACTGCCAGCGCATCAACAATATTTTCACCTG
AATCAGGATATTCTTCTAATACCTGGAATGCTGTTTTCCCGGGGATCGCAGTGGTGAGTAACCA
TGCATCATCAGGAGTACGGATAAAATGCTTGATGGTCGGAAGAGGCATAAATTCCGTCAGCCA
GTTTAGTCTGACCATCTCATCTGTAACATCATTGGCAACGCTACCTTTGCCATGTTTCAGAAACA
ACTCTGGCGCATCGGGCTTCCCATACAATCGATAGATTGTCGCACCTGATTGCCCGACATTATC
GCGAGCCCATTTATACCCATATAAATCAGCATCCATGTTGGAATTTAATCGCGGCCTAGAGCAA
GACGTTTCCCGTTGAATATGGCTCATAACACCCCTTGTATTACTGTTTATGTAAGCAGACAGTTT

TATTGTTCATGACCAAAATCCCTTAACGTGAGTTTTCGTTCCACTGAGCGTCAGACCCCGTAGAA
AAGATCAAAGGATCTTCTTGAGATCCTTTTTTTCTGCGCGTAATCTGCTGCTTGCAAACAAAAAA
ACCACCGCTACCAGCGGTGGTTTGTTTGCCGGATCAAGAGCTACCAACTCTTTTTCCGAAGGTA
ACTGGCTTCAGCAGAGCGCAGATACCAAATACTGTCCTTCTAGTGTAGCCGTAGTTAGGCCACC
ACTTCAAGAACTCTGTAGCACCGCCTACATACCTCGCTCTGCTAATCCTGTTACCAGTGGCTGCT
GCCAGTGGCGATAAGTCGTGTCTTACCGGGTTGGACTCAAGACGATAGTTACCGGATAAGGCGC
AGCGGTCGGGCTGAACGGGGGGTTCGTGCACACAGCCCAGCTTGGAGCGAACGACCTACACCG
AACTGAGATACCTACAGCGTGAGCTATGAGAAAGCGCCACGCTTCCCGAAGGGAGAAAGGCGG
ACAGGTATCCGGTAAGCGGCAGGGTCGGAACAGGAGAGCGCACGAGGGAGCTTCCAGGGGGA
AACGCCTGGTATCTTTATAGTCCTGTCGGGTTTCGCCACCTCTGACTTGAGCGTCGATTTTTGTG
ATGCTCGTCAGGGGGGCGGAGCCTATGGAAAAACGCCAGCAACGCGGCCTTTTTACGGTTCCTG
GCCTTTTGCTGGCCTTTTGCTCACATGTTCTTTCCTGCGTTATCCCCTGATTCTGTGGATAACCGT
ATTACCGCCTTTGAGTGAGCTGATACCGCTCGCCGCAGCCGAACGACCGAGCGCAGCGAGTCA
GTGAGCGAGGAAGCGGAAGAGCGCCTGATGCGGTATTTTCTCCTTACGCATCTGTGCGGTATTT
CACACCGCATATATGGTGCACTCTCAGTACAATCTGCTCTGATGCCGCATAGTTAAGCCAGTAT
ACACTCCGCTATCGCTACGTGACTGGGTCATGGCTGCGCCCCGACACCCGCCAACACCCGCTGA
CGCGCCCTGACGGGCTTGTCTGCTCCCGGCATCCGCTTACAGACAAGCTGTGACCGTCTCCGGG
AGCTGCATGTGTCAGAGGTTTTCACCGTCATCACCGAAACGCGCGAGGCAGCTGCGGTAAAGCT
CATCAGCGTGGTCGTGAAGCGATTCACAGATGTCTGCCTGTTCATCCGCGTCCAGCTCGTTGAG
TTTCTCCAGAAGCGTTAATGTCTGGCTTCTGATAAAGCGGGCCATGTTAAGGGCGGTTTTTTCCT
GTTTGGTCACTGATGCCTCCGTGTAAGGGGGATTTCTGTTCATGGGGGTAATGATACCGATGAA
ACGAGAGAGGATGCTCACGATACGGGTTACTGATGATGAACATGCCCGGTTACTGGAACGTTGT
GAGGGTAAACAACTGGCGGTATGGATGCGGCGGGACCAGAGAAAAATCACTCAGGGTCAATGC
CAGCGCTTCGTTAATACAGATGTAGGTGTTCCACAGGGTAGCCAGCAGCATCCTGCGATGCAGA
TCCGGAACATAATGGTGCAGGGCGCTGACTTCCGCGTTTCCAGACTTTACGAAACACGGAAACC
GAAGACCATTCATGTTGTTGCTCAGGTCGCAGACGTTTTGCAGCAGCAGTCGCTTCACGTTCGCT
CGCGTATCGGTGATTCATTCTGCTAACCAGTAAGGCAACCCCGCCAGCCTAGCCGGGTCCTCAA
CGACAGGAGCACGATCATGCGCACCCGTGGGGCCGCCATGCCGGCGATAATGGCCTGCTTCTCG
CCGAAACGTTTGGTGGCGGGACCAGTGACGAAGGCTTGAGCGAGGGCGTGCAAGATTCCGAAT
ACCGCAAGCGACAGGCCGATCATCGTCGCGCTCCAGCGAAAGCGGTCCTCGCCGAAAATGACC
CAGAGCGCTGCCGGCACCTGTCCTACGAGTTGCATGATAAAGAAGACAGTCATAAGTGCGGCG
ACGATAGTCATGCCCCGCGCCCACCGGAAGGAGCTGACTGGGTTGAAGGCTCTCAAGGGCATC
GGTCGAGATCCCGGTGCCTAATGAGTGAGCTAACTTACATTAATTGCGTTGCGCTCACTGCCCG
CTTTCCAGTCGGGAAACCTGTCGTGCCAGCTGCATTAATGAATCGGCCAACGCGCGGGGAGAG
GCGGTTTGCGTATTGGGCGCCAGGGTGGTTTTTCTTTTCACCAGTGAGACGGGCAACAGCTGAT
TGCCCTTCACCGCCTGGCCCTGAGAGAGTTGCAGCAAGCGGTCCACGCTGGTTTGCCCCAGCAG
GCGAAAATCCTGTTTGATGGTGGTTAACGGCGGGATATAACATGAGCTGTCTTCGGTATCGTCG
TATCCCACTACCGAGATATCCGCACCAACGCGCAGCCCGGACTCGGTAATGGCGCGCATTGCGC
CCAGCGCCATCTGATCGTTGGCAACCAGCATCGCAGTGGGAACGATGCCCTCATTCAGCATTTG
CATGGTTTGTTGAAAACCGGACATGGCACTCCAGTCGCCTTCCCGTTCCGCTATCGGCTGAATTT
GATTGCGAGTGAGATATTTATGCCAGCCAGCCAGACGCAGACGCGCCGAGACAGAACTTAATG

GGCCCGCTAACAGCGCGATTTGCTGGTGACCCAATGCGACCAGATGCTCCACGCCCAGTCGCGT
ACCGTCTTCATGGGAGAAAATAATACTGTTGATGGGTGTCTGGTCAGAGACATCAAGAAATAAC
GCCGGAACATTAGTGCAGGCAGCTTCCACAGCAATGGCATCCTGGTCATCCAGCGGATAGTTAA
TGATCAGCCCACTGACGCGTTGCGCGAGAAGATTGTGCACCGCCGCTTTACAGGCTTCGACGCC
GCTTCGTTCTACCATCGACACCACCACGCTGGCACCCAGTTGATCGGCGCGAGATTTAATCGCC
GCGACAATTTGCGACGGCGCGTGCAGGGCCAGACTGGAGGTGGCAACGCCAATCAGCAACGAC
TGTTTGCCCGCCAGTTGTTGTGCCACGCGGTTGGGAATGTAATTCAGCTCCGCCATCGCCGCTTC
CACTTTTTCCCGCGTTTTCGCAGAAACGTGGCTGGCCTGGTTCACCACGCGGGAAACGGTCTGA
TAAGAGACACCGGCATACTCTGCGACATCGTATAACGTTACTGGTTTCACATTCACCACCCTGA
ATTGACTCTCTTCCGGGCGCTATCATGCCATACCGCGAAAGGTTTTGCGCCATTCGATGGTGTCC
GGGATCTCGACGCTCTCCCTTATGCGACTCCTGCATTAGGAAGCAGCCCAGTAGTAGGTTGAGG
CCGTTGAGCACCGCCGCCGCAAGGAATGGTGCATGCAAGGAGATGGCGCCCAACAGTCCCCCG
GCCACGGGGCCTGCCACCATACCCACGCCGAAACAAGCGCTCATGAGCCCGAAGTGGCGAGCC
CGATCTTCCCCATCGGTGATGTCGGCGATATAGGCGCCAGCAACCGCACCTGTGGCGCCGGTGA
TGCCGGCCACGATGCGTCCGGCGTAGAGGATCGAGATCTCGATCCCGCGAAATTAATACGACTC
ACTATAGGGGAATTGTGAGCGGATAACAATTCCCCTCTAGATAACGAGGGCAAAAAATGAAAA
AGACAGCTATCGCGATTGCAGTGGCACTGGCTGGTTTCGCTACCGTAGCGCAGGCCGCTAGCTG
GAGCCACCCGCAGTTCGAAAAAATCGAAGGGCGCCATCACCATCACCATCACGGGGCCCAGCC
GGCCATGGCCCAGGTGAAACTGCAGCAGTCTGGACCTGAGCTGGTGAAGCCTGGGGCCTCAGT
GAAGATTTCCTGCAAAGCTTCTGGCTACGCATTCAGTAGGTCTTGGATGAACTGGGTGAAGCAG
AGGCCTGGACAGGGTCTTGAGTGGATTGGACGGATTTATCCTGGAGATGGAGATACTAACTACA
ATGGGAAGTTCAAGGGCAAGGCCACACTGACTGCAGACAAATCCTCCAGCACAGCCTACATGC
AGGTCAGCAGCCTGACCTCTGTGGACTCTGCGGTCTATTTCTGTGCAAGAGGGAATACGGTAGT
AGTTCCCTATACTATGGACTACTGGGGTCAAGGAACCACCGTGACCGTGAGTTCGGGTGGCGGT
GGATCCGGTGGTGGCGGCAGCGGTGGTGGCGGCAGCGATATTGAACTGACGCAATCTCCAGCT
TCTTTGGCTGTGTCTCTAGGGCAGAGGGCCACCATATCCTGCAGAGCCAGTGAAAGTGTTGATA
GTTATGGCAATAGTTTTATGCACTGGTACCAGCAGAAACCAGGACAGCCACCCAAACTCCTCAT
CTATCTTGCATCCAACCTAGAATCTGGGGTCCCTGCCAGGTTCAGTGGCAGTGGATCTAGGACA
GACTTCACCCTCACCATTGATCCTGTGGAGGCTGATGATGCTGCAACCTATTACTGTCAACAAA
ATAATGAAGACCCTCTGACGTTTGGCGGCGGGACCAAGCTGGAACTGAAACGGGCGGCCGCAA
TGGCTGAACCCCGCCAGGAGTTCGAAGTGATGGAAGATCACGCTGGGACGTACGGGTTGGGGG
ACAGGAAAGATCAGGGGGGCTACACCATGCACCAAGACCAAGAGGGTGACACGGACGCTGGC
CTGAAAGCTGAAGAAGCAGGCATTGGAGACACCCCCAGCCTGGAAGACGAAGCTGCTGGTCAC
GTGACCCAAGCTCGCATGGTCAGTAAAAGCAAAGACGGGACTGGAAGCGATGACAAAAAAGC
CAAGGGGGCTGATGGTAAAACGAAGATCGCCACACCGCGGGGAGCAGCCCCTCCAGGCCAGAA
GGGCCAGGCCAACGCCACCAGGATTCCAGCAAAAACCCCGCCCGCTCCAAAGACACCACCCAG
CTCTGGTGAACCTCCAAAATCAGGGGATCGCAGCGGCTACAGCAGCCCCGGCTCCCCAGGCACT
CCCGGCAGCCGCTCCCGCACCCCGGCCCTTCCAACCCCACCCACCCGGGAGCCCAAGAAGGTG
GCAGTGGTCCGTACTCCACCCAAGTCGCCGTCTTCCGCCAAGAGCCGCCTGCAGACAGCCCCCG
TGCCCATGCCAGACCTGAAGAATGTCAAGTCCAAGATCGGCGCCACTGAGAACCTGAAGCACC
AGCCGGGAGGCGGGAAGGTGCAGATAATTAATAAGAAGCTGGATCTTAGCAACGTCCAGTCCA

AGTGTGGCTCAAAGGATAATATCAAACACGTCCCGGGAGGCGGCAGTGTGCAAATAGTCTACA
AACCAGTTGACCTGAGCAAGGTGACCTCCAAGTGTGGCTCATTAGGCAACATCCATCATAAACC
AGGAGGTGGCCAGGTGGAAGTAAAATCTGAGAAGCTTGACTTCAAGGACAGAGTCCAGTCGAA
GATTGGGTCCCTGGACAATATCACCCACGTCCCTGGCGGAGGAAATAAAAAGATTGAAACCCA
CAAGCTGACCTTCCGCGAGAACGCCAAAGCCAAGACAGACCACGGGGCGGAGATCGTGTACAA
GTCGCCAGTGGTGTCTGGGGACACGTCTCCACGGCATCTCAGCAATGTCTCCTCCACCGGCAGC
ATCGACATGGTAGACTCGCCCCAGCTCGCCACGCTAGCTGACGAGGTGTCTGCCTCCCTGGCCA
AGCAGGGTTTGCCCAAAAAAAAAAGGAAAGTGTGAGCTGAGCAATAACTAGCATAACCCCTTG
GGGCCTCTAAACGGGTCTTGAGGGGTTTTTTGCTGAAAGGAGGAACTATATCCGGATTG

### *VI.3.6 PMS-ANTI-EPCAM_SNAP_IV*

GCTAGCCACCATGGAGACAGACACACTCCTGCTATGGGTACTGCTGCTCTGGGTTCCAGGTTCC
ACTGGTGACGCGGCCCAGCCGGCCATGGCCCAGGTGCAGCTGGTGCAGTCTGGGGCTGAGGTG
AAGAAGCCTGGGTCCTCGGTGAGGGTCTCCTGCAAGGCTTCTGGAGGCACCTTCAGCAGCTATG
CTATCAGCTGGGTGCGACAGGCCCCTGGACAAGGGCTTGAGTGGATGGGAGGGATCATCCCTA
TCTTTGGTACAGCAAACTACGCACAGAAGTTCCAGGGCAGAGTCACGATTACCGCGGACGAAT
CCACGAGCACAGCCTACATGGAGCTGAGCAGCCTGAGATCTGAGGACACGGCTGTGTATTACT
GTGCAAGAGACCCGTTTCTTCACTATTGGGGCCAAGGTACCCTGGTCACCGTCTCGAGTGGTGG
AGGCGGTTCAGGCGGAGGTGGCTCTGGCGGTGGCGGATCGGAAATTGAGCTCACTCAGTCTCC
ACTCTCCCTGCCCGTCACCCCTGGAGAGCCGGCCTCCATCTCCTGCAGGTCTAGTCAGAGCCTCC
TGCATAGTAATGGATACAACTATTTGGATTGGTACCTGCAGAAGCCAGGGCAGTCTCCACAGCT
CCTGATCTATTTGGGTTCTAATCGGGCCTCCGGGGTCCCTGACAGGTTCAGTGGCAGTGGATCA
GGCACAGATTTTACACTGAAAATCAGCAGAGTGGAGGCTGAGGATGTTGGGGTTTATTACTGCA
TGCAAGCTCTACAAACTTTCACTTTCGGCCCTGGGACCAAGGTGGAGATCAAACGTGCGGCCGC
ACTCGAGTCTAGAATGGACAAAGACTGCGAAATGAAGCGCACCACCCTGGATAGCCCTCTGGG
CAAGCTGGAACTGTCTGGGTGCGAACAGGGCCTGCACGAGATCAAGCTGCTGGGCAAAGGAAC
ATCTGCCGCCGACGCCGTGGAAGTGCCTGCCCCAGCCGCCGTGCTGGGCGGACCAGAGCCACT
GATGCAGGCCACCGCCTGGCTCAACGCCTACTTTCACCAGCCTGAGGCCATCGAGGAGTTCCCT
GTGCCAGCCCTGCACCACCCAGTGTTCCAGCAGGAGAGCTTTACCCGCCAGGTGCTGTGGAAAC
TGCTGAAAGTGGTGAAGTTCGGAGAGGTCATCAGCTACCAGCAGCTGGCGGCCCTGGCGGGCA
ATCCCGCCGCCACCGCCGCCGTGAAAACCGCCCTGAGCGGAAATCCCGTGCCCATTCTGATCCC
CTGCCACCGGGTGGTGTCTAGCTCTGGCGCCGTGGGGGGCTACGAGGGCGGGCTCGCCGTGAA
AGAGTGGCTGCTGGCCCACGAGGGCCACAGACTGGGCAAGCCTGGGCTGGGCGCTGAGCACGA
ATTTCGAGGAGGGCCCGAACAAAAACTCATCTCAGAAGAGGATCTGAATAGCGCCGTCGACCA
TCATCATCATCATCATTGAGTTTTGAGCACGAATTCTGGAATTAATTCGCTGTCTGCGAGGGCCA
GCTGTTGGGGTGAGTACTCCCTCTCAAAAGCGGGCATGACTTCTGCGCTAAGATTGTCAGTTTC
CAAAAACGAGGAGGATTTGATATTCACCTGGCCCGCGGTGATGCCTTTGAGGGTGGCCGCGTCC
ATCTGGTCAGAAAAGACAATCTTTTTGTTGTCAAGCTTGAGGTGTGGCAGGCTTGAGATCTGGC
CATACACTTGAGTGACAATGACATCCACTTTGCCTTTCTCTCCACAGGTGTCCACTCCCAGGTCC
AACTGCAGGTCGAGCATGCATCTAGGGCGGCCAATTCCGCCCCTCTCCCTCCCCCCCCCCTAAC

GTTACTGGCCGAAGCCGCTTGGAATAAGGCCGGTGTGCGTTTGTCTATATGTGATTTTCCACCAT
ATTGCCGTCTTTTGGCAATGTGAGGGCCCGGAAACCTGGCCCTGTCTTCTTGACGAGCATTCCTA
GGGGTCTTTCCCCTCTCGCCAAAGGAATGCAAGGTCTGTTGAATGTCGTGAAGGAAGCAGTTCC
TCTGGAAGCTTCTTGAAGACAAACAACGTCTGTAGCGACCCTTTGCAGGCAGCGGAACCCCCCA
CCTGGCGACAGGTGCCTCTGCGGCCAAAAGCCACGTGTATAAGATACACCTGCAAAGGCGGCA
CAACCCCAGTGCCACGTTGTGAGTTGGATAGTTGTGGAAAGAGTCAAATGGCTCTCCTCAAGCG
TATTCAACAAGGGGCTGAAGGATGCCCAGAAGGTACCCCATTGTATGGGATCTGATCTGGGGCC
TCGGTGCACATGCTTTACATGTGTTTAGTCGAGGTTAAAAAAACGTCTAGGCCCCCCGAACCAC
GGGGACGTGGTTTTCCTTTGAAAAACACGATGATAAGCTTGCCACAACCCGGGATCCACCGGTC
GCCACCATGGTGAGCAAGGGCGAGGAGCTGTTCACCGGGGTGGTGCCCATCCTGGTCGAGCTG
GACGGCGACGTAAACGGCCACAAGTTCAGCGTGTCCGGCGAGGGCGAGGGCGATGCCACCTAC
GGCAAGCTGACCCTGAAGTTCATCTGCACCACCGGCAAGCTGCCCGTGCCCTGGCCCACCCTCG
TGACCACCCTGACCTACGGCGTGCAGTGCTTCAGCCGCTACCCCGACCACATGAAGCAGCACGA
CTTCTTCAAGTCCGCCATGCCCGAAGGCTACGTCCAGGAGCGCACCATCTTCTTCAAGGACGAC
GGCAACTACAAGACCCGCGCCGAGGTGAAGTTCGAGGGCGACACCCTGGTGAACCGCATCGAG
CTGAAGGGCATCGACTTCAAGGAGGACGGCAACATCCTGGGGCACAAGCTGGAGTACAACTAC
AACAGCCACAACGTCTATATCATGGCCGACAAGCAGAAGAACGGCATCAAGGTGAACTTCAAG
ATCCGCCACAACATCGAGGACGGCAGCGTGCAGCTCGCCGACCACTACCAGCAGAACACCCCC
ATCGGCGACGGCCCCGTGCTGCTGCCCGACAACCACTACCTGAGCACCCAGTCCGCCCTGAGCA
AAGACCCCAACGAGAAGCGCGATCACATGGTCCTGCTGGAGTTCGTGACCGCCGCCGGGATCA
CTCTCGGCATGGACGAGCTGTACAAGTAAGTTTAAACCCGCTGATCAGCCTCGACTGTGCCTTC
TAGTTGCCAGCCATCTGTTGTTTGCCCCTCCCCCGTGCCTTCCTTGACCCTGGAAGGTGCCACTC
CCACTGTCCTTTCCTAATAAAATGAGGAAATTGCATCGCATTGTCTGAGTAGGTGTCATTCTATT
CTGGGGGGTGGGGTGGGGCAGGACAGCAAGGGGGAGGATTGGGAAGACAATAGCAGGCATGC
TGGGGATGCGGTGGGCTCTATGGCTTCTGAGGCGGAAAGAACCAGCTGGGGCTCTAGGGGGTA
TCCCCACGCGCCCTGTAGCGGCGCATTAAGCGCGGCGGGTGTGGTGGTTACGCGCAGCGTGACC
GCTACACTTGCCAGCGCCCTAGCGCCCGCTCCTTTCGCTTTCTTCCCTTCCTTTCTCGCCACGTTC
GCCGGCTTTCCCCGTCAAGCTCTAAATCGGGGCATCCCTTTAGGGTTCCGATTTAGTGCTTTACG
GCACCTCGACCCCAAAAAACTTGATTAGGGTGATGGTTCACGTAGTGGGCCATCGCCCTGATAG
ACGGTTTTTCGCCCTTTGACGTTGGAGTCCACGTTCTTTAATAGTGGACTCTTGTTCCAAACTGG
AACAACACTCAACCCTATCTCGGTCTATTCTTTTGATTTATAAGGGATTTTGGGGATTTCGGCCT
ATTGGTTAAAAAATGAGCTGATTTAACAAAAATTTAACGCGAATTAATTCTGTGGAATGTGTGT
CAGTTAGGGTGTGGAAAGTCCCCAGGCTCCCCAGCAGGCAGAAGTATGCAAAGCATGCATCTC
AATTAGTCAGCAACCAGGTGTGGAAAGTCCCCAGGCTCCCCAGCAGGCAGAAGTATGCAAAGC
ATGCATCTCAATTAGTCAGCAACCATAGTCCCGCCCCTAACTCCGCCCATCCCGCCCCTAACTCC
GCCCAGTTCCGCCCATTCTCCGCCCCATGGCTGACTAATTTTTTTTATTTATGCAGAGGCCGAGG
CCGCCTCTGCCTCTGAGCTATTCCAGAAGTAGTGAGGAGGCTTTTTTGGAGGCCTAGGCTTTTGC
AAAAAGCTCCCGGGAGCTTGTATATCCATTTTCGGATCTGATCAGCACGTGTTGACAATTAATC
ATCGGCATAGTATATCGGCATAGTATAATACGACAAGGTGAGGAACTAAACCATGGCCAAGTT
GACCAGTGCCGTTCCGGTGCTCACCGCGCGCGACGTCGCCGGAGCGGTCGAGTTCTGGACCGAC
CGGCTCGGGTTCTCCCGGGACTTCGTGGAGGACGACTTCGCCGGTGTGGTCCGGGACGACGTGA

CCCTGTTCATCAGCGCGGTCCAGGACCAGGTGGTGCCGGACAACACCCTGGCCTGGGTGTGGGT
GCGCGGCCTGGACGAGCTGTACGCCGAGTGGTCGGAGGTCGTGTCCACGAACTTCCGGGACGC
CTCCGGGCCGGCCATGACCGAGATCGGCGAGCAGCCGTGGGGGCGGGAGTTCGCCCTGCGCGA
CCCGGCCGGCAACTGCGTGCACTTCGTGGCCGAGGAGCAGGACTGACACGTGCTACGAGATTTC
GATTCCACCGCCGCCTTCTATGAAAGGTTGGGCTTCGGAATCGTTTTCCGGGACGCCGGCTGGA
TGATCCTCCAGCGCGGGGATCTCATGCTGGAGTTCTTCGCCCACCCCAACTTGTTTATTGCAGCT
TATAATGGTTACAAATAAAGCAATAGCATCACAAATTTCACAAATAAAGCATTTTTTTCACTGC
ATTCTAGTTGTGGTTTGTCCAAACTCATCAATGTATCTTATCATGTCTGTATACCGTCGACCTCT
AGCTAGAGCTTGGCGTAATCATGGTCATAGCTGTTTCCTGTGTGAAATTGTTATCCGCTCACAAT
TCCACACAACATACGAGCCGGAAGCATAAAGTGTAAAGCCTGGGGTGCCTAATGAGTGAGCTA
ACTCACATTAATTGCGTTGCGCTCACTGCCCGCTTTCCAGTCGGGAAACCTGTCGTGCCAGCTGC
ATTAATGAATCGGCCAACGCGCGGGGAGAGGCGGTTTGCGTATTGGGCGCTCTTCCGCTTCCTC
GCTCACTGACTCGCTGCGCTCGGTCGTTCGGCTGCGGCGAGCGGTATCAGCTCACTCAAAGGCG
GTAATACGGTTATCCACAGAATCAGGGGATAACGCAGGAAAGAACATGTGAGCAAAAGGCCAG
CAAAAGGCCAGGAACCGTAAAAAGGCCGCGTTGCTGGCGTTTTTCCATAGGCTCCGCCCCCCTG
ACGAGCATCACAAAAATCGACGCTCAAGTCAGAGGTGGCGAAACCCGACAGGACTATAAAGAT
ACCAGGCGTTTCCCCCTGGAAGCTCCCTCGTGCGCTCTCCTGTTCCGACCCTGCCGCTTACCGGA
TACCTGTCCGCCTTTCTCCCTTCGGGAAGCGTGGCGCTTTCTCAATGCTCACGCTGTAGGTATCT
CAGTTCGGTGTAGGTCGTTCGCTCCAAGCTGGGCTGTGTGCACGAACCCCCCGTTCAGCCCGAC
CGCTGCGCCTTATCCGGTAACTATCGTCTTGAGTCCAACCCGGTAAGACACGACTTATCGCCAC
TGGCAGCAGCCACTGGTAACAGGATTAGCAGAGCGAGGTATGTAGGCGGTGCTACAGAGTTCT
TGAAGTGGTGGCCTAACTACGGCTACACTAGAAGGACAGTATTTGGTATCTGCGCTCTGCTGAA
GCCAGTTACCTTCGGAAAAAGAGTTGGTAGCTCTTGATCCGGCAAACAAACCACCGCTGGTAGC
GGTGGTTTTTTTGTTTGCAAGCAGCAGATTACGCGCAGAAAAAAAGGATCTCAAGAAGATCCTT
TGATCTTTTCTACGGGGTCTGACGCTCAGTGGAACGAAAACTCACGTTAAGGGATTTTGGTCAT
GAGATTATCAAAAAGGATCTTCACCTAGATCCTTTTAAATTAAAAATGAAGTTTTAAATCAATC
TAAAGTATATATGAGTAAACTTGGTCTGACAGTTACCAATGCTTAATCAGTGAGGCACCTATCT
CAGCGATCTGTCTATTTCGTTCATCCATAGTTGCCTGACTCCCCGTCGTGTAGATAACTACGATA
CGGGAGGGCTTACCATCTGGCCCCAGTGCTGCAATGATACCGCGAGACCCACGCTCACCGGCTC
CAGATTTATCAGCAATAAACCAGCCAGCCGGAAGGGCCGAGCGCAGAAGTGGTCCTGCAACTT
TATCCGCCTCCATCCAGTCTATTAATTGTTGCCGGGAAGCTAGAGTAAGTAGTTCGCCAGTTAAT
AGTTTGCGCAACGTTGTTGCCATTGCTACAGGCATCGTGGTGTCACGCTCGTCGTTTGGTATGGC
TTCATTCAGCTCCGGTTCCCAACGATCAAGGCGAGTTACATGATCCCCCATGTTGTGCAAAAAA
GCGGTTAGCTCCTTCGGTCCTCCGATCGTTGTCAGAAGTAAGTTGGCCGCAGTGTTATCACTCAT
GGTTATGGCAGCACTGCATAATTCTCTTACTGTCATGCCATCCGTAAGATGCTTTTCTGTGACTG
GTGAGTACTCAACCAAGTCATTCTGAGAATAGTGTATGCGGCGACCGAGTTGCTCTTGCCCGGC
GTCAATACGGGATAATACCGCGCCACATAGCAGAACTTTAAAAGTGCTCATCATTGGAAAACGT
TCTTCGGGGCGAAAACTCTCAAGGATCTTACCGCTGTTGAGATCCAGTTCGATGTAACCCACTC
GTGCACCCAACTGATCTTCAGCATCTTTTACTTTCACCAGCGTTTCTGGGTGAGCAAAAACAGG
AAGGCAAAATGCCGCAAAAAAGGGAATAAGGGCGACACGGAAATGTTGAATACTCATACTCTT
CCTTTTTCAATATTATTGAAGCATTTATCAGGGTTATTGTCTCATGAGCGGATACATATTTGAAT

GTATTTAGAAAAATAAACAAATAGGGGTTCCGCGCACATTTCCCCGAAAAGTGCCACCTGACGT
CGACGGATCGGGAGATCTCCCGATCCCCTATGGTCGACTCTCAGTACAATCTGCTCTGATGCCG
CATAGTTAAGCCAGTATCTGCTCCCTGCTTGTGTGTTGGAGGTCGCTGAGTAGTGCGCGAGCAA
AATTTAAGCTACAACAAGGCAAGGCTTGACCGACAATTGCATGAAGAATCTGCTTAGGGTTAG
GCGTTTTGCGCTGCTTCGCGATGTACGGGCCAGATATACGCGTTGACATTGATTATTGACTAGTT
ATTAATAGTAATCAATTACGGGGTCATTAGTTCATAGCCCATATATGGAGTTCCGCGTTACATA
ACTTACGGTAAATGGCCCGCCTGGCTGACCGCCCAACGACCCCCGCCCATTGACGTCAATAATG
ACGTATGTTCCCATAGTAACGCCAATAGGGACTTTCCATTGACGTCAATGGGTGGACTATTTAC
GGTAAACTGCCCACTTGGCAGTACATCAAGTGTATCATATGCCAAGTACGCCCCCTATTGACGT
CAATGACGGTAAATGGCCCGCCTGGCATTATGCCCAGTACATGACCTTATGGGACTTTCCTACT
TGGCAGTACATCTACGTATTAGTCATCGCTATTACCATGGTGATGCGGTTTTGGCAGTACATCAA
TGGGCGTGGATAGCGGTTTGACTCACGGGGATTTCCAAGTCTCCACCCCATTGACGTCAATGGG
AGTTTGTTTTGGCACCAAAATCAACGGGACTTTCCAAAATGTCGTAACAACTCCGCCCCATTGA
CGCAAATGGGCGGTAGGCGTGTACGGTGGGAGGTCTATATAAGCAGAGCTCTCTGGCTAACTA
GAGAACCCACTGCTTACTGGCTTATCGAAATTAATACGACTCACTATAGGGAGACCCAAGCTG

### *VI.3.7 PMS-ANTI-CSPG4-SNAP_IV*

GCTAGCCACCATGGAGACAGACACACTCCTGCTATGGGTACTGCTGCTCTGGGTTCCAGGTTCC
ACTGGTGACGCGGCCCAGCCGGCCATGGCCCAGGTGAAACTGCAGCAGTCTGGACCTGAGCTG
GTGAAGCCTGGGGCCTCAGTGAAGATTTCCTGCAAAGCTTCTGGCTACGCATTCAGTAGGTCTT
GGATGAACTGGGTGAAGCAGAGGCCTGGACAGGGTCTTGAGTGGATTGGACGGATTTATCCTG
GAGATGGAGATACTAACTACAATGGGAAGTTCAAGGGCAAGGCCACACTGACTGCAGACAAAT
CCTCCAGCACAGCCTACATGCAGGTCAGCAGCCTGACCTCTGTGGACTCTGCGGTCTATTTCTGT
GCAAGAGGGAATACGGTAGTAGTTCCCTATACTATGGACTACTGGGGTCAAGGAACCACCGTG
ACCGTGAGTTCGGGTGGCGGTGGATCCGGTGGTGGCGGCAGCGGTGGTGGCGGCAGCGATATT
GAACTGACGCAATCTCCAGCTTCTTTGGCTGTGTCTCTAGGGCAGAGGGCCACCATATCCTGCA
GAGCCAGTGAAAGTGTTGATAGTTATGGCAATAGTTTTATGCACTGGTACCAGCAGAAACCAGG
ACAGCCACCCAAACTCCTCATCTATCTTGCATCCAACCTAGAATCTGGGGTCCCTGCCAGGTTC
AGTGGCAGTGGATCTAGGACAGACTTCACCCTCACCATTGATCCTGTGGAGGCTGATGATGCTG
CAACCTATTACTGTCAACAAAATAATGAAGACCCTCTGACGTTTGGCGGCGGGACCAAGCTGGA
ACTGAAACGGGCGGCCGCACTCGAGTCTAGAATGGACAAAGACTGCGAAATGAAGCGCACCAC
CCTGGATAGCCCTCTGGGCAAGCTGGAACTGTCTGGGTGCGAACAGGGCCTGCACGAGATCAA
GCTGCTGGGCAAAGGAACATCTGCCGCCGACGCCGTGGAAGTGCCTGCCCCAGCCGCCGTGCT
GGGCGGACCAGAGCCACTGATGCAGGCCACCGCCTGGCTCAACGCCTACTTTCACCAGCCTGAG
GCCATCGAGGAGTTCCCTGTGCCAGCCCTGCACCACCCAGTGTTCCAGCAGGAGAGCTTTACCC
GCCAGGTGCTGTGGAAACTGCTGAAAGTGGTGAAGTTCGGAGAGGTCATCAGCTACCAGCAGC
TGGCGGCCCTGGCGGGCAATCCCGCCGCCACCGCCGCCGTGAAAACCGCCCTGAGCGGAAATC
CCGTGCCCATTCTGATCCCCTGCCACCGGGTGGTGTCTAGCTCTGGCGCCGTGGGGGGCTACGA
GGGCGGGCTCGCCGTGAAAGAGTGGCTGCTGGCCCACGAGGGCCACAGACTGGGCAAGCCTGG
GCTGGGCGCTGAGCACGAATTTCGAGGAGGGCCCGAACAAAAACTCATCTCAGAAGAGGATCT

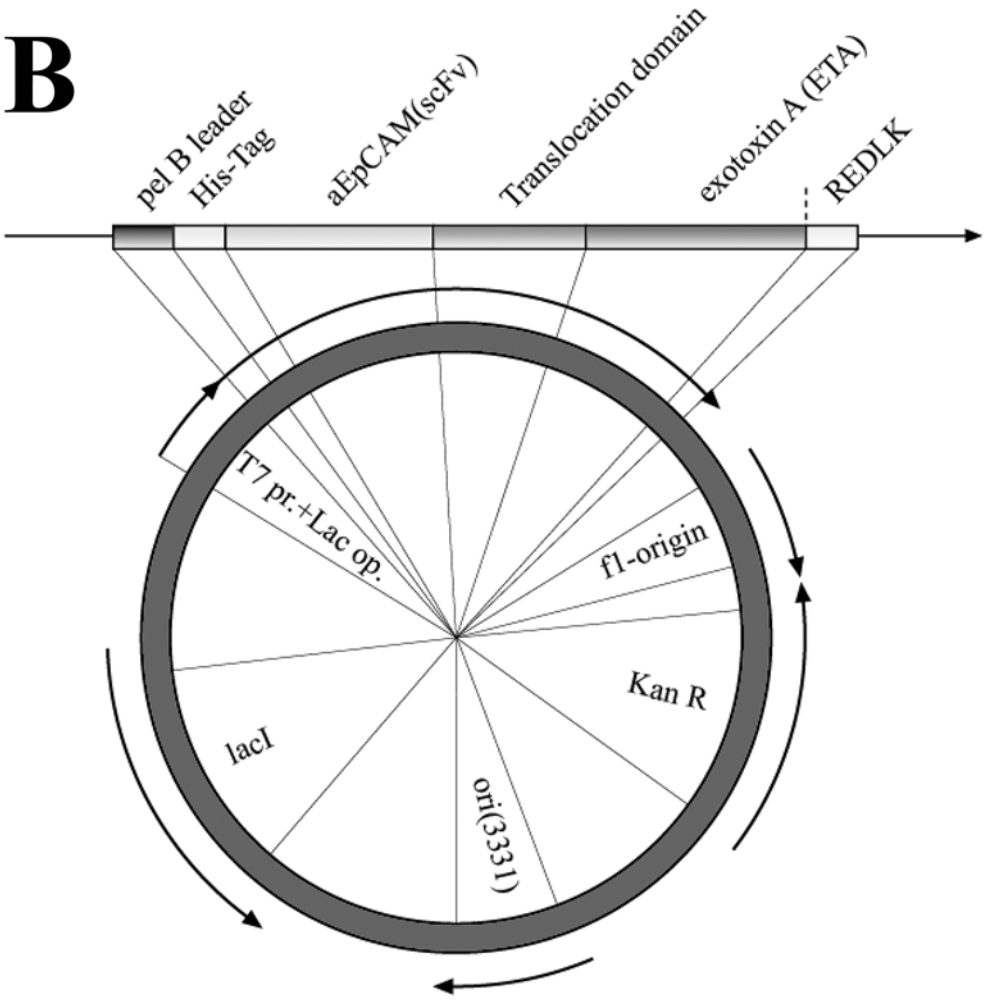
GAATAGCGCCGTCGACCATCATCATCATCATTGAGTTTTGAGCACGAATTCTGGAATTAAT
TCGCTGTCTGCGAGGGCCAGCTGTTGGGGTGAGTACTCCCTCTCAAAAGCGGGCATGACTTCTG
CGCTAAGATTGTCAGTTTCCAAAAACGAGGAGGATTTGATATTCACCTGGCCCGCGGTGATGCC
TTTGAGGGTGGCCGCGTCCATCTGGTCAGAAAAGACAATCTTTTTGTTGTCAAGCTTGAGGTGT
GGCAGGCTTGAGATCTGGCCATACACTTGAGTGACAATGACATCCACTTTGCCTTTCTCTCCACA
GGTGTCCACTCCCAGGTCCAACTGCAGGTCGAGCATGCATCTAGGGCGGCCAATTCCGCCCCTC
TCCCTCCCCCCCCCCTAACGTTACTGGCCGAAGCCGCTTGGAATAAGGCCGGTGTGCGTTTGTCT
ATATGTGATTTTCCACCATATTGCCGTCTTTTGGCAATGTGAGGGCCCGGAAACCTGGCCCTGTC
TTCTTGACGAGCATTCCTAGGGGTCTTTCCCCTCTCGCCAAAGGAATGCAAGGTCTGTTGAATGT
CGTGAAGGAAGCAGTTCCTCTGGAAGCTTCTTGAAGACAAACAACGTCTGTAGCGACCCTTTGC
AGGCAGCGGAACCCCCCACCTGGCGACAGGTGCCTCTGCGGCCAAAAGCCACGTGTATAAGAT
ACACCTGCAAAGGCGGCACAACCCCAGTGCCACGTTGTGAGTTGGATAGTTGTGGAAAGAGTC
AAATGGCTCTCCTCAAGCGTATTCAACAAGGGGCTGAAGGATGCCCAGAAGGTACCCCATTGTA
TGGGATCTGATCTGGGGCCTCGGTGCACATGCTTTACATGTGTTTAGTCGAGGTTAAAAAAACG
TCTAGGCCCCCCGAACCACGGGGACGTGGTTTTCCTTTGAAAAACACGATGATAAGCTTGCCAC
AACCCGGGATCCACCGGTCGCCACCATGGTGAGCAAGGGCGAGGAGCTGTTCACCGGGGTGGT
GCCCATCCTGGTCGAGCTGGACGGCGACGTAAACGGCCACAAGTTCAGCGTGTCCGGCGAGGG
CGAGGGCGATGCCACCTACGGCAAGCTGACCCTGAAGTTCATCTGCACCACCGGCAAGCTGCCC
GTGCCCTGGCCCACCCTCGTGACCACCCTGACCTACGGCGTGCAGTGCTTCAGCCGCTACCCCG
ACCACATGAAGCAGCACGACTTCTTCAAGTCCGCCATGCCCGAAGGCTACGTCCAGGAGCGCA
CCATCTTCTTCAAGGACGACGGCAACTACAAGACCCGCGCCGAGGTGAAGTTCGAGGGCGACA
CCCTGGTGAACCGCATCGAGCTGAAGGGCATCGACTTCAAGGAGGACGGCAACATCCTGGGGC
ACAAGCTGGAGTACAACTACAACAGCCACAACGTCTATATCATGGCCGACAAGCAGAAGAACG
GCATCAAGGTGAACTTCAAGATCCGCCACAACATCGAGGACGGCAGCGTGCAGCTCGCCGACC
ACTACCAGCAGAACACCCCCATCGGCGACGGCCCCGTGCTGCTGCCCGACAACCACTACCTGAG
CACCCAGTCCGCCCTGAGCAAAGACCCCAACGAGAAGCGCGATCACATGGTCCTGCTGGAGTT
CGTGACCGCCGCCGGGATCACTCTCGGCATGGACGAGCTGTACAAGTAAGTTTAAACCCGCTGA
TCAGCCTCGACTGTGCCTTCTAGTTGCCAGCCATCTGTTGTTTGCCCCTCCCCCGTGCCTTCCTTG
ACCCTGGAAGGTGCCACTCCCACTGTCCTTTCCTAATAAAATGAGGAAATTGCATCGCATTGTC
TGAGTAGGTGTCATTCTATTCTGGGGGGTGGGGTGGGGCAGGACAGCAAGGGGGAGGATTGGG
AAGACAATAGCAGGCATGCTGGGGATGCGGTGGGCTCTATGGCTTCTGAGGCGGAAAGAACCA
GCTGGGGCTCTAGGGGGTATCCCCACGCGCCCTGTAGCGGCGCATTAAGCGCGGCGGGTGTGGT
GGTTACGCGCAGCGTGACCGCTACACTTGCCAGCGCCCTAGCGCCCGCTCCTTTCGCTTTCTTCC
CTTCCTTTCTCGCCACGTTCGCCGGCTTTCCCCGTCAAGCTCTAAATCGGGGCATCCCTTTAGGG
TTCCGATTTAGTGCTTTACGGCACCTCGACCCCAAAAAACTTGATTAGGGTGATGGTTCACGTA
GTGGGCCATCGCCCTGATAGACGGTTTTTCGCCCTTTGACGTTGGAGTCCACGTTCTTTAATAGT
GGACTCTTGTTCCAAACTGGAACAACACTCAACCCTATCTCGGTCTATTCTTTTGATTTATAAGG
GATTTTGGGGATTTCGGCCTATTGGTTAAAAAATGAGCTGATTTAACAAAAATTTAACGCGAAT
TAATTCTGTGGAATGTGTGTCAGTTAGGGTGTGGAAAGTCCCCAGGCTCCCCAGCAGGCAGAAG
TATGCAAAGCATGCATCTCAATTAGTCAGCAACCAGGTGTGGAAAGTCCCCAGGCTCCCCAGCA
GGCAGAAGTATGCAAAGCATGCATCTCAATTAGTCAGCAACCATAGTCCCGCCCCTAACTCCGC

CCATCCCGCCCCTAACTCCGCCCAGTTCCGCCCATTCTCCGCCCCATGGCTGACTAATTTTTTTT
ATTTATGCAGAGGCCGAGGCCGCCTCTGCCTCTGAGCTATTCCAGAAGTAGTGAGGAGGCTTTT
TTGGAGGCCTAGGCTTTTGCAAAAAGCTCCCGGGAGCTTGTATATCCATTTTCGGATCTGATCA
GCACGTGTTGACAATTAATCATCGGCATAGTATATCGGCATAGTATAATACGACAAGGTGAGGA
ACTAAACCATGGCCAAGTTGACCAGTGCCGTTCCGGTGCTCACCGCGCGCGACGTCGCCGGAGC
GGTCGAGTTCTGGACCGACCGGCTCGGGTTCTCCCGGGACTTCGTGGAGGACGACTTCGCCGGT
GTGGTCCGGGACGACGTGACCCTGTTCATCAGCGCGGTCCAGGACCAGGTGGTGCCGGACAAC
ACCCTGGCCTGGGTGTGGGTGCGCGGCCTGGACGAGCTGTACGCCGAGTGGTCGGAGGTCGTGT
CCACGAACTTCCGGGACGCCTCCGGGCCGGCCATGACCGAGATCGGCGAGCAGCCGTGGGGGC
GGGAGTTCGCCCTGCGCGACCCGGCCGGCAACTGCGTGCACTTCGTGGCCGAGGAGCAGGACT
GACACGTGCTACGAGATTTCGATTCCACCGCCGCCTTCTATGAAAGGTTGGGCTTCGGAATCGT
TTTCCGGGACGCCGGCTGGATGATCCTCCAGCGCGGGGATCTCATGCTGGAGTTCTTCGCCCAC
CCCAACTTGTTTATTGCAGCTTATAATGGTTACAAATAAAGCAATAGCATCACAAATTTCACAA
ATAAAGCATTTTTTTCACTGCATTCTAGTTGTGGTTTGTCCAAACTCATCAATGTATCTTATCATG
TCTGTATACCGTCGACCTCTAGCTAGAGCTTGGCGTAATCATGGTCATAGCTGTTTCCTGTGTGA
AATTGTTATCCGCTCACAATTCCACACAACATACGAGCCGGAAGCATAAAGTGTAAAGCCTGGG
GTGCCTAATGAGTGAGCTAACTCACATTAATTGCGTTGCGCTCACTGCCCGCTTTCCAGTCGGG
AAACCTGTCGTGCCAGCTGCATTAATGAATCGGCCAACGCGCGGGGAGAGGCGGTTTGCGTATT
GGGCGCTCTTCCGCTTCCTCGCTCACTGACTCGCTGCGCTCGGTCGTTCGGCTGCGGCGAGCGGT
ATCAGCTCACTCAAAGGCGGTAATACGGTTATCCACAGAATCAGGGGATAACGCAGGAAAGAA
CATGTGAGCAAAAGGCCAGCAAAAGGCCAGGAACCGTAAAAAGGCCGCGTTGCTGGCGTTTTT
CCATAGGCTCCGCCCCCCTGACGAGCATCACAAAAATCGACGCTCAAGTCAGAGGTGGCGAAA
CCCGACAGGACTATAAAGATACCAGGCGTTTCCCCCTGGAAGCTCCCTCGTGCGCTCTCCTGTT
CCGACCCTGCCGCTTACCGGATACCTGTCCGCCTTTCTCCCTTCGGGAAGCGTGGCGCTTTCTCA
ATGCTCACGCTGTAGGTATCTCAGTTCGGTGTAGGTCGTTCGCTCCAAGCTGGGCTGTGTGCAC
GAACCCCCCGTTCAGCCCGACCGCTGCGCCTTATCCGGTAACTATCGTCTTGAGTCCAACCCGG
TAAGACACGACTTATCGCCACTGGCAGCAGCCACTGGTAACAGGATTAGCAGAGCGAGGTATG
TAGGCGGTGCTACAGAGTTCTTGAAGTGGTGGCCTAACTACGGCTACACTAGAAGGACAGTATT
TGGTATCTGCGCTCTGCTGAAGCCAGTTACCTTCGGAAAAAGAGTTGGTAGCTCTTGATCCGGC
AAACAAACCACCGCTGGTAGCGGTGGTTTTTTTGTTTGCAAGCAGCAGATTACGCGCAGAAAAA
AAGGATCTCAAGAAGATCCTTTGATCTTTTCTACGGGGTCTGACGCTCAGTGGAACGAAAACTC
ACGTTAAGGGATTTTGGTCATGAGATTATCAAAAAGGATCTTCACCTAGATCCTTTTAAATTAA
AAATGAAGTTTTAAATCAATCTAAAGTATATATGAGTAAACTTGGTCTGACAGTTACCAATGCT
TAATCAGTGAGGCACCTATCTCAGCGATCTGTCTATTTCGTTCATCCATAGTTGCCTGACTCCCC
GTCGTGTAGATAACTACGATACGGGAGGGCTTACCATCTGGCCCCAGTGCTGCAATGATACCGC
GAGACCCACGCTCACCGGCTCCAGATTTATCAGCAATAAACCAGCCAGCCGGAAGGGCCGAGC
GCAGAAGTGGTCCTGCAACTTTATCCGCCTCCATCCAGTCTATTAATTGTTGCCGGGAAGCTAG
AGTAAGTAGTTCGCCAGTTAATAGTTTGCGCAACGTTGTTGCCATTGCTACAGGCATCGTGGTG
TCACGCTCGTCGTTTGGTATGGCTTCATTCAGCTCCGGTTCCCAACGATCAAGGCGAGTTACATG
ATCCCCCATGTTGTGCAAAAAAGCGGTTAGCTCCTTCGGTCCTCCGATCGTTGTCAGAAGTAAG
TTGGCCGCAGTGTTATCACTCATGGTTATGGCAGCACTGCATAATTCTCTTACTGTCATGCCATC

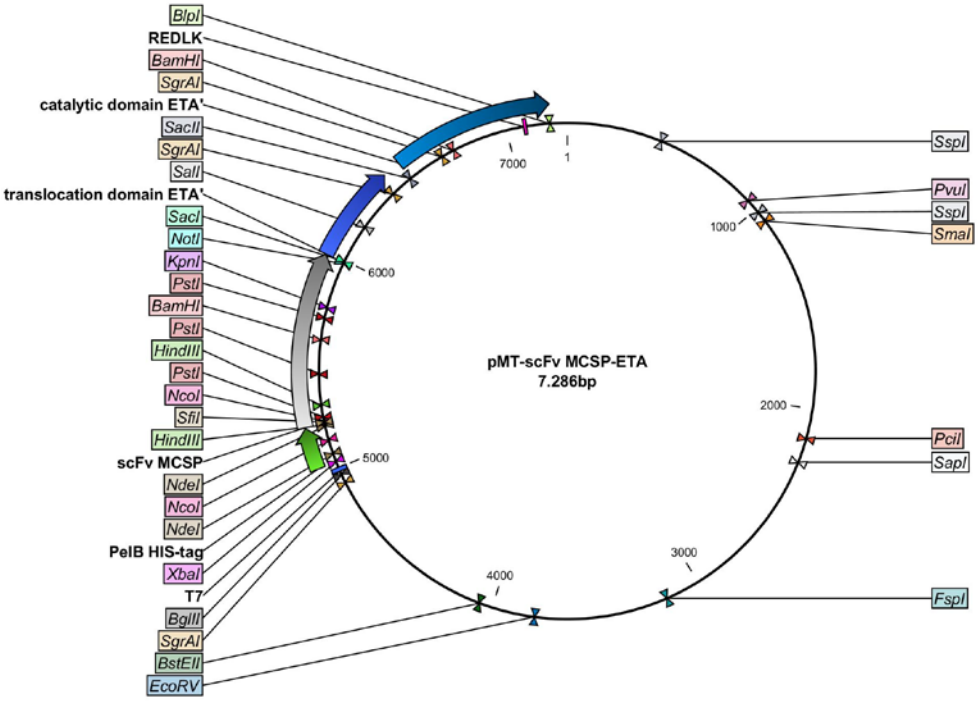
CGTAAGATGCTTTTCTGTGACTGGTGAGTACTCAACCAAGTCATTCTGAGAATAGTGTATGCGG
CGACCGAGTTGCTCTTGCCCGGCGTCAATACGGGATAATACCGCGCCACATAGCAGAACTTTAA
AAGTGCTCATCATTGGAAAACGTTCTTCGGGGCGAAAACTCTCAAGGATCTTACCGCTGTTGAG
ATCCAGTTCGATGTAACCCACTCGTGCACCCAACTGATCTTCAGCATCTTTTACTTTCACCAGCG
TTTCTGGGTGAGCAAAAACAGGAAGGCAAAATGCCGCAAAAAAGGGAATAAGGGCGACACGG
AAATGTTGAATACTCATACTCTTCCTTTTTCAATATTATTGAAGCATTTATCAGGGTTATTGTCTC
ATGAGCGGATACATATTTGAATGTATTTAGAAAAATAAACAAATAGGGGTTCCGCGCACATTTC
CCCGAAAAGTGCCACCTGACGTCGACGGATCGGGAGATCTCCCGATCCCCTATGGTCGACTCTC
AGTACAATCTGCTCTGATGCCGCATAGTTAAGCCAGTATCTGCTCCCTGCTTGTGTGTTGGAGGT
CGCTGAGTAGTGCGCGAGCAAAATTTAAGCTACAACAAGGCAAGGCTTGACCGACAATTGCAT
GAAGAATCTGCTTAGGGTTAGGCGTTTTGCGCTGCTTCGCGATGTACGGGCCAGATATACGCGT
TGACATTGATTATTGACTAGTTATTAATAGTAATCAATTACGGGGTCATTAGTTCATAGCCCATA
TATGGAGTTCCGCGTTACATAACTTACGGTAAATGGCCCGCCTGGCTGACCGCCCAACGACCCC
CGCCCATTGACGTCAATAATGACGTATGTTCCCATAGTAACGCCAATAGGGACTTTCCATTGAC
GTCAATGGGTGGACTATTTACGGTAAACTGCCCACTTGGCAGTACATCAAGTGTATCATATGCC
AAGTACGCCCCCTATTGACGTCAATGACGGTAAATGGCCCGCCTGGCATTATGCCCAGTACATG
ACCTTATGGGACTTTCCTACTTGGCAGTACATCTACGTATTAGTCATCGCTATTACCATGGTGAT
GCGGTTTTGGCAGTACATCAATGGGCGTGGATAGCGGTTTGACTCACGGGGATTTCCAAGTCTC
CACCCCATTGACGTCAATGGGAGTTTGTTTTGGCACCAAAATCAACGGGACTTTCCAAAATGTC
GTAACAACTCCGCCCCATTGACGCAAATGGGCGGTAGGCGTGTACGGTGGGAGGTCTATATAA
GCAGAGCTCTCTGGCTAACTAGAGAACCCACTGCTTACTGGCTTATCGAAATTAATACGACTCA
CTATAGGGAGACCCAAGCTG

## *VI.4 Plasmid maps*

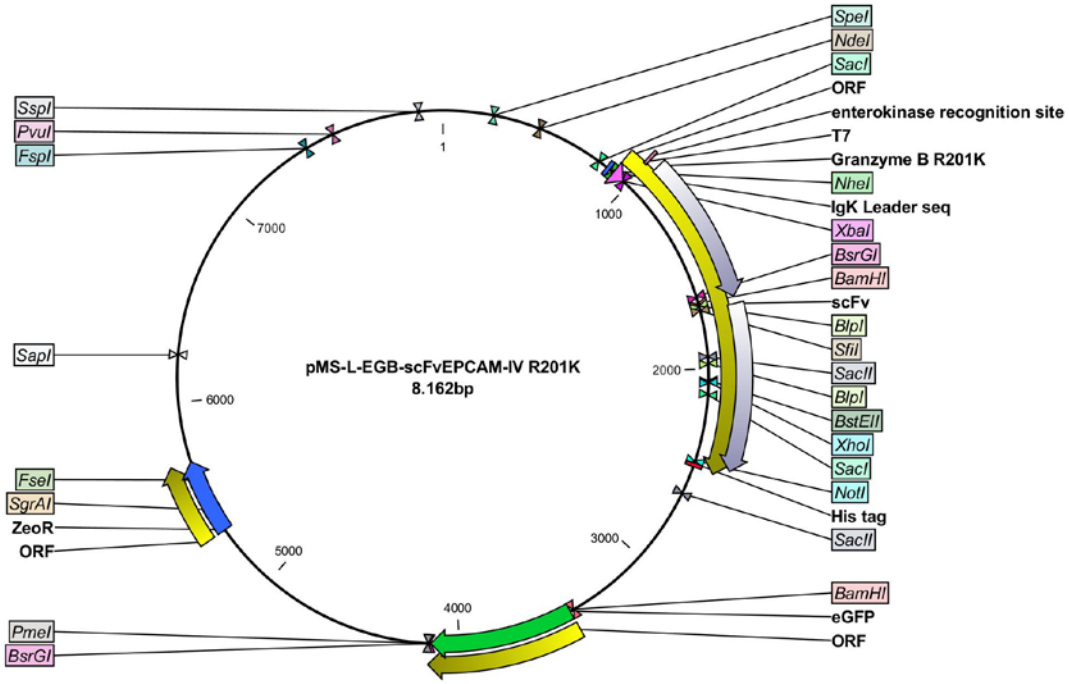
### *VI.4.1 pMT-anti-EpCAM-ETA*



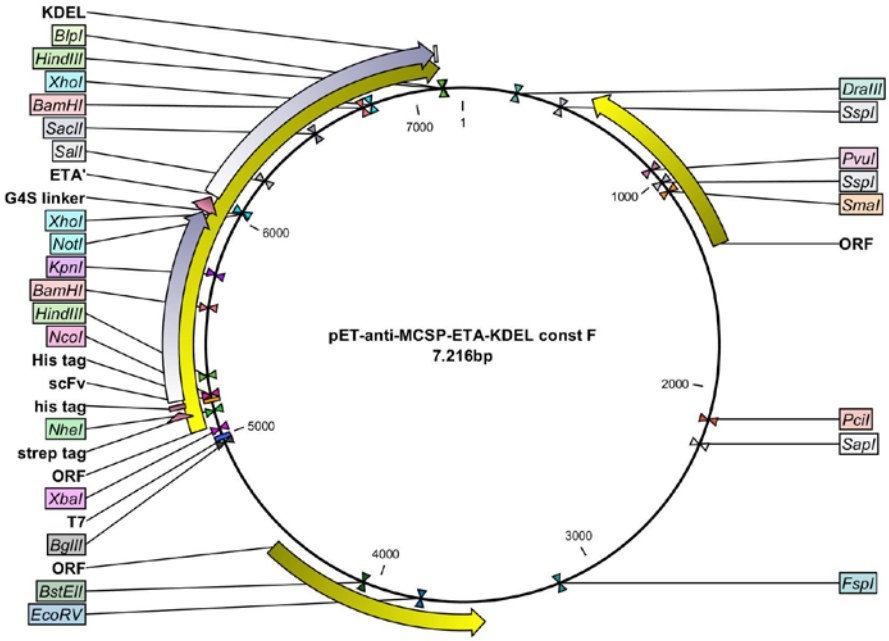
### *VI.4.2 pMT-anti-CSPG4-ETA*



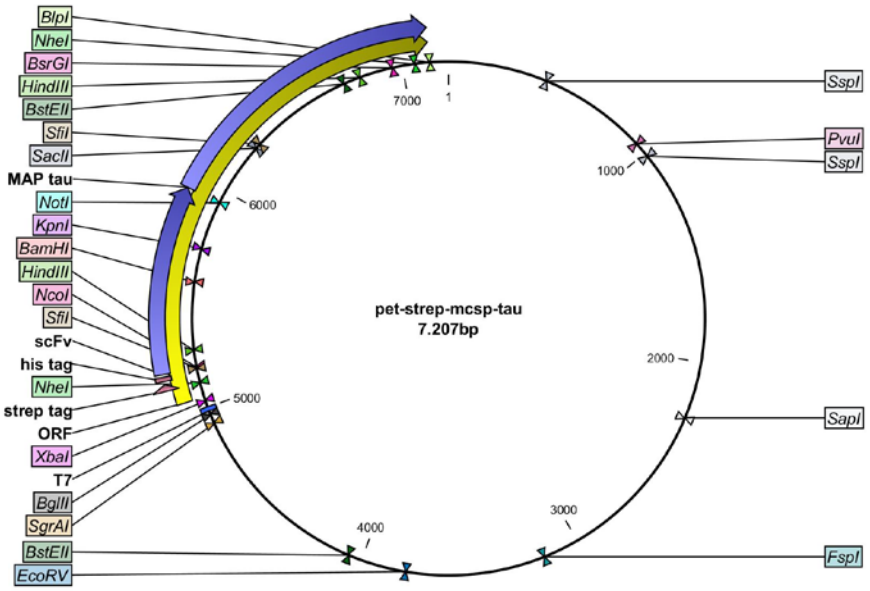

### *VI.4.3 pMS-L-EGB-anti-EpCAM-IV*



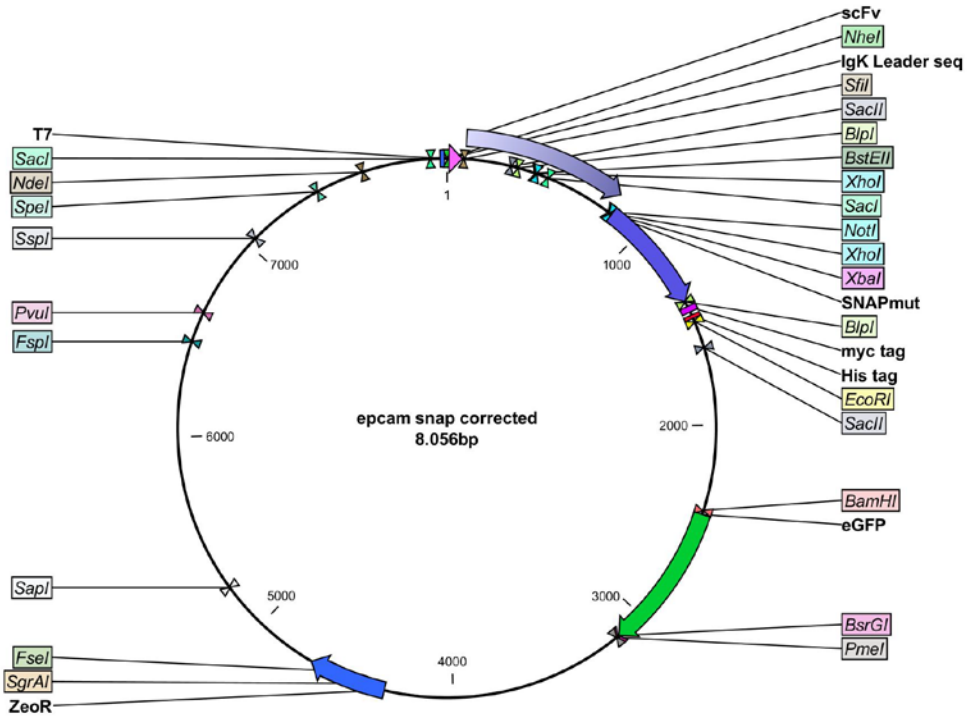
### *VI.4.4 pET-strep-anti-CSPG4-ETA-KDEL*



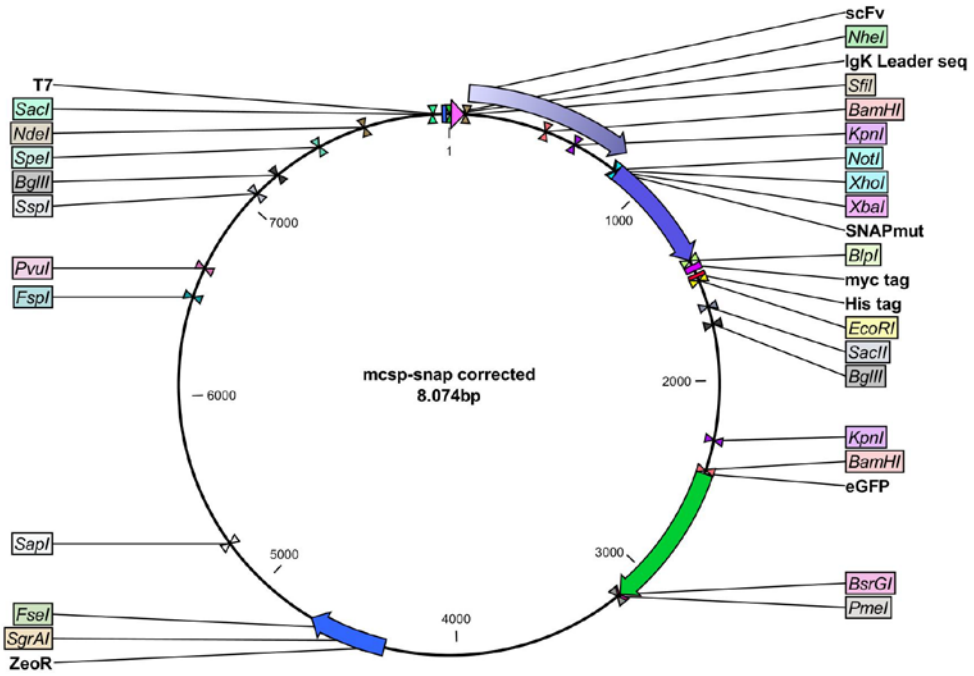

### *VI.4.5 pET-strep-anti-CSPG4-MAP*



### *VI.4.6 pMS-anti-EpCAM-SNAP-IV*



### *VI.4.7 pMS-anti-CSPG4-SNAP-IV*



# VII Thesis related scientific publications

1. A novel approach for targeted elimination of CSPG4-positive triple-negative breast cancer cells using a MAP tau-based fusion protein.
**Amoury M**, Mladenov R, Nachreiner T, Pham AT, Hristodorov D, Di Fiore S, Helfrich W, Pardo A, Fey G, Schwenkert M, Thepen T, Kiessling F, Hussain AF, Fischer R, Kolberg K, Barth S.
Internationl Journal of Cancer. 2016 Apr 1.

2. Granzyme B-based cytolytic fusion protein targeting EpCAM specifically kills triple negative breast cancer cells in vitro and inhibits tumor growth in a subcutaneous mouse tumor model.
**Amoury M**, Kolberg K, Pham AT, Hristodorov D, Mladenov R, Di Fiore S, Helfrich W, Kiessling F, Fischer R, Pardo A, Thepen T, Hussain AF, Nachreiner T, Barth S.
Cancer Letters. 2016 Mar 28;372(2):201-9.

3. EpCAM-selective elimination of carcinoma cells by a novel MAP-based cytolytic fusion protein.
Hristodorov D*, **Amoury M***, Mladenov R, Niesen J, Arens K, Berges N, Hein L, Di Fiore S, Pham AT, Huhn M, Helfrich W, Fischer R, Thepen T, Barth S.
Molecular Cancer Therpeutics. 2014 Sep;13(9):2194-202. * ***shared first authors.***

4. SNAP-tag technology: a powerful tool for site specific conjugation of therapeutic and imaging agents.
Hussain AF, **Amoury M**, Barth S.
Current Pharmaceutical Design. 2013;19(30):5437-42. Review.

5. SNAP-tag based agents for preclinical in vitro imaging in malignant diseases.
**Amoury M**, Blume T, Brehm H, Niesen J, Tenhaef N, Barth S, Gattenlöhner S, Helfrich W, Fitting J, Nachreiner T, Pardo A.
Current Pharmaceutical Design. 2013;19(30):5429-36.

**6.** Photoimmunotheranostic agents for triple-negative breast cancer diagnosis and therapy that can be activated on demand.
**Amoury M**, Bauerschlag D, Zeppernick F, von Felbert V, Berges N, Di Fiore S, Mintert I, Bleilevens A, Maass N, Bräutigam K, Meinhold-Heerlein I, Stickeler E, Barth S, Fischer R, Hussain AF. ***(Accepted for publication, Oncotarget, May 2016).***

# VIII Acknowledgements

I would like to thank my doctoral advisor **Prof. Dr. Rainer Fischer** for supervising this thesis.

I would like to thank **Prof. Dr. Dr. Stefan Barth** for giving me the chance to work in his department, for co-supervising me, and for giving me working freedom during the last years.

I wish also to thank **and Prof. Dr. Fabian Kiessling** for agreeing to act as co-referents.
I also thank Prof. Elmar Stickeler for agreeing to take act as PhD examiner.
I thank **Dr. Theo Thepen** for practically supervising the animal experiments.
I am thankful to **Dr. Stefano Di Fiore for** helping me with all immunofluorescence assays and microscopy.

My special thanks go to my friends and colleagues **Radoslav, Ahmad, Dmitrij, Swati, Markus, Tanja, Holger and Alda** for helping me with experiments and with trouble-shooting, for teaching me new techniques and for the great times and fun moments we had in and outside the lab.

For their kind help in the lab, I am very grateful to **Reinhard Rosinke and Anh-Tuan Pham**.

Finally, I would like to give my greatest thanks and my gratitude for my supporting and loving family, my life partner **Saib**, my Mom **Laila**, and my sisters **Hana, Ibtisam, Hiba** and **Tala** for always being there, always encouraging and always loving me.

And to my beautiful and amazing son **Joud** who was born towards the end of my PhD, you made everything better, you gave me hope and strength to get to the finish line…